CE-MS for metabolomics: advancing performance and detection sensitivity

Zhang, W.

CE-MS for metabolomics:

advancing performance and detection sensitivity

Wei Zhang

CE-MS for metabolomics:
advancing performance and detection sensitivity

Proefschrift

ter verkrijging van
de graad van Doctor aan de Universiteit Leiden,
op gezag van Rector Magnificus Prof. Mr. C.J.J.M. Stolker,
volgens besluit van het college voor Promoties
te verdedigen op dinsdag 31 Maart 2020
klokke 16:15 uur

door

Wei Zhang | 张伟

geboren te Yangzhou, China in 1989

Promotor

Prof. dr. Thomas Hankemeier

Copromotor

Dr. Rawi Ramautar

Promotiecommissie

Prof. dr. Hubertus Irth (Chair)

Leiden University, the Netherlands

Prof. dr. Joke Bouwstra (Secretary)

Leiden University, the Netherlands

Prof. dr. Erik Danen

Leiden University, the Netherlands

Prof. dr. Philip Britz-McKibbin

McMaster University, Canada

Prof. dr. Govert W. Somsen

Vrije Universiteit Amsterdam, the Netherlands

Prof. dr. Marie-José Goumans

Leiden University Medical Center, the Netherlands

This work was financially supported as indicated in each chapter.

Contents

Chapter 1

General Introduction and Scope

Introduction

Drug discovery and systems biology

Drug discovery is an interdisciplinary endeavor that involves iterative process of chemical, biochemical, and pharmacological assays [1-3]. Over the last five decades, the capitalized cost estimate for developing a new drug from concept has increased from millions to a few billion dollars [4], however, the success rate for drugs entering into the market is no higher than 24% [5, 6]. Reducing the attrition rate of drug candidates in clinical development is the key challenge for pharmaceutical researches, and important for sustaining the viability of the entire industry [7, 8]. Advancements in various technical aspects can help researchers avoid unnecessary costs. Preclinical characterization of pharmacokinetic and toxicological properties of chemical entities has already reduced downstream attrition [9]. On the contrast, the attrition rates in clinical trial stage are still unacceptably high, and one of the major issues is the lack of understanding about the nature of (new) drug targets, which increases the uncertainty about the desired therapeutic efficacy. Pharmaceutical industry has experienced a string of failed clinical trials in developing modifying therapies for Alzheimer's disease over last two decades. Sperling et al. proposed three assumptions in an attempt to explain those failures and emphasized the importance of the combination of the right target, the right drug, and the right time in order for the drug to exert its efficacy [10]. Selecting drug targets and employing discovered targets for early pharmacological evaluation are two key steps in drug discovery and aid in the reduction of high attrition rates in clinical trials [7].

Whether it is drug target identification or efficacy evaluation, systems biology appears to be a promising tool. Systems biology is a knowledge-based approach that attempts to understand biology at the system level and has the capability of integrating large quantities of complex data obtained by genomic, proteomic and metabolic analyses [11]. An important application of systems biology lies within the rapidly developing field of personalized medicine. Systems biology approach screens variations, mutations, gene variants, and metabolic profiles by analyzing human DNA, RNA and proteins, which reveals pathologically relevant information such as diagnosis, susceptibility and risk factors, and disease progression and therapy [12]. In this way, the current healthcare strategies can be optimized and therapeutic therapies personally customized.

Among the technologies applied for systems biology, genomics and proteomics first came to the spotlight and were expected to result in a plethora of validated new drug targets [6]. Genomics and proteomics only take into consideration the intermediate steps in the central dogma, while metabolomics explores the downstream products from genes and proteins [13]. It is the integration of metabolomics with genomics and proteomics that enables researchers to gain a holistic understanding about pathways and ultimately better assists with drug discovery and personalized medicine. However, it still remains to be a challenge to conduct multi-omics

integration because a lot of the analytical techniques and experimental designs lack the versatility to permit proper comparison or integration among different omics disciplines. Pinu et at. [14] pointed out that metabolomics is capable of providing a "common denominator" to the design and analysis of many other omics works due to its closeness to phenotypes, thus an increased awareness of metabolomics by fellow researchers conducting other omics could greatly benefit the quality of integrated-omics research.

Metabolomics

Metabolomics seeks to provide a comprehensive profile of all the (endogenous) metabolites present in a given sample at a specific point of time [15]. Metabolomic analysis of biological samples has found applications in pathology, diagnostics, and toxicology [16-20]. The field of metabolomics has developed significantly over the past decade and basically progressed from a fundamental research topic studied by a relatively small number of highly specialized research groups into a major field now used by hundreds of laboratories, core facilities and national centers.

The ultimate aim of metabolomics research is to effectively address a specific biological or clinical problem. For this purpose, two analytical strategies are generally employed, i.e. non-targeted and targeted metabolomics. Non-targeted metabolomics approaches are often used for explorative, discovery-based studies and involves the profiling of biological samples (often body fluids) without having *a priori* knowledge on the nature and identity of the measured metabolites. Such strategies may be referred to as metabolic profiling or fingerprinting. The second approach is focused on the quantitative analysis of pre-selected (target) metabolites in a biological sample. Both approaches can be used in a single study, where the first approach is used to discover putative biomarkers of disease, which are then validated and subsequently quantified by the second approach. The requirements on analytics for these two approaches are diverging, notably when it comes to sample pre-treatment, standardization, matrix effects, etc. The decision on which metabolomics approach to use is determined by the aim of the study.

Current techniques used in metabolomics mainly include two categories: nuclear magnetic resonance (NMR) spectroscopy and mass spectrometry (MS)-based techniques. NMR is a non-destructive strategy that does not require complicated and laborious sample preparation [21], which sometimes, in turn, increases the difficulty of analyzing NMR spectra derived from complex mixtures. In terms of analysis time and cost per sample, NMR is more suitable for high-throughput studies than MS [22]. The major drawback of NMR in metabolomics applications is the relatively low sensitivity, thus its acquired metabolic coverage isn't comparable to MS.

Mass spectrometry (MS)-based techniques such as GC-MS and LC-MS are the most commonly used analytical platforms for metabolomics studies. GC-MS is the method of choice for volatile and thermally stable metabolites, and it involves complex and laborious sample derivatization procedures. LC-MS benefits from its widespread availability and continuous instrumentation

development and has been applied in a plethora of metabolomics explorations. The profiling of endogenous metabolites is predominantly performed with *state-of-the-art* reverse phase LC-MS (RPLC-MS) methods. However, RPLC-MS is highly suitable for analyzing compounds of medium or low polarity, but often problematic for highly polar metabolites. The analysis of polar compounds could then be alternatively analyzed by employing hydrophilic interaction liquid chromatography (HILIC) columns. HILIC utilizes modified LC columns that possess strong retention capability for highly polar compounds, which renders HILIC a complementary technique to RPLC and has been applied in various research fields as described in the literature [23-25]. The drawbacks of HILIC usually include poor retention time reproducibility and analytical drift after analyzing multiple samples [26].

CE-MS for metabolomics

Within the metabolomics field, another useful analytical technique for the profiling of (highly) polar and charged metabolites is capillary electrophoresis (CE) hyphenated to MS (CE-MS). In CE, compounds are separated on the basis of differences in their intrinsic electrophoretic mobility, which is dependent on the charge and size of the analyte. Therefore, CE is especially suited for the analysis of polar and charged metabolites. Compared to chromatographic-based separation methods, the separation efficiency of CE is very high due to the flat flow profile of the electro-osmotic flow and there is no mass transfer between phases and as only longitudinal diffusion contributes to band broadening under proper experimental conditions. The intrinsically high separation efficiency of CE is very advantageous for the high resolution separation of structurally similar metabolites in complex samples. Moreover, as the separation mechanism of CE is fundamentally different from chromatographic-based separation techniques, a complementary view on the composition of metabolites present in a given biological sample is provided [27-29]. HILIC and CE are both suited for the analysis of polar metabolome, and the extent of overlapping in their metabolic coverage triggered some interesting studies. Kok et al. employed both CE-MS and HILIC-MS for anionic profiling of rat urine and discovered that these methods exhibited a high degree of orthogonality [30]. Although the proposed HILIC method obtained more features and high intensities (mainly due to the much larger injection volume), CE-MS detected over 200 unique features.

CE coupling to MS is accomplished via electrospray ionization (ESI) with different interfacing designs. The development of interfacing technologies has helped expand the applications of CE-MS. So far the most commonly used interface is coaxial sheath liquid interface, and sheath liquid CE-MS has found usefulness in profiling various biological samples [31-33]. Due to the limited volume of injected samples and the dilution effect caused by the sheath liquid, the compromised concentration sensitivity has always been an issue with this setup. To overcome the sample injection limitation, various online sample preconcentration techniques have been investigated, including dynamic pH injunction, transient isotachophoresis (tITP), field amplification sample

stacking (FASS), field amplification sample injection (FASI), and sweeping [34-37]. Moreover, efforts have also been devoted to developing more sensitive interfaces by minimizing or circumventing the direct mixing of sheath liquid with CE effluent [38-42], thus improving detection sensitivity. To date, the most successful alternative interface has been the sheathless nanospray interface with a porous tip emitter developed by Moini [40], which has greatly benefited the detection sensitivity and metabolome coverage, as showcased in the literature [43-46].

Notably, a strong advantage of CE-MS over HILIC-MS is that it is especially useful for analyzing volume-restricted samples. Volume restricted samples are intrinsically small and often low in metabolite concentrations, such as mouse cerebrospinal fluid (CSF), samples from microfluidic organ-on-a-chip models, and circulating tumor cells in bloodstream, but they can be information-rich and could be the key to unravelling certain biomedical mysteries. The heterogeneous tumor cell populations that reside in the tumor ecosystem represent a considerable challenge for tumor therapy [47, 48]. Insights into the metabolic patterns of these small tumor cell populations can contribute to the understanding about tumor cell heterogeneity. Better understanding about the cell heterogeneity in tumors will lead to a better chance of eradicating all different cell subpopulations and smother any possibility of inducing drug resistance. Sheathless CE-MS has proved to be a useful technique in the metabolic profiling mouse CSF samples [45] and low numbers of cancer cells [49].

Challenges in CE-MS for metabolomics

Until now, CE-MS has only been used by a limited number of research groups for metabolomics studies. The coupling of CE to MS is often perceived as technically challenging by the scientific community. Moreover, there is a lack of standard operating procedures, which are critical for performing (long-term and inter-laboratory) reproducibility studies. The major drawback of CE is the inadequate robustness. However, it is important to note that a number of recent studies clearly exemplify the usefulness of CE-MS for metabolic profiling of large sample sets [50, 51]. For example, the group of Soga and co-workers, the group that introduced the first CE-MS methods for metabolomics in 2003 [52], has assessed the long-term performance of CE-MS for metabolic profiling of more than 8000 human plasma samples from the Tsuruoka Metabolomics Cohort Study over a 52-month period [50]. The study provided an absolute quantification for 94 polar metabolites in plasma with a similar reproducibility when compared to other analytical platforms, i.e. reversed-phase LC-MS and GC-MS, employed for large-scale metabolomics studies.

Nonetheless, there is still a lack of reliable CE-MS methods for the efficient profiling of highly polar and charged metabolites in the literature, especially in volume-limited samples. In this thesis, a key aim was to develop viable CE-MS approaches for the highly efficient and sensitive profiling of polar and charged metabolites. For achieving this purpose, both the conventional and the sheathless porous tip interface have been considered for coupling CE to MS. The repeatability of CE-MS methods for peak areas and migration times of metabolites was closely monitored. Special

attention has been devoted to highlight relevant methodological aspects for metabolomics studies in protocol papers and to share experimental procedures via peer-reviewed (video) articles. Conveying the work in this way is urgently needed to convince the scientific community about the unique and complementary capabilities of CE-MS for metabolomics.

Scope and outline of the thesis

At the start of this work, some efforts had already been devoted to downscaling analytical techniques and/or workflows for the analysis of (endogenous) metabolites in minute sample amounts. These analytical technologies, though very promising, were not suited for the highly sensitive and efficient profiling of a large number of metabolites in small-volume biological samples in a robust way [53-55]. Therefore, in this thesis, CE-MS strategies employing both a sheath-liquid and sheathless porous tip interface were developed and evaluated for the global profiling of metabolites in low amounts of sample material. These methods covered a wide range of cationic and anionic metabolites, including compounds like amino acids, amines, organic acids and nucleotides, etc. This evaluation was conducted by considering aspects such as migration-time and peak area repeatability, separation efficiency, linearity and detection limits. The applicability of the developed CE-MS methods has been tested by analyzing clinically relevant volume/material limited samples. Special attention has been devoted to highlighting relevant methodological aspects in order to expand the (complementary) role of CE-MS in metabolomics.

An overview of CE-MS advancements in metabolic profiling is presented in **Chapter 2**. This chapter discusses aspects such as interfacing designs and provides an overview of strategies on how to improve metabolic coverage, and sample throughput. The applicability of CE-MS for metabolic profiling of especially limited sample amounts is demonstrated by the analysis of cell culture extracts. The advancements in CE-MS interfaces, such as the sheathless interface with a porous tip emitter, have shown great promise in enhancing the coverage of the polar metabolome. However, the general application of CE-MS in metabolomics research is still limited as this approach is considered as technically challenging and lacking reproducibility.

In order to expand the utility of CE-MS in metabolomics research, standardized protocols are urgently needed. **Chapter 3** includes two technical notes, introducing both the basic operations and biological applications of CE-MS. The first part introduces a protocol on how the CE system is coupled to MS via a sheathless porous tip interface, including a description of an extensive conditioning procedure for the first use of the capillary. This section also showcased the versatility of CE-MS for the global profiling of anionic and cationic metabolites using a single capillary and buffer composition. The second part in this chapter described an analytical workflow based on sheathless CE-MS for metabolic profiling of low amounts of HepG2 cells, with special attention on the sample preparation step.

In **Chapter 4**, the utility of CE-MS employing a sheathless porous tip interface is demonstrated for metabolic profiling of limited amounts of HepG2 cells, using the sample preparation procedure described in the previous chapter. By using sheathless CE-MS in combination with transient isotachophoresis (tITP), this chapter illustrated the feasibility of CE-MS for highly sensitive profiling of metabolites in material-limited samples. It is shown that the proposed approach allows to obtain metabolomics data from an injection volume corresponding to the content of less than a single HepG2 cell.

In **Chapter 5** a sheathless CE-MS method is proposed for the profiling of nucleotides at high pH separation conditions. In this work, nucleotides were separated while negatively charged and detected by MS in the positive ion mode, thereby fully circumventing the commonly observed *corona discharge* when coupling high pH nanoscale separations to negative ESI-MS mode. The proposed sheathless CE-MS method was validated in aspects of linearity, precision, accuracy and matrix effect. Overall, the developed approach allows highly efficient and sensitive profiling of nucleotides in HepG2 cells, down to the injection content equivalent to less than a single cell.

CE-MS approaches employing a conventional sheath-liquid interface have been widely used for metabolic profiling studies, however, the robustness and usefulness of this technique has not been assessed in detail for biomarker discovery studies yet. Therefore, **chapter 6** outlines an innovative validation strategy to illustrate the utility of CE-MS for biomarker discovery studies using metabolomics. In essence, the approach was based on the determination of simulated biomarkers in spiked human plasma. Different strategies were adopted in creating differences among sample groups, and those artificial “biomarkers” could be accurately identified with the use of CE-MS analysis combined with multivariate data analysis.

Chapter 7 demonstrates our work using conventional CE-MS in biomarker discovery using volume-limited plasma samples from a mouse model for epilepsy. The mouse model was created by direct electric shock on mouse corneal and blood samples were collected from both the control group and model group By using our previously developed and validated CE-MS method for biomarker discovery. The study clearly revealed the advantage of CE-MS in profiling volume-restricted samples and revealed metabolic markers potentially indicative of epilepsy onsets in mice.

Chapter 8 reports the first quantitative assessment of polar and charged metabolites in the nanomaterial corona using a CE-MS-based metabolomics approach. This study revealed that polar ionogenic metabolites adsorb to nanomaterials and that nanomaterial properties have a significant impact upon the qualitative and quantitative composition of the metabolite corona. Furthermore, formation of metabolite corona was quantitatively assessed using protein-free and complete human plasma samples, which revealed that the presence of proteins in the sample is vital to characterizing a biologically relevant metabolite corona as differences between protein-free and intact plasma are significant and lead to different corona formation.

Finally, **Chapter 9** offers a general conclusion of the studies described in this thesis. Perspectives and recommendations on further improvement and applications of the proposed CE-MS methods are also discussed.

References

1. Mohs, R.C. and N.H. Greig, *Drug discovery and development: Role of basic biological research.* Alzheimers Dement (N Y), 2017. **3**(4),651-657.
2. Tamimi, N.A. and P. Ellis, *Drug development: from concept to marketing!* Nephron Clin Pract, 2009. **113**(3),c125-31.
3. Zon, L.I. and R.T. Peterson, *In vivo drug discovery in the zebrafish.* Nat Rev Drug Discov, 2005. **4**(1),35-44.
4. Morgan, S., et al., *The cost of drug development: A systematic review.* Health Policy, 2011. **100**(1),4-17.
5. Adams, C.P. and V.V. Brantner, *Estimating the cost of new drug development: Is it really $802 million?* Health Affairs, 2006. **25**(2),420-428.
6. Paul, S.M., et al., *How to improve R&D productivity: the pharmaceutical industry's grand challenge.* Nature Reviews Drug Discovery, 2010. **9**(3),203-214.
7. Waring, M.J., et al., *An analysis of the attrition of drug candidates from four major pharmaceutical companies.* Nature Reviews Drug Discovery, 2015. **14**(7),475-486.
8. Kavanagh, S., et al., *Reducing attrition in drug development: Smart loading pre-clinical safety assessment.* Toxicology Letters, 2014. **229**,S167-S167.
9. Kramer, J.A., J.E. Sagartz, and D.L. Morris, *The application of discovery toxicology and pathology towards the design of safer pharmaceutical lead candidates.* Nat Rev Drug Discov, 2007. **6**(8),636-49.
10. Sperling, R.A., C.R. Jack, and P.S. Aisen, *Testing the Right Target and Right Drug at the Right Stage.* Science Translational Medicine, 2011. **3**(111).
11. Davidov, E.J., et al., *Advancing drug discovery through systems biology.* Drug Discovery Today, 2003. **8**(4),175-183.
12. Di Sanzo, M., et al., *Clinical Applications of Personalized Medicine: A New Paradigm and Challenge.* Current Pharmaceutical Biotechnology, 2017. **18**(3),194-203.
13. Baharum, S.N. and K.A. Azizan, *Metabolomics in Systems Biology.* Adv Exp Med Biol, 2018. **1102**,51-68.
14. Pinu, F.R., et al., *Systems Biology and Multi-Omics Integration: Viewpoints from the Metabolomics Research Community.* Metabolites, 2019. **9**(4).
15. Fiehn, O., *Metabolomics—the link between genotypes and phenotypes*, in *Functional genomics*. 2002, Springer. p. 155-171.
16. Ussher, J.R., et al., *The Emerging Role of Metabolomics in the Diagnosis and Prognosis of Cardiovascular Disease.* Journal of the American College of Cardiology, 2016. **68**(25),2850-2870.
17. Kumar, B., et al., *Potential of metabolomics in preclinical and clinical drug development.* Pharmacological Reports, 2014. **66**(6),956-963.
18. Guleria, A., et al., *NMR Based Metabolomics: An Exquisite and Facile Method for Evaluating Therapeutic Efficacy and Screening Drug Toxicity.* Current Topics in Medicinal Chemistry, 2018. **18**(20),1827 - 1849.

19. Bujak, R., et al., *Metabolomics for laboratory diagnostics.* Journal of Pharmaceutical and Biomedical Analysis, 2015. **113**,108-120.
20. Rysz, J., et al., *Novel Biomarkers in the Diagnosis of Chronic Kidney Disease and the Prediction of Its Outcome. .* International Journal of Molecular Sciences, 2017. **18**(8),1702.
21. Shulaev, V., *Metabolomics technology and bioinformatics.* Briefings in Bioinformatics, 2006. **7**(2),128-139.
22. Miggiels, P., et al., *Novel technologies for metabolomics: More for less.* TrAC Trends in Analytical Chemistry, 2018.
23. Tang, D.Q., et al., *HILIC-MS for metabolomics: An attractive and complementary approach to RPLC-MS.* Mass Spectrom Rev, 2016. **35**(5),574-600.
24. Hendrickx, S., E. Adams, and D. Cabooter, *Recent advances in the application of hydrophilic interaction chromatography for the analysis of biological matrices.* Bioanalysis, 2015. **7**(22),2927-45.
25. Li, Z., et al., *Hydrophilic Interaction Liquid Chromatography/Mass Spectrometry: An Attractive and Prospective Method for the Quantitative Bioanalysis in Drug Metabolism.* Curr Drug Metab, 2016. **17**(4),386-400.
26. Buszewski, B. and S. Noga, *Hydrophilic interaction liquid chromatography (HILIC)-a powerful separation technique.* Analytical and Bioanalytical Chemistry, 2012. **402**(1),231-247.
27. Ramautar, R., G.W. Somsen, and G.J. de Jong, *CE-MS for metabolomics: Developments and applications in the period 2016-2018.* Electrophoresis, 2019. **40**(1),165-179.
28. Barbas, C., E.P. Moraes, and A. Villasenor, *Capillary electrophoresis as a metabolomics tool for non-targeted fingerprinting of biological samples.* Journal of Pharmaceutical and Biomedical Analysis, 2011. **55**(4),823-831.
29. Soga, T., *Capillary electrophoresis-mass spectrometry for metabolomics.* Methods Mol Biol, 2007. **358**,129-37.
30. Kok, M.G., G.W. Somsen, and G.J. de Jong, *Comparison of capillary electrophoresis-mass spectrometry and hydrophilic interaction chromatography-mass spectrometry for anionic metabolic profiling of urine.* Talanta, 2015. **132**,1-7.
31. Celebier, M., et al., *A Foodomics Approach: CE-MS for Comparative Metabolomics of Colon Cancer Cells Treated with Dietary Polyphenols.* Methods Mol Biol, 2019. **1855**,303-313.
32. Zhang, W., et al., *Assessing the suitability of capillary electrophoresis-mass spectrometry for biomarker discovery in plasma-based metabolomics.* Electrophoresis, 2019. **40**(18-19),2309-2320.
33. Mayboroda, O.A., et al., *Amino acid profiling in urine by capillary zone electrophoresis - mass spectrometry.* J Chromatogr A, 2007. **1159**(1-2),149-53.
34. Kawai, T., *Recent Studies on Online Sample Preconcentration Methods in Capillary Electrophoresis Coupled with Mass Spectrometry.* Chromatography, 2017. **38**(1),1-8.
35. Hempel, G., *Strategies to improve the sensitivity in capillary electrophoresis for the analysis of drugs in biological fluids.* Electrophoresis, 2000. **21**(4),691-8.
36. Tomlinson, A.J., N.A. Guzman, and S. Naylor, *Enhancement of concentration limits of detection in CE and CE-MS: a review of on-line sample extraction, cleanup, analyte preconcentration, and microreactor technology.* J Capillary Electrophor, 1995. **2**(6),247-66.
37. Mala, Z., et al., *Contemporary sample stacking in analytical electrophoresis.* Electrophoresis, 2015. **36**(1),15-35.
38. Hirayama, A., et al., *Development of a sheathless CE-ESI-MS interface.* Electrophoresis, 2018. **39**(11),1382-1389.
39. Kawai, T., et al., *Ultrasensitive Single Cell Metabolomics by Capillary Electrophoresis-Mass Spectrometry with a Thin-Walled Tapered Emitter and Large-Volume Dual Sample Preconcentration.* Anal Chem, 2019. **91**(16),10564-10572.

40. Moini, M., *Simplifying CE-MS operation. 2. Interfacing low-flow separation techniques to mass spectrometry using a porous tip.* Anal Chem, 2007. **79**(11),4241-6.
41. Hocker, O., C. Montealegre, and C. Neususs, *Characterization of a nanoflow sheath liquid interface and comparison to a sheath liquid and a sheathless porous-tip interface for CE-ESI-MS in positive and negative ionization.* Anal Bioanal Chem, 2018. **410**(21),5265-5275.
42. Nguyen, T.T., N.J. Petersen, and K.D. Rand, *A simple sheathless CE-MS interface with a sub-micrometer electrical contact fracture for sensitive analysis of peptide and protein samples.* Anal Chim Acta, 2016. **936**,157-67.
43. Gulersonmez, M.C., et al., *Sheathless capillary electrophoresis-mass spectrometry for anionic metabolic profiling.* Electrophoresis, 2016. **37**(7-8),1007-14.
44. Sanchez-Lopez, E., et al., *Sheathless CE-MS based metabolic profiling of kidney tissue section samples from a mouse model of Polycystic Kidney Disease.* Sci Rep, 2019. **9**(1),806.
45. Ramautar, R., et al., *Metabolic profiling of mouse cerebrospinal fluid by sheathless CE-MS.* Anal Bioanal Chem, 2012. **404**(10),2895-900.
46. Shyti, R., et al., *Plasma metabolic profiling after cortical spreading depression in a transgenic mouse model of hemiplegic migraine by capillary electrophoresis--mass spectrometry.* Mol Biosyst, 2015. **11**(5),1462-71.
47. Schmidt, F. and T. Efferth, *Tumor Heterogeneity, Single-Cell Sequencing, and Drug Resistance.* Pharmaceuticals (Basel), 2016. **9**(2).
48. Sasaki, N. and H. Clevers, *Studying cellular heterogeneity and drug sensitivity in colorectal cancer using organoid technology.* Current Opinion in Genetics & Development, 2018. **52**,117-122.
49. Gulersonmez, M.C., et al., *Sheathless capillary electrophoresis-mass spectrometry for anionic metabolic profiling.* Electrophoresis, 2016. **37**(7-8),1007-1014.
50. Harada, S., et al., *Reliability of plasma polar metabolite concentrations in a large-scale cohort study using capillary electrophoresis-mass spectrometry.* Plos One, 2018. **13**(1).
51. Kuehnbaum, N.L., A. Kormendi, and P. Britz-McKibbin, *Multisegment injection-capillary electrophoresis-mass spectrometry: a high-throughput platform for metabolomics with high data fidelity.* Anal Chem, 2013. **85**(22),10664-9.
52. Soga, T., et al., *Quantitative metabolome analysis using capillary electrophoresis mass spectrometry.* Journal of Proteome Research, 2003. **2**(5),488-494.
53. Krylov, S.N. and N.J. Dovichi, *Single-cell analysis using capillary electrophoresis: Influence of surface support properties on cell injection into the capillary.* Electrophoresis, 2000. **21**(4),767-773.
54. Fujii, T., et al., *Direct metabolomics for plant cells by live single-cell mass spectrometry.* Nature Protocols, 2015. **10**(9),1445-1456.
55. Tsuyama, N., et al., *Live single-cell molecular analysis by video-mass spectrometry.* Anal Sci, 2008. **24**(5),559-61.

Chapter 2

Next-generation capillary electrophoresis–mass spectrometry approaches in metabolomics

Based on

Wei Zhang, Thomas Hankemeier, and Rawi Ramautar

Next-generation capillary electrophoresis–mass spectrometry approaches in metabolomics

Current opinion in biotechnology 43 (2017): 1-7

Abstract

Capillary electrophoresis-mass spectrometry has shown considerable potential for profiling polar ionogenic compounds in metabolomics. Hyphenation of capillary electrophoresis to mass spectrometry is generally performed via a sheath-liquid interface. However, the electrophoretic effluent is significantly diluted in this configuration thereby limiting the utility of this method for highly sensitive metabolomics studies. Moreover, in this set-up the intrinsically low-flow property of capillary electrophoresis is not effectively utilized in combination with electrospray ionization. Here, advancements that significantly improved the performance of capillary electrophoresis-mass spectrometry are considered, with a special emphasis on the sheathless porous tip interface. Attention is also devoted to various technical aspects that still need to be addressed to make capillary electrophoresis-mass spectrometry a robust approach for probing the polar metabolome.

Introduction

The major and ultimate aim of metabolomics is to obtain an answer to a specific biological or clinical question [1]. For this purpose, advanced analytical separation techniques are generally used for the global profiling of endogenous metabolites in biological samples [2]. Currently, the profiling of endogenous metabolites is commonly performed with mass spectrometry (MS) in combination with an on-line front-end chromatographic separation method [3, 4]. Despite significant developments in liquid chromatography column technology and methodology, such as hydrophilic interaction liquid chromatography, the selective and efficient analysis of highly polar and charged metabolites is still highly challenging. Capillary zone electrophoresis, referred to here as CE instead of CZE, separates compounds on the basis of differences in their intrinsic electrophoretic mobility, which is dependent on the charge and size of the analyte, in a capillary filled with separation buffer only under the influence of an electric field. Therefore, CE is highly suited for the analysis of polar ionogenic metabolites. Moreover, as the separation mechanism of CE is fundamentally different from chromatographic-based separation techniques, a complementary view on the composition of metabolites present in a given biological sample is provided. In comparison to chromatographic-based methods the separation efficiency of CE is very high as there is no mass transfer between phases. Actually, under ideal conditions the only source of band broadening in CE is from longitudinal diffusion.

A critical need for metabolomics is also the introduction of analytical methods allowing metabolic profiling of those samples for which the amount is severely limited [5]. CE-MS can be considered an attractive microscale analytical platform for this purpose, as in CE nanoliter injection volumes are employed from (sub-)microliter sample amounts. Therefore, CE-MS is highly suited for the analysis of polar ionogenic metabolites in ultra-small biological samples, as has been recently demonstrated for the analysis of cerebrospinal fluid of mice and extracts from small tissues or a single cell [6-8].

At present, the use of CE-MS for metabolomics studies is disproportionately low in comparison to other analytical separation techniques [2]. The scientific community still perceives CE-MS as a technically challenging approach suffering from a relatively poor reproducibility and sensitivity [9]. An important reason for this perception is lack of expertise with this technology. In this context, it is of interest to note that CE-MS has been used for the global profiling of native peptides and endogenous metabolites in a clinical context for more than a decade now [10-13]. For example, Mischak and co-workers have analyzed peptides in more than 20,000 human urine samples at different laboratories with an acceptable inter-laboratory reproducibility [10, 14].

Over the past few years, various novel CE-MS approaches have been developed which show a strong potential for improving the sensitivity/metabolic coverage and sample throughput in metabolomics. In this paper, attention will be paid to advancements that significantly improved

the analytical performance, particularly with regard to improving the metabolic coverage, of CE-MS for metabolomics studies. Analytical aspects that still need to be addressed to make CE-MS a viable approach in the metabolomics field are also discussed. Strategies to improve the stability of CE-MS in terms of migration times, data pre-processing aspects, procedures for the identification of metabolites and preconcentration techniques to improve the loadability of CE are not covered in this paper. The reader is referred to more dedicated literature for an overview concerning these topics [15-21].

Interfacing techniques for seamless integration of CE and ESI-MS

CE is fundamentally a low flow nanoscale separation technique reaching its optimal separation performance at very low flow-rates, which is typically in the range of 20 to 100 nL/min depending on the pH of the separation buffer when using a bare fused-silica capillary. Actually, a high separation resolution is obtained in CE by solely separating the compounds on the basis of their electrophoretic mobilities, i.e. under (near-)zero electro-osmotic flow conditions. The intrinsically low flow-rates of CE are also advantageous from a viewpoint of the ESI mechanism. In ESI, smaller droplets are generated under low-flow separation conditions, which results in a more efficient desolvation and an improved transfer of ions to the MS [22-24]. Moreover, at very low flow-rates (≤20 nL/min) ion suppression is significantly reduced resulting in an improved concentration sensitivity [22], which is important for in-depth metabolic profiling studies.

In a standard CE set-up both ends of the separation capillary are immersed in buffer vials to which electrodes are added to provide a high voltage gradient. To couple CE to MS, the outlet vial must be replaced by an interface to close the electrical circuit and which provides contact with the ESI stream. Therefore, a CE-MS interface needs to apply voltage to the capillary outlet while maintaining independent CE and ESI electrical circuits. A co-axial solvent delivery as a terminal electrolyte reservoir (i.e., a sheath-liquid interface) and various other interfacing techniques have been subsequently developed to enable the hyphenation of CE to MS. So far, most CE-MS-based metabolomics studies have been performed with a sheath-liquid interface [13, 25-30]. CE-MS approaches utilizing a sheath-liquid interface for global metabolic profiling studies were first developed by Soga and co-workers [12, 31]. The sheath-liquid interface, originally developed by Smith and co-workers [32], has been used for a broad range of bio-analytical applications with acceptable analytical figures of merit. However, the sheath-liquid is generally provided at a flow-rate between 5 to 10 μL/min, thereby significantly diluting the CE effluent resulting in compromised detection sensitivities for metabolomics applications. Still, an important advantage of the sheath-liquid interface is that the composition of the sheath-liquid can be tuned to modify the ionization efficiency without affecting CE selectivity and efficiency. For example, to improve the detection sensitivity, supplementation of the sheath-liquid with modifiers has been investigated [33]. Enhanced supercharging of analytes in ESI-MS has also been explored by adding various supercharging agents to the sheath-liquid [34]. The effect of these agents on metabolic

profiling studies by CE-MS needs to be studied. Overall, considering the fact that both CE and ESI-MS perform most optimally at low flow-rate conditions, the coupling of CE to MS should preferably be carried out via an interfacing technique which effectively utilizes the inherently low flow separation property of CE and the improved ESI efficiency under these conditions.

Currently, the design of new interfacing techniques for CE-MS and assessing their potential for proteomics and metabolomics studies is an active area of research [35-41]. New methods that abolish or minimize the usage of a sheath-liquid have been introduced to the market or are on the verge of being commercialized. In this context, three interfacing designs have been evaluated in detail for a wide range of bio-analytical studies, i.e. the flow-through microvial interface, the sheathless porous tip interface and the electrokinetic-based sheath-liquid interface [42-44]. Concerning metabolomics, thus far the most promising results have been obtained by the sheathless porous tip interface (**Fig. 1**), which was developed by Moini [43]. In this design, the porous tip interface was created by removing the polyimide coating of the capillary outlet and etching the capillary wall with 49% solution of hydrofluoric acid to a thickness of about 5 µm. The etched conductor was inserted into an ESI needle which was filled with separation buffer. Redox reactions of water at the ESI needle and transport of these small ions through the porous tip into the capillary provides the electrical connection for the ESI and for the CE outlet electrode. The sheathless porous tip design is especially useful for interfacing narrow (<30 µm id) capillaries and for low flow-rate (<20-30 nL/min) nano-ESI-MS analyses [45].

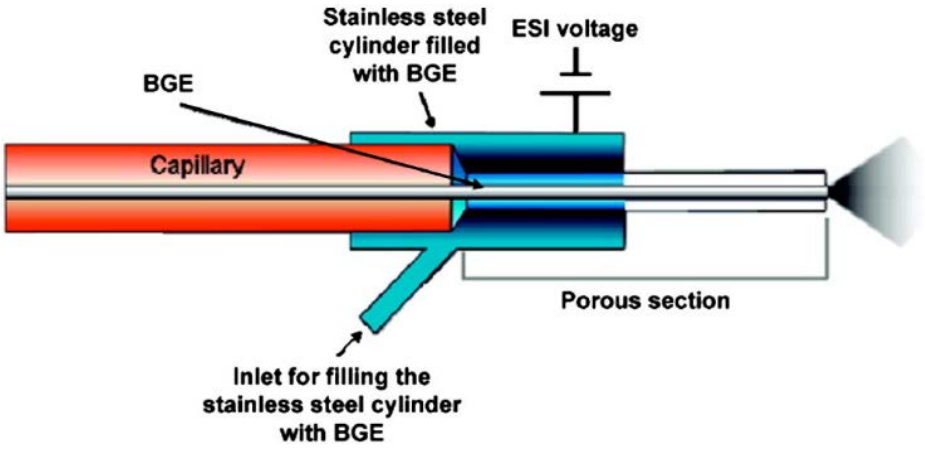

Figure 1. Design of the sheathless porous tip interface. A scheme of the porous tip interface, originally developed by Moini, is depicted. *Source*: Reproduced from ref. [43] with permission.

Enhancing the coverage of the polar metabolome

The performance of CE-MS utilizing a sheathless porous tip interface has been evaluated for the profiling of cationic metabolites in human urine (1:1 dilution with separation buffer) at low-pH separation conditions resulting in an information-rich metabolic profile [46]. The use of the sheathless interface enhanced the concentration sensitivity by over two orders of magnitude

while maintaining high separation efficiency relative to the use of a sheath-liquid interface. This approach allowed for an improved coverage of the urinary metabolome with nanomolar detection limits for a broad range of polar ionogenic metabolites (**Fig. 2**). Approximately 900 molecular features were detected with sheathless CE-MS, whereas 300 were found with sheath-liquid CE-MS. The enhanced sensitivity resulted in the detection of many compounds, including many low abundance ions above *m/z* 300, such as small peptides. Hirayama and co-workers also assessed the performance of this approach for urinary metabolomics and found a tenfold increase in the number of detected peaks compared with conventional CE-MS methods [47]. Though a single sheathless porous tip capillary could be used for more than 180 successive runs of a tenfold-diluted human urine sample, the long-term performance of this new CE-MS interface still needs to be assessed in more extended studies analyzing large numbers of diverse clinical samples.

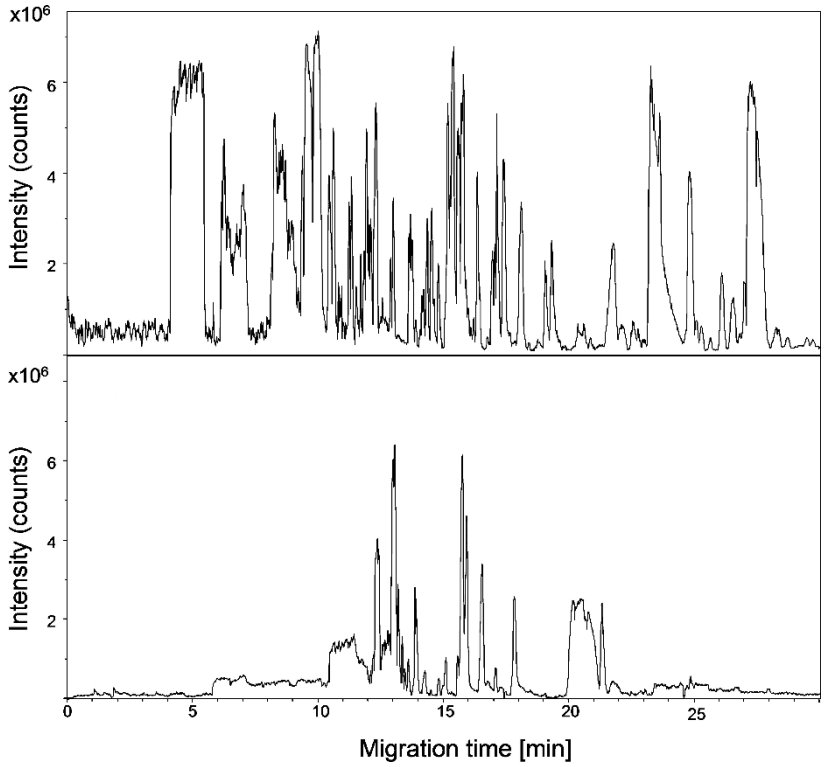

Figure 2. Comparison of sheathless and sheath–liquid CE–MS for metabolic profiling of human urine. (Top) Base peak electropherogram (*m/z* 50–450) of human urine obtained with sheathless CE-MS using a porous tip sprayer. Conditions: separation buffer, 10% acetic acid (pH 2.2); sample injection, 2.0 psi for 30 s (1% of capillary volume). (Bottom) Base peak electropherogram (*m/z* 50–450) of human urine obtained with CE–MS using a sheath–liquid interface. Conditions: separation buffer, 10% acetic acid (pH 2.2); sample injection, 0.5 psi for 30 s (1% of capillary volume).
Source: Reproduced from ref. [46] with permission.

Sheath-liquid CE-MS approaches for anionic metabolic profiling used in reversed polarity CE mode lack robustness due to oxidation and corrosion of the stainless steel ESI spray needle under these conditions, unless a platinum ESI needle is used [48]. Recently, the utility of the sheathless porous tip interface was examined for the profiling of anionic metabolites in biological samples [49], using exactly the same separation conditions as used for the profiling of cationic metabolites,

only the MS detection and CE separation voltage polarity were switched/reversed. A broad range of anionic metabolite classes could be profiled under these conditions, including sugar phosphates, nucleotides and organic acids, as shown in **Figure 3**. An injection volume of about 20 nL resulted in nanomolar detection limits, which corresponded to a significant enhancement as compared to the micromolar detection limits typically obtained with classical sheath-liquid CE-MS methods. Structural isomers of phosphorylated sugars as well as isobaric metabolites could be selectively analyzed by the proposed sheathless CE-MS method without using any derivatization. A front-end (partially) separation of these compounds is key in order to allow selective detection by MS. The methodology was applied to anionic metabolic profiling of glioblastoma cell line extracts. The low-pH separation buffer used for anionic metabolic profiling may not be the most optimal for achieving a baseline separation of structurally related sugar phosphates. Also important is that only anionic metabolites can be analyzed which are (partially) negatively charged under the used separation conditions. Still, the proposed single sheathless CE-MS approach can be used for the analysis of a wide range of highly polar anionic and cationic metabolites, thereby showing potential for global metabolic profiling studies.

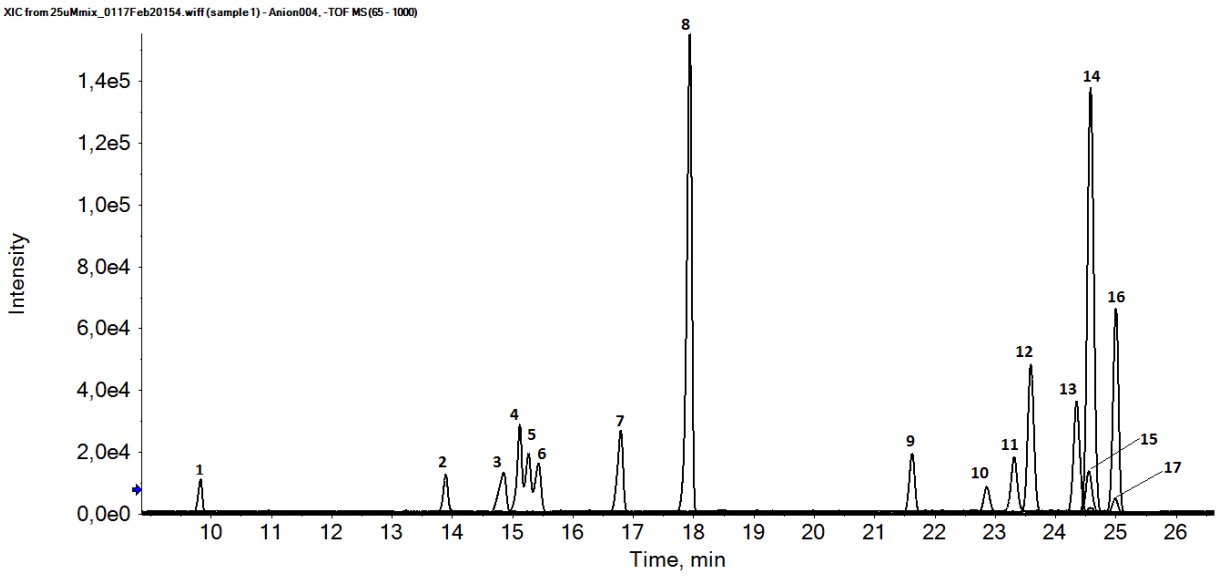

Figure 3. Performance of CE–MS using a sheathless porous tip sprayer for anionic metabolic profiling. Multiple extracted ion electropherograms for the metabolite test mixture (25 µM) obtained with sheathless CE–MS in negative ion mode using a porous tip sprayer. Peaks: 1, 2-naphtol-3,6-disulfonic acid; 2, d(+)2-phosphoglyceric acid; 3, d-ribose-5-phosphate; 4, d-glucose-1-phosphate; 5, d-glucose-6-phosphate; 6, d-fructose-6-phosphate; 7, inosine 5′-monophosphate (IMP); 8, guanosine 3′,5′-cyclic monophosphate (cGMP); 9, guanosine 5′-monophosphate; 10, citric acid; 11, trimesic acid; 12, isocitric acid; 13, gluconic acid; 14, adenosine 3′,5′-cyclic monophosphate (cAMP); 15, 2-hydroxybutyric acid; 16, b-diphosphopyridine nucleotide (NAD+); 17, 3-hydroxybutyric acid. Experimental conditions: separation buffer, 10% acetic acid (pH 2.2); separation voltage, −30 kV (+0.5 psi applied at the inlet of the CE capillary); sample injection, 2.0 psi for 60 s. *Source*: Reproduced from ref. [49] with permission.

Multi-segment injection for enhancing sample throughput

Clinical metabolomics studies require high-throughput analytical technologies. Currently, the flexibility of using shorter capillary lengths with the commercially available sheathless porous tip interface emitters is limited, i.e. the dimensions of the porous tip capillary emitter are fixed (length is 90 cm and inner diameter is 30 µm). In this context, the multi-segment injection approach developed for CE-MS-based metabolomics studies by Kuehnbaum et al. may be used in sheathless CE-MS to enable high-throughput metabolic profiling of clinical samples [50]. Multi-segment injection can be considered a multiplexing technique in which multiple samples are injected into the capillary prior to applying the separation voltage. Each sample is injected followed by the injection of a short plug of separation buffer which provides a differentiating gap between samples during the injection process.

Careful optimization of the multi-segment injection process is critical in order to minimize overlap of the same metabolite peak from different sample injections during the electrophoretic separation. For example, the injection of too short separation buffer plugs between sample plugs may result in loss in resolution of metabolites and their isomers between adjacent sample plugs. The use of multi-segment injection in sheath-liquid CE-MS increased sample throughput up to one order of magnitude, thereby maintaining the separation of structurally similar metabolites without ion suppression (**Fig. 4**). Overall, an acceptable precision was obtained for the quantification of various cationic metabolites in human plasma filtrates (RSD ≈ 10%, n = 70).

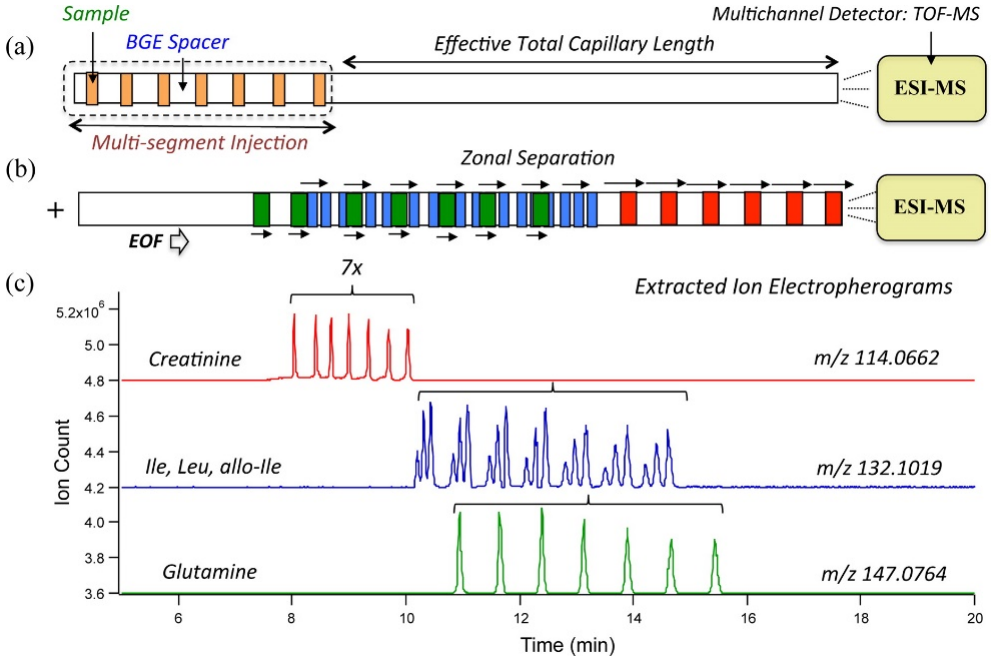

Figure 4. Multi-segment injection in CE–MS. (a) Multiplexed separation based on serial injection of seven discrete sample segments within a single capillary by multi-segment injection CE–MS; (b) ions migrate as a series of zones in free solution before ionization; (c) the procedure enables reliable quantification of polar metabolites and their isomers in different samples as ionization occurs within a short-time interval (≈2–6 min) under steady-state conditions when using ESI–MS. *Source*: Reproduced from ref. [50] with permission.

Concluding remarks

New CE-MS approaches have been developed for metabolomics showing improved analytical performances as compared to conventional CE-MS methods over the past few years. Here, the potential of CE-MS using a sheathless porous tip sprayer for the analysis of highly polar and charged metabolites has been highlighted. Though exquisite concentration sensitivities can be obtained with this approach, the next important step is to show its utility for large-scale clinical metabolomics studies. Such data are crucial to endorse the sheathless CE-MS method as a potential diagnostic tool. Sheathless CE-MS provides low nanomolar detection limits for a wide range of polar metabolite classes by only using an injection volume of 20 nL (or less) from a few microliters of sample in the vial. Therefore, this approach can be considered a highly attractive and unique analytical tool for probing the polar metabolome in ultra-small biological samples.

The use of an effective interfacing technique for CE-MS should preferably be used in conjunction with an effective injection strategy which allows the selective transfer of target analytes into the CE system. Pre-analytics and injection are especially important for metabolic profiling of low-abundance metabolites in ultra-small biological samples. An efficient and selective transfer of ions into the separation capillary will significantly increase the durability of a single sheathless porous tip emitter, which at this stage can only be used for the analysis of up to 200 samples, and which may increase the overall sensitivity even further if a larger portion of the sample is injected. Further developments in this field will result in a viable CE-MS approach for probing the polar metabolome.

Acknowledgements

Rawi Ramautar would like to acknowledge the financial support of the Veni grant scheme of the Netherlands Organization of Scientific Research (NWO Veni 722.013.008). Wei Zhang would like to acknowledge the Chinese Scholarship Council (CSC, No. 201507060011). We would like to express our gratitude to Christian Ramakers for the creation of the graphical abstract. The graphical abstract is a modified version of a design originally developed by Sciex.

References

1. Ramautar, R., et al., *Human metabolomics: strategies to understand biology.* Curr Opin Chem Biol, 2013. **17**(5),841-6.
2. Kuehnbaum, N.L. and P. Britz-McKibbin, *New advances in separation science for metabolomics: resolving chemical diversity in a post-genomic era.* Chemical reviews, 2013. **113**(4),2437-68.
3. Gika, H.G., et al., *Current practice of liquid chromatography-mass spectrometry in metabolomics and metabonomics.* Journal of pharmaceutical and biomedical analysis, 2014. **87**,12-25.

4. Ramautar, R. and G.J. de Jong, *Recent developments in liquid-phase separation techniques for metabolomics.* Bioanalysis, 2014. **6**(7),1011-26.
5. Nevedomskaya, E., et al., *CE-MS for metabolic profiling of volume-limited urine samples: application to accelerated aging TTD mice.* Journal of proteome research, 2010. **9**(9),4869-74.
6. Ramautar, R., et al., *Metabolic profiling of mouse cerebrospinal fluid by sheathless CE-MS.* Analytical and bioanalytical chemistry, 2012. **404**(10),2895-900.
7. Liu, J.X., et al., *Analysis of endogenous nucleotides by single cell capillary electrophoresis-mass spectrometry.* The Analyst, 2014. **139**(22),5835-42.
8. Knolhoff, A.M., et al., *Combining small-volume metabolomic and transcriptomic approaches for assessing brain chemistry.* Analytical chemistry, 2013. **85**(6),3136-43.
9. Ramautar, R., *CE-MS in metabolomics: status quo and the way forward.* Bioanalysis, 2016. **8**(5),371-4.
10. Pontillo, C., et al., *CE-MS-based proteomics in biomarker discovery and clinical application.* Proteomics. Clinical applications, 2015. **9**(3-4),322-34.
11. Pejchinovski, M., et al., *Capillary zone electrophoresis on-line coupled to mass spectrometry: A perspective application for clinical proteomics.* Proteomics. Clinical applications, 2015. **9**(5-6),453-68.
12. Soga, T., et al., *Quantitative metabolome analysis using capillary electrophoresis mass spectrometry.* Journal of proteome research, 2003. **2**(5),488-94.
13. Hirayama, A., M. Wakayama, and T. Soga, *Metabolome analysis based on capillary electrophoresis-mass spectrometry.* Trac-Trends in Analytical Chemistry, 2014. **61**,215-222.
14. Klein, J., et al., *The role of urinary peptidomics in kidney disease research.* Kidney international, 2016. **89**(3),539-45.
15. Huhn, C., et al., *Relevance and use of capillary coatings in capillary electrophoresis-mass spectrometry.* Analytical and bioanalytical chemistry, 2010. **396**(1),297-314.
16. Nevedomskaya, E., et al., *Alignment of capillary electrophoresis-mass spectrometry datasets using accurate mass information.* Analytical and bioanalytical chemistry, 2009. **395**(8),2527-33.
17. Sugimoto, M., et al., *Prediction of metabolite identity from accurate mass, migration time prediction and isotopic pattern information in CE-TOFMS data.* Electrophoresis, 2010. **31**(14),2311-8.
18. Sugimoto, M., et al., *Differential metabolomics software for capillary electrophoresis-mass spectrometry data analysis.* Metabolomics : Official journal of the Metabolomic Society, 2010. **6**(1),27-41.
19. Barbas, C., E.P. Moraes, and A. Villasenor, *Capillary electrophoresis as a metabolomics tool for non-targeted fingerprinting of biological samples.* Journal of pharmaceutical and biomedical analysis, 2011. **55**(4),823-31.
20. Breadmore, M.C., et al., *Recent advances in enhancing the sensitivity of electrophoresis and electrochromatography in capillaries and microchips (2012-2014).* Electrophoresis, 2015. **36**(1),36-61.
21. Ramautar, R., G.W. Somsen, and G.J. de Jong, *Developments in coupled solid-phase extraction-capillary electrophoresis 2013-2015.* Electrophoresis, 2016. **37**(1),35-44.
22. Schmidt, A., M. Karas, and T. Dulcks, *Effect of different solution flow rates on analyte ion signals in nano-ESI MS, or: when does ESI turn into nano-ESI?* Journal of the American Society for Mass Spectrometry, 2003. **14**(5),492-500.
23. Wilm, M. and M. Mann, *Analytical properties of the nanoelectrospray ion source.* Analytical chemistry, 1996. **68**(1),1-8.
24. Valaskovic, G.A., N.L. Kelleher, and F.W. McLafferty, *Attomole protein characterization by capillary electrophoresis-mass spectrometry.* Science, 1996. **273**(5279),1199-202.
25. Ramautar, R., G.W. Somsen, and G.J. de Jong, *The Role of CE–MS in Metabolomics*, in *Metabolomics in Practice*. 2013, Wiley-VCH Verlag GmbH & Co. KGaA. p. 177-208.

26. Ramautar, R., G.W. Somsen, and G.J. de Jong, *CE-MS for metabolomics: developments and applications in the period 2012-2014.* Electrophoresis, 2015. **36**(1),212-24.
27. Ramautar, R., *Capillary Electrophoresis-Mass Spectrometry for Clinical Metabolomics.* Advances in clinical chemistry, 2016. **74**,1-34.
28. Wakayama, M., A. Hirayama, and T. Soga, *Capillary electrophoresis-mass spectrometry.* Methods in molecular biology, 2015. **1277**,113-22.
29. Wang, X., et al., *Capillary electrophoresis-mass spectrometry in metabolomics: the potential for driving drug discovery and development.* Current drug metabolism, 2013. **14**(7),807-13.
30. Bonvin, G., J. Schappler, and S. Rudaz, *Capillary electrophoresis-electrospray ionization-mass spectrometry interfaces: fundamental concepts and technical developments.* Journal of chromatography. A, 2012. **1267**,17-31.
31. Soga, T., et al., *Simultaneous determination of anionic intermediates for Bacillus subtilis metabolic pathways by capillary electrophoresis electrospray ionization mass spectrometry.* Analytical chemistry, 2002. **74**(10),2233-9.
32. Smith, R.D., C.J. Barinaga, and H.R. Udseth, *Improved electrospray ionization interface for capillary zone electrophoresis-mass spectrometry.* Analytical chemistry, 1988. **60**(18),1948-1952.
33. Causon, T.J., et al., *Addition of reagents to the sheath liquid: a novel concept in capillary electrophoresis-mass spectrometry.* Journal of chromatography. A, 2014. **1343**,182-7.
34. Bonvin, G., S. Rudaz, and J. Schappler, *In-spray supercharging of intact proteins by capillary electrophoresis-electrospray ionization-mass spectrometry using sheath liquid interface.* Analytica chimica acta, 2014. **813**,97-105.
35. Lindenburg, P.W., et al., *Developments in Interfacing Designs for CE-MS: Towards Enabling Tools for Proteomics and Metabolomics.* Chromatographia, 2015. **78**(5-6),367-377.
36. Heemskerk, A.A., A.M. Deelder, and O.A. Mayboroda, *CE-ESI-MS for bottom-up proteomics: Advances in separation, interfacing and applications.* Mass spectrometry reviews, 2016. **35**(2),259-71.
37. Sun, L., et al., *Third-generation electrokinetically pumped sheath-flow nanospray interface with improved stability and sensitivity for automated capillary zone electrophoresis-mass spectrometry analysis of complex proteome digests.* Journal of proteome research, 2015. **14**(5),2312-21.
38. Guo, X., et al., *Capillary Electrophoresis-Nanoelectrospray Ionization-Selected Reaction Monitoring Mass Spectrometry via a True Sheathless Metal-Coated Emitter Interface for Robust and High-Sensitivity Sample Quantification.* Analytical chemistry, 2016. **88**(8),4418-25.
39. Wang, C., et al., *Capillary isotachophoresis-nanoelectrospray ionization-selected reaction monitoring MS via a novel sheathless interface for high sensitivity sample quantification.* Analytical chemistry, 2013. **85**(15),7308-15.
40. Tycova, A., J. Prikryl, and F. Foret, *Reproducible preparation of nanospray tips for capillary electrophoresis coupled to mass spectrometry using 3D printed grinding device.* Electrophoresis, 2016. **37**(7-8),924-30.
41. Gonzalez-Ruiz, V., et al., *Evaluation of a new low sheath-flow interface for CE-MS.* Electrophoresis, 2016. **37**(7-8),936-46.
42. Maxwell, E.J., et al., *Decoupling CE and ESI for a more robust interface with MS.* Electrophoresis, 2010. **31**(7),1130-7.
43. Moini, M., *Simplifying CE-MS operation. 2. Interfacing low-flow separation techniques to mass spectrometry using a porous tip.* Analytical chemistry, 2007. **79**(11),4241-6.
44. Wojcik, R., et al., *Simplified capillary electrophoresis nanospray sheath-flow interface for high efficiency and sensitive peptide analysis.* Rapid communications in mass spectrometry : RCM, 2010. **24**(17),2554-60.
45. Busnel, J.M., et al., *High capacity capillary electrophoresis-electrospray ionization mass spectrometry: coupling a porous sheathless interface with transient-isotachophoresis.* Analytical chemistry, 2010. **82**(22),9476-83.

46. Ramautar, R., et al., *Enhancing the coverage of the urinary metabolome by sheathless capillary electrophoresis-mass spectrometry.* Analytical chemistry, 2012. **84**(2),885-92.
47. Hirayama, A., M. Tomita, and T. Soga, *Sheathless capillary electrophoresis-mass spectrometry with a high-sensitivity porous sprayer for cationic metabolome analysis.* The Analyst, 2012. **137**(21),5026-33.
48. Soga, T., et al., *Metabolomic profiling of anionic metabolites by capillary electrophoresis mass spectrometry.* Analytical chemistry, 2009. **81**(15),6165-74.
49. Gulersonmez, C., et al., *Sheathless capillary electrophoresis-mass spectrometry for anionic metabolic profiling.* Electrophoresis, 2015.
50. Kuehnbaum, N.L., A. Kormendi, and P. Britz-McKibbin, *Multisegment injection-capillary electrophoresis-mass spectrometry: a high-throughput platform for metabolomics with high data fidelity.* Analytical chemistry, 2013. **85**(22),10664-9.

Chapter 3

Part 1. Sheathless Capillary Electrophoresis–Mass Spectrometry for Metabolic Profiling of Biological Samples

Based on

Wei Zhang, Mehmet Can Gulersonmez, Thomas Hankemeier, and Rawi Ramautar

Sheathless Capillary Electrophoresis–Mass Spectrometry for Metabolic Profiling of Biological Samples

JoVE (Journal of Visualized Experiments) 116 (2016): e54535

Abstract

In metabolomics, a wide range of analytical techniques is used for the global profiling of (endogenous) metabolites in complex samples. In this paper, a protocol is presented for the analysis of anionic and cationic metabolites in biological samples by capillary electrophoresis–mass spectrometry (CE-MS). CE is well-suited for the analysis of highly polar and charged metabolites as compounds are separated on the basis of their charge-to-size ratio. A recently developed sheathless interfacing design, *i.e.,* a porous tip interface, is used for coupling CE to electrospray ionization (ESI) MS. This interfacing approach allows the effective use of the intrinsically low-flow property of CE in combination with MS, resulting in nanomolar detection limits for a broad range of polar metabolite classes. The protocol presented here is based on employing a bare fused-silica capillary with a porous tip emitter at low-pH separation conditions for the analysis of a broad array of metabolite classes in biological samples. It is demonstrated that the same sheathless CE-MS method can be used for the profiling of cationic metabolites, including amino acids, nucleosides and small peptides, or anionic metabolites, including sugar phosphates, nucleotides and organic acids, by only switching the MS detection and separation voltage polarity. Highly information-rich metabolic profiles in various biological samples, such as urine, cerebrospinal fluid and extracts of the glioblastoma cell line, can be obtained by this protocol in less than 1 hour of CE-MS analysis.

Introduction

In contemporary metabolomics, high-end analytical separation techniques are used to analyze a wide range of metabolite classes in order to obtain a representative read-out of the physiological status of an organism [1]. The ultimate objective of a metabolomics study is to obtain an answer to a given biological/clinical question. At present, the Human Metabolome Database is comprised of more than 40000 metabolite entries representing both endogenous and exogenous compounds (the latter originating from nutrients, microbiota, drugs and other sources) [2]. Given the huge diversity in physico-chemical properties and concentration range of these metabolites, multiple analytical techniques with different separation mechanisms should be used in conjunction in order to profile as many metabolites as possible in a given biological sample. For example, Psychogios *et al.* used a combination of five analytical separation techniques for metabolic profiling of human serum resulting in the detection of more than 4000 chemically diverse metabolites [3].

In this paper, attention will be paid to recently developed CE-MS strategies for metabolic profiling of biological samples [4, 5]. In CE, more specifically capillary zone electrophoresis (CZE; normally referred as CE), compounds are separated on the basis of their charge-to-size ratio and, therefore, this analytical technique is highly suited for the analysis of polar and charged metabolites. The separation mechanism of CE is fundamentally different from chromatographic-based techniques, thereby providing a complementary view on the metabolic composition of biological samples [6-8]. Soga and co-workers were the first to show the utility of CE-MS for the global profiling of metabolites in biological samples [9, 10]. Until now, the feasibility and usefulness of CE–MS for metabolomics has been widely demonstrated [11-15]. CE is generally coupled to MS via a sheath-liquid interfacing technique [16, 17]; however, due to dilution of the capillary effluent by the sheath-liquid, the detection sensitivity is intrinsically compromised.

Recently, it was demonstrated that the use of a sheathless interface significantly improved the detection coverage of metabolites present in various biological samples as compared to CE-MS utilizing a classical sheath-liquid interface [5, 18, 19]. For example, about 900 molecular features were detected in human urine by sheathless CE-MS whereas about 300 molecular features were observed with sheath-liquid CE-MS [5]. The sheathless interface used was based on a porous tip emitter, which was invented by Moini [20], allowing the effective use of the intrinsically low-flow property of CE in combination with nano–ESI-MS.

In order to stimulate the use of sheathless CE-MS in the field of metabolomics, a protocol is presented describing how this approach can be used for the analysis of highly polar metabolites in biological samples, as exemplified for the analysis of extracts from the glioblastoma cell line. It is shown that the sheathless CE-MS method for the profiling of cationic metabolites can also be used for the profiling of anionic metabolites using exactly the same capillary and separation

conditions, thereby reducing analysis time and providing one single analytical platform for the global profiling of charged metabolites. The protocol also describes a strategy for the effective alignment of the sheathless porous tip emitter with the MS instrument.

Protocol

NOTE: The protocol described here for the use of sheathless CE-MS for metabolic profiling studies is for laboratory use only. The procedures outlined below are based on recently published work [4, 5]. Further experimental details can be found in these papers. Prior to using this protocol, consult all relevant material safety data sheets (MSDS). Please use all appropriate laboratory safety procedures, including safety glasses, lab coat and gloves, when conducting the experiments outlined in this protocol.

1. Preparation of Reagents Solutions and Samples

1. Preparation of the background electrolyte (BGE)

1. Prepare a new BGE solution (10% (v/v) acetic acid, pH 2.2) every day.
2. Add 9.0 ml of water into a 10 ml glass vial and add 1.0 ml of acetic acid to the water in a fume hood. Mix the solution thoroughly using a vortex mixer.

2. Preparation of metabolite standard mixture

1. Dissolve 50 µl of a 50 µM cation standard mixture containing 60 cationic metabolites into 50 µl of water and mix the solution thoroughly. Store at -80 °C when not in use.
2. Dissolve 50 µl of a 50 µM anion standard mixture containing 30 anionic metabolites into 50 µl of water and mix the solution thoroughly. Store this solution, in aliquots to prevent freeze/thaw cycles of the same standard mixture, at -80 °C when not in use. **NOTE**: The metabolite standard mixtures are stable for 3 months when stored properly at -80 °C.

3. Preparation of extracts from the glioblastoma cell line

1. Wash the adherent human U-87 MG glioblastoma cells three times with 1 ml ice-cold 0.9% sodium chloride solution [21].
2. Add 2 ml ice-cold methanol/water solution (8/2, v/v) to the adherent cells and scrape using a rubber tipped cell scraper [21].
3. Collect the methanol/water solution in a tube and ultrasonicate for 2 min.
4. Add chloroform to the methanol/water fraction (final ratio 8/8/2, v/v/v) and centrifuge the sample for 10 min at 16,100 g and 4 °C.
5. Collect the methanol/water layer and evaporate this fraction using a vacuum concentrator. Reconstitute the dried material in 50 µl water for analysis by sheathless CE-MS. When not in use store the sample at -80 °C.

2. Setting up the Sheathless CE-MS System

1. Installation of the bare fused-silica cartridge with the porous tip emitter

1. Place a new bare fused-silica cartridge with a porous tip emitter (30 μm inner diameter x 90 cm total length) in the CE instrument.
2. Apply a forward rinse at 50 psi for 15 min with the software controlling the CE instrument using 100% methanol and visually check whether liquid is flowing out from the capillary outlet during this rinsing step. Also perform a rinse in the opposite direction at 50 psi for 5 min using the BGE solution to visually examine whether liquid is flowing out from the conductive capillary.
3. Repeat step 2.1.2 at a pressure of 100 psi in case no liquid drop formation has been observed at the capillary outlet. Install a new bare fused-silica cartridge if no liquid drop formation was observed during this step.
4. Rinse the separation capillary with water at 50 psi for 10 min, followed by 0.1 M NaOH at 50 psi for 10 min, then by water at 50 psi for 10 min and finally with BGE at 50 psi for 10 min. **NOTE**: Steps 2.1.1 until 2.1.4 are only required for the installation of a new capillary cartridge.

2. Coupling of the capillary porous tip emitter to ESI-MS

NOTE: Prior to coupling the CE capillary to MS, ensure that the MS instrument has been calibrated and connected to the CE system. Set the ESI voltage to 0. Fit the MS instrument with a nanospray source. Gas 1, gas 2 and interface heater temperature were not applied as ESI at very low flow rates occurs by just applying the ion spray voltage set at 1500 V. Set the curtain gas at 5 psi.

1. Remove the sprayer tip of the fused-silica cartridge from the water tube and install it in the nanospray source adapter for coupling to the MS instrument. Ensure that the height of the BGE vials in the CE instrument matches the height of the sprayer tip.
2. Check for flow of liquid through the conductive capillary by rinsing with BGE at 50 psi for 5 min. During this rinsing step a drop formation at the base of the ESI sprayer needle should be observed.
3. Flush the separation capillary with BGE at 50 psi for 10 min in the forward direction. Drop formation should be observed at the tip of the porous tip emitter (sprayer tip) during this step.
4. Position the porous tip emitter to the entrance of the MS inlet at a distance of about 2 to 3 mm.
5. Apply a voltage of 30 kV using a ramp time of 1 min and start acquiring MS data in the *m/z* range from 65 to 1,000 *m/z* for metabolic profiling studies using first an ESI voltage of 0. **NOTE**: The mass spectrum should be void of signal as there should be no electrospray.

6. Set the ESI voltage to 1,000 V while carry on measuring data. Increase the ESI voltage with increments of 200 V until a constant background signal is observed for at least 15 min.
7. Optimize the porous tip emitter position with respect to the center of the MS inlet by moving it in the x, y, or z-direction in order to see which position provides the maximal and most stable MS signal (total ion electropherogram).
8. After optimizing the position of the porous tip emitter and determining the optimal ESI voltage, set the ESI voltage to 0 V and decrease the CE voltage from 30 kV to 1 kV using a ramp time of 5 min.
9. Create a MS method using the optimal ESI voltage and a CE method on the CE instrument for the analysis of metabolite standards and biological samples.

3. Analysis of Metabolite Standards and Biological Samples

1. Performance evaluation of the sheathless CE-MS system

1. Transfer 20 µl of the anionic metabolite standard mixture into an empty 100 µl microvial (PCR vial) which fits into a CE vial and put this vial in the inlet sample tray. **NOTE:** The minimum volume required in the microvial for a reliable injection is 2 µl.
    1. Start the MS acquisition negative ion mode method created during step 2.2.9 and subsequently start the CE sequence using the software controlling the CE instrument.
    2. Rinse the separation capillary with BGE at 50 psi for 3 min followed by injection at 2.0 psi for 60 sec (20 nL corresponding to 3% of the capillary volume) and then by BGE injection at 1.0 psi for 10 sec. NOTE: Subsequently, MS data acquisition is triggered.
    3. Apply a voltage of -30 kV with a ramp time of 1.0 min with a pressure of 0.5 psi for 30 min at the inlet. After a 30 min electrophoretic separation, stop MS data acquisition and decrease the CE voltage to -1 kV using a ramp time of 5 min (a gradual decrease of the CE voltage after the electrophoretic separation improves the durability of the porous tip capillary emitter).
2. Between sample injections, rinse the capillary with water, 0.1 M sodium hydroxide, water and BGE each at 30 psi for 3 min.
3. Analyze the recorded data by determining the migration times and the signal intensity of the analyzed anionic metabolite mixture.
4. Assess whether the anionic metabolite standards appear in the region between 10 and 28 min.
5. Check whether three structurally related isomers, *i.e.*, D-Glucose-1-phosphate, D-Glucose-6-phosphate and D-Fructose-6-phosphate are partially separated, *i.e.*, the resolution between the first two peaks is about 0.75 and of the last two peaks is about

0.50 (see **Fig. 1**). **NOTE:** A resolution of 1.5 indicates a baseline separation of two adjacent peaks.

6. Repeat steps 3.1.1 and 3.1.2 for the cationic metabolite mixture. Ensure that MS detection is now in positive ion mode and CE voltage is +30 kV.
7. Analyze the recorded data by determining the migration times and the signal intensity of the analyzed cationic metabolite mixture.
8. Assess whether the cationic metabolite standards appear in the region between 8 and 22 min. Check whether isoleucine and leucine are migrating between 15 and 15.5 min and determine if the resolution is about 0.5.

2. Analysis of biological samples

1. Repeat steps 3.1.1 and 3.1.2 for anionic metabolic profiling of the extract of the glioblastoma cell line. **NOTE:** The metabolic content obtained after sample pretreatment corresponds to a cell density of about 20 cells/nL, therefore, a 20 nL injection is the equivalent of 400 cells per analysis.
2. Create an extracted ion electropherogram for the metabolite lactic acid (*m/z* 89.0243) using 5 mDa mass accuracy and check whether the signal intensity is above 100,000 counts.
3. Repeat steps 3.1.1 and 3.1.2 for cationic metabolic profiling of the extract of the glioblastoma cell line. **NOTE:** A highly information-rich total ion electropherogram should be observed for a 20 nL injection in this mode.
4. After the analyses or when not in use, rinse the capillary with water at 50 psi for 15 min and store the inlet part of the capillary in a vial containing water and the porous section (outlet part) in a tube also containing water.

Representative results

The proposed sheathless CE-MS method is capable of providing highly efficient, *i.e.,* plate numbers ranging from 60,000 to 400,000, profiles for anionic and cationic metabolites at nanomolar detection limits using 10% acetic acid (pH 2.2) as BGE. The separation performance of the method for the analysis of highly polar anionic metabolites is demonstrated for three structurally related sugar phosphate isomers (**Fig. 1**). Though a baseline separation was not obtained for these three analytes, a partial separation is sufficient to allow their selective detection by MS as these analytes have the same exact mass. The potential of the sheathless CE-MS method for metabolic profiling of limited number of cells, *i.e.*, a 20 nL injection corresponds to 400 cells (cell density is about 20 cells/nL), is demonstrated for the analysis of cationic metabolites in an extract of the glioblastoma cell line (**Fig. 2**), in which more than 300 molecular features were detected above a S/N ratio ≥ 5.

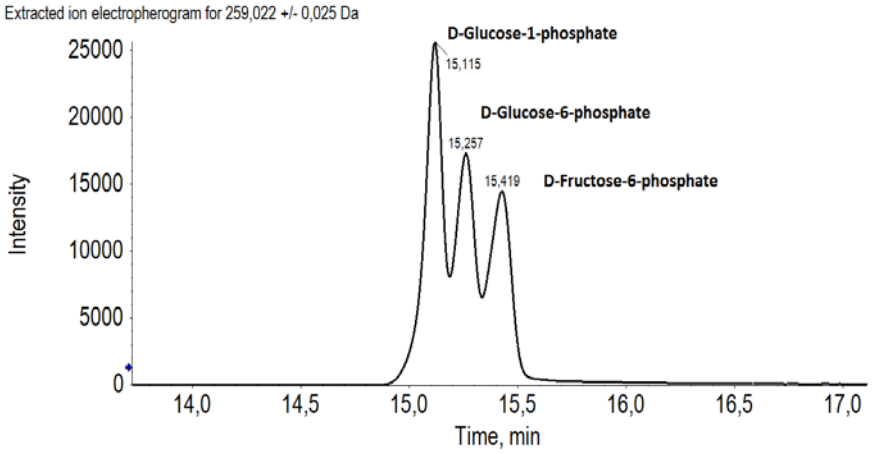

Figure 1. Analysis of sugar phosphate isomers by sheathless CE-MS. Analysis of sugar phosphate isomers by sheathless CE-MS. Extracted ion electropherogram for three sugar phosphate isomers (25 µM) obtained with sheathless CE-MS in negative ion mode. Experimental conditions: BGE, 10% acetic acid (pH 2.2); separation voltage, -30 kV (+0.5 psi applied at the inlet of the CE capillary); sample injection, 2.0 psi for 60 sec. Reproduced from ref. [4] with permission.

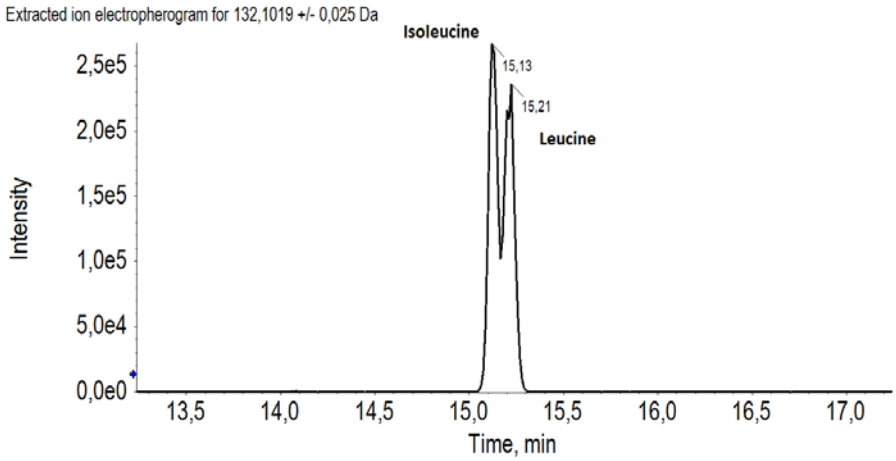

Figure 2. Analysis of isoleucine and leucine by sheathless CE-MS. Extracted ion electropherogram of two amino acid isomers (25 µM) obtained with sheathless CE-MS in positive ion mode. Experimental conditions: BGE, 10% acetic acid (pH 2.2); separation voltage, +30 kV; sample injection, 2.0 psi for 60 sec.

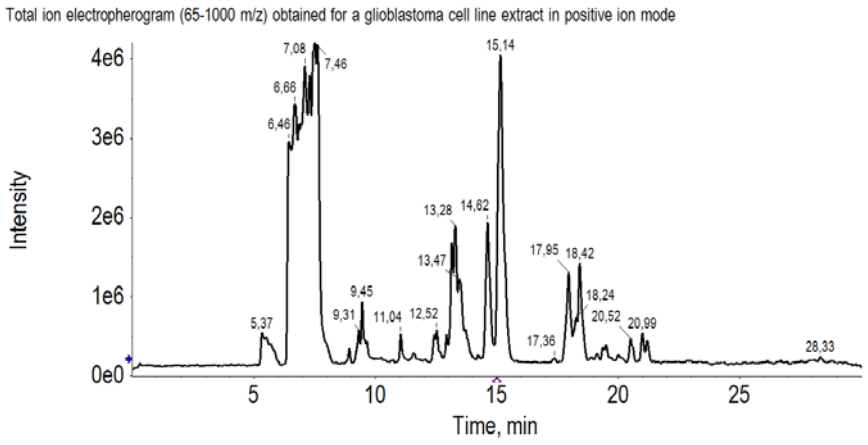

Figure 3. Potential of sheathless CE-MS for profiling cationic metabolites in a cell line extract. Metabolic profile (total ion electropherogram) observed in an extract of a glioblastoma cell line with

sheathless CE-MS in positive ion mode. Experimental conditions: BGE, 10% acetic acid (pH 2.2); separation voltage, +30 kV; sample injection, 2.0 psi for 60 sec.
Reproduced from ref. [4] with permission.

Discussion

A sheathless CE-MS method employing a porous tip emitter has been presented for the analysis of highly polar and charged metabolites. A unique feature of this approach is that anionic or cationic metabolites can be profiled by only switching the MS detection and CE voltage polarity. A wide range of highly polar and charged metabolites in biological samples can be analyzed with a high separation efficiency, which is crucial for structurally similar metabolites, and with limits of detection in the (low) nanomolar range. The presented protocol focused on the use of sheathless CE-MS for metabolic profiling of cell extracts in order to exemplify the utility of the method for metabolic profiling of a biological sample. The approach described here can also be used for metabolic profiling of other types of biological samples, such as human urine [5], given that a proper sample pretreatment procedure is used.

The sheathless CE-MS method is based on a porous tip emitter which allows the usage of the intrinsically low-flow property of CE. In this context, a stable ESI signal is a pre-requisite for reproducible metabolic profiling studies. Thus, it is important that the sprayer tip is properly positioned in front of the MS inlet. In this set-up, the ESI process is mainly dependent on the nature of the BGE and therefore, BGE optimization is critical. The sheathless configuration is less versatile in comparison to sheath-liquid CE-MS systems where all kinds of sheath-liquid compositions can be added to improve the ionization efficiency. The sheathless ESI sprayer needle needs to be completely filled with conductive liquid (i.e., BGE solution). An unstable ESI signal may result from a partial or fully plugged capillary. Rinsing at high pressures with BGE may solve this issue. Otherwise the separation capillary needs to be replaced. Prior to assessment of the analytical performance, a stable ESI background signal should be generated first which is consistent from one day to another.

The analytical performance of the sheathless CE-MS method for metabolic profiling studies needs to be checked daily using metabolite standard mixtures. Under the same experimental conditions, consistent migration times, i.e. variation below 3% for within-day (n=10) and between-day (n=5) using a 20 nL injection of a metabolite standard mixture (12.5 μM), peak heights/areas (variation below 15%) and plate numbers (ranging between 60000-400000) should be obtained. Limits of detection should be in the nanomolar range for most metabolite standards. Only when these criteria are met is the method ready for metabolic profiling of biological samples. If not, the MS instrument needs to be tuned and re-calibrated or the porous tip capillary emitter needs to be changed.

An effective rinsing step between CE-MS analyses is of high importance, not only to prevent potential carryover but also to maintain the separation performance. Potential carryover may be

caused by BGE vials contaminated with the sample and therefore solved by replacement with new BGE vials. When the sheathless CE-MS method is not in use, it is important to disconnect the separation capillary and to store the inlet side of the capillary in water and the outside submerged with the protective sleeve in a tube containing water to prolong capillary lifetime.

In summary, the proposed sheathless CE-MS method shows a strong potential for metabolic profiling of biological samples when used according to the procedures reported in this protocol. At this stage, inter-laboratory comparison data are definitely needed for sheathless CE-MS in order to assess the (long-term) reproducibility and robustness of this approach for metabolomics. This protocol may stimulate such a study. Various analytical challenges still need to be considered. For optimal performance, the CE current should be kept preferably below 5 μA and at this stage the capillary porous tip emitters are only provided at a length of 91 cm which may hamper the development of high-throughput assays. Moreover, a low pH separation buffer was used for anionic metabolic profiling which may not be the most optimal for achieving a baseline separation of structurally related sugar phosphates. Also important is that only anionic metabolites can be analyzed which are (partially) negatively charged under the used separation conditions. The next step is to assess the utility of the sheathless CE-MS method for clinical metabolic profiling studies as currently, a single porous tip capillary emitter can only be used for the analysis of up to 100 biological samples.

Overall, further development in the sheathless CE-MS approach will open a new direction in the field of metabolomics, i.e. towards a deeper understanding of biological functions in sample-restricted cases.

Acknowledgements

Dr. Rawi Ramautar would like to acknowledge the financial support of the Veni grant scheme of the Netherlands Organization of Scientific Research (NWO Veni 722.013.008).

References

1. Ramautar, R., et al., *Human metabolomics: strategies to understand biology.* Current opinion in chemical biology, 2013. **17**(5),841-6.
2. Wishart, D.S., et al., *HMDB 3.0--The Human Metabolome Database in 2013.* Nucleic acids research, 2013. **41**(Database issue),D801-7.
3. Psychogios, N., et al., *The human serum metabolome.* PloS one, 2011. **6**(2),e16957.
4. Gulersonmez, M.C., et al., *Sheathless capillary electrophoresis-mass spectrometry for anionic metabolic profiling.* Electrophoresis, 2016. **37**(7-8),1007-14.
5. Ramautar, R., et al., *Enhancing the coverage of the urinary metabolome by sheathless capillary electrophoresis-mass spectrometry.* Anal Chem, 2012. **84**(2),885-92.

6. Ramautar, R., et al., *CE-MS for metabolomics: Developments and applications in the period 2008-2010.* Electrophoresis, 2011. **32**(1),52-65.
7. Naz, S., A. Garcia, and C. Barbas, *Multiplatform analytical methodology for metabolic fingerprinting of lung tissue.* Analytical chemistry, 2013. **85**(22),10941-8.
8. Ibanez, C., et al., *CE/LC-MS multiplatform for broad metabolomic analysis of dietary polyphenols effect on colon cancer cells proliferation.* Electrophoresis, 2012. **33**(15),2328-36.
9. Soga, T., et al., *Simultaneous determination of anionic intermediates for Bacillus subtilis metabolic pathways by capillary electrophoresis electrospray ionization mass spectrometry.* Analytical chemistry, 2002. **74**(10),2233-9.
10. Soga, T., et al., *Quantitative metabolome analysis using capillary electrophoresis mass spectrometry.* Journal of proteome research, 2003. **2**(5),488-94.
11. Britz-McKibbin, P., *Capillary electrophoresis-electrospray ionization-mass spectrometry (CE-ESI-MS)-based metabolomics.* Methods in molecular biology, 2011. **708**,229-46.
12. Ibanez, C., et al., *A new metabolomic workflow for early detection of Alzheimer's disease.* Journal of chromatography. A, 2013. **1302**,65-71.
13. Kuehnbaum, N.L. and P. Britz-McKibbin, *New advances in separation science for metabolomics: resolving chemical diversity in a post-genomic era.* Chemical reviews, 2013. **113**(4),2437-68.
14. Nemes, P., et al., *Qualitative and quantitative metabolomic investigation of single neurons by capillary electrophoresis electrospray ionization mass spectrometry.* Nature protocols, 2013. **8**(4),783-99.
15. Hirayama, A., M. Wakayama, and T. Soga, *Metabolome analysis based on capillary electrophoresis-mass spectrometry.* Trac-Trends in Analytical Chemistry, 2014. **61**,215-222.
16. Maxwell, E.J. and D.D. Chen, *Twenty years of interface development for capillary electrophoresis-electrospray ionization-mass spectrometry.* Analytica chimica acta, 2008. **627**(1),25-33.
17. Bonvin, G., J. Schappler, and S. Rudaz, *Capillary electrophoresis-electrospray ionization-mass spectrometry interfaces: fundamental concepts and technical developments.* Journal of chromatography. A, 2012. **1267**,17-31.
18. Hirayama, A., M. Tomita, and T. Soga, *Sheathless capillary electrophoresis-mass spectrometry with a high-sensitivity porous sprayer for cationic metabolome analysis.* The Analyst, 2012. **137**(21),5026-33.
19. Bonvin, G., J. Schappler, and S. Rudaz, *Non-aqueous capillary electrophoresis for the analysis of acidic compounds using negative electrospray ionization mass spectrometry.* Journal of chromatography. A, 2014. **1323**,163-73.
20. Moini, M., *Simplifying CE-MS operation. 2. Interfacing low-flow separation techniques to mass spectrometry using a porous tip.* Analytical chemistry, 2007. **79**(11),4241-6.
21. Dettmer, K., et al., *Metabolite extraction from adherently growing mammalian cells for metabolomics studies: optimization of harvesting and extraction protocols.* Anal Bioanal Chem, 2011. **399**(3),1127-39.

Chapter 3

Part 2. Capillary Electrophoresis-Mass Spectrometry for Metabolic Profiling of Biomass-Limited Samples

Based on

Wei Zhang, Thomas Hankemeier, and Rawi Ramautar

Capillary Electrophoresis-Mass Spectrometry for Metabolic Profiling of Biomass-Limited Samples

Clinical Applications of Capillary Electrophoresis. Humana Press, New York, NY, 2019. 165-172

Abstract

Capillary electrophoresis-mass spectrometry (CE-MS) is a strong separation technique for the highly efficient and selective analysis of polar and charged metabolites in biological samples. The CE approach is especially suited for the analysis of limited sample amounts due to its nanoliter injections from only a few microliters of material in the sample injection vial. In this protocol, a CE-MS strategy is outlined for the profiling of cationic metabolites in biomass-limited samples using a small amount of human hepatocellular carcinoma (HepG2) cells as a model system. By employing a sheathless interfacing design for coupling CE to MS, it is shown that information-rich profiles for cationic metabolites can be obtained when working with a starting amount of 10,000 HepG2 cells and even lower. Overall, the proposed CE-MS-based analytical workflow may be considered a useful tool for biomass-limited metabolomics studies.

Introduction

Metabolomics aims at the comprehensive profiling of small (endogenous) molecules in a living system, unraveling biological processes and helping to tackle physiological issues [1-3]. This relatively new field of –omics has therefore assisted researchers in understanding the compositions and functions of living organisms and the environment. Various analytical tools have been introduced in order to deliver metabolic profiles that cover crucial metabolites, including nuclear magnetic resonance spectroscopy (NMR) and mass spectrometry (MS)-based platforms. Over the last few years, MS-based platforms have emerged as the main technique in the field of metabolomics [4]. In spite of the advancements made on liquid chromatography column technology and methodology, the analytical selectivity and efficiency for especially highly polar and charged metabolites still remains a challenge. Capillary electrophoresis (CE) separates compounds based on the difference in their size-to-charge ratios, which makes this approach highly suitable for the analysis of polar and charged metabolites. Due to the distinctive and unique separation mode of CE, it can offer complementary information about the composition of metabolites in a given biological sample.

At present, CE-MS is not as widely used as other techniques in global metabolic profiling studies [5], as within the separations science community this analytical technique is still often perceived to be a technically challenging approach. In 2015, Christian Wenz *et al*. reported a peptide mapping study involving 13 different labs, using the same sample, method and PVA-coated capillaries and a different set of instrumentations [6]. The results showed that by employing well-described suitability tests and protocols, CE-MS is capable of delivering reproducible outcomes for peptide mapping and that analytical method transfer can be performed in an effective manner among different laboratories. Recently, Harada *et al*. has used CE-MS for a large-scale metabolomics study [7]. In this study, 8000 human plasma samples were analyzed over a 52-month period. A unique and broad coverage of 94 polar metabolites was obtained with a similar or better reproducibility when compared to other analytical platforms employed for large-scale targeted metabolomics studies.

With the introduction of a recently developed software denoted as ROMANCE, researchers now can easily convert typical CE-MS timescales into electrophoretic mobility scales by using a reference peak with known electrophoretic mobility, enabling better peak alignment and normalized peak areas, provided that the same background electrolyte is used [8]. As such, this tool may facilitate comparative metabolic profiling studies by CE-MS.

In the classical CE-MS approach, the CE effluent is significantly diluted by the sheath-liquid which is provided at a flow-rate between 2 to 10 µL/min, resulting in compromised detection sensitivities. A lot of efforts have been dedicated to abolishing or minimizing the usage of the sheath-liquid, among which the sheathless porous tip interface has yielded very encouraging

results so far. Developed by Moini [9], the sheathless porous tip interface is now commercially available and has been recently applied in areas like proteomics [10] and metabolomics [11, 12].

The sheathless CE-MS approach has very strong analytical features for the highly sensitive analysis of metabolites especially in small-volume biological samples. In order to demonstrate the usefulness of sheathless CE-MS for biomass-limited metabolomics studies, a protocol is presented here.

Materials

Water used for the preparation of all solutions is obtained from a Milli-Q system equipped with 0.22 μM pore-size filter. Reagents used are of analytical grade unless stated otherwise.

1. Solutions and samples for analysis

1. Background electrolyte (BGE) solution: 10% (v/v) acetic acid, pH 2.2. Add 1 mL acetic acid into 9.0 mL of water and sonicate the mixture for 10 minutes under room temperature. Store at 4 °C.
2. Other solutions: Weigh 3.854 grams ammonium acetate into a 50 mL volumetric flask and add water to the marked line. Vortex thoroughly till the solid is completely dissolved. Transfer the solution to a 50 mL falcon tube (***Solution 1***, 1 M ammonium acetate). Weigh 0.112 gram of sodium hydroxide into a 25 mL volumetric flask and add water up to the mark. Vortex and sonicate the mixture till no solid is observed. Transfer the solution to a vial (***Solution 2***, 0.1 M sodium hydroxide). Store the prepared solutions at 4 °C prior to use.
3. Metabolite standard mixture: Weigh and dissolve 31 cationic metabolite standards separately in small tainted vials with a mixture of water and acetonitrile (95:5, containing 0.1% formic acid) to a concentration of 10 mM (unless otherwise stated). The cation mixture includes (1) spermine; (2) homoserine; (3) hypoxanthine (1 mM); (4) GSSG; (5) adenosine; (6) histidine; (7) methionine; (8) L-alanine; (9) tyrosine (1 mM); (10) threonine; (11) proline; (12) glutamine; (13) asparagine (6.67 mM); (14) serine; (15) valine; (16) glutamic acid; (17) glycine; (18) 4-hydroxyproline; (19) phenylalanine (6.67 mM); (20)cytidine; (21) lysine; (22) aspartic acid; (23) isoleucine; (24) leucine; (25) spermidine; (26) tryptophan; (27) anthranilic acid; (28) cytosine (6.67 mM); (29) tyramine (6.67 mM); (30) adenine (6.67 mM); and (31) creatine. Add 50 μL of each stock solution (10 mM; 75 μL for 6.67 mM; 500 μL for 1 mM) into a 10 mL volumetric flask and fill the flask up to the marked line with water: acetonitrile (95:5, containing 0.1% formic acid) mixture to make a standard mix of 50 μM. Shake the flask vigorously. Transfer the solution to a glass vial and store at -20 °C.

2. Analytical equipment

1. The reported protocol here can only be conducted on a sheathless CE instrument, CESI 8000. The sheathless CE is hyphenated to MS via a dedicated nanospray source, and relevant information can be acquired from references [13, 14].
2. For the electrophoretic separations, fused-silica capillary cartridges (30 μm I.D. x 90 cm total length) are used.

Methods

The protocol presented here for the application of sheathless CE-MS in biomass-limited cationic profiling studies is for laboratory use only. Please comply with proper laboratory safety procedures, and wear safety goggles, lab coats and gloves, when carrying out the experiments described below.

The set-up of sheathless CE-MS has been described previously and interested readers are referred to another publication [13].

1. Preparation of Extracts from the Human Hepatocellular Carcinoma (HepG2) Cell Line

1. Culture the human hepatocellular carcinoma (HepG2) cell line in Dulbecco's Modified Eagle's Medium/Nutrient Mixture F-12 Ham (DMEM) supplemented with 10% (v/v) fetal calf serum and 1% (v/v) of penicillin/streptomycin (see **Note 1**). The medium is replaced every three days.

2. The harvesting of the cells is done by detaching the adherent cells using trypsinization. Cells are stained with Trypan Blue and counted using an automated cell counting system.

3. Re-suspend the cells in 37 °C PBS to the concentration of 2x 10^6 /mL and distribute the mixture to clean Eppendorf tubes (1 mL per tube). Centrifuge the tubes and remove the PBS. Store the dry cell pellets at -80 °C.

4. Add 2 metal beads (see **Note 2**) and 1 mL cold methanol: water (80:20, v/v) mixture to the cell pellet. Subject the mixture to a bullet blender for 2 min at high speed.

5. Take 50 μL of the lysed cell mixture and mix it with 450 μL cold methanol: water (80:20, v/v) mixture, so that the diluted mixture has the concentration of 10,000 cells per 50 μL (see **Note 3**).

6. Transfer 50 μL of the diluted mixture (**Step 5**) to a clean Eppendorf tube for metabolite extraction. Add chloroform, methanol, water and internal standard solution to make a final mixture of 750 μL, with the ratio of methanol:water:chloroform being 2:2:1. Vortex for 1 min and centrifuge the mixture for 10 min at 16,100 g.

7. Transfer 500 μL of the supernatant after centrifuge and subject it to ultrafiltration using 5 kDa cutoff membrane filters to further remove (residual) proteins by centrifugation at 9,000 g for 2.0 hours. Collect 380 μL of the filtered aqueous phase and evaporate it to dryness in a LabConco SpeedVac. Store the dried extracts at -20 °C briefly before analysis.

8. Add 50 µL of 250 mM ammonium acetate solution to reconstitute the dry material. Vortex and centrifuge for 10 min at 16,100 g prior to sheathless CE-MS analysis.

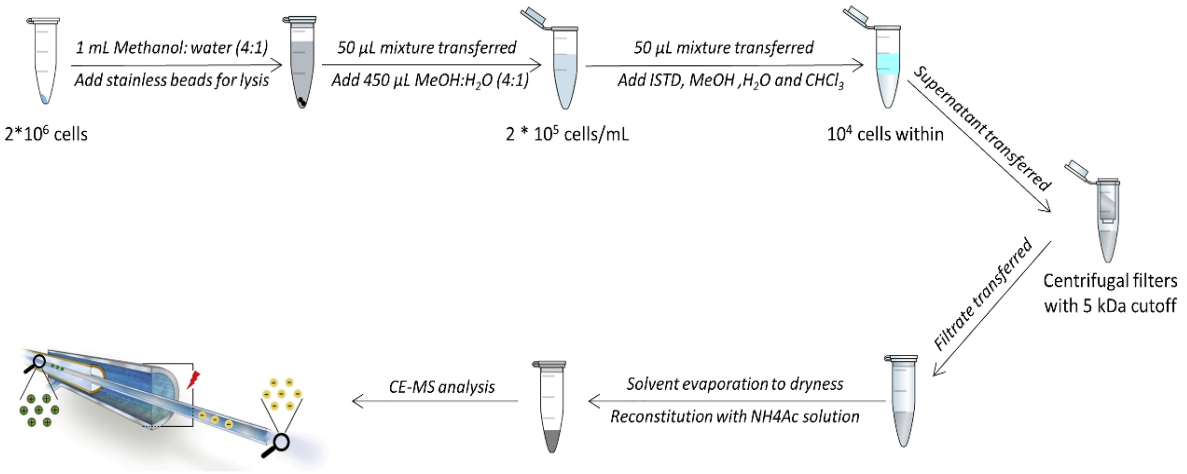

Figure. 1 An overview of the analytical workflow used for the preparation of extracts from HepG2 cells

2. Analysis of Metabolites Standards and Biological Samples

1. Add 50 µL of the cationic standard mix into an empty 250 µL microvial and 50 µL 500 mM ammonium acetate. Mix well and put the vial in the inlet sample tray, where the temperature is maintained at 10 °C.

2. Between runs, precondition the capillary by flushing with water (forward, 50 psi for 2 min), 0.1 M NaOH (forward, 50 psi for 3 min), water (forward, 50 psi for 2 min), and BGE (forward, 50 psi for 3 min; reverse, 50 psi for 2 min) (see **Note 4**). Inject the sample hydrodynamically at 6 psi for 60 s, which corresponds to about 42 nL or 6.6% of the total capillary volume. Then perform a BGE injection at 1 psi for 10 s.

3. Start MS data acquisition and apply a voltage of 30 kV (ramp time of 1.0 min) for cationic metabolic profiling for 22 min. After the electrophoretic separation, stop MS data acquisition, and decrease the CE voltage to 1 kV using a ramp time of 5 min.

4. Assess the recorded data by determining the migration times of the signal intensity of the analyzed cation standard mix (see **Note 5**).

5. Use the procedures described in Subheading 3.1, **steps 1-8**, for cationic metabolic profiling of extracts of the human hepatocellular carcinoma (HepG2) cell line. A typical profile for cationic metabolites extracted from the HepG2 cells by sheathless CE-MS is shown in Fig. 2 (see **Note 6**).

6. After the analyses or when not in use, rinse the capillary with water (forward, 50 psi for 10 min; reverse, 50 psi for 3 min), and put the capillary on water and rinse at 5 psi until further use (see **Notes 7 and 8**).

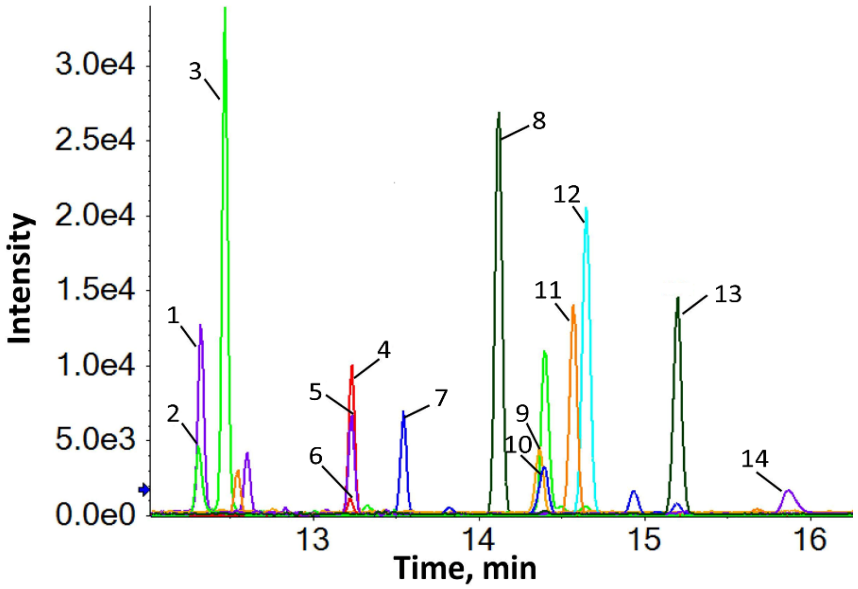

Figure. 2 Multiple extraction ion electropherograms for a selected number of metabolites obtained in an extract of about 10,000 HepG2 cells with sheathless CE-MS in positive ion mode using a porous tip emitter. Peaks: (1) lysine; (2) s-adenosylmethionine; (3) histidine; (4) glycine; (5) creatine; (6) cytidine; (7) L-alanine; (8) serine; (9) asparagine; (10) anthranilic acid; (11) phenylalanine; (12) tyrosine; (13) hypoxanthine; (14) hydroxyproline

Notes

1. The cells are incubated in 75 cm^2 tissue culture flasks at 37 °C under 5% CO_2 in an incubator.
2. The metal beads can come in different sizes, the ones used are about 2 mm in diameter. When dealing with smaller beads, more beads can be added to ensure thorough lysis.
3. The dilution process can be further repeated to achieve the targeted cell concentration as required for the experiment. The whole sample extraction procedure is performed on ice.
4. The sheathless capillary cartridge consists of a separation capillary and a conductive capillary. Both of them need to be thoroughly flushed before the start of measurements (see references [13-15]).
5. Please check for the following test compounds of the standard mixture whether the migration times are around the indicated values, i.e., for histidine: 12.4 min; L-alanine: 13.5 min; phenylalanine: 14.7 min and 4-hydroxyproline: 15.4 min.
6. Check the resolution for the two peaks of phenylalanine and tyrosine and determine whether their resolution factor is around 0.9.
7. When the sheathless CE-MS method is not in use, it is important to avoid drying out the porous tip capillary. One practice is to disconnect the separation capillary from the MS instrument and to store the outlet section of the capillary in water. The practice mentioned here is to rinse the capillary with water at a low flow-rate, i.e. at 5 psi for 10 min in reverse mode and at 5 psi for 300 min in forward mode, which procedure also guarantees that the position of the porous tip emitter in front of the MS inlet will remain the same, thereby making follow-up analyses easier.

8. Concerning durability of a single porous tip capillary emitter, at this stage up to 100 samples, including both standards and HepG2 cell extracts, can be analyzed. Further improvement of the sample preparation procedure is needed to improve the long-term performance of sheathless CE-MS for metabolic profiling of extracts from HepG2 cells.

Acknowledgements

Wei Zhang would like to acknowledge the Chinese Scholarship Council (CSC, No. 201507060011). Dr. Rawi Ramautar would like to acknowledge the financial support of the Veni and Vidi grant scheme of the Netherlands Organization for Scientific Research (NWO Veni 722.013.008 and Vidi 723.016.003). This work was also supported by the European Union´s Seventh Framework Programme for research, technological development and demonstration (FP7/CAM-PaC) under grant agreement no 602783.

References

1. Patti, G.J., O. Yanes, and G. Siuzdak, *Innovation: Metabolomics: the apogee of the omics trilogy.* Nat Rev Mol Cell Biol, 2012. **13**(4),263-9.
2. Gitto, S., et al., *Study of the Serum Metabolomic Profile in Nonalcoholic Fatty Liver Disease: Research and Clinical Perspectives.* Metabolites, 2018. **8**(1).
3. Ramautar, R., et al., *Human metabolomics: strategies to understand biology.* Curr Opin Chem Biol, 2013. **17**(5),841-6.
4. Theodoridis, G.A., et al., *Liquid chromatography-mass spectrometry based global metabolite profiling: a review.* Anal Chim Acta, 2012. **711**,7-16.
5. Kuehnbaum, N.L. and P. Britz-McKibbin, *New advances in separation science for metabolomics: resolving chemical diversity in a post-genomic era.* Chem Rev, 2013. **113**(4),2437-68.
6. Wenz, C., et al., *Interlaboratory study to evaluate the robustness of capillary electrophoresis-mass spectrometry for peptide mapping.* J Sep Sci, 2015.
7. Harada, S., et al., *Reliability of plasma polar metabolite concentrations in a large-scale cohort study using capillary electrophoresis-mass spectrometry.* Plos One, 2018. **13**(1).
8. Gonzalez-Ruiz, V., et al., *ROMANCE: A new software tool to improve data robustness and feature identification in CE-MS metabolomics.* Electrophoresis, 2018.
9. Moini, M., *Simplifying CE-MS operation. 2. Interfacing low-flow separation techniques to mass spectrometry using a porous tip.* Anal Chem, 2007. **79**(11),4241-6.
10. Gahoual, R., et al., *Full antibody primary structure and microvariant characterization in a single injection using transient isotachophoresis and sheathless capillary electrophoresis-tandem mass spectrometry.* Anal Chem, 2014. **86**(18),9074-81.
11. Gulersonmez, M.C., et al., *Sheathless capillary electrophoresis-mass spectrometry for anionic metabolic profiling.* Electrophoresis, 2016. **37**(7-8),1007-14.
12. Ramautar, R., et al., *Metabolic profiling of mouse cerebrospinal fluid by sheathless CE-MS.* Anal Bioanal Chem, 2012. **404**(10),2895-900.
13. Zhang, W., et al., *Sheathless Capillary Electrophoresis-Mass Spectrometry for Metabolic Profiling of Biological Samples.* J Vis Exp, 2016(116).

14. Ramautar, R., *Sheathless Capillary Electrophoresis-Mass Spectrometry for the Profiling of Charged Metabolites in Biological Samples.* Methods Mol Biol, 2018. **1738**,183-192.
15. Zhang, W., et al., *Utility of sheathless capillary electrophoresis-mass spectrometry for metabolic profiling of limited sample amounts.* J Chromatogr B Analyt Technol Biomed Life Sci, 2019. **1105**,10-14.

Chapter 4

Utility of sheathless capillary electrophoresis-mass spectrometry for metabolic profiling of limited sample amounts

Based on

Wei Zhang, Faisa Guled, Thomas Hankemeier, and Rawi Ramautar

Utility of sheathless capillary electrophoresis-mass spectrometry for metabolic profiling of limited sample amounts

Journal of Chromatography B 1105 (2019): 10-14

Abstract

Metabolomics studies using a small amount of cells may save time and money, while in some cases (e.g., profiling pathogenic cells in an early-stage tissue), only a small number of cells are accessible for analysis. The analysis of small amounts of biological samples challenges the analytical toolbox used in present-day metabolomics studies, and a significant number of crucial biological questions cannot be properly addressed. To allow metabolic profiling of limited sample amounts, the potential of capillary electrophoresis-mass spectrometry (CE-MS) using a sheathless porous tip interface has been assessed using HepG2 cells in starting amounts of 500 and 10,000 cells as a model system in this work. It is shown that highly efficient and information-rich metabolic profiles for cationic metabolites at low-pH separation conditions could be obtained by sheathless CE-MS using an injection volume of only about 42 nL, which equals to the content/aliquot of about 0.25 and 5 HepG2 cells, respectively. With as little as the content of 0.25 cell injected, more than 24 cationic metabolites could be identified. A further improvement of sample preparation and/or the injection part is required in order to effectively analyze the compounds of interest in very low sample amounts by sheathless CE-MS. However, the results obtained so far clearly indicate the strong potential of the proposed method for metabolic profiling of limited sample amounts.

Introduction

The final aim of a metabolomics study is to find an answer to a given (well-defined) biological or clinical question [1]. For this purpose, advanced analytical separation techniques are used for targeted or non-targeted analysis of (endogenous) metabolites in biological samples to determine the influence of genetic variation or external stimuli [2]. If performed properly, the metabolomics study may reveal important insights into pathogenic factors or compromised metabolic pathways, which eventually may lead to an improved diagnosis and a personalized therapy [3-5].

Currently, the conventional analytical techniques can be used in a reliable way for metabolomics studies, however, these analytical tools are often not suited for the profiling of metabolites in small amounts of biological samples. There is a strong interest for analytical tools capable of providing highly sensitive metabolic profiles for microscale cell culture samples. For example, for researches focused on stem cells [6], circulating tumor cells in blood [7], cancer stem cells, and primary tumor cells in early-stage tissues [8, 9], often only a small amount of cells are available. Another type of biomass-limited samples come from the emerging microfluidic 3D cell models, which can simulate physiological tissues by arranging different cell types in a 3D environment within a proper micro-environment [10]. These microfluidic cell culture systems intrinsically deal with relatively low amount of cell numbers, i.e. typically in the range of hundreds to thousands of cells.

Therefore, highly sensitive microscale (or nanoscale) analytical tools are needed to enable metabolomics studies of limited sample amounts. CE-MS may be considered an attractive analytical tool for metabolic profiling of limited samples due to its nanoliter sample injection requirement from only a few microliters of samples in a vial [11].

Although, a conventional CE-MS method employing a co-axial sheath-liquid interface is suited for analyzing volume-restricted biological samples, the detection sensitivity obtained by such an approach is often not sufficient for the reliable and global screening of trace-level metabolites in small sample amounts. In this work, we have considered a sheathless CE-MS approach, which was originally developed by Moini [12], for metabolic profiling of limited amounts of cells, as this approach has provided very promising results for metabolic profiling of volume-limited samples, such as mouse urine and cerebrospinal fluid (CSF) [13]. For example, in case of metabolic profiling of CSF samples from mice after a simple 1:1 dilution with water, more than 300 molecular features could be observed by only employing an injection volume of about 9 nL. Recently, we have developed a sheathless CE-MS method for the profiling of anionic and cationic metabolites employing a single bare fused-silica capillary emitter at low-pH separation conditions and applied it to the analysis of extracts from the glioblastoma cell line [14, 15]. By using an injection volume of about 20 nL, the developed CE-MS approach allowed the profiling of cationic metabolites in an amount corresponding to 400 glioblastoma cells. This encouraging result triggered us to assess the utility of sheathless CE-MS for highly sensitive profiling of cationic metabolites in limited

amounts of mammalian cells. In order to do this, HepG2 cells were used as a model system and the cell pellet was lysed, diluted, processed and analyzed as microscale cell cultures. An on-line preconcentration strategy, transient isotachophoresis (t-ITP), was used in this study to further improve the detection sensitivity of the proposed sheathless CE-MS method.

Materials and methods

The reagents, background electrolyte (BGE), sheathless CE equipment (CESI 8000) and mass spectrometer are as described in our previous work [15]. HepG2 cells were cultured, harvested and rinsed with PBS (37 °C) before being split into Eppendorf tubes (about 2,000,000 cells per tube); the amount of rinsing solvent was minimized. Cell pellets were kept at -80 °C prior to quenching with cold methanol/water mixture (v/v, 80/20). The quenched cell lysate mixture was further diluted to 10,000 and 500 cells per 50 µL using the same methanol/water mixture. For cationic metabolic profiling, the intracellular metabolites were extracted in a similar manner as reported in ref. [15]. 50 µL of the aforementioned samples was used for sample preparation, where 50 µL of cell-free isotope-labeled amino acids solution (0.2 µg/mL) was added as internal standards (ISTD). Pre-chilled water, methanol and chloroform were then added to the mix resulting in a final ratio of 1:1:0.5 (v/v/v). After vigorous vortex shaking and centrifugation, the supernatant was transferred to centrifugal filters with a 5 kDa cutoff filter to further remove interfering residues. Prior to analysis, dried metabolite extracts were reconstituted in 50 µL of 250 mM ammonium acetate (pH 7.0) solution in order to allow the use of t-ITP. About 42 nL (corresponding to about 6.6% of the total capillary volume) was hydrodynamically injected (i.e., by using a pressure of 6 psi for 60 seconds) into the sheathless CE-MS system, which in case for the HepG2 cell samples corresponded to an aliquot/content of about 5 and 0.25 HepG2 cells, respectively. The calculation of the number of cells per injection was based on the following procedure: a mixture of water, methanol and chloroform was used for liquid-liquid extraction, using in total 600 µL of water and methanol. The highly polar and charged compounds will be in the water-methanol layer. After ultrafiltration, 360 µL of this fraction was evaporated and the dried extract was reconstituted in 50 µL of ammonium acetate solution, which contains the content of 10,000 × (360/600) cells if we start with 10,000 HepG2 cells. For CE-MS analyses, an injection of volume of 42 nL is used, which corresponds to the content of about 5 cells based on 42 nL/50,000 nL × 10,000 × (360/600).

Sheathless CE-MS experiments were performed employing a 30 µm i.d. x 91 cm bare fused-silica capillary, which was thermostated using recirculating liquid coolant regulated at 25 °C, and coupled to a Sciex TripleTOF 5600+ MS system using the NanoSpray III source. ESI was performed in positive ionization mode by setting the ionspray voltage at 1100 V while the values for gas 1, gas 2, and interface heating temperature were set at 0, 0 and 50 respectively. MS data were recorded in the *m/z* range of 65 to 1000. Declustering potential was set at 50, which favors the detection of compounds in the low mass region. Electrophoretic separation was conducted in normal polarity mode by applying 30 kV to the CE inlet electrode. Prior to CE-MS, the MS

instrument was optimized using an ESI tuning mix for positive ion mode. 10% acetic acid (pH = 2.2) was used as BGE. The OptiMS cartridge was pre-conditioned and rinsed as described in ref. [14]. Plate numbers of a few representative compounds were calculated using their migration time and the peak width at half height. Limits of detection (LODs) for the metabolites in the test mixture were determined as the concentration yielding a S/N-ratio of 3 via extrapolation of the S/N-ratio produced by the lowest concentration used for the design of calibration curves (extracted ion electropherograms were used for this purpose). The identification of the peaks detected in HepG2 cell extracts by sheathless CE-MS was based on a comparison of the recorded *m/z* values and migration times with that obtained for the metabolites from the standard mixture.

Results and discussion

The aim of this study was to develop a sheathless CE-MS method for the profiling of metabolites in limited amount of cells, using HepG2 cells as a model system for this purpose. First, we have evaluated the performance of sheathless CE-MS for the analysis of a home-made cationic metabolite mixture and subsequently applied this approach to the profiling of intracellular metabolites in extracts from HepG2 cells. An injection volume of about 4.7 nL (which corresponds to 0.73% of the total capillary volume) of a 5 µM cationic metabolite mixture resulted in an acceptable detector response for most test compounds. The LOD values (S/N=3) obtained for the test compounds, by extrapolating the S/N-ratio obtained for the injection of a 5 µM metabolite mixture, ranged from 1.4 to 92 nM (except for aspartic acid, 417 nM), which is a significant improvement as compared to the LOD values (0.1 to 10 µM) typically found for these compounds when employing conventional sheath-liquid CE-MS systems [16, 17], and also with comparison to CE-MS using a flow-through microvial interface in which LODs from 0.1 to 12 µM were obtained for a cationic metabolite mixture [18]. It should be noted, however, that these are rough comparisons as different MS systems have been used in the other works. Recently, Hirayama *et al*. developed a new sheathless interface for coupling CE to MS [19]. The interface was designed by creating a small crack approximately 2 cm from the end of the capillary, which was covered with an electrodialysis membrane (cellulose acetate, molecular weight cut-off of 100 Da) to minimize the migration of small metabolites across the crack. This approach provided LODs for cationic metabolites in the range from 30 nM to 1.7 µM (when using an injection volume of 1.4 nL), which were rather comparable with results obtained by the sheathless CE-MS method proposed here when considering the difference in injection volume. However, the new CE-MS approach of Hirayama and co-workers is not suited for the profiling of compounds with a molecular weight below 100 Da, therefore, many relevant metabolites may not be detected by this approach.

Though, a significant improvement in LODs was provided by the sheathless CE-MS method using a porous tip interface, these values may not be sufficient for the highly sensitive profiling of metabolites in small sample amounts. Therefore, t-ITP was applied to further increase the injection volume to about 42 nL. The cationic metabolite mixture with different physico-chemical

properties was first analyzed using this method. **Figure 1** shows a typical result obtained by sheathless CE-MS for the analysis of a 1 µM cationic metabolite mixture employing t-ITP for preconcentration. Compared with the results from injection without t-ITP, the plate numbers for a few selected compounds like phenylalanine, tyrosine and lysine increased from 76659, 89493 and 273631 to 444761, 397870 and 637912, respectively, thereby indicating a significant decrease of peak widths at half height and as a result higher peak heights. The LOD values obtained with t-ITP injections ranged from 0.06 to 8.41 nM, with nearly one-third of the compounds achieving sub-nanomolar LOD values. It should be noted that these values were extrapolated from S/N-ratios obtained for the injection of a 1 µM metabolite mixture. The improvement in efficiency and especially in detection sensitivity as compared to previously reported sheathless CE-MS methods renders this method applicable for metabolomics studies of biomass-limited samples. The generation of calibration curves using the same cationic metabolite mixture showed that a linear detector response was observed for most test compounds in the range from 5 (or 10) to 500 nM (see **Supplementary Table S1**). On the basis of the lowest concentration used for the construction of the calibration curves, LODs have been determined again and listed in **Supplementary Table 1**. Still, these reported LODs need to be verified by the injection of a metabolite mixture in this concentration range.

Next, the sheathless CE-MS method was applied to the profiling of cationic metabolites in an extract of HepG2 cells using an injection volume of about 42 nL. **Figure 2** shows that a reasonable amount of metabolites could be detected by sheathless CE-MS in an injected amount corresponding to the content of 5 HepG2 cells only. The number of compounds detected was manually determined in the *m/z* range from 65 to 900, thereby only including peaks with a detection response above 1,000 counts. In total, 67 compounds were detected in the HepG2 cell extract, for which highly efficient peaks were obtained (**Fig. 2**). **Table 1** shows the compounds observed with sheathless CE-MS by comparing the *m/z* ratio of the compounds with that of the metabolite standards. In order to assess the repeatability of the sheathless CE-MS method for profiling metabolites in limited amounts of HepG2 cells, a single extract from 10,000 HepG2 cells (corresponding to the injection content of 5 HepG2 cells) was analyzed using seven consecutive runs. The relative standard deviation (RSD) values for migration times and peak areas of 18 selected endogenous metabolites (amino acids) were determined, which were below 3% and 10%, respectively (see **Supplementary Table S2**). These are acceptable values when considering the use of sheathless CE-MS at nano-ESI-MS conditions. **Figure 3** depicts multiple extraction ion electropherograms generated from the analysis using 500 HepG2 cells as the starting material, in which case as little as the content of 0.25 HepG2 cell was injected. Preliminary screening and comparison led to the identification of 24 known metabolites, thereby clearly indicating the potential of sheathless CE-MS for metabolic profiling of biomass-limited samples. Though, primarily introduced here as a screening method, we have also compared the detector response (using peak area as read-out) for a few selected endogenous metabolites as a function of the

starting amount of HepG2 cells. This analysis revealed a linear detector response when going from 10,000 to 500 HepG2 cells (see **Supplementary Figure S1**), which corresponds to an injection content from 5 cells to 0.25 cell, indicating the potential of the sheathless CE-MS method for quantitative metabolomics studies of limited sample amounts.

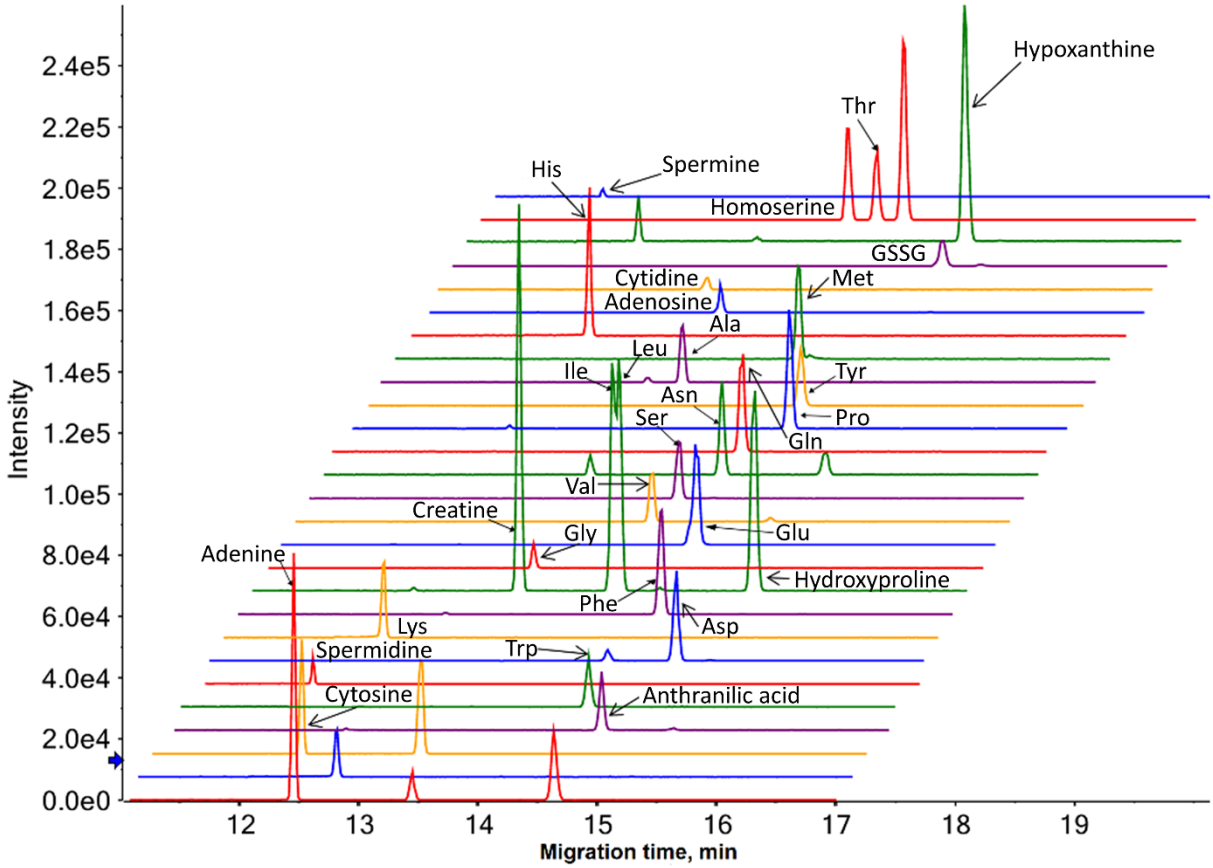

Figure 1. Multiple extracted ion electropherograms obtained for the analysis of a home-made cationic metabolite mixture (1 µM) by sheathless CE–MS in positive ion mode using a porous tip emitter. Separation conditions: BGE, 10% acetic acid (pH 2.2); Separation voltage: 30 kV; sample injection: 6.0 psi for 60 s.

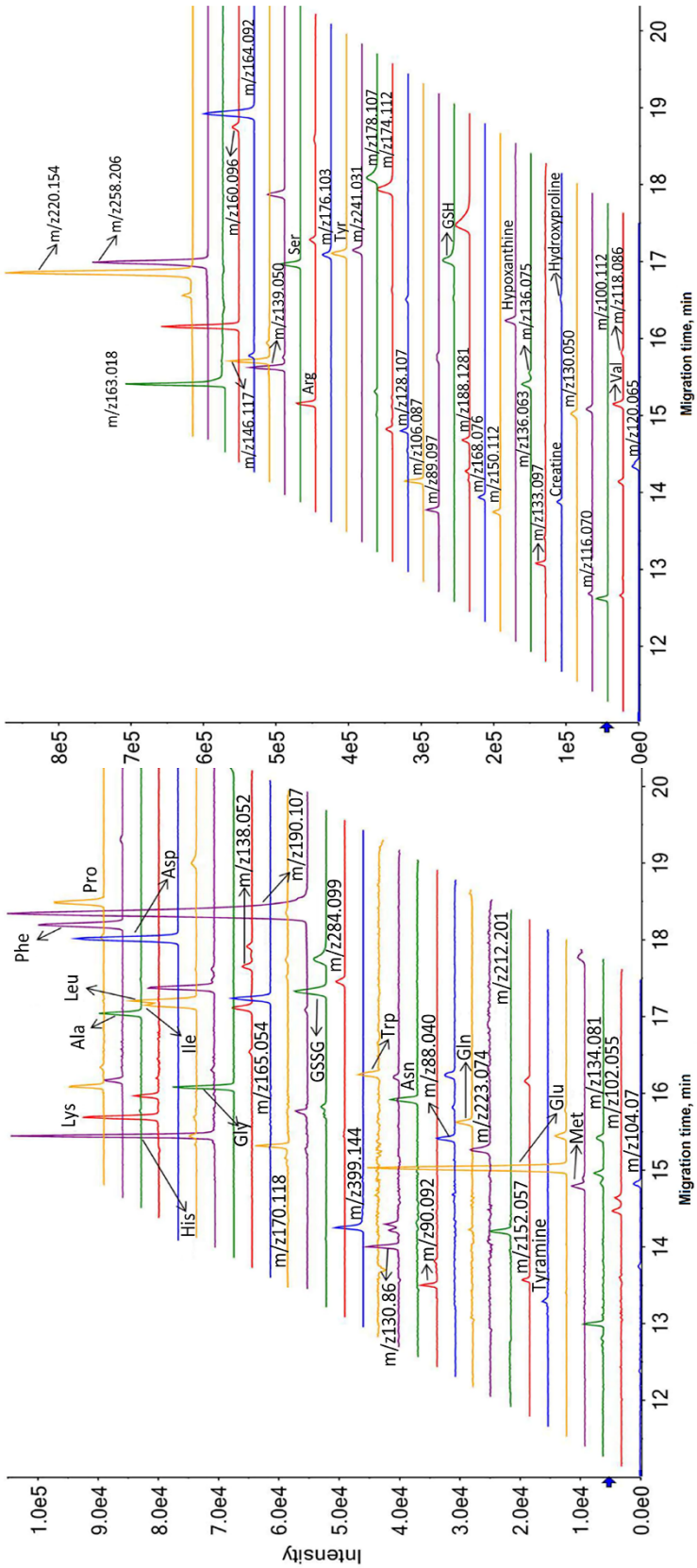

Figure 2. Multiple extracted ion electropherograms for a selected number of metabolite peaks detected in an extract of 10,000 HepG2 cells by sheathless CE–MS in positive ion mode using a porous tip emitter. Separation conditions: BGE, 10% acetic acid (pH 2.2); Separation voltage: 30 kV; sample injection: 6.0 psi for 60 s.

Table 1. List of compounds detected in an extract of HepG2 cells with sheathless CE-MS in positive ion mode using a porous tip emitter by comparing the migration time and *m/z* ratio with those obtained for in-house metabolite standards. Separation conditions: BGE, 10% acetic acid (pH 2.2); separation voltage: +30 kV; sample injection: 6.0 psi for 60 s.

Metabolites determined			
Detected *m/z*	**Metabolites**	**Detected *m/z***	**Metabolites**
76.0393	Glycine	138.0913	Tyramine
90.0550	Alanine	147.0764	Glutamine
106.0499	Serine	147.1128	Lysine
116.0706	Proline	148.0604	Glutamic acid
118.0863	Valine	150.0583	Methionine
120.0655	Threonine	156.0768	Histidine
132.0655	Hydroxyproline	166.0863	Phenylalanine
132.0768	Creatine	175.1190	Arginine
132.1019	Isoleucine	182.0812	Tyrosine
132.1019	Leucine	205.0972	Tryptophan
133.0608	Asparagine	307.0833	GSSG
134.0448	Aspartic acid	308.0911	GSH*
137.0458	Hypoxanthine		
Metabolites to be determined			
Detected m/z	**Detected m/z**	**Detected m/z**	**Detected m/z**
86.0972	130.0499	152.0562	188.1281
88.0402	130.0859	160.0965	190.1071
90.0918	133.0972	163.0179	212.2008
100.1120	134.0809	164.0917	220.1544
102.0550	136.0634	165.0543	221.1544
102.0550	136.0754	168.0761	223.0740
104.0701	138.0520	170.1181	241.0313
106.0866	139.0495	174.1123	258.2065
116.0703	139.0499	176.1030	284.0989
118.0863	146.1173	178.1071	399.1445
128.1067	150.1120		

*Though detected, GSH is not stable under the employed conditions as it is prone to oxidation.

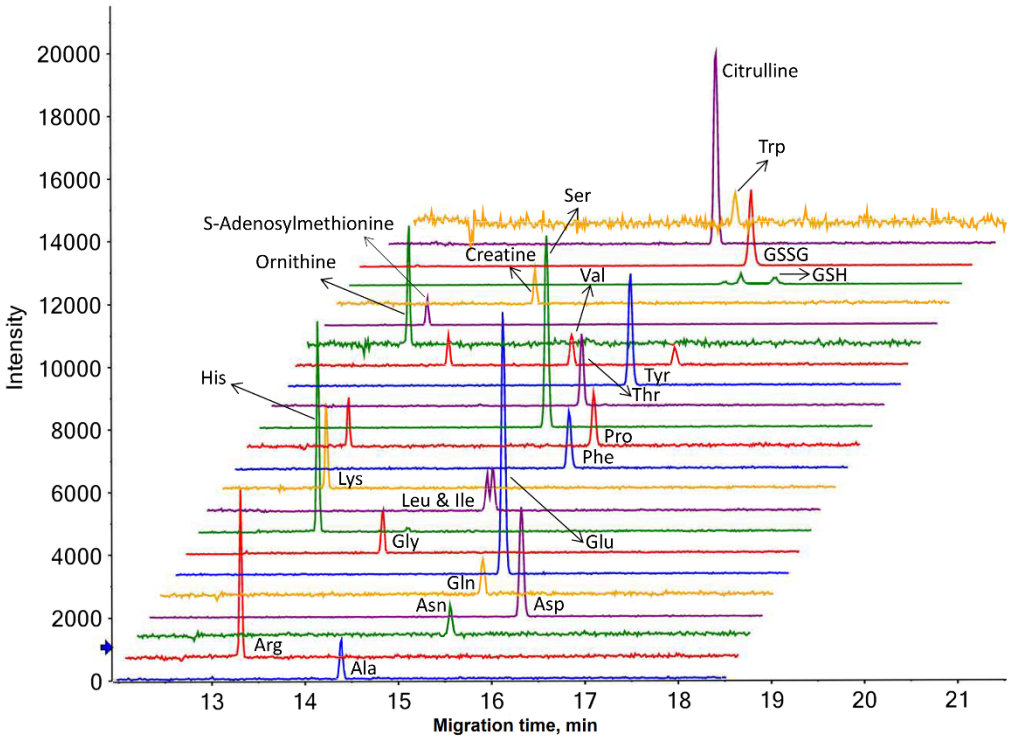

Figure 3. Multiple extracted ion electropherograms for a selected number of metabolite peaks detected in an extract of 500 HepG2 cells by sheathless CE–MS in positive mode using a porous tip emitter. Separation conditions: BGE, 10% acetic acid (pH 2.2); Separation voltage: 30 kV; sample injection: 6.0 psi for 60 s.

In the present work, the primary focus was on developing an assay for profiling cationic metabolites in limited amounts of cells. Follow-up work will focus on the profiling of anionic metabolites, including compounds like nucleotides and sugar phosphates, in order to further expand the metabolic coverage of this method. In this context, (further) optimization of BGE composition and the in-capillary preconcentration procedure is needed, notably for anionic metabolites. Another important aspect to consider is the sample preparation strategy used for a given material-limited cell line based metabolomics study, as we anticipate that the chosen sample preparation strategy, instead of the type of cell, will have a major influence on the performance of the analytical method. In the work outlined here, the final dried cell extract was reconstituted in 50 µL of solvent, however, the reconstitution volume may be dramatically reduced by the use of nanovials and, as such, we expect that the we can further improve the detection sensitivity of our method for material-limited metabolomics studies. The sample throughput of the current approach is limited, however, the group of Britz-McKibbbin recently developed a multi-segment injection strategy which significantly improved the sample throughput for targeted metabolomics studies [20]. We will also explore the possibility of multi-segment injection for improving analysis times in sheathless CE-MS-based metabolomics studies. Overall, the aim is to use the proposed sheathless CE-MS method for metabolic profiling of cell culture samples from 3D microfluidic organ-on-a-chip systems developed in our laboratory [21].

Acknowledgements

Wei Zhang would like to acknowledge the China Scholarship Council (CSC, No. 201507060011). Dr. Rawi Ramautar would like to acknowledge the financial support of the Vidi grant scheme of the Netherlands Organization of Scientific Research (NWO Vidi 723.016.003). This project has also received funding from the European Union´s Seventh Framework Programme for research, technological development and demonstration (FP7/CAM-PaC) under grant agreement number 602783.

References

1. Ramautar, R., et al., *Human metabolomics: strategies to understand biology.* Curr Opin Chem Biol, 2013. **17**(5),841-6.
2. Johnson, C.H., J. Ivanisevic, and G. Siuzdak, *Metabolomics: beyond biomarkers and towards mechanisms.* Nat Rev Mol Cell Biol, 2016. **17**(7),451-9.

3. Jack, C.R., Jr., et al., *Hypothetical model of dynamic biomarkers of the Alzheimer's pathological cascade.* Lancet Neurol, 2010. **9**(1),119-28.
4. Dona, A.C., S. Coffey, and G. Figtree, *Translational and emerging clinical applications of metabolomics in cardiovascular disease diagnosis and treatment.* Eur J Prev Cardiol, 2016. **23**(15),1578-89.
5. Shah, S.H., W.E. Kraus, and C.B. Newgard, *Metabolomic profiling for the identification of novel biomarkers and mechanisms related to common cardiovascular diseases: form and function.* Circulation, 2012. **126**(9),1110-20.
6. Shyh-Chang, N. and H.H. Ng, *The metabolic programming of stem cells.* Genes Dev, 2017. **31**(4),336-346.
7. Jackson, J.M., et al., *Materials and microfluidics: enabling the efficient isolation and analysis of circulating tumour cells.* Chem Soc Rev, 2017. **46**(14),4245-4280.
8. Mitra, A., L. Mishra, and S. Li, *Technologies for deriving primary tumor cells for use in personalized cancer therapy.* Trends in biotechnology, 2013. **31**(6),347-354.
9. Tredan, O., et al., *Drug resistance and the solid tumor microenvironment.* J Natl Cancer Inst, 2007. **99**(19),1441-54.
10. van Duinen, V., et al., *Microfluidic 3D cell culture: from tools to tissue models.* Curr Opin Biotechnol, 2015. **35**,118-26.
11. Onjiko, R.M., et al., *In Situ Microprobe Single-Cell Capillary Electrophoresis Mass Spectrometry: Metabolic Reorganization in Single Differentiating Cells in the Live Vertebrate (Xenopus laevis) Embryo.* Anal Chem, 2017. **89**(13),7069-7076.
12. Moini, M., *Simplifying CE-MS operation. 2. Interfacing low-flow separation techniques to mass spectrometry using a porous tip.* Anal Chem, 2007. **79**(11),4241-6.
13. Ramautar, R., et al., *Metabolic profiling of mouse cerebrospinal fluid by sheathless CE-MS.* Anal Bioanal Chem, 2012. **404**(10),2895-900.
14. Zhang, W., et al., *Sheathless Capillary Electrophoresis-Mass Spectrometry for Metabolic Profiling of Biological Samples.* J Vis Exp, 2016(116).
15. Gulersonmez, M.C., et al., *Sheathless capillary electrophoresis-mass spectrometry for anionic metabolic profiling.* Electrophoresis, 2016. **37**(7-8),1007-14.
16. Ramautar, R., et al., *Enhancing the coverage of the urinary metabolome by sheathless capillary electrophoresis-mass spectrometry.* Anal Chem, 2012. **84**(2),885-92.
17. Soga, T., et al., *Quantitative metabolome analysis using capillary electrophoresis mass spectrometry.* Journal of proteome research, 2003. **2**(5),488-494.
18. Lindenburg, P.W., et al., *Capillary electrophoresis-mass spectrometry using a flow-through microvial interface for cationic metabolome analysis.* Electrophoresis, 2014. **35**(9),1308-1314.
19. Hirayama, A., et al., *Development of a sheathless CE-ESI-MS interface.* Electrophoresis, 2018. **39**(11),1382-1389.
20. Kuehnbaum, N.L., A. Kormendi, and P. Britz-McKibbin, *Multisegment injection-capillary electrophoresis-mass spectrometry: a high-throughput platform for metabolomics with high data fidelity.* Anal Chem, 2013. **85**(22),10664-9.
21. Moreno, E.L., et al., *Differentiation of neuroepithelial stem cells into functional dopaminergic neurons in 3D microfluidic cell culture.* Lab on a Chip, 2015. **15**(11),2419-2428.

Supplementary Materials

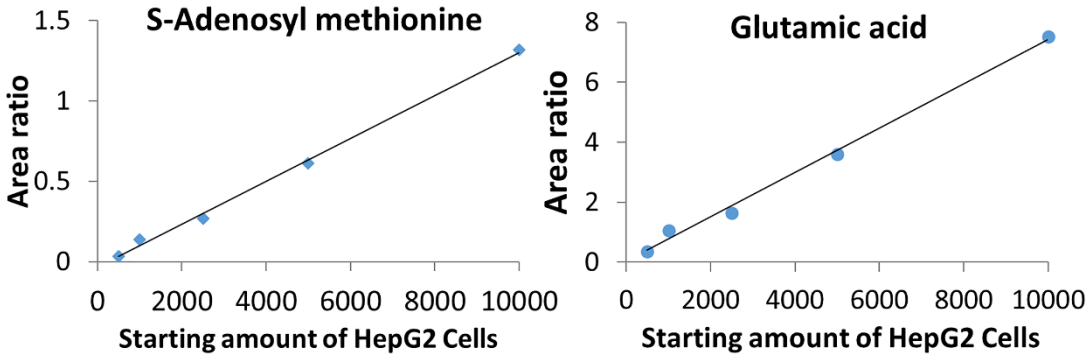

Figure S1. Analysis of selected endogenous metabolites in extracts from HepG2 cells using starting amounts from 10,000 to 500 cells by sheathless CE-MS in positive ion mode using a porous tip emitter. Separation conditions: BGE, 10% acetic acid (pH 2.2); Separation voltage: 30 kV; sample injection: 6.0 psi for 60 s.

Table S1. An overview of the calibration curves obtained for the analysis of the cationic metabolite mixture by sheathless CE-MS.

Compounds	Linear range (nM)	R^2	LOD (nM)
4-Hydroxyproline	5-500	0.9934	4.2
Adenine	10-500	0.9944	5.5
Adenosine	5-500	0.9884	0.5
Anthranilic acid	10-500	0.992	4.4
Asparagine	10-500	0.9892	5.6
Creatine	5-500	0.9823	2.3
Cytidine	5-500	0.9989	1.7
Cytosine	10-500	0.9982	4.8
Glutamic acid	10-500	0.9957	1
Glutamine	10-500	0.9948	5.7
GSSG	5-500	0.9988	0.9
Histidine	10-500	0.9952	0.7
Hypoxanthine	5-500	0.9958	4.5
L-Alanine	10-500	0.9719	4.5
Leucine & Isoleucine	10-500	0.9836	1.3
Lysine	10-500	0.9905	1.8
Methionine	10-500	0.9961	6.3
Phenylalanine	10-500	0.992	1
Proline	10-500	0.9849	2
Threonine	10-500	0.9935	3
Tryptophan	10-500	0.9967	7.9
Tyramine	5-500	0.9915	3
Tyrosine	10-500	0.9934	0.7
Valine	5-500	0.9854	2.5

Table S2. Repeated analysis (n=7) of selected endogenous metabolites in an extract from 10,000 HepG2 cells by sheathless CE-MS in positive ion mode using a porous tip emitter. Separation conditions: BGE, 10% acetic acid (pH 2.2); Separation voltage: 30 kV; sample injection: 6.0 psi for 60 s.

Amino acid	Average peak area	RSD (%) for peak area	Average migration time (min)	RSD (%) for migration time
Ala	19849	8.4	14.00	2.5
Arg	70888	4.9	12.89	2.7
Asn	16374	9.0	14.84	2.4
Asp	69931	7.8	15.44	2.4
Gln	9827	7.4	14.94	2.4
Glu	126807	7.9	14.99	2.4
Gly	30098	9.0	13.69	2.5
His	88947	4.8	12.92	2.7
Ile & Leu (co-migrated)	60498	5.2	14.55	2.4
Tyr	76004	5.1	15.13	2.4
Lys	32384	2.7	12.78	2.8
Met	7183	5.4	14.88	2.4
Phe	49203	7.1	15.05	2.4
Pro	29426	5.6	15.18	2.4
Ser	87979	6.1	14.59	2.4
Thr	48738	6.8	14.82	2.4
Trp	12687	9.5	14.92	2.4
Val	21783	6.6	14.48	2.4

Chapter 5

Profiling nucleotides in low numbers of mammalian cells by sheathless CE-MS in positive ion mode: circumventing corona discharge

Based on

Wei Zhang, Faisa Guled, Thomas Hankemeier, and Rawi Ramautar

Profiling nucleotides in low numbers of mammalian cells by sheathless CE-MS in positive ion mode: circumventing corona discharge

Electrophoresis (2020)

Abstract

Negative ion mode nano-ESI-MS is often considered for the analysis of acidic compounds, including nucleotides. However, under high aqueous separation conditions, corona discharge is frequently observed at emitter tips, which may result in low ion abundances and reduced nano-ESI needle emitter lifetimes. In this work, we introduce a sheathless CE-MS method for the highly efficient and sensitive analysis of nucleotides employing ESI in positive ion mode, thereby fully circumventing corona discharge. By using a background electrolyte of 16 mM ammonium acetate (pH 9.7) a mixture of 12 nucleotides, comprised of mono-, di- and tri-phosphates, could be efficiently analyzed with plate numbers per meter above 220,000 and with limits of detection in the range from 0.06 to 1.3 nM, corresponding to 0.4 to 8.6 attomole, when using an injection volume of about 6.5 nL only. The utility of the method was demonstrated for the profiling of nucleotides in low numbers of mammalian cells using HepG2 cells as a model system. Endogenous nucleotides could be efficiently analyzed in extracts from 50,000 down to 500 HepG2 cells only. Moreover, apart from nucleotides, also some nicotinamide-adenine dinucleotides and amino acids could be analyzed under these conditions, thereby clearly illustrating the utility of this approach for metabolic profiling of low amounts of biological material.

Introduction

In metabolomics, liquid chromatography (LC) hyphenated to high-resolution accurate mass TOF-MS is now routinely used for discovery studies. However, the highly efficient profiling of polar and charged metabolites remains a challenge with modern LC columns including HILIC and ion-exchange LC, especially for phosphorylated metabolites such as nucleotides [1], which play key roles in cell signaling and metabolism. The latter compounds have the tendency to interact with stainless steel in the LC-MS system and an additive to the mobile phase needs to be applied to deactivate the steel surfaces [2]. Moreover, method development for nucleotide profiling by ion-pair reversed-phase LC-MS, anion-exchange LC-MS and HILIC-MS is often not straightforward. Another challenge concerns the analysis of nucleotides in low numbers of mammalian cells with the aim to get insight into how a small population of cells within a tumor or organoid responds to a drug as compared to another (adjacent) small population of cells. For this, a highly efficient microscale separation technique coupled to a high end MS instrument is required in order to enable the analysis of nucleotides in low amounts of biological material.

Capillary zone electrophoresis (CE) is a highly efficient microscale separation technique and as compounds are separated on the basis of their charge-to-size ratio, CE is especially suited for the profiling of polar and charged compounds under biocompatible conditions [3]. Moreover, CE-MS is well-suited for the sensitive analysis of compounds in material- or volume-limited samples as only nanoliter injection volumes are required from just a few microliters of sample or less in the injection vial [4-8]. A number of recent studies have clearly shown the utility of CE-MS for metabolic profiling of large sample sets. For example, Harada *et al*. assessed the long-term performance of CE-MS for metabolic profiling of more than 8000 human plasma samples from the Tsuruoka Metabolomics Cohort Study over a 52-month period [9]. The study provided an absolute quantification for 94 polar metabolites in plasma with a reproducibility comparable to other analytical platforms, i.e. reversed-phase LC-MS and GC-MS, commonly employed for large-scale metabolomics studies.

The first CE-MS methods for the global profiling of polar and charged metabolites were developed by Soga and co-workers [10, 11]. For nucleotides and other anionic metabolites, a positively charged capillary coating was employed in combination with reversed CE separation polarity to allow their relatively fast analysis by CE-MS [10]. However, adsorption of compounds carrying multiple negative charges, such as ATP and ADP, to the positively charged capillary wall was an issue. Moreover, a conventional sheath-liquid interface was employed for coupling CE to MS and it was found that under these conditions the stainless steel ESI spray needle showed oxidation and corrosion due to electrolysis [12]. The resulting precipitation of iron oxides plugged the capillary outlet and shortened capillary lifetime. In addition, many of the anionic metabolites appeared to form complexes with iron oxides and nickel ions from the steel needle. The metal-metabolite complex formation caused ionization suppression and significantly reduced detection sensitivity for

anionic metabolites. In 2009, this issue was resolved by the use of a platinum ESI needle, however, the adsorption of some nucleotides and other acidic metabolites to the positively charged capillary wall remained an issue [12]. A platinum ESI needle is not needed when analyzing anionic metabolites in normal CE polarity mode at high pH separation conditions and negative ESI-MS mode. However, the CE effluent is significantly diluted in CE-MS employing a conventional sheath-liquid interface, resulting in limits of detection (LODs) around the low µM-range for nucleotides which may not be sufficient for their reliable analysis in low numbers of mammalian cells.

In order to enable the analysis of nucleotides in limited amounts of cells or in even a single cell, CE has been coupled to nano-ESI-MS using custom-built low-flow sheath-liquid interfaces and detection in negative ion mode. For example, Liu *et al*. developed a CE-MS method for the profiling of nucleotides in extracts of single neuronal cells from *Aplysia californica* using MS in negative ionization mode [13]. A modified coaxial sheath-liquid nanospray interface was used which had a smaller diameter capillary outlet, that is 40 µm instead of 75 µm internal diameter, thereby allowing to use a sheath-liquid flow-rate of 600 nL/min. These modifications reduced sample dilution and improved detection limits. The interface used in this study was constructed with a microtee assembly containing a platinum alloy emitter in order to prevent corrosion. The method provided a good separation for 16 mono-, di- and triphosphate nucleosides with LODs ranging from 2 to 22 nM using an injection volume of only 10 nL. Though, low nanomolar detection sensitivities could be obtained for nucleotides under these conditions, a serious concern is corona discharge when employing low-flow separations in combination with nano-ESI-MS in negative ion mode [14]. This effect can be attenuated by the addition of organic solvents, nitrogen gas, oxygen or other reagents acting as electron scavengers. For example, Portero *et al*. complemented a home-made low-flow sheath-liquid interface design for CE-MS with a nitrogen gas filled chamber to minimize electrical discharges and to obtain a stable ESI spray in the negative ion mode [15]. In order to avoid corona discharge, Dodbiba *et al*. analyzed nucleotides in the positive ion mode by employing different cationic ion-pairing reagents that associate with nucleotides resulting in overall positively charged complexes [16]. Under these conditions, improved LODs were obtained for most of the studied nucleotides, however, for the nucleotide triphosphate compounds, such as for example ATP, low LODs were more difficult to obtain with the employed cationic ion-pairing agents.

In the present work, our aim was to develop a microscale analytical platform for the highly sensitive and efficient profiling of nucleotides in low numbers of mammalian cells under nano-ESI conditions and to fully circumvent corona discharge. For this purpose, CE was coupled to nano-ESI-MS via a sheathless porous tip interface, originally developed by Moini [17] and now commercially available as CESI (Sciex), and the detection of nucleotides was performed in the positive ion mode, whereas they were electrophoretically separated at high-pH separation conditions. It is shown that apart from nucleotides also some nicotinamide-adenine dinucleotides and amino acids could be analyzed in low number of mammalian cells under these conditions,

thereby clearly illustrating the utility of this approach for metabolic profiling of low amounts of biological samples.

Materials and methods

1. Chemicals and reagents

Ammonium acetate (99%), Dulbecco's Phosphate Buffered Saline (PBS) and Dulbecco's Modified Eagle's Medium/Nutrient Mixture F-12 Ham (DMEM F-12) were purchased from Sigma Aldrich (St. Louis, USA). Ammonium bicarbonate (99.5%) was provided by Fluka (Steinheim,Germany). Ammonium carbonate was obtained from Scharlau (Barcelona, Spain). Sodium hydroxide (analytical grade) was acquired from Merck (Darmstadt, Germany). Hydrochloric acid (37% solution in water) and ammonia (28~30% NH_3 in water) were supplied by Across Organics (Geel, Belgium). Methanol (ultra LC-MS grade) was purchased from ACTU-ALL chemicals (Oss, the Netherlands). HPLC grade chloroform and MS grade acetic acid were provided by Biosolve Chemicals (Valkensweerd, the Netherlands). Water used in this work was produced by a Milli-Q® Advantage A10 Water Purification System from Millipore. Fetal calf serum HC-20C (Biowest) was obtained from VWR (Amsterdam, the Netherlands). Penicillin-streptomycin (Pen/Strep, 100 mg/mL each) was supplied by Duchefa (Haarlem, the Netherlands). Centrifugal filters with 3 kDa cutoff membrane were also provided by Merck. Standards of nucleotides, including NMP, NDP, and NTP (N=A, U, C, G), cyclic AMP (cAMP, used as reference when calculating relative apparent electrophoretic mobility), and isotope-labeled nucleotides (used as internal standards), UMP (^{15}N2), ATP (^{15}N5), and GMP (^{15}N5), were all acquired from Sigma Aldrich.

2. Preparation of solutions

Solutions of ammonium acetate, ammonium bicarbonate and ammonium carbonate were prepared by dissolving proper amounts of powder in corresponding volumes of water. The pH of each solution was then adjusted with 28%-30% ammonia to desired values, including 8.5, 9.0 and 9.7. The concentration of all tested buffers was 12.5 mM at the start. Stock solutions of all the nucleotides were prepared individually by dissolving dry powders in a mixture of 95% water and 5% methanol. A mix of standards was then generated by mixing aforementioned solutions in a volumetric flask and the final concentration was 100 μM for every compound. This mixture was then divided over separate Eppendorf tubes and stored at -80 °C. The same preparation procedure was conducted for labeled ATP and GMP, and 40 μL of mixed internal standard (ISTD) solution (50 μg/mL) was divided over aliquots in clean Eppendorf tubes for single uses later.

3. Sample preparation

Prior to sample preparation, chloroform saturated with water and methanol was prepared by vigorously mixing chloroform, methanol and water at a 1:1:1 (v/v/v) ratio and removing the upper layer after centrifugation. A series of working solutions were diluted from a 100 μM stock

solution with water, covering the range of 3.9 nM to 2 µM for calibration curves. ISTD mixture was diluted with methanol to a final concentration of 400 ng/mL for each compound. Into clean Eppendorf tubes, 120 µL methanol, 30 µL ISTD solution, 100 µL water, 50 µL working solution (substituted with water for blanks), and 125 µL saturated chloroform were added. The final ratio of methanol/water/chloroform was 1:1:0.83 (v/v/v) in sample mixture. The mixtures were then vortexed for 1 min followed by centrifugation using 20817 g at 4 °C for 10 min. 220 µL supernatant was then transferred to 500 µL Eppendorf tubes and placed in a Savant SC210A SpeedVac Concentrator (Thermo Scientific) for solvent evaporation at room temperature. Dried residues were reconstituted with 30 µL of ice-cold MeOH/H_2O (1:1, v/v) mixture, followed by vigorous vortex and centrifugation using 20817 g at 4 °C for 15 min prior to analysis.

4. Cell Lysate Preparation

500 mL DMEM F12 was supplemented with 45 mL FCS and 1 mL Pen/Strep and used as the culture medium in this work. HepG2 cells were cultured and harvested in house. Harvested cells were counted with a TC10 Automated Cell Counter (Bio-Rad Laboratories) and live cell density arrived at 7.4*10^6 cells/mL. 5 mL of pre-warmed (37 °C) culture medium was firstly added onto petri dishes (60 mm, *n*=3), and 135 µL of the obtained cell mixture (containing about 10^6 live cells) was gently pipetted into the medium right after the cell mixture was properly dispersed. The petri dishes were then gently shaken to help distribute the cells evenly before incubation at 37 °C in 95% air/5% CO_2. The petri dishes were taken out of the incubator after all the cells had adhered to the bottom of the dishes (after roughly 7.5 hours). The medium was then aspirated and 6 mL pre-warmed (37 °C) PBS was carefully added into each dish to wash away residual culture medium. The PBS was then removed and 1 mL ice-cold methanol/H_2O (80:20, v/v) mixture was added into every petri dish to quench intracellular enzymatic reactions. The dishes were then moved onto ice and scraping was employed to get all the cells off the surface. Cell lysates were transferred into separate Eppendorf tubes and centrifuged using 14000 RPM at 4 °C for 10 min. The supernatant from each tube was then filtered with centrifugal filters with 3 kDa cutoffs and centrifuged using 10,000 g at 4 °C for 1.5 hours. Filtered cell lysates were then transferred and stored at -80 °C prior to further sample preparation. The cell lysate samples were processed in a similar manner as previously described [18]. The cell lysate obtained corresponded to a cell density of 50000 cells/50 µL and was further diluted to 10000, 5000, 2500, 1000 and 500 cells/50 µL with ice-cold methanol/water (80:20, v/v). 50 µL of every (diluted) cell lysate was transferred to clean Eppendorf tubes, followed by addition of methanol, water, ISTD solution and saturated chloroform to reach the same final ratio as aforementioned. The rest was conducted exactly as previously stated.

5. CE-MS analysis

Sheathless CE–MS experiments were conducted employing a 30 µm i.d. × 91 cm bare fused-silica capillary, regulated at 25 °C with recirculating liquid coolant, and coupled to a Sciex TripleTOF

6600 MS system via NanoSpray III source equipped with an XYZ stage. The porous tip of the sheathless capillary was positioned roughly 3 mm away from the MS inlet. ESI was performed in positive ionization mode and manual tuning was conducted after installation of the capillary to determine the optimal IonSpray Voltage Floating (ISVF) and curtain gas values. Different ISVF values ranging from 1600 V to 1850 V were selected for different BGEs tested and curtain gas values varied between 10 and 15 psi. During the method validation process and cell lysate analysis, ISVF values were set between 1920 to 1960 **V** and curtain gas values between 12 to 14 psi. The values for gas 1, gas 2, interface heating temperature and declustering potential were set at 0, 0, 50 °C, and 50 V respectively. An accumulation time of 0.25 second was used and the collision cell was set at 10.0 eV. MS data were recorded in the *m/z* range of 65 to 1000. The OptiMS cartridge was pre-conditioned and rinsed as described in our previous work. Sample tray was kept at 8°C. Samples were hydrodynamically injected into the capillary at 2 psi for 30 seconds, which corresponds to about 6.5 nL (i.e., 1% of the total capillary volume). A push plug of BGE injected at 5 psi for 60 seconds was introduced right after sample injection. Electrophoretic separation was performed in normal polarity mode by applying 30 kV to the CE inlet electrode and 1 psi forward pressure was applied during the separation. The selection of an optimal BGE was done by testing different BGEs in combination with nucleotides dissolved in water. The selection of optimal BGE was based on the separation resolution, peak shapes, intensities and S/N ratios obtained for NTPs.

6. Determination of analytical performance characteristics

Calibration curves were generated by plotting peak area ratios (i.e., peak area of nucleotide divided by peak area of internal standard) against their corresponding concentrations employing 5, 10, 25, 50, 100, 250, 500 and 1000 nM as concentration for each nucleotide. Labeled UMP was used as internal standard at a fixed concentration of 200 nM. Values for the slope, intercept, and correlation coefficient were obtained by linear-regression analysis of the calibration curves. LODs were calculated as the concentrations providing a signal intensity equivalent to S/N of 3 based on an injected concentration of 5 nM or 10 nM (extracted ion electropherograms were used for this purpose). As LLE is required for the analysis of nucleotides in HepG2 cells, calibration curves were also constructed for nucleotide standard solutions in the concentration range as listed in **Table 2** using liquid-liquid extraction (LLE) in combination with sheathless CE-MS.

Accuracy was determined by comparing calculated concentrations of nucleotides with established calibration curves with the nominal concentrations using a concentration of 250 nM. Intra- and inter-day variation of relative migration time and peak area were determined by analyzing four replicates of a 250-nM nucleotide mixture, which were processed by LLE, within a day and on 3 consecutive days. Relative migration time (RMT) ratios were calculated using the migration times of corresponding internal standards. For determination of cellular energy status, adenylate energy charge (AEC) was calculated using obtained concentrations of AMP, ADP, and ATP, with the formula expressed as AEC=([ATP] + 0.5*[ADP])/([ATP] + [ADP] + [AMP]) [19].

In order to evaluate the repeatability of this method for profiling nucleotides in cell lysates, cell samples were prepared in triplicates for the cell lysate obtained from one petri dish at 1000 and 2500 cells/50 µL, respectively, and cell lysates from the other two dishes were also diluted to the same cell densities and analyzed, which could reveal information regarding intra- and inter-dish variability.

Results and discussion

As outlined in the Introduction, the profiling of anionic (i.e., acidic) metabolites by CE-MS has only been considered by a few groups as it is a challenging endeavor to develop robust CE-MS methods when employing ESI in negative ion mode in combination with high aqueous separation conditions. In this context, we have previously developed a CE-MS method utilizing a sheathless porous tip interface, which was first developed by Moini [17], for the profiling of anionic metabolites at low-pH separation conditions in combination with ESI in negative ion mode [20]. Under these conditions we observed that corona discharge was minimal, while at high-pH separation conditions employing ammonium acetate with a low percentage of isopropanol as BGE corona discharge rapidly decreased the lifetime of a single porous tip emitter. Recently, Sarver *et al*. also reported on the detrimental effect of corona discharge when using borosilicate emitters in an electrokinetic sheath-liquid interface for coupling CE to MS in negative ion mode [21]. Though, corona discharge could be attenuated in our previously developed CE-MS method for anionic metabolic profiling, the employed low-pH separation conditions were not optimal for profiling acidic compounds, especially for the analysis of nucleoside triphosphates, such as ATP, GTP and UTP, which were not detected. The chemical stability of these compounds at low-pH separation conditions may be limited and it was recently proposed by Siegel *et al*. that these compounds should be preferably analyzed at high pH (separation) conditions [2]. Given this context and our interest to profile nucleotides in low numbers of mammalian cells, the aim of this work was to develop a highly sensitive sheathless CE-MS method for nucleotide profiling at high-pH separation conditions using ESI-TOF-MS in the positive ion mode, thereby fully circumventing corona discharge.

1. CE-MS method optimization for nucleotide analysis

Prior to assessing the performance of the sheathless CE-MS method for the profiling of nucleotides, three types of volatile BGEs (selected on the basis of the examination of the literature), including ammonium acetate, ammonium carbonate and ammonium bicarbonate, were tested first for the analysis of nucleotides by CE-MS. As a starting point, 12.5 mM of each BGE using different pH values in the range from 8.5 to 10.5 was considered, followed by further optimization of the BGE concentration. All the nucleotides studied were negatively charged during the electrophoretic separation performed in normal polarity mode (i.e., anode at inlet side) with the different BGE conditions. Their detection by TOF-MS was performed in positive ion mode, thereby fully

circumventing corona discharge, by focusing on the signal intensity obtained for the protonated compounds. Optimization of the BGE conditions revealed that 16 mM ammonium acetate with a pH of 9.7 provided most optimal signal intensities, peak shapes and resolution for the nucleotides with acceptable CE currents (~4.1 µA). A representative electropherogram for a 100 nM nucleotide standard mixture is shown in **Figure 1A**, which clearly indicates that very narrow peaks were obtained by sheathless CE-MS under the employed separation conditions. The most intense signal intensities were attained for protonated nucleotides ($[M+H]^+$), whereas very low signal intensities were observed for ammonium and/or sodium adducts.

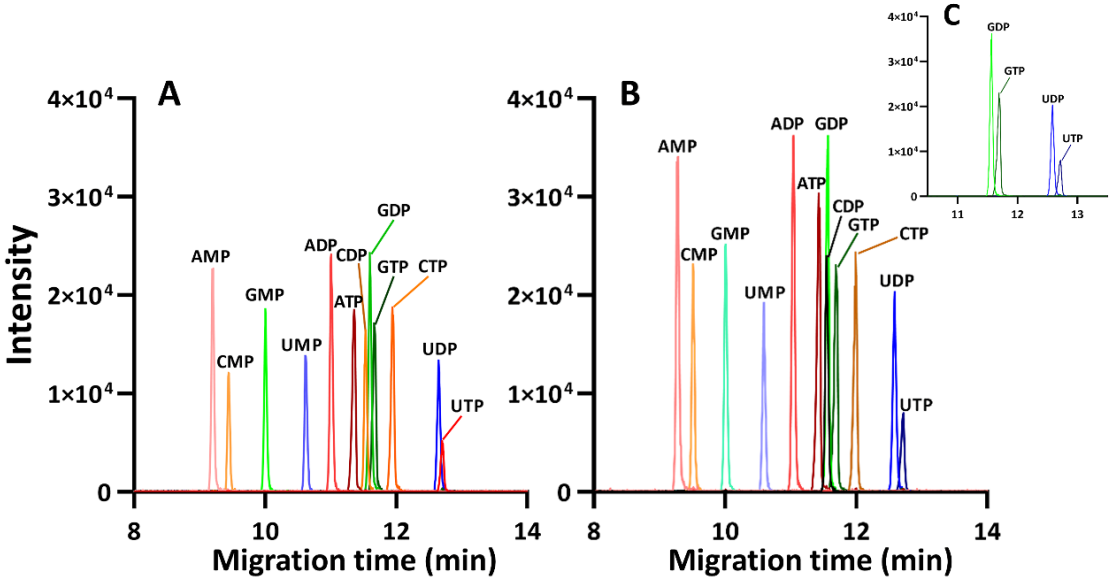

Figure 1. Multiple extracted ion electropherograms obtained for the analysis of a standard nucleotide mixture (100 nM) by sheathless CE-MS in positive ion mode. Separation conditions: BGE, 16 mM ammonium acetate (pH 9.7); Separation voltage: +30 kV; sample injection: 2.0 psi for 30 s. A. Nucleotides dissolved in water; B. Nucleotides dissolved in methanol:water (1:1, v/v); C. Zoom-in of Figure 1B showing the (partial) separation for GDP/GTP and UDP/UTP.

By dissolving the nucleotides in methanol/water (1:1, v/v) instead of water only, and keeping the injection volume (about 6.5 nL) constant, slightly enhanced peak intensities and improved S/N-ratios were obtained as a result of field-amplified sample stacking (**Fig. 1B**). Under the final optimal conditions, plate numbers obtained for the nucleotides ranged from 200,000 to 250,000. These values clearly indicate the high separation efficiency of the proposed sheathless CE-MS method.

Recently, Yamamoto *et al*. have demonstrated that the use of alkaline aqueous ammonia solutions (with a pH above 9.0) as BGE leads to chemical degradation of the outer polyimide capillary coating, causing incidental capillary fractures [22]. In our approach, this is not an issue as the outer part of the capillary, which is the porous tip emitter, does not contain an outer polyimide layer.

2. Analytical performance evaluation

The performance of the sheathless CE-MS method was evaluated by establishing calibration curves, LODs, migration time and peak area precision. Eight-point response curves (based on extracted-ion peak area vs. concentration) were established using working solutions with individual nucleotide concentrations in the range from 5 to 1000 nM. For all nucleotides, apart from UTP, a good linearity was observed with R^2 values above 0.994 (**Supplementary Table S1**). For all analyzed nucleotides, LODs were calculated as the concentrations providing a signal intensity equivalent to S/N of 3 based on an injected concentration of 5 (or 10) nM. The LODs ranged from 0.06 to 1.33 nM, thereby clearly indicating that the proposed sheathless CE-MS method provides very high sensitivity for nucleotides, allowing detection down to 0.4 to 8.6 amol of injected amount. To our knowledge these are the lowest LOD values reported for nucleotides by CE-MS so far. When compared to the *state-of-the-art* ion-pair nanoscale RP-LC-MS method developed for profiling nucleotides and other anionic metabolites [23], which provided absolute LOD values of 100, 250 and 750 amol for AMP, ADP and ATP, respectively, our method showed an improvement in LOD of 19, 104, and 326-fold, respectively, for these compounds. More recently developed ion-pair reversed-phase LC-MS methods yielded LODs in the range from 1 to 10 nM for AMP, ADP and ATP using multiple reaction monitoring and an injection volume of 5 µL [24, 25]. HILIC-MS-based approaches recently developed for nucleotide profiling in various biological samples provided LODs typically in the range from 2 to 100 nM using MS/MS mode and employing an injection volume of 5 µL [26-28]. In this context, the proposed sheathless CE-MS method (used in full scan MS mode only) provided concentration LODs for the studied nucleotides which are comparable to or better than LODs obtained by LC-MS-based approaches employing multiple reaction monitoring. It is anticipated that lower LODs can be obtained by sheathless CE-MS by also using MS/MS and/or by injecting more using in-capillary preconcentration techniques. When considering the obtained LODs in terms of absolute amount injected, it is obvious that the proposed sheathless CE-MS method has very promising characteristics for the sensitive profiling of nucleotides in biomass-limited samples.

For the analysis of nucleotides in HepG2 cells by sheathless CE-MS, a liquid-liquid extraction (LLE) step is required to selectively remove proteins and apolar compounds from the highly polar and charged metabolites in the cell lysate. As sample preparation is often the most crucial step in the entire analytical workflow, we have determined the analytical performance of the sheathless CE-MS method with LLE included. **Table 1** gives an overview of the analytical performance characteristics showing that excellent linearity was observed for all nucleotides with coefficients of determination (R^2) between 0.9943 to 0.9993 over the tested linear ranges. The LODs and LOQs ranged, respectively, from 0.1 to 0.9 nM and from 0.5 to 3.0 nM (**Table 1**), indicating the strong potential of the method to profile nucleotides in low numbers of mammalian cells, but also to potentially profile these compounds in human plasma samples [26].

Table 1 . Analytical performance characteristics of the optimized sheathless CE-MS method including LLE for the analysis of nucleotides

Nucleotides	Linear range (nM)	Slope (n=3) (Mean ± SD%)	R^2 (n=3) (Mean ± SD%)	LOD (nM)	LOQ (nM)	Accuracy (n=4) (Mean ± SD%)	Matrix effect (n=4)(Mean ± SD%)
ADP	3.9 - 2000	1.804 ± 0.055	0.9970 ± 0.0033	0.2	0.5	95.2 ± 2.4	93.6 ± 6.4
AMP	3.9 - 2000	3.424 ± 0.203	0.9943 ± 0.0021	0.5	1.8	100.8 ± 2.9	92.0 ± 8.1
ATP	3.9 - 2000	1.897 ± 0.022	0.9994 ± 0.0006	0.3	1.1	98.4 ± 1.5	93.9 ± 6.2
CDP	3.9 - 2000	1.224 ± 0.016	0.9972 ± 0.0025	0.7	2.4	97.9 ± 2.0	96.4 ± 7.8
CMP	15.6 - 2000	2.064 ± 0.259	0.9952 ± 0.0026	0.5	1.6	102.0 ± 2.9	90.9 ± 8.6
CTP	3.9 - 2000	1.503 ± 0.201	0.9978 ± 0.0007	0.1	0.5	102.4± 4.3	94.7 ± 9.8
GDP	3.9 - 2000	1.565 ± 0.234	0.9960 ± 0.0034	0.4	1.4	96.1 ± 2.3	91.9 ± 10.0
GMP	3.9 - 2000	2.503 ± 0.221	0.9995 ± 0.0005	0.4	1.2	94.1 ± 1.2	92.2 ± 6.9
GTP	3.9 - 2000	1.416 ± 0.115	0.9966 ± 0.0029	0.7	2.4	90.7 ± 0.8	94.9 ± 6.3
UDP	7.8 - 2000	1.026 ± 0.035	0.9977 ± 0.0011	0.5	1.6	99.5 ± 1.1	92.9 ± 5.2
UMP	3.9 - 2000	2.156 ± 0.170	0.9976 ± 0.0019	0.9	3.0	99.1 ± 3.5	96.3 ± 8.0
UTP	7.8 - 2000	0.472 ± 0.011	0.9988 ± 0.0009	0.2	0.5	99.1 ± 7.2	95.1 ± 4.7
ATP ^{15}N5	NA	NA	NA	NA	NA	NA	NA
GMP ^{15}N5	NA	NA	NA	NA	NA	NA	NA

Precision of the sheathless CE-MS method for nucleotide analysis was assessed based on the repeated analyses of samples prepared at the intermediate concentration level (250 nM). Intra-day RSD values (*n*=4) for peak areas and migration times of all the analytes were better than 8.40% and 1.99%, respectively, while inter-day RSDs (*n*=12) were below 14.64% and 6.75%, respectively (**Table 2**). By using relative migration times (RMT) instead of migration times, inter-day RSD values for RMTs were below 1.10%. Peak area ratios were calculated for all nucleotides with inter-day RSD values lower than 9.5% (**Table 2**). Even without internal standard correction, acceptable RSD values (i.e. below 14.64%) for inter-day peak areas were obtained by the sheathless CE-MS method. Next, accuracy was investigated for the proposed method by back calculating the concentration of nucleotides spiked to the cell extract with established calibration curves and comparing the calculated and nominal concentrations (250 nM). The accuracy for every nucleotide included was shown to be between 90.7 to 102.4% (**Table 1**). In order to study the matrix effect, a HepG2 sample matrix extracted from 5000 cells (*n*=4) was prepared in which subsequently the responses (peak areas) obtained for post-extraction spiked nucleotides (and corrected for endogenous nucleotides) were compared with the responses obtained for standards. As shown in **Table 1**, a marginal to negligible matrix effect was observed for all the nucleotides, which is of crucial importance when analyzing nucleotides present at trace levels in biological samples.

Table 2. Precision data (RSD, %) obtained for migration time and peak area of a 250-nM nucleotide mixture by sheathless CE-MS in positive ion mode

Nucleotides	Intra-day MT (RSD ,%) (*n*=4)	Intra-day peak area (RSD, %) (*n*=4)	Inter-day MT (RSD, %) (*n*=12)	RMT (mean) (*n*=12)	Inter-day RMT ratio (RSD ,%) (*n*=12)	Inter-day peak area (RSD ,%) (*n*=12)	Inter-day peak area ratio (RSD ,%) (*n*=12)
ADP	1.78	7.04	5.82	0.91	0.68	8.45	5.96

AMP*	1.50	5.25	4.77	0.99	0.53	12.80	4.37
ATP	1.91	7.22	6.43	1.00	0.00	6.98	3.46
CDP	1.87	8.40	6.10	0.96	0.46	8.36	5.24
CMP*	1.51	5.10	4.90	1.02	0.65	12.16	5.76
CTP	1.99	7.05	6.75	1.06	0.32	8.14	5.38
GDP	1.59	8.05	5.32	0.90	1.10	9.65	6.72
GMP*	1.28	4.87	4.23	1.00	0.01	14.64	2.59
GTP	1.78	7.91	6.01	0.98	0.41	8.23	1.66
UDP	1.72	7.20	5.70	0.99	0.74	7.28	3.74
UMP*	1.34	6.16	4.39	1.06	0.16	10.42	7.41
UTP	1.89	6.84	6.48	1.09	0.15	9.05	9.44
ATP ^{15}N5	1.91	7.67	6.42	NA	NA	8.64	NA
GMP ^{15}N5	1.29	4.57	4.24	NA	NA	16.51	NA

* Peak areas and migration times of these nucleotides were normalized with isotope-labeled GMP ^{15}N5, whereas the other compounds were normalized with isotope-labeled ATP ^{15}N5 for determining the inter-day RMT and peak area ratio.

3. Profiling nucleotides in low numbers of mammalian cells

The applicability of this method for profiling nucleotides in low numbers of mammalian cells was evaluated using HepG2 cells as a model system. For this, a serial dilution of cell lysate with a methanol/water (8:2, v/v) mixture was performed, yielding a sample range from 50,000 to 500 HepG2 cells per 50 µL, in which then the nucleotides were analyzed by the proposed sheathless CE-MS method. **Figure 2** shows a representative electropherogram obtained by sheathless CE-MS for the analysis of nucleotides in an extract from 10,000 HepG2 cells.

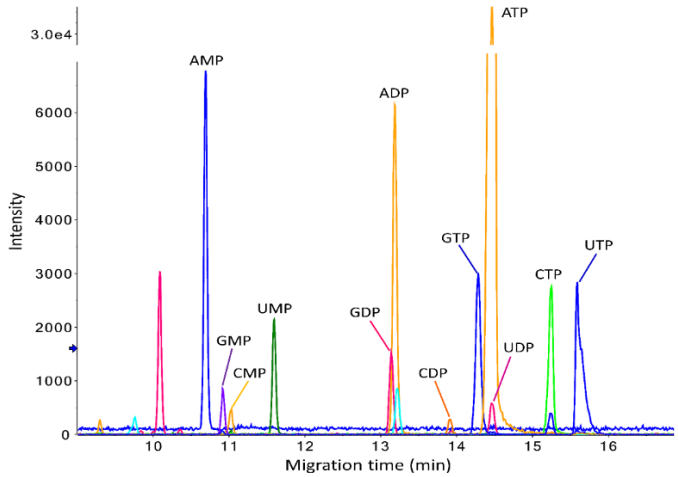

Figure 2. Reconstructed ion electropherograms obtained from the analysis using 10,000 HepG2 cells as the starting material by sheathless CE-MS in positive ion mode using a porous tip emitter. Separation conditions: BGE, 16 mM ammonium acetate (pH 9.7); Separation voltage: 30 kV; Sample injection: 2.0 psi for 30 s.

Figure 3A shows reconstructed electropherograms for seven nucleotides that could be observed in 500 HepG2 cells only under these conditions. **Figure 3B** shows that a linear detector response was obtained for endogenous ATP concentrations when going from 500 to 50,000 HepG2 cells as starting amount. Throughout the analysis of cell lysates at different cell densities, no sign of

degradation or in-source fragmentation was observed for compounds like ATP and ADP. This is important for quantitative studies, as ATP/ADP ratios are used for the determination of the adenylate energy charge (AEC), which is a measure of chemical energy available for metabolic processes. AEC is a common key feature to all cellular organisms and maintains a value between 0.7 and 0.95 in most cell types grown under optimal conditions. The calculated AEC values were between 0.72 and 0.85 for all different cell content concentrations in our work, indicating that the proposed method can be a useful tool in assessing AEC values in biomedical/clinical studies intrinsically dealing with low amounts of mammalian cells. Actually, we would like to propose AEC as an additional metric for evaluating the reliability of the sampling and sample preparation process when working with low amounts of cells.

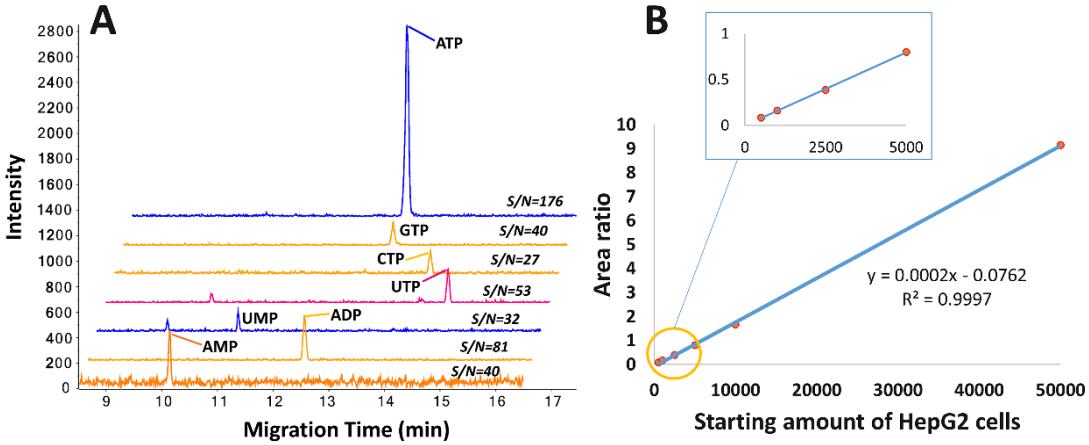

Figure 3. A. Multiple extracted ion electropherograms obtained for nucleotides in an extract from 500 HepG2 cells by sheathless CE-MS in positive ion mode. Separation conditions: BGE, 16 mM ammonium acetate (pH 9.7); Separation voltage: 30 kV; sample injection: 2.0 psi for 30 s. B. Scatter plot generated by plotting the area ratios of endogenous ATP to labeled ATP (ISTD) against corresponding starting numbers of HepG2 cells.

The repeatability of the method for profiling nucleotides in biological samples was demonstrated by analyzing triplicates from the same cell lysate and comparing cell lysate aliquots from different culture dishes using 1000 and 2500 cells as starting amounts in the analytical procedure. **Table 3** clearly indicates that good repeatability could be obtained using both 1000 and 2500 HepG2 cells with intra-dish CV values of no more than 11.4% and 11.6%, respectively. However, for the comparison between different dishes cultured at the same time, overall greater variation was observed for the evaluated metabolites, notably for low abundant metabolites (**Table 3**).

Table 3. Concentrations determined for some nucleotides in extracts from 1000 and 2500 HepG2 cells by sheathless CE-MS. Intra-dish refers to analyzing nucleotide concentrations from the same cell lysate extract, whereas inter-dish refers to analyzing concentrations from three different culture dishes.

Nucleotides	1000 HepG2 cells				2500 HepG2 cells			
	Intra-dish (*n*=3)		Inter-dish (*n*=3)		Intra-dish (*n*=3)		Inter-dish (*n*=3)	
	Concentration (nM)	Precision (RSD, %)	Concentration (nM)	Precision (RSD, %)	Concentration (nM)	Precision (RSD, %)	Concentration (nM)	Precision (RSD, %)

AMP	13.9	11.4	15.9	10.6	32.5	11.6	34.4	6.9
ADP	13.8	1.8	15.7	11.8	37.2	9.8	41.4	13.4
ATP	87.5	0.6	85.5	3.0	228.1	0.2	219.1	3.9
CTP	9.2	7.5	8.5	6.6	22.5	3.4	21.9	3.4
GTP	14.9	4.5	13.9	3.5	29.4	10.3	29.6	19.9
UMP	4.5	10.7	3.5	21.2	10.6	9.1	9.5	20.0
UTP	41.2	5.1	39.9	8.2	105.6	3.9	101.3	8.3

The detection sensitivity of the proposed sheathless CE-MS method can be further improved by using in-capillary preconcentration techniques, such as for example transient-isotachophoresis (t-ITP). When using 2 M acetic acid as a leading electrolyte and an injection volume of about 39 nL, improved peak intensities and S/N ratios of nucleotides in an extract from 500 HepG2 cells, as shown for AMP, ADP and ATP, were obtained (**Fig. 4B** compared to **Fig. 4A**). The increase in S/N ratios obtained for AMP, ADP and ATP was 5.75, 3.71, and 6.21 folds, respectively, as compared to the results obtained for these compounds using standard injection. Therefore, the implementation of t-ITP in sheathless CE-MS may be considered for the detection of nucleotides present at trace levels in very low amounts of biological material.

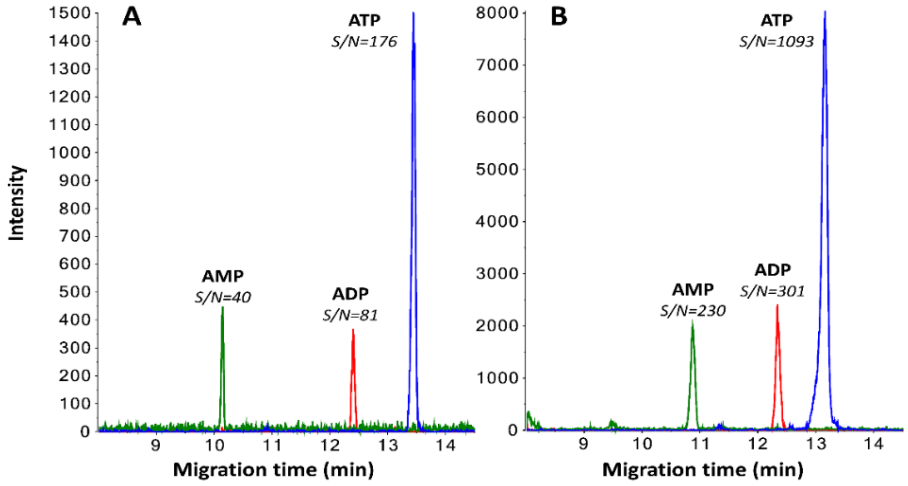

Figure 4. Peaks for AMP, ADP, and ATP obtained from the analysis of 500 HepG2 cells as starting material by sheathless CE-MS in positive ion mode using a porous tip emitter. Separation conditions: BGE, 16 mM ammonium acetate (pH 9.7); Separation voltage: 30 kV; A. Sample injection: 2.0 psi for 30 s. B. 2 M acetic acid as the leading electrolyte. Sample injection: 6.0 psi for 60 s using t-ITP for in-capillary preconcentration.

To assess whether the proposed method could be used for the analysis of other compounds beyond nucleotides, more features were extracted and provisionally annotated with standards or theoretical *m/z* values using the data obtained for 10,000 HepG2 cells as starting material (**Supplementary Fig. S1**). It was noticed that amino acids, such as proline, glutamic acid and aspartic acid, showed satisfactory peak shapes with good intensities. Other key metabolites, such as NAD+, NADH, and FAD, were also detected though with a relatively low detector response. Further optimization of the sheathless CE-MS method is needed in order to improve the detection sensitivity for the latter compounds.

Concluding remarks

In this work, we have developed a sheathless CE-MS method for the highly sensitive and efficient profiling of nucleotides in low numbers of mammalian cells. To fully circumvent corona discharge, which is typically observed in nano-ESI employing negative ion mode detection for acidic compounds, nucleotides were analyzed in the positive ion mode. Sub-nanomolar detection limits were obtained for the nucleotides by sheathless CE-MS by using an injection volume of only about 6.5 nL, corresponding to low attomoles injected into the capillary. Compared to other *state-of-the-art* methods developed for nucleotide profiling, the proposed method provided the lowest LOD values in terms of absolute amounts and clearly shows the value of the approach for analyzing these compounds in low amounts of biological material, as exemplified here for nucleotide profiling in extracts from 50,000 to 500 HepG2 cells only. The detection sensitivity of the method for nucleotide profiling in extracts from HepG2 cells can be further improved by reconstituting the dried extract in 5 µL instead of 30 µL using microvials. In order to apply the proposed method for comparative metabolic profiling studies, a more thorough validation is needed. An aspect not studied in detail in the present work is the injection technique for material-limited samples, i.e. how to get the relevant fraction/compounds of the sample effectively into the CE system. In this context, miniaturization and optimization of injection techniques and sample preparation will be crucial for material-limited metabolomics studies.

Acknowledgements

Wei Zhang would like to acknowledge the China Scholarship Council (CSC, No. 201507060011). Dr. Rawi Ramautar would like to acknowledge the financial support of the Vidi grant scheme of the Netherlands Organization of Scientific Research (NWO Vidi 723.016.003).

References

1. Drouin, N., et al., *Effective mobility as a robust criterion for compound annotation and identification in metabolomics: Toward a mobility-based library.* Anal Chim Acta, 2018. **1032**,178-187.
2. Siegel, D., et al., *Chemical and technical challenges in the analysis of central carbon metabolites by liquid-chromatography mass spectrometry.* J Chromatogr B Analyt Technol Biomed Life Sci, 2014. **966**,21-33.
3. Kuehnbaum, N.L. and P. Britz-McKibbin, *New advances in separation science for metabolomics: resolving chemical diversity in a post-genomic era.* Chem Rev, 2013. **113**(4),2437-68.
4. Lapainis, T., S.S. Rubakhin, and J.V. Sweedler, *Capillary electrophoresis with electrospray ionization mass spectrometric detection for single-cell metabolomics.* Anal Chem, 2009. **81**(14),5858-64.
5. Ramautar, R., et al., *Metabolic profiling of mouse cerebrospinal fluid by sheathless CE-MS.* Anal Bioanal Chem, 2012. **404**(10),2895-900.

6. Onjiko, R.M., et al., *Microprobe Capillary Electrophoresis Mass Spectrometry for Single-cell Metabolomics in Live Frog (Xenopus laevis) Embryos.* J Vis Exp, 2017(130).
7. Onjiko, R.M., et al., *In Situ Microprobe Single-Cell Capillary Electrophoresis Mass Spectrometry: Metabolic Reorganization in Single Differentiating Cells in the Live Vertebrate (Xenopus laevis) Embryo.* Anal Chem, 2017. **89**(13),7069-7076.
8. Kawai, T., et al., *Ultrasensitive Single Cell Metabolomics by Capillary Electrophoresis-Mass Spectrometry with a Thin-Walled Tapered Emitter and Large-Volume Dual Sample Preconcentration.* Anal Chem, 2019. **91**(16),10564-10572.
9. Harada, S., et al., *Reliability of plasma polar metabolite concentrations in a large-scale cohort study using capillary electrophoresis-mass spectrometry.* PLoS One, 2018. **13**(1),e0191230.
10. Soga, T., et al., *Simultaneous determination of anionic intermediates for Bacillus subtilis metabolic pathways by capillary electrophoresis electrospray ionization mass spectrometry.* Anal Chem, 2002. **74**(10),2233-9.
11. Soga, T., et al., *Quantitative metabolome analysis using capillary electrophoresis mass spectrometry.* J Proteome Res, 2003. **2**(5),488-94.
12. Soga, T., et al., *Metabolomic profiling of anionic metabolites by capillary electrophoresis mass spectrometry.* Anal Chem, 2009. **81**(15),6165-74.
13. Liu, J.X., et al., *Analysis of endogenous nucleotides by single cell capillary electrophoresis-mass spectrometry.* Analyst, 2014. **139**(22),5835-5842.
14. McClory, P.J. and K. Hakansson, *Corona Discharge Suppression in Negative Ion Mode Nanoelectrospray Ionization via Trifluoroethanol Addition.* Anal Chem, 2017. **89**(19),10188-10193.
15. Portero, E.P. and P. Nemes, *Dual cationic-anionic profiling of metabolites in a single identified cell in a live Xenopus laevis embryo by microprobe CE-ESI-MS.* Analyst, 2019. **144**(3),892-900.
16. Dodbiba, E., et al., *Detection of nucleotides in positive-mode electrospray ionization mass spectrometry using multiply-charged cationic ion-pairing reagents.* Anal Bioanal Chem, 2010. **398**(1),367-76.
17. Moini, M., *Simplifying CE-MS operation. 2. Interfacing low-flow separation techniques to mass spectrometry using a porous tip.* Anal Chem, 2007. **79**(11),4241-6.
18. Zhang, W., et al., *Utility of sheathless capillary electrophoresis-mass spectrometry for metabolic profiling of limited sample amounts.* J Chromatogr B Analyt Technol Biomed Life Sci, 2019. **1105**,10-14.
19. Atkinson, D.E. and G.M. Walton, *Adenosine triphosphate conservation in metabolic regulation. Rat liver citrate cleavage enzyme.* J Biol Chem, 1967. **242**(13),3239-41.
20. Gulersonmez, M.C., et al., *Sheathless capillary electrophoresis-mass spectrometry for anionic metabolic profiling.* Electrophoresis, 2016. **37**(7-8),1007-14.
21. Sarver, S.A., et al., *Capillary electrophoresis coupled to negative mode electrospray ionization-mass spectrometry using an electrokinetically-pumped nanospray interface with primary amines grafted to the interior of a glass emitter.* Talanta, 2017. **165**,522-525.
22. Yamamoto, M., et al., *Robust and High-Throughput Method for Anionic Metabolite Profiling: Preventing Polyimide Aminolysis and Capillary Breakages under Alkaline Conditions in Capillary Electrophoresis-Mass Spectrometry.* Anal Chem, 2016. **88**(21),10710-10719.
23. Kiefer, P., N. Delmotte, and J.A. Vorholt, *Nanoscale ion-pair reversed-phase HPLC-MS for sensitive metabolome analysis.* Anal Chem, 2011. **83**(3),850-5.
24. Fu, X.R., et al., *Targeted Determination of Tissue Energy Status by LC-MS/MS.* Analytical Chemistry, 2019. **91**(9),5881-5887.
25. Cortese, M., et al., *Validation of a LC/MSMS method for simultaneous quantification of 9 nucleotides in biological matrices.* Talanta, 2019. **193**,206-214.

26. Zhang, G., et al., *Strategies for quantitation of endogenous adenine nucleotides in human plasma using novel ion-pair hydrophilic interaction chromatography coupled with tandem mass spectrometry.* J Chromatogr A, 2014. **1325**,129-36.
27. Teleki, A. and R. Takors, *Quantitative Profiling of Endogenous Metabolites Using Hydrophilic Interaction Liquid Chromatography–Tandem Mass Spectrometry (HILIC-MS/MS)*, in *Microbial Metabolomics: Methods and Protocols*, E.E.K. Baidoo, Editor. 2019, Springer New York: New York, NY. p. 185-207.
28. Teleki, A., A. Sanchez-Kopper, and R. Takors, *Alkaline conditions in hydrophilic interaction liquid chromatography for intracellular metabolite quantification using tandem mass spectrometry.* Analytical Biochemistry, 2015. **475**,4-13.

Supplementary Materials

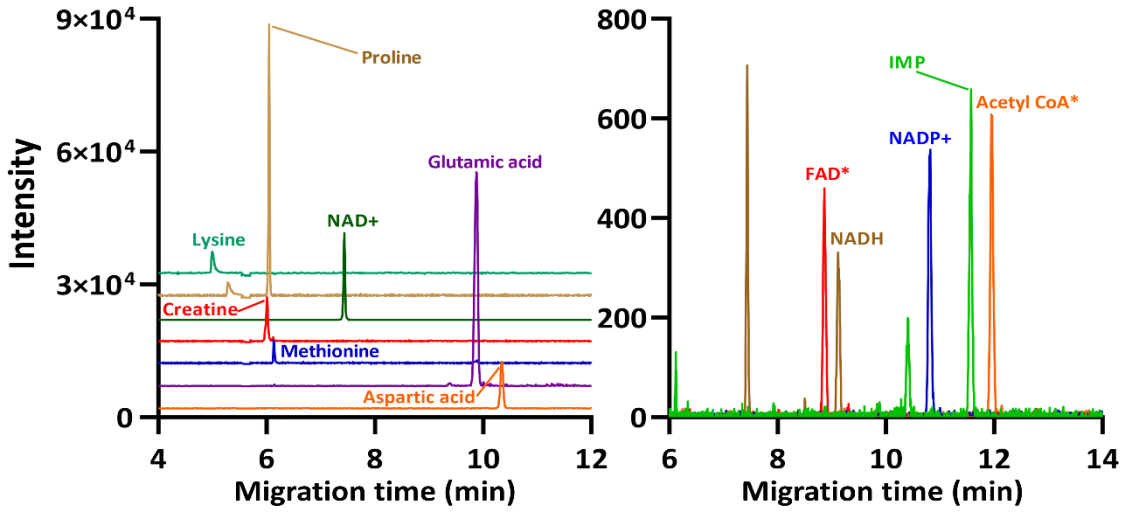

Figure S1. Multiple extracted ion electropherogram obtained from the analysis using 10,000 HepG2 cells as the starting material by sheathless CE-MS in positive ion mode using a porous tip emitter. Separation conditions: BGE, 16 mM ammonium acetate (pH 9.7); Separation voltage: 30 kV; Sample injection: 2.0 psi for 30 s. *Peaks tentatively identified based on accurate *m/z* values (error ≤ 5ppm).

Table S1. Overview of linearity and detection limits obtained for nucleotide standards by sheathless CE-MS in positive ion mode

Nucleotides	Linear range (nM)	Calibration curve*	R^2	LOD (nM)#	LOD (amol)$
ADP	5-1000	y = 3.1364x + 0.0381	0.9948	0.37	2.4
AMP	5-1000	y = 2.2887x + 0.0029	0.9997	0.81	5.3
ATP	5-1000	y = 3.5678x + 0.0115	0.9998	0.36	2.3
CDP	5-1000	y = 2.5117x - 0.018	0.9987	0.96	6.2
CMP	10-1000	y = 1.3989x + 0.0011	0.9998	1.21	7.9
CTP	5-1000	y = 2.9691x - 0.0075	0.9992	0.93	6.0
GDP	5-1000	y = 3.2378x + 0.0234	0.9979	0.67	4.4
GMP	10-1000	y = 3.8133x + 0.0165	0.9986	1.33	8.6
GTP	5-1000	y = 2.9579x + 0.0067	0.9996	0.06	0.4
UDP	5-1000	y = 2.1084x + 0.0086	0.9996	1.17	7.6
UMP	5-1000	y = 1.2213x + 0.0607	0.9986	0.22	1.4
UTP	10-1000	y = 0.9008x + 0.0229	0.9805	1.19	7.7

*^{15}N2-labeled-UMP was used as internal standard

LOD (nM) expressed as concentration in injection solution

$ LOD (amol) expressed as injected amount in CE capillary

Chapter 6

Assessing the suitability of capillary electrophoresis-mass spectrometry for biomarker discovery in plasma-based metabolomics

Based on

Wei Zhang*, Karen Segers*, Debby Mangelings, Ann Van Eeckhaut, Thomas Hankemeier, Yvan Vander Heyden, and Rawi Ramautar

Assessing the suitability of capillary electrophoresis-mass spectrometry for biomarker discovery in plasma-based metabolomics

Electrophoresis (2019)

* Authors contributed equally

Abstract

In metabolomics, CE-MS is a useful analytical technique for the profiling of polar and charged metabolites. However, the actual utility of this approach for biomarker discovery using metabolomics still needs to be assessed. Therefore, a simulated comparative metabolic profiling study for biomarker discovery by conventional CE-MS at low-pH separation conditions was performed, using pooled human plasma samples with spiked biomarkers. In this context, two studies have been carried out in this work. The focus of study I was on comparing two sets of plasma samples, in which one set (class I) was spiked with five isotope-labeled compounds, whereas another set (class II) was spiked with six different isotope-labeled compounds. In study II, the focus was also on comparing two sets of plasma samples, however, in this case the isotope-labeled compounds were spiked to both class I and class II samples but with concentrations which differ by a factor of two between both classes, and with the absence of one compound in each class. In both studies, blank pooled human plasma was used as a quality control sample. The main aim was to determine whether the CE-MS-based metabolomics approach could reveal the spiked biomarkers as the main classifiers, applying two different data analysis software tools (namely, MetaboAnalyst and Matlab). Unsupervised analysis of the recorded metabolic profiles revealed a clear distinction between class I and class II plasma samples in both studies. This classification was mainly attributed to the spiked isotope-labeled compounds, thereby emphasizing the utility of CE-MS in metabolomics for biomarker discovery.

Introduction

Metabolomics offers a new approach to explore changes in patterns for a large number of (endogenous) metabolites in biological media, such as blood, urine and cerebrospinal fluid [1-6]. Currently, a wide range of advanced analytical separation techniques are used for metabolic profiling of biological samples. The complex data sets generated by these analytical tools can be processed by software tools, for example XCMS [7], MZmine [8], MetAlign [9], or SpectConnect [10], and the main output is a peak table with the intensity of each chromatographic or electrophoretic peak, characterized by a specific retention or migration time, respectively, and one or more *m/z* values. Supervised and unsupervised chemometric approaches are often used to get visualization of the relations between the metabolic profiles and to define borders between groups of samples. Global profiling of (endogenous) metabolites in organisms has been vastly explored for its potential application in research areas, such as diagnosis of diseases [1, 3, 6], guidance for personalized medicine [11], and evaluation of therapeutic treatments [12, 13]. Despite the efforts dedicated to metabolomics for biomarker discovery, its impact on recent clinical practice is still rather limited due to various challenges encountered during the analytical process, including study design, sample handling, data acquisition and data analysis [14], which may potentially lead to contradictory results in reported biomarkers. For example, Slupsky *et al*. [15] indicated succinic acid to be among the down-regulated urinary metabolites in ovarian cancer patients, whereas Zhang *et al*. [16] obtained the opposite finding for this compound using a different analytical technique. Therefore, these studies clearly underscore the need for assessing the capability of a given analytical technique for delivering the right biomarkers in metabolomics using preferably multiple data analysis procedures. In principle, each data analysis procedure should provide the same chemical information/output when employing a single analytical technique for metabolic profiling. In this work, we have used MetaboAnalyst and Matlab as two data analysis software tools for analyzing metabolomics data obtained by CE-MS (**Fig. 1**).

CE is a separation technique that is well-suited for the highly efficient profiling of polar and charged metabolites, as compounds are separated according to their charge-to-size ratios. It provides complementary metabolic information compared to chromatography-based techniques. Until now, CE coupled to MS has been utilized for metabolic profiling of a wide range of biological samples in various application fields [17]. However, in comparison to other analytical techniques the use of CE-MS in metabolomics is still underrepresented [18]. CE-MS is often still considered by the scientific community as a rather complicated or not robust technique, in this case specifically the coupling of CE to MS, and often not fulfilling the criteria of repeatability and sensitivity for metabolomics studies.

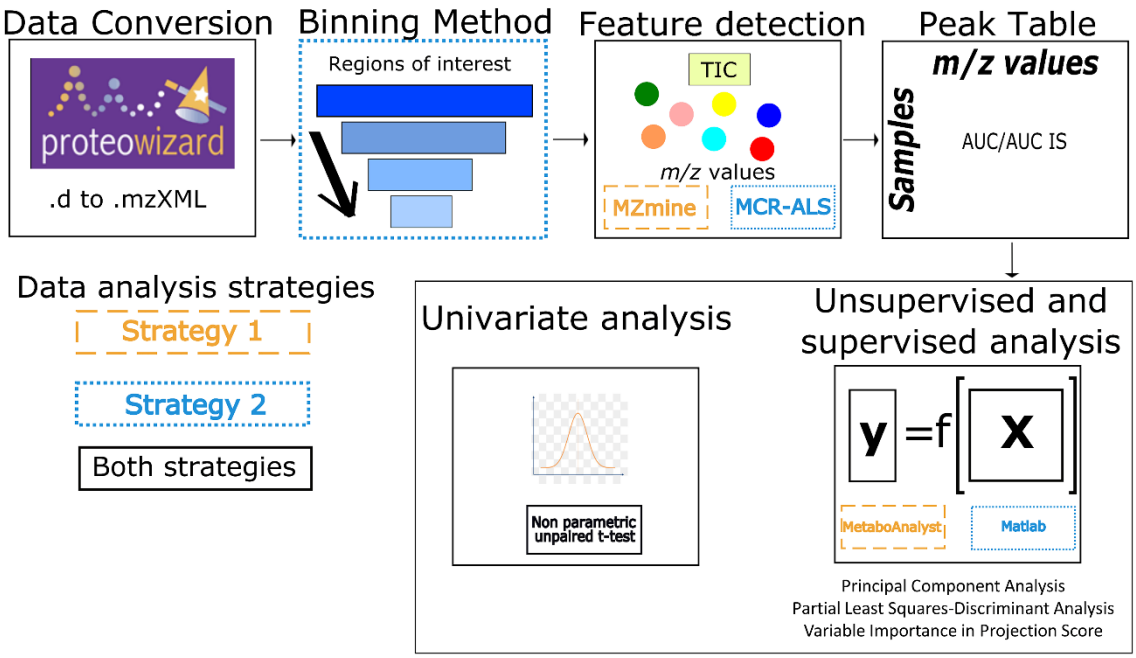

Figure 1. Overview of the data analysis tools used in this study. The tools of the first data analysis strategy are shown in orange (stripes) while in blue (dots) those for the second strategy are given. The workflow is similar starting with the data conversions to a readable file. Subsequently, data compression is needed for the MCR-ALS feature detection of the second strategy. After selecting the features a peak table is generated containing the corrected peak areas for each sample. The generated peak table can be further investigated using univariate, unsupervised and supervised analysis to discover potential biomarkers.

Over the past years, various studies have clearly indicated the long-term performance of CE-MS for metabolomics and peptide profiling studies [19-21]. For example, the group of Soga and co-workers, who introduced the first CE-MS methods for metabolomics in 2003 [22], has recently assessed the long-term performance of CE-MS for metabolic profiling of more than 8000 human plasma samples from the Tsuruoka Metabolomics Cohort Study over a 52-month period [20]. The study provided an absolute quantification of 94 polar metabolites in plasma with a similar or better reproducibility than other analytical platforms employed for large-scale metabolomics studies. The issue of migration-time repeatability for metabolic profiling studies can be tackled by converting migration times into electrophoretic mobilities, as recently demonstrated by Drouin *et al.* [23]. This group has designed an experimental database for effective mobilities (μ_{eff}) measured for a large variety of charged metabolites, which was successfully implemented for the characterization of metabolites observed by CE-MS in tumor cell samples. Overall, we expect that this approach will be of great value for metabolomics studies, especially for the identification of metabolites when employing a library based on electrophoretic mobilities. Other improvements in CE-MS analyses, such as the use of novel interfaces [24, 25] and multi-segment injection (MSI) [26], have clearly contributed to the potential of CE-MS of becoming a sensitive and high-throughput technique for metabolic profiling studies. Apart from increasing sample throughput, the MSI approach, developed by the group of Britz-McKibbin [26], could also be used to distinguish authentic

metabolite features from spurious signals in biological samples. The latter could readily be annotated based on their temporal signal pattern when using the MSI approach in combination with high-resolution tandem mass spectrometry.

Up till now, CE-MS has been used by various research groups for a wide range of metabolomics studies providing useful insights into questions/problems from different fields. Still, it is important to show the actual utility of CE-MS for comparative metabolic profiling studies, especially in order to convince the scientific community about the usefulness of this approach for biomarker discovery. An artificial metabolomics study was therefore designed to test the capability of CE-MS in finding the correct biomarkers in a comparative metabolic profiling study. For this, two studies have been carried out, in which the focus of study I was on comparing two sets of plasma samples, i.e. class I was spiked with five isotope-labeled compounds, whereas class II was spiked with six different isotope-labeled compounds. In study II, the focus was also on comparing two sets of plasma samples, however, in this case the isotope-labeled compounds were spiked to both class I and class II samples but with concentrations which differ by a factor of two between both classes, and with the absence of one compound in each class. Blank pooled human plasma (without spiking) was used as quality control (QC) sample to assess the performance of CE-MS over time. Overall, the strategy outlined in this paper could be considered as an approach to validate a (conventional) CE-MS method for metabolomics studies.

Materials and Methods

1. Chemicals and reagents

HPLC grade methanol and acetonitrile were obtained from Actu-All Chemicals (Oss, the Netherlands). HPLC grade chloroform was provided by Biosolve Chemicals (Valkensweerd, the Netherlands). Acetic acid (99-100%) and sodium hydroxide were purchased from VWR (Amsterdam, the Netherlands). Ammonium hydroxide (28-30%) was acquired from Acros Organics (Amsterdam, the Netherlands). Water in this work was produced by a Milli-Q® Advantage A10 Water Purification System from Millipore (Amsterdam-Zuidoost, the Netherlands). The standards of eleven ^{13}C, ^{15}N and/or D-isotope-labeled amino acids were purchased from Cambridge Isotope Laboratories (Apeldoorn, the Netherlands). In Study I, DL-phenyl-D5-alanine from CDN ISOTOPES (Nieuwegein, the Netherlands) was used as the internal standard (IS). In study II, an L-methionine sulfone-containing solution from Human Metabolome Technologies (Leiden, the Netherlands) was employed as IS. All compounds were dissolved in a mixture of water:acetonitrile (95:5, containing 0.5% v/v formic acid) and subsequently diluted to desired concentrations with water (see **Tables 1 and 2**). A solution of acetic acid (10% v/v in water, pH=2.2) was employed as BGE.

Table 1. An overview of the design of class I and class II plasma samples for study I (IS: DL-phenyl-D5-alanine). Sample 1 within class I is prepared by spiking Mix 1 to the blank plasma sample, and sample 2 within class I is prepared by spiking Mix 2 to the plasma sample, etc.

Compound	*m/z*	Concentration (µM)					
		Class I (*n*=6 samples per mix)					
		Mix 1	Mix 2	Mix 3	Mix 4	Mix 5	
L-Isoleucine (^{13}C; ^{15}N)	134.099	40	36	50	40	36	
L-Asparagine ($^{13}C2$;$^{15}N2$)	139.066	100	80	90	80	80	
L-Glutamine ($^{13}C2$)	149.081	20	15	30	30	30	
L-Lysine (4,4,5,5-D4)	151.135	10	10	15	12	15	
L-Tryptophan ($^{13}C11$;$^{15}N2$)	218.124	40	48	50	36	50	
		Class II (*n*=5 samples per mix)					
		Mix 6	Mix 7	Mix 8	Mix 9	Mix 10	Mix 11
Creatinine (N-methyl-D3)	117.088	40	30	45	50	45	50
L-Valine (D5)	126.134	5	7.5	10	7.5	10	7.5
L-Asparagine (2,3,3-D3)	136.078	100	80	90	100	80	90
L-Glutamine (2,3,3,4,4-D5)	152.11	100	90	100	80	90	80
L-Lysine ($^{13}C6$)	153.129	40	35	50	45	35	40
L-Glutamic acid ($^{13}C5$;D5;^{15}N)	159.103	40	45	30	50	30	40

2. Plasma sample preparation

Pooled human plasma, anti-coagulated with citrate, was obtained from Sanquin Blood Bank (Leiden, the Netherlands). For protein precipitation, methanol was added to pooled human plasma at a 5:1 ratio. The plasma/methanol mixture was vortexed for 1 min at room temperature before centrifugation at 16100 g at 4 °C for 10 min. Subsequently, 120 µL of the supernatant was transferred to an Eppendorf tube for liquid-liquid extraction, for which 300 µL methanol, 450 µL chloroform, 140 µL water, 50 µL internal standard solution (200 µmol/L for L-methionine and 60 µ µmol/L for DL-phenyl-D5-alanine), and 50 µL isotope-labeled compounds mix for classes I and II (50 µL water was used for the QC samples) were used to extract polar metabolites. **Tables 1 and 2** provide an overview of how the samples were prepared for each class of plasma samples within study I and II, respectively. The samples were vortexed for 2 min and then centrifuged at 16100 g at 4 °C for 10 min. 500 µL of the supernatant was centrifugally filtered using a 5 kDa cutoff filter (Millipore) at 12000 g at 4 °C for 1.5 h to further remove proteins. The filtered sample was evaporated in a CentriVap Concentrator (Labconco) and stored at -80 °C. The dried extract was reconstituted in 50 µL water prior to CE-MS analysis. Standards for calibration curves were generated by spiking the pooled human plasma with the mix of isotope labeled compounds at 10, 20, 40, 60, 80 and 100 µM, respectively.

Table 2. Design of class I and class II plasma samples for study II (IS: L-methionine sulfone).

Compound	*m/z*	Class I (*n*=30 samples)	Class II (*n*=30 samples)
		Concentration (µM)	Concentration (µM)
L-Lysine (4,4,5,5-D4)	151.135	20	10
L-Asparagine ($^{13}C2$;$^{15}N2$)	139.066	100	50
L-Isoleucine (^{13}C; ^{15}N)	134.099	20	40
L-Tryptophan ($^{13}C11$;$^{15}N2$)	218.124	0	20

L-Glutamic acid (^{13}C5;D5;^{15}N)	159.103	20	40
L-Asparagine (2,3,3-D3)	136.078	40	20
L-Valine (D5)	126.134	5	10
L-Lysine (^{13}C6)	153.129	10	20
L-Glutamine (2,3,3,4,4-D5)	152.110	20	0
L-Glutamine (^{13}C2)	149.081	10	20
Creatinine (N-methyl-D3)	117.088	10	20

3. CE-MS analysis

All fused-silica capillaries used were 70 cm in length with an internal diameter of 50 µm and obtained from BGB Analytik (Harderwijk, the Netherlands). Prior to first use a newly installed capillary was conditioned using the following rinsing steps: water for 2 min at 5 bar, 0.1 M sodium hydroxide for 10 min at 5 bar, water for 2 min at 5 bar, and BGE for 2 min at 5 bar. The samples were injected hydrodynamically at 50 mbar for 20 s, which corresponds to about 1.2% (~17 nL) of the total capillary volume.

The analyses were conducted on an Agilent 7100 CE instrument hyphenated to an Agilent 6230 Time of Flight (TOF) mass spectrometer (Agilent Technologies, Santa Clara, California), equipped with an ESI source via a co-axial sheath-liquid interface. The CE-MS approach used in this work was based on the work from Drouin *et al.* [23]. The sheath-liquid, consisting of isopropanol/water (1:1, v/v) and acetic acid (200 µL added to a final volume of 100 mL sheath liquid), was delivered at a final flow-rate of 5 µL/min by an Agilent 1260 Infinity II Isocratic Pump (Agilent Technologies) using a 1:100 splitter. A voltage of 30 kV was used for electrophoretic separation and detection was performed in positive MS mode. The MS parameters were as follows: drying gas was set at 100 °C with a flow-rate of 11 L/min, and the nebulizer gas at 0 psi. The capillary voltage was 5500 V, and the fragmentor, skimmer, and OCT1 RF voltages were set at 100, 50 and 150 V, respectively. The full scan MS acquisition covered the mass range from 50 to 1000 *m/z* at an acquisition rate of 1.5 spectra/s, which was controlled and monitored with MassHunter version B05.01 (Agilent Technologies). Between consecutive biological sample analyses, the capillary was flushed as follows: water for 30 s at 5 bar, methanol for 1 min at 5 bar, water for 30 s at 5 bar, 10% ammonium hydroxide for 1 min at 5 bar, water for 30 s at 5 bar and BGE for 2 min at 5 bar. The CE-MS data were stored as .d files.

The capillary cassette was thermostated at 22 °C and the sample tray maintained at 10 °C by means of a Julabo F12 circulator temperature controller (Boven-Leeuwen, the Netherlands). To assess the repeatability of CE-MS for metabolic profiling of plasma, the RSD for migration time and peak area were determined for 19 endogenous metabolites in a QC sample, which was analyzed in 16 consecutive runs. During the analysis of the individual plasma samples, every ten runs a QC sample was analyzed. In total 23 QC samples were analyzed in each study.

4. Data processing and chemometric analysis

An overview of the data analysis, by the software tools used in this study, is shown in **Figure 1**. Each data analysis strategy is described in detail below.

4.1. Strategy 1

The raw data were converted into mzXML format using ProteoWizard and imported into MZmine 2.32 for feature detection. The detailed detection process is listed in **supplementary file S1**. Considering that the peak area calculation function was not ideal in MZmine, the peak areas were calculated in the Data Acquisition module within MassHunter version B05.01 (Agilent Technologies). The peak areas were integrated based on a standard list generated by an untargeted analysis. Peak areas of the detected metabolites were corrected with the corresponding IS peak area (for study I with DL-phenyl-D5-alanine and for study II with L-methionine sulfone), and the peak area ratios were further used in the statistical analysis.

MetaboAnalyst (http://www.metaboanalyst.ca) was used for multivariate analysis, including principal component analysis (PCA) and partial least squares - discriminant analysis (PLS-DA) to identify the spiked markers as "biomarkers" to distinguish "class I" from "class II". Auto-scaling was done prior to PCA to prevent highly responsive metabolites from dominating the model, and prior to PLS-DA to facilitate the discovery of the "spiked biomarkers" [27]. The peak area ratios were also subjected to an unpaired non-parametric test (Wilcoxon rank-sum test, also known as Mann-Whitney U test) within MetaboAnalyst, and false discovery rates (FDR) were calculated to discover if those *m/z* values are significantly different between class I and II. The compounds responsible for distinguishing class I from class II samples were selected using the variable importance in projection (VIP) score employing the criteria of VIP>1 and false discovery rate (FDR)<0.05.

4.2. Strategy 2

As in strategy 1, data was generated in centroid mode at an Agilent CE-TOF-MS instrument and converted to mzXML files with the open-source file converter ProteoWizard. Compared to strategy 1, these files were imported and further analyzed in Matlab™ R2014a (The Mathworks, Natick, MA) instead of MetaboAnalyst. Due to storage requirements, a binning method was necessary to compress the data [28, 29] (**Fig. 1**). The regions-of-interest (ROI) method was used to compress the generated Total Ion Current profile [30]. Here, ROI values are searched among all measurement times in the recorded CE-MS profile. However, different input variables are needed to define an ROI, such as a signal threshold value, mass accuracy and the minimum time interval to be considered as a peak width [30, 31]. In our study, these parameters were set at 1000 for the signal threshold, mass accuracy was set to 0.01 Da and the minimum time to elute a peak was set to 6 s. All parameter values were based on the protocol by Gorrochategui *et al*. [30]. The following step was the feature detection step, which does not make use of MZmine, but is based on

Multivariate Curve Resolution - Alternating Least Squares (MCR-ALS) using the MCR-ALS toolbox [32].

As in strategy 1, peak areas were further integrated in the Data Acquisition module within MassHunter version B05.01 (Agilent) and corrected with the corresponding IS peak area (for study I with DL-phenyl-D5-alanine and for study II with L-methionine sulfone). The peak area ratios were further utilized in Matlab™ R2014a (The Mathworks) to perform unsupervised PCA analysis, and supervised PLS-DA analysis. Autoscaling was also applied here as data pre-treatment method. The number of latent variables for the PLS-DA model was chosen based on a five-fold venetian-blind cross validation. Additionally, the PLS-DA model evaluation was based on the error rate, non-error rate and accuracy, based on the cross-validation and calibration results. Finally, compounds mainly responsible for distinguishing class I from class II samples were selected based on the variable importance in projection (VIP) score, with the aim to hopefully trace back the spiked markers and confirm the results of strategy 1. An additional confirmation was performed with the same non-parametric test as in strategy 1. All the *m/z* values resulting in a VIP value above 1 were analyzed with this univariate data analysis. Those resulting in a p-value below 0.05 are significantly different between both classes and are important for distinguishing class I from class II samples.

Results and discussion

1. CE-MS for cationic metabolic profiling

Up till now, most metabolomics studies using CE-MS employed a standard co-axial sheath-liquid interface and low-pH separation conditions to target cationic metabolites (i.e. basic compounds). In this study, this CE-MS approach was used in order to assess its capability of delivering proper chemical information in comparative metabolic profiling studies.

For comparative metabolic profiling, the CE-MS method should provide consistent migration times and peak areas over time. Therefore, pretreated blank pooled human plasma was first analyzed for 16 consecutive runs (lasting around 8 hours in total). The RSD values for migration time, peak area, and peak area divided by IS, of 19 selected endogenous metabolites in this QC sample, were determined and are shown in Table 3. RSD values found are below 5.9%, 9.1%, and 4.5%, respectively. However, the lower RSD values are found for the corrected areas by the IS. For 16 of the 19 selected endogenous metabolites, the RSD values for migration time were below 3%. Therefore, we considered the overall findings acceptable to perform the proposed assessment study.

Table 3. Migration-time and peak-area repeatability (n=16) for selected endogenous metabolites in pooled human plasma obtained by CE-MS. Abbreviations: MT, migration time.

Compound	*m/z* value	MT RSD(%)	Area RSD(%)	Area ratio 1 RSD(%)*	Area ratio 2 RSD(%)*

Glycine	76.039	1.6	8.9	3.4	3.3
Serine	106.05	2.1	8.4	3.1	2.8
Proline	116.071	2.4	6.7	2.9	2
Valine	118.086	2.1	6.6	2.4	1.6
Threonine	120.066	2.3	7.9	3.3	3.1
Creatine	132.077	1.7	7.1	2.9	2.5
Asparagine	133.061	2.3	7.1	2.5	2.1
Ornithine	133.097	1.2	7.7	2.8	2.5
Glutamine	147.076	2.3	7.6	2.6	2.2
Glutamic acid	148.06	2.4	6.9	2.9	2.4
Phenyl-D5-alanine (IS2)	171.123	2.4	6.1	NA	NA
Arginine	175.119	1.3	7.2	3.5	3
L-Methionine Sulfone (IS1)	182.048	2.7	6.6	NA	NA
L-Alanine	90.055	1.8	8.2	3.6	3
L-Isoleucine	132.102	2.1	4.4	4.2	3
L-Leucine	132.102	2.2	5.9	2.3	1.1
L-Lysine	147.113	1.2	7.4	2.6	2
L-Methionine	150.058	2.3	9.1	4.3	4.5
L-Histidine	156.077	1.4	6.5	2.4	2.4
L-Phenylalanine	166.086	2.4	6.1	2.8	1.5
L-Tyrosine	182.081	2.5	6.9	4	3.3

* Area ratio 1 is representing the corrected areas for the first internal standard, L-Methionine Sulfone. The second internal standard is Phenyl-D5-alanine and the correction for this internal standard resulted in the RSD values of area ratio 2.

2. Suitability of CE-MS for metabolic profiling of human plasma

To assess whether the CE-MS method for cationic metabolic profiling has the capability to deliver proper chemical information in biomarker discovery studies, a metabolomics study was simulated. For this purpose, isotope-labeled compounds were used as "spiked biomarkers", while the capability of CE-MS to trace them back as biomarkers was examined. The selected isotope-labeled compounds included diverse chemical structures and were evenly spread over the analysis time. Another requirement was that the unlabeled form could be observed with a good detection sensitivity by CE-MS. Prior to performing the simulation study, some performance metrics of CE-MS for the analysis of the selected isotope-labeled compounds were determined. Special focus was on the accuracy of the method. The accuracy was determined comparing the spiked concentrations of the isotope-labeled compounds, with those experimentally estimated using calibration curves. The accuracy for all labeled compounds was found to be in the range of 85% to 115% (**Supplementary Table S1**).

Study I (**Table 1**) focused on analyzing three sets of plasma samples, i.e. class I is spiked with five isotope-labeled compounds, class II is spiked with six different isotope-labeled compounds, and set three consists of blank pooled human plasma (used as QC). In order to mimic a comparative metabolomics study, samples were constructed in a way as indicated in **Table 1**, in which the (introduced) concentration differences for the spiked compounds between the plasma samples can be found. In metabolomics, it is important to include QC samples to provide information about the robustness of the method [33] and to mimic the sample composition, qualitatively and

quantitatively [34]. Study II focused on more subtle differences by spiking the 'markers' in both groups with concentrations which differ by a factor 2 between both classes (**Table 2**), and with the absence of one compound in each class. For comparative metabolic profiling only compounds with RSD values for migration time and corrected peak area below 5 and 30%, respectively, as calculated for each class including QC samples (n=23), were considered for data analysis as those with higher values may be considered as spurious signals [35]. **Supplementary Figure S1** shows extracted ion electropherograms obtained by CE-MS for the analysis of the spiked compounds in plasma samples of Group 2, Study II. **Supplementary Figure S2** shows extracted ion electropherograms obtained for the analysis of selected endogenous compounds in a QC sample by CE-MS (**Supplementary figure S2A**) including a mass spectrum for the same time window after noise subtraction (**Supplementary figure S2B**).

2.1. Data analysis for study I

The design of this first study introduced two groups of metabolites into individual classes, so it was merely the absence/presence of differences that needed to be distinguished. The whole corrected data matrix for the IS, including all the samples, which differs in composition of the mixtures mentioned in **Table 1**, are used for further data-analysis.

The first feature detection approach with MZmine (from strategy 1) resulted in more than 100 features. A feature is defined as a given mass-to-charge number with a defined migration time and intensity. Manual examination was then introduced to exclude falsely identified features, resulting in 70 features with peak heights above 1000. Except for the 11 compounds used for spiking, all the corrected peak areas detected in QC samples and class I and II samples showed variation far below 30% in RSD.

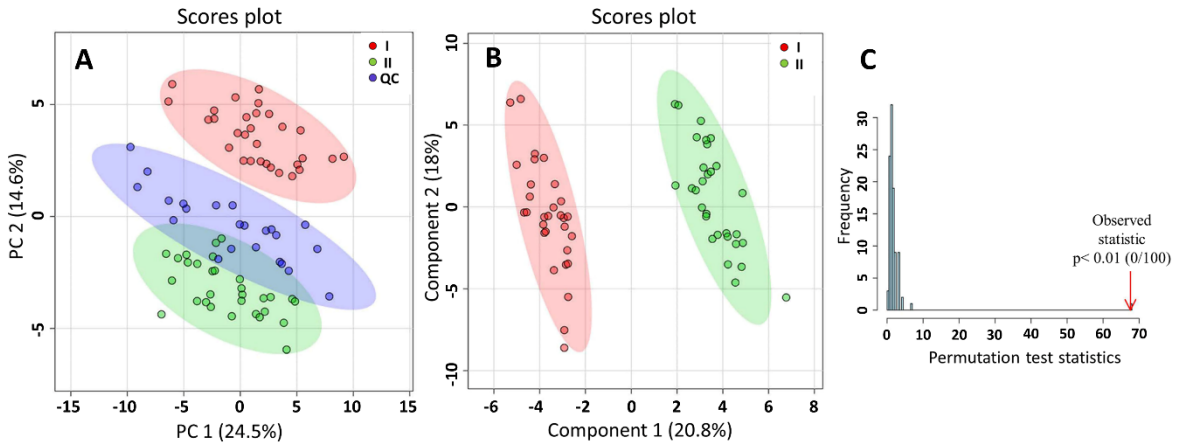

Figure 2. Multivariate results for study I obtained with MetaboAnalyst 4.0. (A) PC1-PC2 score plot for the area corrected by the IS. ●, ● and ● symbols represent samples of class I, class II and QC group, respectively. The elliptic areas represent the 95% confidence regions; (B) PLS-DA scores plot. ● and ● symbols represent samples of class I and II, separately; (C) Permutation test results of the PLS-DA model (statistical test: separation distance (B/W)), number of permutations set at 100.

Strategy 2 does not need alignment of the peaks and is therefore suitable for CE data where, especially the late-migrating analytes, may experience significant migration shifts between samples [31]. 67 features were investigated, resulting in the parameters for the best MCR-ALS model, with an explained variance of 99.1% and an LOF value of 9.3%. For 67 resolved compounds, which can be related to endogenous metabolites or spurious markers, the RSD values for corrected peak areas and migration times were maximally 29.0% and 3.8%, respectively.

PCA was first conducted to investigate relations between groups. Auto-scaling was adopted as data-pretreatment to strip away the dominance of highly responsive/abundant metabolites and to render all metabolites equally important. PCA plots thus generated from study I, using both data-analysis approaches, are displayed in **Figures 2A and 3A**. Good separation of the three groups was observed in both cases. However, **Figure 3A** will result in better separation of the groups, which may be the result of a different number of features in the **X**-matrix resolved by another feature selection method. It is worth noticing that samples in all groups in both PCA plots sprawled mainly along PC1, suggesting that most variation could be explained by the instrumental drift, while the difference between the groups was along PC2. However, no QC correction was performed because of the lack of spiked markers in the QC samples, which are pooled human plasma samples. The two spiked groups were well separated in **Figure 3B**. Then a supervised analysis is performed to build a classification model and to identify the features responsible for the classification.

PLS-DA is a commonly used classification method in metabolomics studies, because of its ability to identify biomarkers from the loadings of the model [29]. In the first data analysis strategy with MetaboAnalyst, a five-component PLS-DA model was established based on the leave-one-out cross validation (LOOCV) results. The obtained PLS-DA plot is shown in **Figure 2B**. The LOOCV parameters, R^2=0.994 and Q^2=0.979, indicated an excellently fitting and predictive PLS-DA model. In order to prevent PLS-DA from overfitting the data, the established model was validated by performing a permutation test to determine whether differences observed between groups are significant [36, 37]. In each permutation, a PLS-DA model is established between the data (**X**) and the permuted class labels (**y**), utilizing the previously determined optimal number of components. Then the ratio of the between-group sum of the squares and the within-group sum of squares, indicated as B/W-ratio, is calculated for the class assignment predictions of each PLS-DA model built. These ratios can be plotted in a histogram known as "the distribution of random class assignments" [36]. If the B/W ratio of the original class assignment is part of this distribution, the differences between the two class assignments cannot be deemed significant. In the permutation test in strategy 1, the class assignment was permuted 100 times (histogram shown in **Fig. 2C**). The bar pointed out by the arrow represents the original sample. A p-value below 0.01 in 100 permutations means that not even once (<0.01*100) did the permutated data yield better performance (higher B/W) than the original label, suggesting the significant difference between these two classes.

The second data analysis approach resulted in a less complex PLS-DA model with only one latent variable, based on the values for the non-error rate and the not-assigned samples. The PLS-DA model was evaluated by five-fold venetian blind cross-validation instead of LOOCV. Good merits of the model were demonstrated with an excellent predictive ability of 100% accuracy and a zero-error rate. Comparing the two PLS-DA models shows that a simpler model was obtained with Strategy 2, which is the result of the better separation of the two classes observed in the unsupervised PCA plot in **Figure 3A**.

The validation of supervised models is often lacking in metabolomics studies [28, 29, 38, 39]. The validation of the established models in both strategies was performed with cross-validation, LOOCV or five-fold venetian blind cross-validation, respectively. These cross-validation approaches are often conducted when only a limited number of samples are involved, as in the present study, but it was also reported that this approach may have the risk of over-fitting, especially LOOCV [29].

VIP scores are often applied to select variables that are important in the projection in PLS-DA models and for the differentiation of the groups. A variable with a VIP value above 1.0 may be considered important [40]. Data analysis strategy 1 revealed 17 features and strategy 2 revealed 16 features (**Supplementary Table S2**) with VIP scores above 1.0. In the results from both data analysis strategies, the 11 spiked "markers" were detected with VIP scores above 2.0. The false discovery rates (FDR) were obtained from the unpaired non-parametric test in order to assess the incidence of false positives. All 17 features had FDR values below 0.05 (data not shown), indicating that these features can indeed be regarded as potential "markers".

The second data analysis strategy also took into consideration the results generated from the non-parametric test to confirm whether the results of the VIP score for the defined features were significantly different for comparing class I with class II, and it resulted in p-values below 0.0001 for all 16 *m/z* values. Furthermore, the PC1-PC2 loadings plot (**Fig. 3C**) showed similar findings as the statistical tests, i.e. five extra features (9, 13, 14, 20, 21), apart from the 11 spiked compounds are among the highest absolute loadings, indicating their contribution to the group classification. Among these detected features, *m/z* 158.101 showed a comparable VIP score to the rest of the spiked features in data analysis strategy 2. The individual standard solutions of the spiked compounds were injected and analyzed in an attempt to determine the source of feature *m/z* 158.101. **Figure 4** clearly shows that *m/z* 158.101 and *m/z* 159.103 are detected at the same migration time, thereby suggesting that *m/z* 158.101 could potentially be another labeled form of the same original compound (L-Glutamic acid). The reason why this feature was not detected in strategy 1 is that the peak height of *m/z* 158.101 did not always meet the peak height threshold of 1000, and got omitted from the feature list by the filtering function within MZmine.

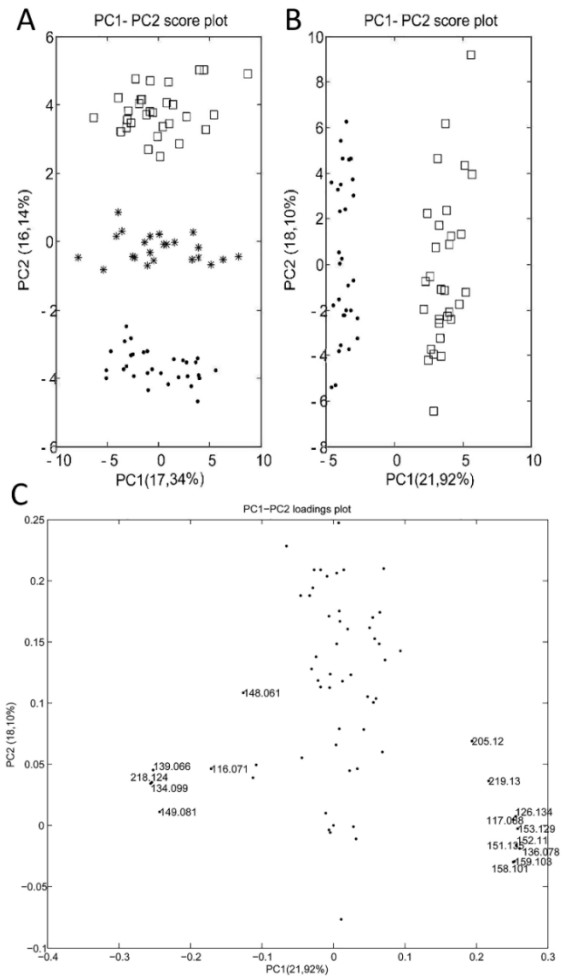

Figure 3. (A) PC1-PC2 score plot obtained for the **X** matrix of study I of the second data analysis strategy using internal standard correction and autoscaling; Quality Control samples are represented by stars; Class I by dots and Class II by squares; (B) PC1-PC2 score plot for the two groups using internal standard correction and autoscaling; (C) PC1-PC2 loadings plot (for numbers see supplementary materials **Table S2**).

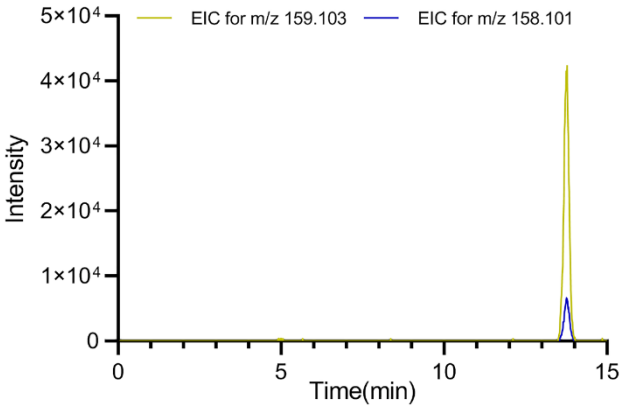

Figure 4. Extracted ion electropherogram obtained by injecting the standard solution of compound *m/z* 159.103, resolving the contaminant *m/z* 158.101.

Apart from the features discussed above, there are still some unaccounted features with a VIP score above 1.0. However, the reason why these variables ended up being "markers" is not clear at this stage. Strategy 2 resulted in 5 unaccounted markers (9, 13, 14, 20, 21), which could be related to an impurity. Strategy 1 resulted in 6 spurious markers (13, 15-19). Strategy 2 resulted in better results for all steps performed in study I. The separation of the different groups was clearer, and the PLS-DA model was much simpler for a better performance and less unknown markers are indicated. In the future, it would be interesting to investigate the importance of the unaccounted markers in more detail.

2.2. Data analysis for study II

Study I showed that spiked "markers" were detected by both data analysis strategies, but it is important to stress that in real-life metabolomics studies, changes in the abundance of metabolites tend to be more subtle than those introduced in study I, where spiked metabolites were present in one group and not in the other. In the second study more subtle differences (**Table 2**) were introduced between the two classes, which anyway still might be larger than the very small metabolic differences that may actually occur between healthy and diseased individuals.

The data from the second study were subjected to the same analysis processes as study I. The application of MZmine resulted in 73 features, among which only 3 features had RSD values above 30%. Those features were deleted prior to further data analysis. The MCR-ALS model in strategy 2 resulted in 90 features with 99.2% explained variance and 9.2% LOF. After removing features with RSD values of peak area ratios over 30%, 84 remained in the data set.

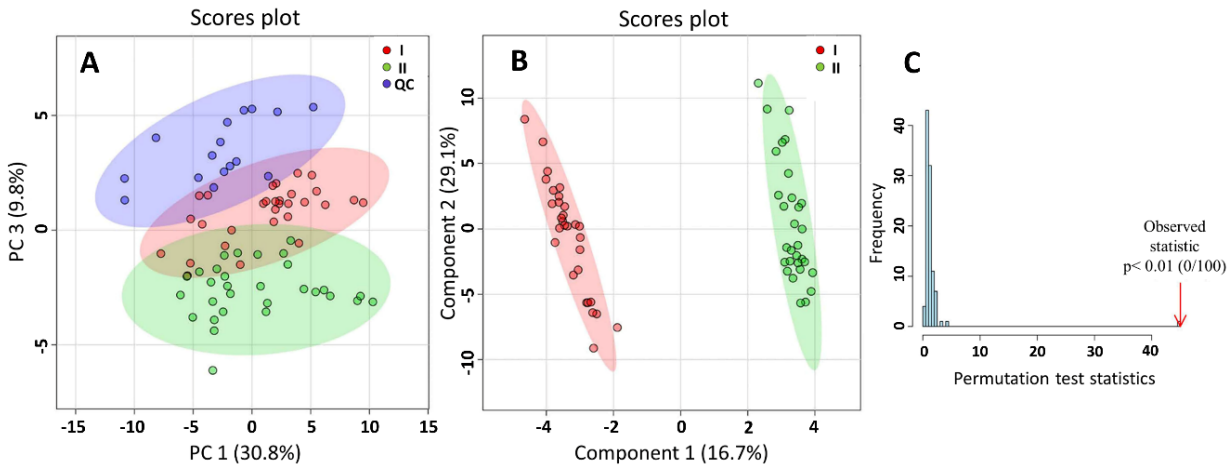

Figure 5. Multivariate results for study II obtained with MetaboAnalyst 4.0. A) PC1-PC3 score plot for the area corrected by the IS. ● , ● and ● symbols represent samples of class I, class II and QC group, respectively. The elliptic areas represent the 95% confidence regions; B) PLS-DA scores plot. ● and ● symbols represent samples of class I and II, respectively; C) Permutation test results of the PLS-DA model (statistical test: separation distance (B/W)), number of permutations set at 100.

PCA score plots were generated after auto-scaling the peak area ratios in both strategies, as shown in **Figures 5A and 6A**. As in study I, the QC samples were distributed along PC1, indicating that the largest variation in the first PC was not related to the group information. The auto-scaled data were well separated along PC3. The PC1-PC2 score plot for only the two spiked groups (**Fig. 6B**) shows that these groups tend to be separated, despite the subtle differences between the profiles.

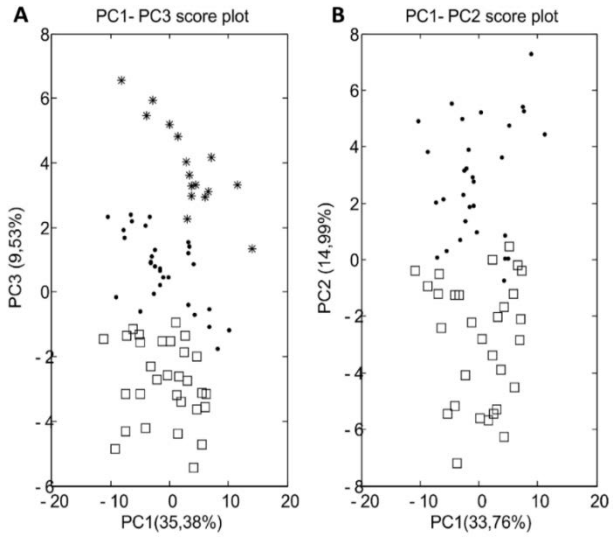

Figure 6. A) PC1-PC3 Score plot of study II obtained with the second data analysis strategy using internal standard correction and autoscaling. Quality Control samples are represented by stars, class I by dots and class II by squares; B) PC1-PC2 Score plot for the two groups using internal standard correction and autoscaling.

A PLS-DA model with five components was established in the first data analysis strategy, using MetaboAnalyst, with parameters R^2=0.998 and Q^2=0.995 acquired by LOOCV. A 100-permutations test using separation distance (B/W) as test parameter, was performed with the observed statistic having a p<0.01 (**Fig. 5C**). The second data analysis strategy resulted in a PLS-DA model with one latent variable, with good predictive ability (100% accuracy and non-error rate) and the model was validated as mentioned above by the same cross-validation method, resulting in good parameters (100% accuracy and non-error rate). Based on the criteria VIP>1.0, and FDR or p<0.05 in the non-parametric tests in both data analysis strategies, the 11 spiked compounds were identified as "biomarkers" in study II (**Supplementary Table S3**). However, again in Strategy 2 the peak with *m/z* value 158.101 was indicated as a biomarker.

Again features with peak heights over 1000 were extracted for further data analysis, because smaller peaks are difficult to measure precisely and might increase the chance of false biomarker identification [41, 42]. For a reliable detection of low abundant metabolites with the current CE-MS set-up, the use of an in-capillary preconcentration technique is needed [43, 44].

In summary, both data processing and analysis strategies resulted in similar findings, despite the small differences observed with the VIP scores. An interesting phenomenon is that the three groups were better separated in the PCA score plots using the second strategy. Additionally, the

better separation may be the result of simpler PLS-DA models in the second strategy compared to the 5 component PLS-DA model in the first strategy. This might be the consequence of the different numbers of *m/z* values included in the **X**-matrix. However, the better separation results between the groups with data analysis strategy 2 makes this method more suitable. However, strategy 2 is more time-consuming and more difficult for an analyst less skilled with data analysis approaches. In real-life cases, targeted metabolomics studies are usually required after untargeted analysis, quantifying the earlier indicated potential "biomarkers", in order to validate and quantify the extent of changes in "biomarkers". The essential message here is that all spiked features could be distinguished by univariate and multivariate analyses of the recorded sheath-liquid CE-MS data. This clearly emphasizes the utility of sheath-liquid CE-MS in metabolomics studies of human plasma samples.

Conclusions and perspectives

In metabolomics, CE-MS has become a useful analytical technique for the profiling of highly polar and charged compounds. In the context of biomarker discovery, it is important to assess whether a given analytical technique provides the proper chemical information and does not result in false positive or negative decisions. In this study, the utility of CE-MS for this purpose was evaluated. Different chemometric analysis procedures were used in order to confirm each other's results and to show that both data analysis strategies give similar information. As shown, the second strategy reveals fewer spurious markers in study I and shows a better separation between the groups in study II. However, the latter approach is more difficult to perform than the use of the MetaboAnalyst software.

Additionally, in this work the two data analysis strategies resulted in very similar outcomes, as expected, and showed that CE-MS in combination with data analysis tools may help to uncover the spiked "biomarkers". Overall, this work emphasized the capability of CE-MS in metabolic profiling studies of human plasma. The usefulness of CE-MS for comparative metabolic profiling may also be evaluated using a comparison or cross-validation with another analytical technique, such as, for example HILIC-MS or NMR spectroscopy. In this case it would be important to focus in such a study on the compounds that can be covered by each analytical technique. For a follow-up study, it would also be interesting to use very small differences in concentration levels for the spiked compounds between sample groups in order to better simulate the actual biological situation in which metabolic differences may be very subtle or to make use of real-life samples.

Acknowledgements

This work was supported by a Travel Grant of the Research Foundation Flanders (FWO) with Grant number V433318N for Karen Segers. Wei Zhang acknowledges the China Scholarship

Council (CSC, No. 201507060011). Dr. Rawi Ramautar acknowledges the financial support of the Vidi grant scheme of the Netherlands Organization of Scientific Research (NWO Vidi 723.016.003).

References

1. Mason, S., C.J. Reinecke, and R. Solomons, *Cerebrospinal Fluid Amino Acid Profiling of Pediatric Cases with Tuberculous Meningitis.* Frontiers in Neuroscience, 2017. **11**(534),1-8.
2. Khamis, M.M., D.J. Adamko, and A. El-Aneed, *Mass spectrometric based approaches in urine metabolomics and biomarker discovery.* Mass Spectrometry Reviews, 2017. **36**,115-134.
3. Stoessel, D., et al., *Promising Metabolite Profiles in the Plasma and CSF of Early Clinical Parkinson's Disease.* Frontiers in Aging Neuroscience, 2018. **10**,1-14.
4. Hernandes, V.V., C. Barbas, and D. Dudzik, *A review of blood sample handling and pre-processing for metabolomics studies.* Electrophoresis, 2017. **38**(18),2232-2241.
5. Andersen, M.-B.S., et al., *Untargeted metabolomics as a screening tool for estimating compliance to a dietary pattern.* Journal of Proteome Research, 2014. **13**(3),1405-1418.
6. Ruiz-Canela, M., et al., *Comprehensive Metabolomic Profiling and Incident Cardiovascular Disease: A Systematic Review.* Journal of the American Heart Association, 2017. **6**(10),1-22.
7. Tautenhahn, R., et al., *XCMS Online: a web-based platform to process untargeted metabolomic data.* Analytical Chemistry, 2012. **84**(11),5035-5039.
8. Pluskal, T., et al., *MZmine 2: modular framework for processing, visualizing, and analyzing mass spectrometry-based molecular profile data.* BMC Bioinformatics, 2010. **11**(1),1-11.
9. Lommen, A., *Data (pre-) processing of nominal and accurate mass LC-MS or GC-MS data using MetAlign*, in *Plant Metabolomics*. 2011, Springer. p. 229-253.
10. Styczynski, M.P., et al., *Systematic identification of conserved metabolites in GC/MS data for metabolomics and biomarker discovery.* Analytical Chemistry, 2007. **79**(3),966-973.
11. Kohler, I., et al., *Integrating clinical metabolomics-based biomarker discovery and clinical pharmacology to enable precision medicine.* Eur J Pharm Sci, 2017. **109s**,S15-S21.
12. van Hasselt, J.G.C., et al., *Disease Progression/Clinical Outcome Model for Castration-Resistant Prostate Cancer in Patients Treated With Eribulin.* CPT: Pharmacometrics & Systems Pharmacology, 2015. **4**(7),386-395.
13. Kim, K.B., et al., *Potential metabolomic biomarkers for evaluation of adriamycin efficacy using a urinary 1H-NMR spectroscopy.* Journal of Applied Toxicology, 2013. **33**(11),1251-1259.
14. Kohler, I., et al., *Analytical pitfalls and challenges in clinical metabolomics.* Bioanalysis, 2016. **8**(14),1509-32.
15. Slupsky, C.M., et al., *Urine metabolite analysis offers potential early diagnosis of ovarian and breast cancers.* Clinical Cancer Research, 2010. **16**(23),5835-5841.
16. Zhang, T., et al., *Identification of potential biomarkers for ovarian cancer by urinary metabolomic profiling.* Journal of Proteome Research, 2012. **12**(1),505-512.
17. García, A., et al., *Capillary electrophoresis mass spectrometry as a tool for untargeted metabolomics.* Bioanalysis, 2017. **9**(1),99-130.
18. Miggiels, P., et al., *Novel technologies for metabolomics: More for less.* TrAC Trends in Analytical Chemistry, 2018.
19. Macedo, A.N., et al., *The Sweat Metabolome of Screen-Positive Cystic Fibrosis Infants: Revealing Mechanisms beyond Impaired Chloride Transport.* ACS Central Science, 2017. **3**(8),904-913.

20. Harada, S., et al., *Reliability of plasma polar metabolite concentrations in a large-scale cohort study using capillary electrophoresis-mass spectrometry.* PloS One, 2018. **13**(1),e0191230.
21. Delles, C., et al., *Urinary proteomic diagnosis of coronary artery disease: identification and clinical validation in 623 individuals.* Journal of Hypertension, 2010. **28**(11),2316-2322.
22. Soga, T., et al., *Quantitative metabolome analysis using capillary electrophoresis mass spectrometry.* Journal of proteome research, 2003. **2**(5),488-494.
23. Drouin, N., et al., *Effective mobility as a robust criterion for compound annotation and identification in metabolomics: Toward a mobility-based library.* Analytica Chimica Acta, 2018. **1032**,178-187.
24. Moini, M., *Simplifying CE–MS operation. 2. Interfacing low-flow separation techniques to mass spectrometry using a porous tip.* Analytical Chemistry, 2007. **79**(11),4241-4246.
25. Höcker, O., C. Montealegre, and C. Neusüß, *Characterization of a nanoflow sheath liquid interface and comparison to a sheath liquid and a sheathless porous-tip interface for CE-ESI-MS in positive and negative ionization.* Analytical and Bioanalytical Chemistry, 2018. **410**(21),5265-5275.
26. Kuehnbaum, N.L., A. Kormendi, and P. Britz-McKibbin, *Multisegment injection-capillary electrophoresis-mass spectrometry: a high-throughput platform for metabolomics with high data fidelity.* Analytical Chemistry, 2013. **85**(22),10664-10669.
27. Ivosev, G., L. Burton, and R. Bonner, *Dimensionality reduction and visualization in principal component analysis.* Analytical Chemistry, 2008. **80**(13),4933-4944.
28. Lindon, J.C., et al., *Summary recommendations for standardization and reporting of metabolic analyses.* Nature Biotechnology, 2005. **23**,833-838.
29. Madsen, R., T. Lundstedt, and J. Trygg, *Chemometrics in metabolomics—a review in human disease diagnosis.* Analytica Chimica Acta, 2010. **659**(1-2),23-33.
30. Gorrochategui, E., J. Jaumot, and R. Tauler, *A protocol for LC-MS metabolomic data processing using chemometric tools.* Protocol Exchange, 2015.
31. Ortiz-Villanueva, E., et al., *Knowledge integration strategies for untargeted metabolomics based on MCR-ALS analysis of CE-MS and LC-MS data.* Analytica Chimica Acta, 2017. **978**,10-23.
32. Jaumot, J., A. de Juan, and R. Tauler, *MCR-ALS GUI 2.0: new features and applications.* Chemometrics and Intelligent Laboratory Systems, 2015. **140**,1-12.
33. Gika, H.G., et al., *A QC approach to the determination of day-to-day reproducibility and robustness of LC–MS methods for global metabolite profiling in metabonomics/metabolomics.* Bioanalysis, 2012. **4**(18),2239-2247.
34. Dunn, W.B., et al., *The importance of experimental design and QC samples in large-scale and MS-driven untargeted metabolomic studies of humans.* Bioanalysis, 2012. **4**(18),2249-2264.
35. Zhang, T. and D.G. Watson, *Evaluation of the technical variations and the suitability of a hydrophilic interaction liquid chromatography-high resolution mass spectrometry (ZIC-pHILIC-Exactive orbitrap) for clinical urinary metabolomics study.* Journal of Chromatography B, 2016. **1022**,199-205.
36. Bijlsma, S., et al., *Large-scale human metabolomics studies: a strategy for data (pre-) processing and validation.* Analytical Chemistry, 2006. **78**(2),567-574.
37. Barberini, L., et al., *Multivariate data validation for investigating primary HCMV infection in pregnancy.* Data in Brief, 2016. **9**,220-230.
38. Goodacre, R., et al., *Proposed minimum reporting standards for data analysis in metabolomics.* Metabolomics, 2007. **3**(3),231-241.
39. Gromski, P.S., et al., *A tutorial review: Metabolomics and partial least squares-discriminant analysis–a marriage of convenience or a shotgun wedding.* Analytica Chimica Acta, 2015. **879**,10-23.
40. Gorrochategui, E., et al., *Data analysis strategies for targeted and untargeted LC-MS metabolomic studies: Overview and workflow.* TrAC Trends in Analytical Chemistry, 2016. **82**,425-442.
41. Kosmides, A.K., et al., *Metabolomic fingerprinting: challenges and opportunities.* Critical Reviews™ in Biomedical Engineering, 2013. **41**(3).

42. Griffin, J.L., *The Cinderella story of metabolic profiling: does metabolomics get to go to the functional genomics ball?* Philosophical Transactions of the Royal Society B: Biological Sciences, 2005. **361**(1465),147-161.
43. Kawai, T., *Recent Studies on Online Sample Preconcentration Methods in Capillary Electrophoresis Coupled with Mass Spectrometry.* Chromatography, 2017. **38**(1),1-8.
44. Jiang, Y., et al., *Recent advances of capillary electrophoresis-mass spectrometry instrumentation and methodology.* Chinese Chemical Letters, 2017. **28**(8),1640-1652.

Supplementary Materials

Supplementary file S1: MZMine 2.32 procedure and settings

Raw data import

Peak detection

- Mass detection:
  - Mass detector: Centroid
  - Noise level: 10^3
  - MS level:1
- Chromatogram builder:
  - Min time span (min): 0.02
  - Min height: 10^3
  - *M/Z* tolerance: 0.01 *m/z* or 12 ppm
  - Retention time: 5-20 min
- Chromatogram deconvolution:
  - Algorithm: Local minimum search
  - Chromatographic threshold: 65%
  - Search minimum in RT range (min): 0.05
  - Minimum relative height: 5%
  - Minimum absolute height: 1000
  - Min ratio of peak top/edge: 2
  - Peak duration range(min): 0.05-0.8

Alignment

- Retention time normalizer:
  - MZ tolerance: 0.01 *m/z* or 12 ppm
  - Retention time tolerance: 15% Relative
  - Minimum standard intensity: 1000
- Alignment: RANSAC Aligner
  - MZ tolerance: 0.01 *m/z* or 12 ppm
  - RT tolerance: 10% Relative
  - RT tolerance after correction: 5% Relative
  - RANSAC iterations 10000
  - Minimum number of points 20%
  - Threshold value: 0.05
  - Linear model ☒
- Filtering: peak list rows filter
  - Minimum peaks in a row: 14
  - Minimum peaks in an isotope pattern: 0
  - *m/z*: auto range
  - Retention time: 5-20 min
  - Peak duration range: 0-0.8
- Gap filling: Same RT and *m/z* gap filler
  - MZ tolerance: 0.005 *m/z* or 12 ppm
- Filtering: duplicate peak filter
  - MZ tolerance: 0.005 *m/z* or 12 ppm
  - RT tolerance: 5%

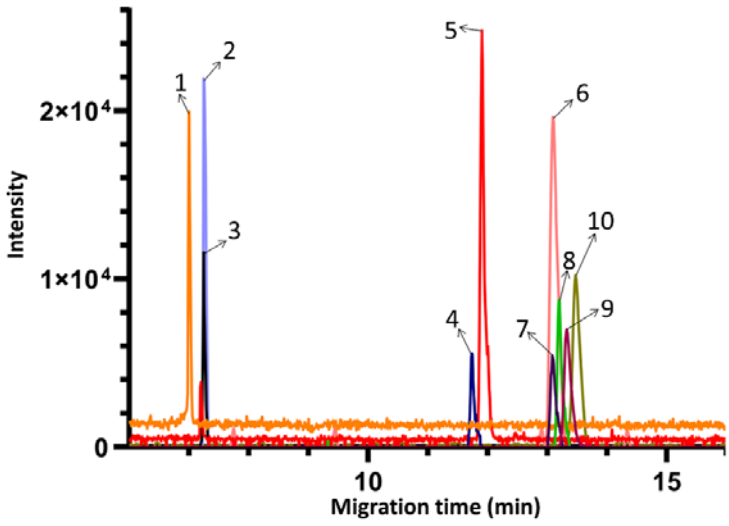

Figure S1. Extracted ion electropherograms obtained by CE-MS for the analysis of spiked compounds in plasma samples from Group 2, Study II. The highlighted compounds are: 1. Creatinine (N-methyl-D3); 2. L-Lysine (^{13}C6); 3. L-Lysine (4,4,5,5-D4); 4. L-Valine (D5); 5. L-Isoleucine (^{13}C; ^{15}N); 6. L-Asparagine (^{13}C2;^{15}N2); 7. L-Asparagine (2,3,3-D3); 8. L-Tryptophan (^{13}C11;^{15}N2); 9.L-Glutamine (^{13}C2); 10. L-Glutamic acid (^{13}C5;D5;^{15}N).

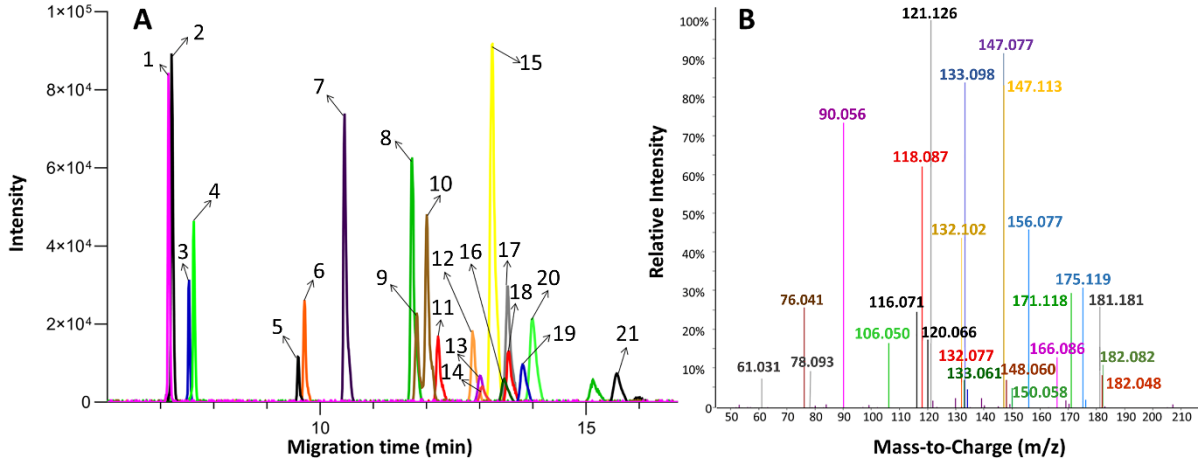

Figure S2. Extracted ion electropherograms. (A) obtained for selected endogenous compounds in a QC sample from Study II by CE-MS, and mass spectrum (B) extracted from the same time window after noise subtraction. The highlighted compounds are as follows: 1. Ornithine (*m/z* 133.098); 2. L-Lysine (*m/z* 147.113); 3. Arginine (*m/z* 175.119); 4. L-Histidine (*m/z* 156.077); 5. Creatine (*m/z* 132.077); 6. Glycine (*m/z* 76.041); 7. L-Alanine (*m/z* 90.056); 8. Valine (*m/z* 118.087); 9. L-Isoleucine (*m/z* 132.102); 10. L-Leucine (*m/z* 132.102); 11. Serine (*m/z* 106.050); 12. Threonine (*m/z* 120.066); 13. Asparagine (*m/z* 133.061); 14. L-Methionine (*m/z* 150.058); 15. Glutamine (*m/z* 147.077); 16. Glutamic acid (*m/z* 148.060); 17. Phenyl-D5-alanine (IS2) (*m/z* 171.118); 18. L-Phenylalanine (*m/z* 166.086); 19. L-Tyrosine (*m/z* 182.082); 20. Proline (*m/z* 116.071); 21. L-Methionine sulfone (IS1) (*m/z* 182.048).

Table S1. CE-MS performance metrics for the analysis of isotope-labeled compounds in plasma. Precision and accuracy of peak areas were based on the analysis of three plasma samples spiked with 40 µM of the labeled compounds.

Metrics	Determination coefficient (R2)*	Precision (%RSD) (n=3)	Accuracy (Mean± SD) (n=3)
Creatinine(N-methyl-D3)	0.9992	8.10%	100.27 ± 5.45
L-Asparagine (^{13}C2;^{15}N2)	0.9909	3.00%	89.37 ± 1.35
L-Asparagine (2,3,3-D3)	0.9973	7.50%	95.60 ± 3.30
L-Glutamic acid (^{13}C5;D5;^{15}N)	0.9995	4.20%	102.40 ± 2.95
L-Glutamine (^{13}C2)	0.9987	5.30%	94.10 ± 1.56
L-Glutamine (2,3,3,4,4-D5)	0.998	5.10%	98.40 ± 1.14
L-Isoleucine (^{13}C; ^{15}N)	0.9992	7.70%	104.27 ± 6.26
L-Lysine (^{13}C6)	0.9991	9.50%	92.93 ± 5.39
L-Lysine (4,4,5,5-D4)	0.9991	12.80%	91.43 ± 8.04
L-Tryptophan (^{13}C11;^{15}N2)	0.9988	4.80%	102.80 ± 3.38
L-Valine (D5)	0.9991	3.70%	101.47 ± 1.91

*Peak areas were corrected with IS2. Linearity determined in the range from 10 to 100 µM.

Table S2. Variable Importance in Projection (VIP) scores obtained for study I using data analysis strategies 1 and 2. The reported *m/z* values have VIP values above 1.0.

Number	*m/z* value	Compound	VIP score strategy 1	VIP score strategy 2
1	152.110*	L-Glutamine (2,3,3,4,4-D5)	2.27	2.17
2	151.135*	L-Lysine (4,4,5,5-D4)	2.16	2.17
3	136.078*	L-Asparagine (2,3,3-D3)	2.26	2.17
4	218.124*	L-Tryptophan (^{13}C11;^{15}N2)	2.25	2.15
5	134.099*	L-Isoleucine (^{13}C;^{15}N)	2.24	2.14
6	153.129*	L-Lysine (^{13}C6)	2.23	2.14
7	139.066*	L-Asparagine (^{13}C2;^{15}N2)	2.14	2.12
8	159.103*	L-Glutamic Acid (^{13}C5;D5;^{15}N)	2.20	2.11
9	158.101	Unknown	NA	2.09
10	126.134*	L-Valine (D5)	2.14	2.09
11	117.088*	Creatinine (N-methyl-D3)	2.18	2.08
12	149.081*	L-Glutamine (^{13}C2)	2.13	2.05
13	116.071	Proline	1.33	1.27
14	148.061	Glutamic acid	NA	1.16
15	158.154	Unknown	1.49	NA
16	148.079	Unknown	1.30	NA
17	246.205	Unknown	1.06	NA
18	184.170	Unknown	1.24	NA
19	104.111	Unknown	1.30	NA
20	219.130	Unknown	NA	1.58
21	205.120	Unknown	NA	1.37

* These *m/z* values are related to the 11 spiked compounds. NA, not applicable

Table S3. Variable Importance in Projection (VIP) scores obtained for study II using data analysis strategies 1 and 2. All *m/z* values have VIP values above 1.0.

***m/z* value**	**Compound**	**VIP score strategy 1**	**VIP score strategy 2**
218.124*	L-Tryptophan (^{13}C11,^{15}N2)	2.50	2.63
136.078*	L-Asparagine (2,3,3-D3)	2.47	2.60
159.103*	L-Glutamic acid (^{13}C5;D5;^{15}N)	2.38	2.57
126.134*	L-Valine (D5)	2.45	2.57
149.081*	L-Glutamine (^{13}C2)	2.45	2.57
158.101	Unknown	NA	2.57
134.099*	L-Isoleucine (^{13}C;^{15}N)	2.46	2.55
139.066*	L-Asparagine (^{13}C2;^{15}N2)	2.46	2.55
151.135*	L-Lysine (4,4,5,5-D4)	2.41	2.53
117.088*	Creatinine (N-methyl-D3)	2.35	2.50
153.129*	L-Lysine (^{13}C6)	2.38	2.47
152.110*	L-Glutamine (2,3,3,4,4-D5)	2.49	2.44

* These *m/z* values are related to the 11 spiked compounds. NA, not applicable.

Chapter 7

CE-MS metabolic profiling of volume-restricted plasma samples from an acute mouse model for epileptic seizures to discover potentially involved metabolic features

Based on

Karen Segers*, Wei Zhang*, Najat Aourz, Jana Bongaerts, Sven Declerck, Debby Mangelings, Thomas Hankemeier, Dimitri De Bundel, Yvan Vander Heyden, Ilse Smolders, Rawi Ramautar, and Ann Van Eeckhaut

CE-MS metabolic profiling of volume-restricted plasma samples from an acute mouse model for epileptic seizures to discover potentially involved metabolic features

In preparation

* Authors contributed equally

Abstract

Currently, a high variety of analytical techniques to perform metabolomics is available. One of these techniques is capillary electrophoresis coupled to mass spectrometry (CE-MS), which has emerged as a rather strong analytical technique for profiling polar and charged compounds. This work aims to discover with CE-MS potential metabolic consequences of evoked seizures in plasma by using a 6Hz acute corneal seizure mouse model. CE-MS is an appealing technique because of its capability to handle very small sample volumes, such as the 10 µL plasma samples using capillary microsampling in this study. After liquid-liquid extraction, the samples were analyzed with a low-pH CE-MS method, followed by data analysis and biomarker identification. Both electrically induced seizures showed decreased values of methionine, lysine, glycine, phenylalanine and histidine in mice plasma. However, a second provoked seizure, 13 days later, showed a less pronounced decrease of the mean concentrations of these plasma metabolites. A decrease in glutamate levels is only observed after a second evoked seizure, which is known as a marker for seizures and is therefore independent of sample type, experimental design or analytical platform. Other obtained markers related to seizure activities, which are already demonstrated in literature, are isoleucine, serine, histidine, proline, tryptophan, alanine, arginine, valine and asparagine. Most amino acids showed relatively stable plasma concentrations between the basal levels (Time point 1) and the 13-day wash-out period (Time point 3), which suggests its effectiveness. Overall, this work clearly demonstrated the possibility of profiling metabolite consequences related to seizure activities of an intrinsically low amount of body fluid using CE-MS. It would be useful in future to investigate and validate the known and unknown metabolites in different animal models as in humans.

Introduction

Metabolomics has emerged as a valuable tool for diagnostic purposes, to predict and monitor disease progression and to measure therapy efficacy. Moreover, biomarker knowledge provides a deeper understanding of ongoing disease mechanisms, to advance drug discovery and development. Most metabolomics studies were executed by analyzing changes in a single biological sample type, such as tissue, urine, serum or plasma [1, 2]. In this study, plasma metabolites were investigated to gain improved knowledge on the metabolic consequences of refractory seizures evoked in the acute 6 Hz corneal model. An epileptic seizure is defined by the International League Against Epilepsy (ILAE) as a transient occurrence of signs and/or symptoms due to abnormal excessive or synchronous neuronal activity in the brain [3]. A disturbance in the balance between excitation and inhibition in the brain will indeed result in seizures. It is known that these seizures will affect the metabolism [4]. Increased knowledge about global metabolic hallmarks related to a seizure will result in an improved understanding of seizure pathophysiology and can reveal novel pathways to control and prevent seizures.

Metabolomics has already been used to investigate changes in the metabolome after seizures [5] or the effect of anti-seizure drug treatment [6] in patients. Therefore, most studies focus on brain metabolites by studying brain tissue of a chemo convulsive animal model [7-12]. One of those studies focus on the participation of cysteine during a seizure and treatment of epilepsy in a mouse model [7]. Another study analyzed different brain regions by NMR spectroscopy, where they found an overlap in changes of the metabolites lactate, succinate, GABA, choline and taurine in hippocampal tissue and cerebellum of rats [12]. A similar study identified 26 metabolites which are differentiating between the normal group and the rats with a status epilepticus [9]. However, tissue analysis is challenging by several analytical and technical issues [13]. Therefore, circulating blood-based biomarkers are potentially interesting as plasma is more easily accessible than, for instance, cerebrospinal fluid [10, 14, 15]. At the moment, only a few studies make use of plasma metabolite profiling in epilepsy by using an animal model. As for example the study of Heischmann et al. [8], makes use of a kainic acid model of temporal lobe epilepsy to compare the metabolite depletions found in hippocampal tissue with the observations in plasma. Only a small number of similar metabolic consequences were observed in both matrices. The major change in plasma 48 hours after a seizure occurred in triacylglycerols, diacylglycerols, phosphatidylcholines, vitamin D and their derivates.

Besides animal models, the metabolic consequences of epilepsy are also studied in human samples. One example is the study of Detour et al. [16], which analyzed hippocampal tissue of different patients with temporal lobe epilepsy and divided those samples in groups based on classification criteria by ILAE. Concentration variations of glutamine, glutamate, aspartate, taurine and N-acetylaspartate were obtained in the hippocampus of those drug-resistant epilepsy patients. Besides tissue, characterization of drug-resistant epilepsy was conducted in serum

samples. Increased values of 3-OH-butyrate, 2-OH-valerate, 2-OH- butyrate, acetoacetate, acetone, acetate, choline, alanine, glutamate and scyllo-inositol were observed in patients with epilepsy. Besides those increase also a decrease of glucose, lactate and citrate were observed in serum samples of epilepsy patients [17]. However, in a study of Al Zweiri et al. [18], which was conducted a few years earlier than the afore mentioned results, no prominent markers of responsiveness to drug treatments in epilepsy could be obtained in serum. However, other serum metabolic characteristics among different types of seizures revealed comparable increased levels of glutamate and decreased levels of citrate [5] with the study of Murgia et al. [17]. Other findings of this study were the elevated levels of lactate, glutamate and butanoic acid and a reduction of cysteine, glutamine, palmitic acid, linoleic acid, elaidic acid, trans-13-octadecnoic acid, stearic acid, asparagine and glyceraldehyde [5].

However, only a few animal studies compared to studies in patients are making use of blood to obtain metabolic profiles. This is the result of the increased importance of animal welfare (refinement, reduction and replacement) resulting in the use of small sample volumes as it is not allowed to take more than 20 µL mice blood in a serial sampling strategy [19-21]. Alternative sampling techniques, such as volumetric absorptive microsampling [21, 22], dried blood spots [19, 21, 23] and capillary microsampling [19, 21] were developed for that purpose. Capillary microsampling has some benefits compared to other microsampling techniques, such as a shorter handling time of the animals, while the equipment for sampling is less expensive than for dried blood spots [19]. In different pharmacokinetic studies, the capillary microsampling technique has been already applied, resulting in robust and reliable outcomes [24-26]. However, these microsampling methods lead, to the additional challenge of extracting useful information of small sample volumes. For this purpose, the interest in microscale analytical methods has increased in recent years [27, 28].

Capillary electrophoresis mass spectrometry (CE-MS) is an interesting microscale technique allowing to profile polar and charged metabolites in small sample volumes [2, 27-29]. The relatively low number of applications of CE-MS in biomarker discovery is related to reproducibility and sensitivity issues, as well as to the complexity of coupling CE to MS [27]. However, in recent years the CE-MS interface was substantially improved, resulting in an increased sensitivity [30-32]. Several studies have already shown the reliability and repeatability of CE-MS for biomarker discovery [33, 34]. Harada et al. [33] performed a large scale cohort study, which profiled more than 8000 human plasma samples with a coefficient of variation for peak areas below 30 % for 80 metabolites. A more recent study of our research group [34], demonstrated the suitability of CE-MS for plasma metabolomics by a simulated omics study combined with two data-analysis tools to handle the data. Drouin et al. [35] proposed the use of the effective mobility of compounds, instead of the migration time, as a more robust migration index. Their work resulted in a database with the effective mobilities of compounds, which will enable a straightforward annotation of detected features in a biological sample.

In the presented study, using an acute 6Hz corneal mouse model for refractory seizures, plasma metabolic consequences for seizures were observed in a CE-MS profile through multivariate data analysis. Plasma samples were collected using capillary microsampling at four time points, i.e. before and after the seizure, with a wash-out period of 13 days between both evoked seizures. All samples were analyzed with a CE-MS method previously developed in the laboratory [34]. Data analysis was conducted by multivariate curve resolution alternating least squares (MCR-ALS) as feature-selection technique, followed by unsupervised and supervised analyses to indicate some possible biomarkers for the evoked seizures.

Material and methods

Acute 6Hz corneal seizure mouse models

All procedures were carried out according to the National Rules of Animal Experiments (Directive 2010/63) and were approved by the Ethical Committee for Animal Experiments of the Faculty of Medicine and Pharmacy of the Vrije Universiteit Brussel, Belgium (no. 18-213-2). Male NMRI mice, weighing between 38 and 50 g, were obtained from Charles River Laboratories (Sulzfield, Germany) and habituated at least one week at the animal house prior to the experiments. Animals were kept under standard laboratory conditions with a 10/14 h dark/light cycle, with water and food ad libitum. The night before the experiments, the animals were transferred to the experimental room.

A 6Hz seizure model as described and applied by [36-39], was used. Corneal stimulation (6Hz, 0.2 ms rectangle pulse width, 3 s duration) by using corneal electrodes connected to a stimulator (ECT Unit 57800, Ugo-Basile, Italy), induces limbic seizures. The optimal current intensity was determined in 6 animals that showed a seizure duration of more than 20 seconds and was found to be 52 mA. Local anesthesia was obtained by applying 0.5% xylocaine (AstraZeneca, Brussels, Belgium) in saline on the eyes before stimulating. These eye drops additionally result in good conductivity for the electrical stimulation. After stimulation, the animals were placed in an open plastic box to observe the presence or absence of a seizure. Seizures were characterized by a stunned or fixed posture, forelimb clonus and elevated straub-tail. The seizure durations were manually recorded for each animal.

Sample collection

Blood samples of all animals (n=8) were obtained with capillary microsampling before and after each seizure on the first and the second experimental day. In between both experimental days, a 13-day wash-out period was applied. In this period the animals were kept under standard laboratory conditions, as aforementioned, and without manipulations. On the first experimental day, the animals received an injection of saline/propylene glycol (50/50 (V/V)) 15 min before the corneal stimulation. On the second experimental day, the animals were injected with a saline

solution, 45 min before the corneal stimulation. The difference in vehicle and time point of injection before the corneal stimulation between the two days of experiments is due to the solubility and half-life time of the obtained drug in the treated group. On the first day of experiments the treated group received carbamazepine and on the second day the drug treatment was obtained with levetiracetam. However, the samples related to those treated groups were not analysed due to the protection of those animals by the treatment for an evoked seizure. An illustration of the animal experiments with blood sampling time points (1 to 4) is shown in **Figure 1**. Blood was collected using capillary microsampling from the vena saphena [24]. Additional blood was taken from the heart when the animals were sacrificed after the second experimental day.

All blood samples were collected into EDTA-coated 32 µL capillaries (Virtex Medical, Herlev, Denmark) and plugged 3 times with wax (sealing wax plate, Hirschmann, Eberstadt, Germany). The waxed capillaries were transferred to individually pre-labeled 5 mL Falcon® tubes (Corning, Tewksbury, Massachusetts, United States) on ice prior to centrifugation. The capillaries were centrifuged in a precooled centrifuge (4 °C) for 10 min at 1500 g. After centrifugation the capillaries were snapped above the cell layer plug and exactly 10 µL of plasma was end-to-end transferred to 10 µL capillaries (Virtex Medical, Herlev, Denmark) and stored in labeled Cryo.S vials (Greiner Bio-One, Frickenhausen, Germany). Blood from the heart was collected into EDTA coated tubes (Vacutest, Azergrande, Italy) and centrifuged as previously explained. The plasma layer was transferred to a labeled Eppendorf® tube (Eppendorf, Hamburg, Germany). All plasma samples were stored at -80°C till sample preparation.

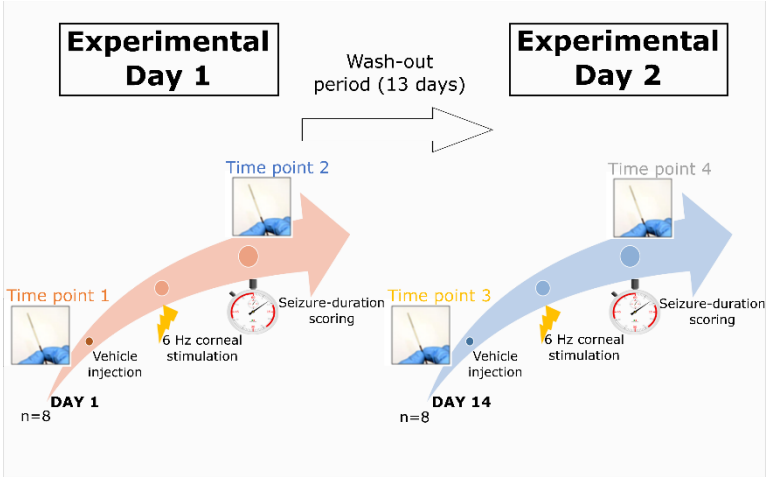

Figure 1. Illustration of the experimental protocol. On the first day, blood samples were collected before given a vehicle to the animals (time point 1). After a 13-days wash-out period the same experiment was repeated (time point 2). Later, a 6Hz stimulation is given, followed by scoring the seizure duration. After the seizure, a second blood sample was collected. In total, 4 blood samples were collected: 1 before and 1 after the provoked seizure on both experimental days (n=8).

Quality control samples

The heart plasma samples of all animals were pooled, 10 µL of these pooled samples was transferred into capillaries in Cryo.S vials (Greiner Bio-One, Frickenhausen, Germany) and pretreated as the other plasma samples of the four different time points.

The day of the analysis, samples were reconstituted in 25 µL water. From each sample (time point 1-4 and the aliquots of the pooled heart samples), 5 µL was taken to generate a pool of them, thereby obtaining quality control (QC) samples to check for and to evaluate system variations. The remaining 20 µL of the samples (time point 1-4 and the aliquots of the pooled heart samples) was used for CE-MS analysis.

The suitability of the CE-MS method for human plasma samples was already demonstrated in [34], but the composition and volume of human plasma is different than that of mice. In order to investigate the effect of capillary microsampling on the sample preparation, 10 µL mouse plasma samples was spiked with four labeled compounds (i.e. L-Alanine-^{13}C2, L-Glutamine-^{13}C2, L-Lysine-^{13}C6, and L-Isoleucine-^{13}C,^{15}N) (Cambridge Isotope Laboratories, Apeldoorn, The Netherlands) at a series of concentrations based on the naturally existing endogenous levels [40]. Moreover, the samples spiked with intermediate concentration levels were prepared in 8 replicates to monitor the variation in the peak area (precision) and estimated concentration (accuracy).

Sample pretreatment

Plasma samples were prepared as described in [34]. To 10 µL stored plasma samples, 250 µL milli-Q water (Millipore, Amsterdam-Zuidoost, the Netherlands), 250 µL MeOH (HPLC grade, Actu-All Chemicals, Oss, the Netherlands), 250 µL $CHCl_3$ (HPLC grade, Biosolve Chemicals, Valkensweerd, the Netherlands) and 20 µL 30 µM internal standard (IS, prepared in Milli-Q water), i.e. DL-methionine sulfone (Human Metabolome Technologies, Leiden, The Netherlands), were added and vortexed followed by centrifugation at 2196 g at 4 °C for 10 min. The supernatant (500 µL) was transferred to centrifugal filters of 5kDa (Millipore) and centrifuged for 1.5 hours at 12000 g. 300 µL of the filtrate was transferred after centrifugation and evaporated under vacuum in a CentriVap Concentrator (Labconco). The dried residues were stored at -80 °C prior to analysis.

Metabolic profiling by CE-MS

The same instruments and analytical methods as in [34] were used. Milli-Q water containing 10% (V/V) acetic acid (99-100%) (VWR, Amsterdam, The Netherlands) was used as background electrolyte (BGE). The sheath liquid was a mixture of isopropanol/water (1:1, V/V), containing 0.2% acetic acid and was delivered at 5 µL/min. Electrophoretic separation was achieved by applying a voltage of 30 kV and the MS detection was done in positive mode. Full scan acquisition, covering the mass range of 50-1000 m/z, was conducted at 1.5 spectra s^{-1} acquisition rate in centroid mode. Between the sample analyses, the capillary was flushed as follows: water for 30 s at 5 bar, methanol for 1 min at 5 bar, water for 30 s at 5 bar, 10% ammonium hydroxide for 1 min at 5 bar, water for 30 s at 5 bar and BGE for 2 min at 5 bar.

Data processing

The obtained data were stored as .d files and converted to mzXML formats with ProteoWizard (Palo Alto, California). These files were imported and further analyzed in MatlabTM R2014a (The Mathworks, Natrick, MA), as described in [34].

First, a binning method was performed and data were compressed through the detection of regions of interest (ROI) [41, 42]. ROI values were searched for each migration time in the CE-MS profile. However, each ROI is defined by a signal threshold, mass accuracy and the minimum time interval to be considered as a peak width [43, 44]. In our study, the parameters are based on the protocol by Gorrochategui et al. [44] and were set at 1000 for the signal threshold, 0.01 atomic mass unites/e was used as mass accuracy and 6 seconds as the minimum time interval.

The subsequent step is the feature detection and is performed with the MCR-ALS toolbox [45]. MCR-ALS does not require peak alignment which makes it very suitable for CE data, since usually significant migrationtime shifts are observed [43]. The number of components in the samples is initially guesses. The Single Value Decomposition (SVD) method is the most suitable method to resolve features. Different SVD-numbers were evaluated in a MCR-ALS model, based on the explained variance and the lack-of-fit (LOF) error of the model. To detect the purest variables, a 10% noise level threshold was used.

The obtained features were integrated in the Data Acquisition module within the MassHunter Workstation (Agilent, Santa Clara, CA). The peak areas of the integrated features were first normalized with that of the internal standard and then auto-scaled prior to further statistical analysis.

1. **Multivariate analysis**

The normalized and auto-scaled data were visualized with unsupervised analysis by clustering analysis (dendrogram-linkage) and principal component analysis (PCA) methods. As supervised analysis method, PLS-DA was performed on the data to link the sample time point with the obtained fingerprint. The numbers of latent variables for the models of the supervised analyses were chosen based on a five-fold venetian-blind cross validation. Subsequently, a model was evaluated based on the error rate, non-error rate and accuracy on the cross-validation and calibration results. In the end, possible seizure biomarkers are reported based on a VIP score above 1.0, which reflects the importance of the variable in the discrimination between the groups of interest, i.e. before and after a seizure.

2. **Univariate analysis**

A paired student t-test was performed on the normalized data to investigate the differences between the time points within and between days illustrated in **Figure 1**. The animals were their own controls, which allowed performing a paired t-test. However, the normal distribution pattern

could not be verified due to the small sample size (n=8). Therefore, besides the parametric paired t-test an additional non-parametric Wilcoxon test was used.

Results and discussion

Evaluation of analytical workflow for metabolic profiling of volume-restricted plasma samples

When performing metabolic profiling of volume-restricted samples, aspects like sampling, sample preparation and analysis by CE-MS need to be carefully studied in order to minimize technical variations. Therefore, we have first assessed whether the plasma sampling technique had an effect on the CE-MS results. For this purpose, plasma samples (n=8) were spiked with four labeled compounds at concentrations reflecting the endogenous levels of the natural counterparts in plasma. Those samples were than stored in 10 µL capillaries, as the actual samples. The relative standard deviations (RSD) obtained for the peak areas of these compounds were below 7.4%. The accuracy was also investigated by comparing the spiked concentration with the experimental concentrations. This resulted in an acceptable accuracy, between 85 to 115% (data not shown).

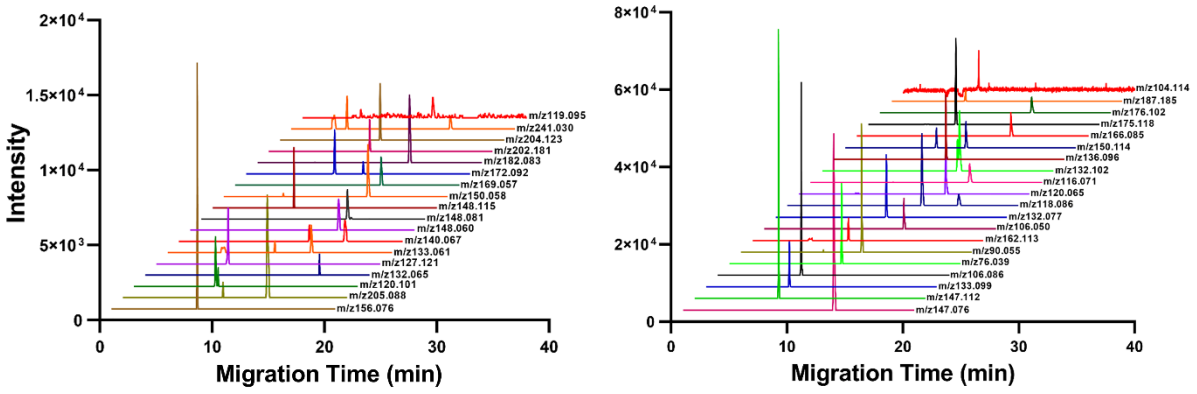

Figure 2. Reconstructed extracted ion electropherograms of the 44 reliable features (m/z values) in a QC sample as obtained by CE-MS.

Before starting the main analysis, one QC sample was analyzed ten times to examine the repeatability of the CE-MS method. After obtaining a signal, repeatable in profile and intensity, the actual samples were analyzed randomly and alternated with blank solutions and QC samples (total number of QC samples=13) and at the end some metabolite standards (including the following compounds: glycine, L-alanine, cytosine, proline, valine, homoserine, threonine, creatine, isoleucine, leucine, asparagine, adenine, anthranilic acid, tyramine, spermidine, glutamine, lysine, glutamic acid, methionine, histidine, phenylalanine, spermine, tryptophan, cytidine, adenosine), which can be used for identification. The analysis of the QC samples will reflect the system variation. As described in literature, to be reliable, RSD values for the resolved features have to be below 30% for the AUC values and below 5% for the migration times [46]. In this study, 44 measured *m/z* values in the QC samples showed acceptable RSD values (below 20.3%

for the corrected areas and below 2.5% for the migration times). Two representative extracted ion electropherograms for the reliable features (44) detected in a QC sample are shown in **Figure 2**. A drift correction was not performed because the instrumental drift was negligible compared to the biological variation.

The variation in sample preparation was verified with the pooled heart plasma sample, which was divided in 10 µL aliquots undergoing the sample pretreatment. The RSD for all features taken into account measured in those heart plasma samples were below 19.5% and 0.7% for the corrected areas and migration times, respectively. The repeatability of injections was examined by injecting the samples of the fourth time point twice, resulting in RSD values between the two injections below 20.2% and 3.5% for the corrected areas and migration times, respectively.

Summarized, all estimated variations were within the acceptance limits, which demonstrates the reliability of the CE-MS and sampling techniques to investigate the metabolites in volume-restricted plasma samples.

Metabolic profiling of plasma samples from a mouse model for epileptic seizures

The focus of this paper is to investigate the applicability of the previously mentioned CE-MS method to detect plasma metabolites related to metabolic consequences for an evoked seizure. In total, 74 samples were analyzed, including 32 from the epileptic mouse model, 8 mouse heart samples, 8 samples from the 4th time point injected a second time, 7 blank solutions, 6 standards, and 13 quality controls which were injected between the different groups ad random. Data compression resulted in 161 resolved *m/z* values. All *m/z* values were manually evaluated to exclude spikes. Spikes can be the result of electrical disturbance occurring in the MS system and are not related to a metabolite. The feature detection allowed to reduce the data to 57 *m/z* values with good predictive ability of the resulting MCR-ALS model; i.e. 99.2% explained variance and 9.2% LOF error. However, this data set also contains *m/z* values with an RSD above 30 % for their peak area ratios and of more than 5% for the migration times. After removing these non-compliant features, 44 *m/z* values remained, which have acceptable variations for migrations time and corrected peak areas measured for the QC samples, i.e. 2.5% and 20.3%, respectively. Multivariate analysis was performed besides parametric and non-parametric paired t-tests on these 44 features after applying auto-scaling to eliminate the dominance of highly abundant features.

First, the sample similarity was investigated by constructing a dendrogram as shown in Figure 3. This dendrogram is constructed using the complete linkage method and the Euclidean distance as similarity parameter. The further the samples are located from each other on the X-axis, the more dissimilar. Three clusters are clearly revealed in the dendrogram. The left group contains all samples after the first seizure (i.e. Time point 2), illustrating high similarities between these profiles and a clear distinction from all other time points. Notice that, sample 23 from Time point 3 (i.e. after the wash-out period) is also present in this cluster. The possible reason for similarity

of sample 23 with these cluster profiles, may be related to the short seizure duration of the animal (22 seconds).

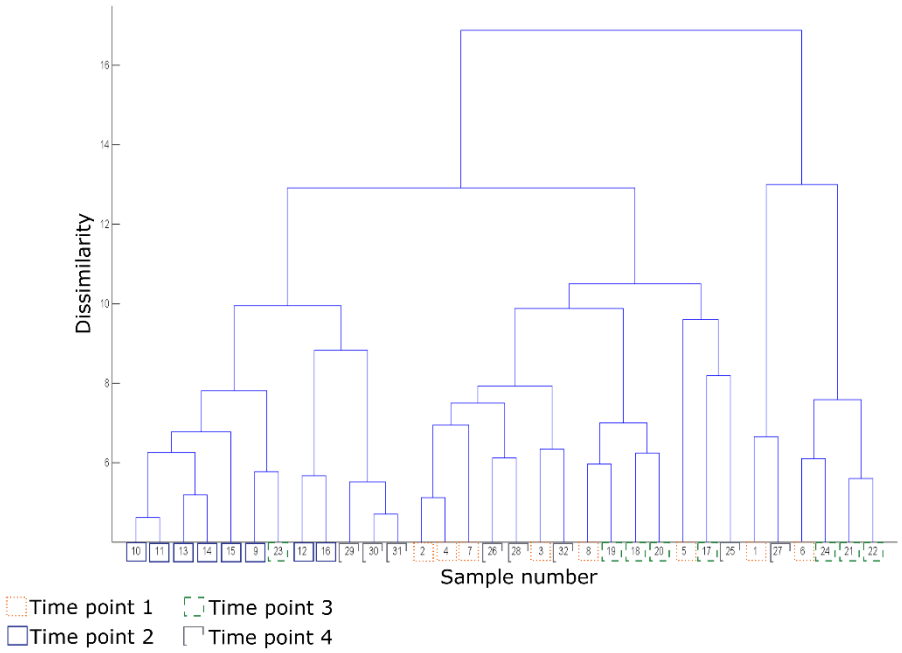

Figure 3. Dendrogram of all samples (n=32) (except the QC sample) to show similarities between the samples. Similarities are based on Euclidean distances, calculated on the autoscaled X matrix.

Only tree samples after the second seizure (Time point 4) are clustering together with samples after the first seizure (Time point 2) in the left cluster, which can be attributed to similar seizure durations for both onsets. The mean durations of the first and second evoked seizures were 3 minutes, 2 seconds and 1 minute, 23 seconds, respectively. However, five samples after the second seizure (Time point 4) are more similar with Time point 1 and 3. These five animals showed a decreased seizure duration compared to the first seizure, which might result in a profile that is more comparable to these at time point 1 and 3. From this clustering information, no clear distinction is observed between the first and third-time-point profiles, suggesting the effectiveness of the wash-out period. The analogies at different time points and the related markers will be studied in more detail by PCA and in the statistical analysis.

The main objective was to find metabolomic consequences of evoked seizures in plasma. This was performed by comparing profiles at time point 1 with 2 and time point 3 with 4. The overall clustering of all groups can be seen in Figure 4A. Here, a clear discrimination between the first sampling time point in the naïve mice with the sample after a seizure can be observed. Clustering tendency of the samples before and after a seizure on the two experimental days is shown in PCA score plots Figures 4B and C. For the first experimental day, the samples before a seizure (represented by solid diamonds in Fig. 4B) are clearly discriminated from those after a seizure (represented by pink squares in Fig. 4B), suggesting a dissimilar profile and changes that occurred by an evoked seizure. The assessment on VIP scores led to the indication of 21 potential markers,

which were all statistically significant based on both univariate statistics (parametric and non-parametric paired t-test resulting in a p-value<0,05). The VIP scores were based on a PLS-DA model with 1 latent variable having good predictive abilities (100% accuracy and non-error rate). Only 14 markers, shown in **Table 1**,could be identified based on an in-house standard mixture and applying the ROMANCE database [47]. All these metabolites were decreased in concentration after a seizure as demonstrated by Figure 5 which contains concentration trends of all identified amino acids of **Table 1**. The decreased concentrations of isoleucine, serine, histidine and proline after a seizure are similar with the study of Heischmann et al. [8]. This study found their observation in rat plasma 48 hours after a seizure occurred in a chemo convulsive model for seizures.

Table 1. Markers obtained after the first provoked seizure based on a variable importance in projection (VIP) score above 1 and p-value below 0.05 (α=95%).

Compound	$[M+H]^+$	Migration time (min)	p-value (parametric)[1]	p-value (non-parametric)[1]	VIP score	Plasma concentration[a]
Methionine	150.058	12.5	0.0002	0.0078	1.5	
Unknown	148.115	7.5	<0.0001	0.0078	1.5	
Lysine	147.113	7.3	<0.0001	0.0078	1.5	
Glycine	76.040	9.5	0.0003	0.0078	1.5	
Alanine	90.055	10.5	0.0020	0.0078	1.4	
Unknown	136.096	9.5	0.007	0.0078	1.4	
Arginine	175.118	7.5	0.0001	0.0078	1.3	
Threonine	120.065	13.0	0.0007	0.0078	1.3	
Unknown	150.111	10.5	0.006	0.0234	1.3	
Unknown	176.121	7.5	0.002	0.0006	1.3	
Leucine/Isoleucine*	132.101	11.5	0.0003	0.0078	1.3	Decreased
Serine	106.050	12.0	0.0006	0.0078	1.3	
Asparagine	133.060	13.0	0.0051	0.0078	1.2	
Unknown	176.102	13.0	0.0003	0.0078	1.2	
Unknown	172.092	10.5	0.0117	0.0078	1.2	
Unknown	119.093	11.5	0.0006	0.0078	1.2	
Phenylalanine	166.085	13.5	0.001	0.0078	1.2	
Ornithine	133.100	7.0	0.0051	0.0078	1.2	
Valine	118.086	11.5	0.0007	0.0078	1.2	
Histidine	156.076	7.5	0.006	0.0078	1.1	
Proline	116.070	13.5	0.0369	0.0391	1.0	

* These compounds are present in the standard mixture, but not baseline separated.

[a] Compared to the basal levels

[1] As a parametric test a paired t-test was used and as a non-parametric test a Wilcoxon test was used.

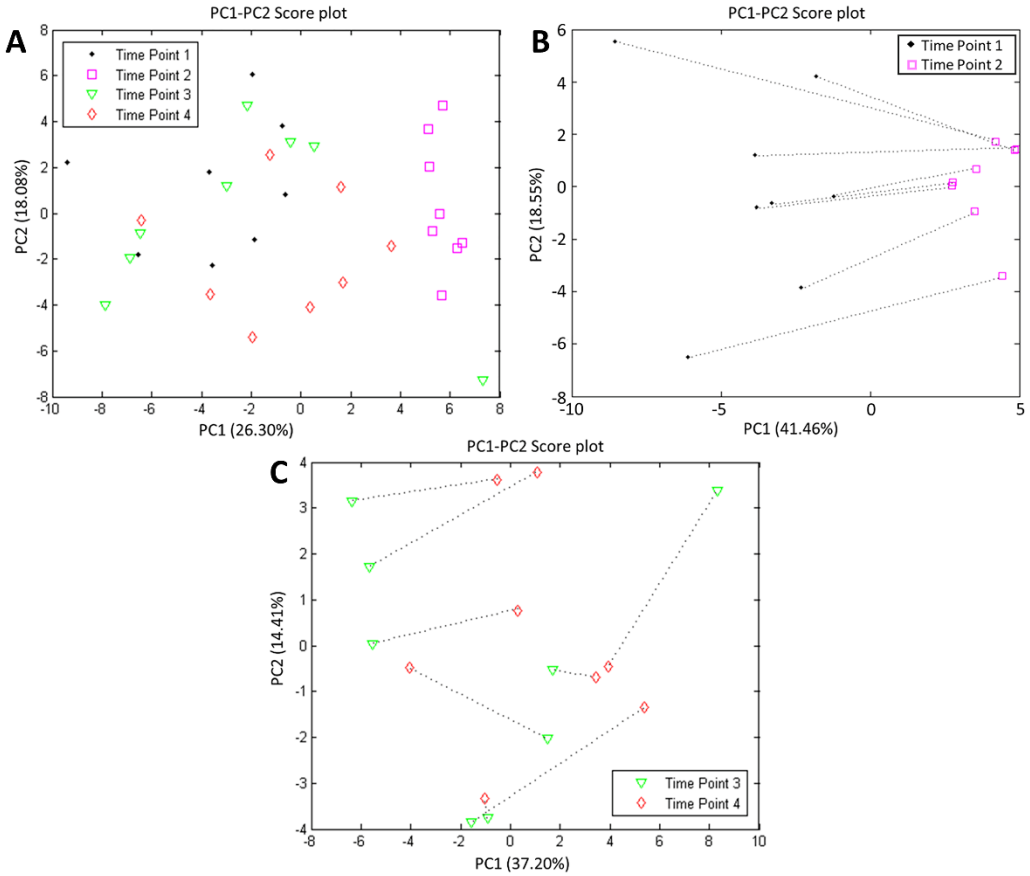

Figure 4. PC1-PC2 score plot for the X matrix to compare the experimental time points (A) all investigated samples before and after an evoked seizure using internal standard correction and autoscaling as data pretreatment (B) the first experimental day (C) the second experimental day. Time point 1 is represented by solid diamonds (◆), time point 2 by squares (□), time point 3 is represented triangles (△) and time point 4 by diamonds (◇).

Less dissimilarity is seen between the samples before (represented by green triangles in **Fig. 4C**) and after a second evoked seizure (represented by red diamonds in **Fig. 4C**) after the 13-days wash-out period. This less dissimilarity may be the result of the injected vehicle, which is different between the first (propylene glycol/saline (50/50 V/V)) and second experimental (saline) day or due to the possibility that a second evoked seizure will induce less metabolic consequences in plasma compared to a first. However, this last consequence is in contradiction with seizures beget seizures, but epilepsy and seizures are brain- specific disorders and many compounds do not cross the blood-brain barrier [8]. Another explanation could be related to the duration of the effects by an evoked seizure. Therefore, this result may suggest the prolonged effect of a first seizure reflected by their metabolite changes. The PLS-DA model resulted in an accuracy of 88% for calibration and 63% for cross-validation results, suggesting less good predictive abilities of the model compared to the previous PLS-DA model for the first day of experiments. Only four metabolites were found statistically significant based on both parametric and non-parametric univariate statistics, i.e. glutamate, glutamine, 4-hydroxyproline and methionine. The latter two amino acids showed a decrease in plasma concentration after the seizure, while glutamate and glutamine plasma

concentrations were increased in this study. Glutamate showed also an increase in human serum samples of Wang et al. [5] and Murgia et al. [17]. Additionally, in a chemo convulsive rat model increased glutamate levels were observed in hippocampal tissue [9]. For both evoked seizures (1st and 2nd) some similar metabolites were indicateby VIP-scores above 1 for the amino acids lysine, glycine, phenylalanine, methionine and histidine, which showed for both seizure a decrease in plasma concentrations as shown in **Figure 5**. However, based on both univariate paired t-test all aforementioned amino acids are significant ($p<0,05$) for the first seizure compared to the significance of only methionine of those aforementioned amino acids for the second evoked seizure.

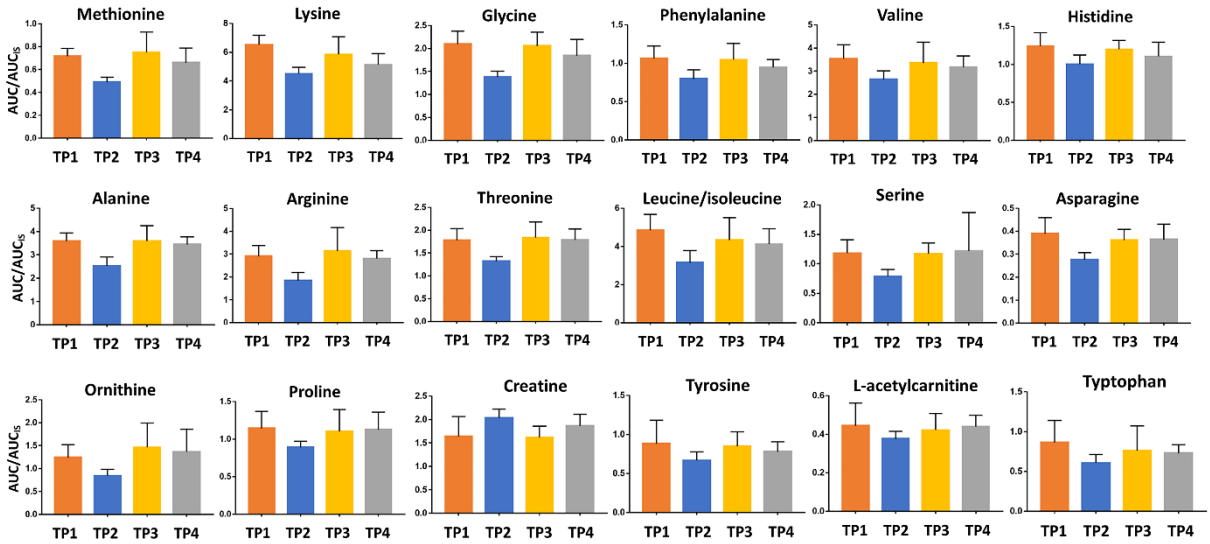

Figure 5. Concentration trends between the different investigated Time Points of some identified amino acids. (TP is short for *time point*)

The decreased plasma concentration of proline after a seizure in the 6Hz mouse model is in contrast with the serum concentrations reported in ref. [5], which compared control groups with patients who had a seizure within 48 hours before sampling. Besides proline, additional markers for seizures were reported by Wang et al. [5] such as lactate, butanoic acid, glutamate, palmitic acid, linoleic acid, elaidic acid, trans-13-octadecenoic acid, stearic acid, citrate, cysteine, glutamine, asparagine and glyceraldehyde.

The lack of effectiveness of the wash-out period could be another explanation to the less pronounced metabolic changes for a second seizure. However, the similarities between time point 1 and 3 suggested an effectiveness of the wash-out period. This similarity was demonstrated by their clustering pattern in the PCA score plot, which is not shown. Still, multivariate analyses revealed some responsible markers for the distinction between the first seizure (Time point 2) and the post wash-out period profiles (Time point 3), which are listed in **Table 2**. Noteworthy, univariate results revealed that most (but not all) metabolites with a VIP score above 1.0 were statistically different after the wash-out period. Therefore, proper selection of a threshold for the

VIP score is important when using this parameter [48]. The threshold is accordingly (study specific) often adjusted to values above 1 [49, 50]. Thus, the VIP score allows to indicate potential biomarker candidates without defining it as a biomarker [48]. In our study, the plasma levels of glycine, serine, asparagine, threonine, methionine, alanine, arginine, histidine, ornithine and lysine were increased (13 days after the first seizure) compared to their post seizure values. These increased values after the wash out demonstrates the influence of sampling time after a seizure, which may result in different interpretations. Additionally, these increased levels, 13 days after the seizure, reflect also the stabilization of the plasma levels during the wash-out period for each mouse according time, as suggested by the concentration trends shown in **Figure 5**. For most metabolites the concentration trend at Time point 1 and 3 are similar.

Table 2. Markers that are different after a seizure (Time point 2) and the recuperation period of 13 days (Time point 3) based on a VIP score above 1. p-values of the performed univariate statistical tests are shown together with the changes in plasma concentration levels between the seizure and recuperation days.

Compound	$[M+H]^+$	Migration time (min)	p-value (parametric)[1]	p-value (non-parametric)[1]	VIP score	Plasma concentration[b]
Glycine	76.040	9.5	0.0003	0.0078	1.6	Increased
Unknown	136.096	9.5	0.0003	0.0078	1.6	
Serine	106.050	12.0	0.0004	0.0078	1.5	
Asparagine	133.060	13.0	0.0015	0.0078	1.5	
Threonine	120.065	13.0	0.0038	0.0078	1.4	
Methionine	150.058	12.5	0.0040	0.0156	1.4	
Alanine	90.055	10.5	0.0085	0.0156	1.4	
Creatine	132.076	9.5	0.0033	0.0078	1.4	Decreased
Unknown	172.092	10.5	0.0099	0.0234	1.3	Increased
Unknown	150.111	10.5	0.0160	0.0234	1.3	
Unknown	176.102	13.0	0.0027	0.0156	1.3	
Arginine	175.118	7.5	0.0091	0.0156	1.3	
Unknown	176.121	7.5	*0.2716*[a]	*0.1215*[a]	1.3	
Histidine	156.076	7.5	0.0044	0.0156	1.3	
Ornithine	133.100	7.0	0.0172	0.0234	1.3	
Phenylalanine	166.085	13.5	0.0265	*0.0547*[a]	1.2	
Lysine	147.113	7.3	0.0165	0.0391	1.2	
Unknown	132.065	9.5	0.0190	0.0078	1.2	Decreased
Unknown	148.115	7.5	0.0368	*0.0781*[a]	1.1	Increased
Leucine/Isoleucine*	132.101	11.5	0.1464[a]	0.1799[a]	1.1	
Tyrosine	182.083	13.5	0.0423	0.0781[a]	1.0	
Unknown	104.114	6.5	*0.0666*[a]	*0.1094*[a]	1.0	Decreased
Unknown	119.093	11.5	*0.0991*[a]	*0.1484*[a]	1.0	Increased

* These compounds are present in the standard mixture, but not baseline separated.

[a] p-values > 0.05 showing that the compounds are statistically not significant based on parametric and/or non-parametric test.

[b] Plasma concentrations observed 13 days later compared to the levels after a first seizure.

[1] As a parametric test a paired t-test was used and as a non-parametric test a Wilcoxon test was used.

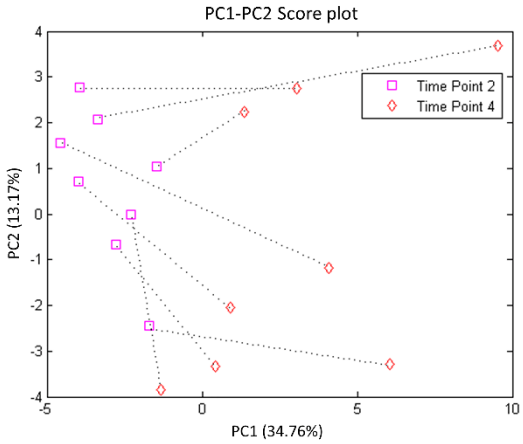

Figure 6. PC1-PC2 score plot for the X matrix to compare the profiles after two different seizures using internal standard correction and autoscaling as data pretreatment. Time point 2 is represented by pink squares (□) and time point 4 by red diamonds (◇).

Table 3. Markers that are different after the two seizures based on a VIP score above 1.0. p-values of the univariate statistical tests are shown together with the changes in plasma concentration levels.

Compound	[M+H]+	Migration time (min)	p-value (parametric)[1]	p-value (non-parametric)[1]	VIP score	Plasma concentration[b]
Arginine	175.118	7.5	0.0006	0.0078	1.7	Increased
Threonine	120.065	13.0	0.0002	0.0078	1.6	
Alanine	90.055	10.5	0.0004	0.0078	1.6	
Unknown	176.121	7.5	*0.1435*[a]	*1.0756*[a]	1.6	
Unknown	150.111	10.5	0.0007	0.0078	1.5	
Unknown	172.092	10.5	0.0054	0.0078	1.5	
Unknown	119.093	11.5	0.0056	0.0156	1.4	
Methionine	150.058	12.5	0.0092	0.0078	1.4	
Glycine	76.040	9.5	0.0097	0.0078	1.4	
Asparagine	133.060	13.0	0.0017	0.0078	1.3	
Unknown	136.096	9.5	0.0143	0.0078	1.3	
Ornithine	133.100	7.0	0.0243	*0.0781*[a]	1.2	
Phenylalanine	166.085	13.5	*0.0722*[a]	*0.0547*[a]	1.2	
Proline	116.070	13.5	*0.0529*[a]	*0.0547*[a]	1.2	
Leucine/Isoleucine*	132.101	11.5	*0.0620*[a]	*0.0781*[a]	1.2	
L-acetylcarnitine	204.123	9.0	*0.0094*[a]	*0.0391*[a]	1.1	
Unknown	104.114	6.5	0.0247	0.0391	1.1	Decreased
Valine	118.086	11.5	*0.0838*[a]	*0.0781*[a]	1.1	Increased
Tryptophan	205.081	13.0	0.0340	0.0391	1.1	
Unknown	176.102	13.0	0.0220	*0.0547*[a]	1.1	

* These compounds are present in the standard mixture, but not baseline separated.

[a] p-values > 0.05 showing that the compounds are statistically not significant based on parametric and/or non-parametric test.

[b] Plasma concentrations compared between a first seizure and second evoked seizure.

[1] As a parametric test a paired t-test was used and as a non-parametric test a Wilcoxon test was used.

Another interesting aspect is the re-use of animals in an acute 6Hz animal model. However, to our knowledge, nothing is currently known about the similarity of the metabolite profiles over the different seizures. Therefore, the comparison between the second and fourth time point is made in **Figure 6**. A clear discrimination of the samples belonging to the first and second evokes seizure

is demonstrated by this score plot, suggesting a difference in metabolic consequences observed in plasma for a second evoked seizure compared to a first. VIP score investigation resulted in the suggestion of 20 markers of which 13 could be identified (see **Table 3**). Higher levels after the second seizure than after the first were obtained for arginine, threonine, alanine, methionine, glycine, asparagine, and tryptophan as shown in **Figure 5**. Our results demonstrate that a second seizure with the same stimulation may result in a less pronounced decrease of the metabolite levels in mouse plasma, compared to the decrease observed after the first evoked seizure, which can also be seen in the concentration trend profiles of **Figure 5**.

Biological significance of the obtained findings

Pathway analysis with the Kyoto Encyclopedia of Genes and Genomes (KEGG) software assigned most of the identified compounds to the nucleotide and amino acid metabolism. The identified markers, which are all amino acids, play important roles in maintaining the equilibrium between inhibitory and excitatory processes.

A seizure is the result of an imbalance between excitation and inhibition. The most important excitatory neurotransmitter is glutamate. Most of the identified compounds in our work are directly or indirectly related to glutamate, which shows elevated levels in our study after a second seizure and in serum and extracellular brain tissues in other publications [51-54]. A precursor of glutamate is glutamine, and a decreased metabolization of glutamate to glutamine causes glutamate accumulation resulting in a seizure [54-56]. This decreased values of glutamine are obtained in plasma samples of a chemo convulsive rat model [8] and in human serum samples [5] and are in contradiction with the increased values observed in our study after a second evoked seizure and in hippocampal sclerosis samples of humans in [16]. Other indirectly involved in the glutamate-glutamine cycle include alanine, asparagine and leucine [57, 58], which are all decreased in our observations after an evoked seizure. This decrease in asparagine is also described by Wang et al. [5] in human serum samples. However, the decreased plasma levels of alanine are additionally observed in human hippocampal sclerosis [16].

Besides an increase in glutamate, the role of norepinephrine, epinephrine, dopamine and serotonin is not fully clarified. Therefore, a decrease of those mono amines has been reported in epileptic seizures [57, 59, 60] besides an increase of those mono amines in other scientific reports which are described in the following review [61]. Therefore, a decrease in the precursors of those neurotransmitters, such as tryptophan, phenylalanine and tyrosine, is expected after a seizure [54, 58, 62] and demonstrated by our findings. This decrease of the precursor levels can be due to the decrease of the mono amines or due to the overconsumption of those mono amines.

GABA is known as inhibitory neurotransmitter. Decreased GABA levels can be found in neurodegenerative and epileptic disorders, as a result of an alternative energy source, instead of isoleucine and valine [57]. Therefore, decreased values of both amino acids are described in our

observations and those decrease of valine is additionally described by Detour et al. [16] in hippocampal tissue. Other metabolites, such as glycine, serine, threonine [54, 55, 58, 63], methionine [54, 64], proline [65], isoleucine, valine [57], arginine [66], creatine [54, 58] and histamine [67], are indirectly involved in a seizure.

In general, the mechanisms of all mentioned compounds are related to brain activities. Therefore, the plasma concentrations should be interpreted with care. The relation brain-plasma concentration depends on the blood-brain barrier permeability of the compounds and may additionally be influenced by specific transporters. For instance, a study reported comparable glutamine concentrations in the hippocampus of kindled and non-kindled rats [55], while lower glutamine concentrations were reported in serum of patients with seizures [5]. In our study, glutamine was identified as a marker for the second evoked seizure. However, the number of similar metabolic changes in the hippocampus and plasma is limited [8]. This is due to the fact that epilepsy and seizures are brain related disorders, but there is an increased need for peripheral markers due to their possibility of a fast screening. The timing of the experimental design, type of research samples may influence the outcomes and even differences in analytical platforms can affect the findings, but in general most of the identified metabolites show similarities with other observations in literature.

Conclusion and future perspectives

In this study, we have demonstrated the utility of our approach, which includes sampling, sample pretreatment and CE-MS analysis of low-volume plasma samples, for finding metabolic consequences of evoked seizures. Seizures were induced in mice by 6Hz corneal stimulation and plasma samples were collected by capillary microsampling before and after stimulation. The 6Hz electrical stimulation was repeated after a 13 days wash-out period to investigate whether the same metabolic changes are observed in naive and previously stimulated mice.

After both evoked seizures a decrease in plasma concentration of methionine, lysine, glycine, phenylalanine and histidine is observed. The decrease of glycine and histidine are also observed in previously reported studies. Additionally, the decrease of glutamate levels after the second seizure is independent of the sample type, experimental design or analytical platform. However, in general most amino acids showed a less pronounced decrease in plasma after a second seizure compared to the first.

The reported decreased levels of isoleucine, serine, histidine, proline and tryptophan after a seizure are similar to observations in literature of a chemo convulsive animal model for seizures. Therefore, those markers are related to some seizure activities and are independent of the obtained seizure model. Additionally, the observed decreased concentrations of alanine, arginine, valine and asparagine are previously investigated in human hippocampal tissue studies or serum

samples. All before mentioned amino acids showed non-significant differences between the basal plasma levels and those obtained after a 13 days wash-out period suggesting their effectiveness.

Besides the similar observations of the previously described changes, in literature, some contradictions are present. As an example, the observed changes of the mono amines and their precursors. Therefore, it would be useful to further investigate and validate their role in different animal models (electrical and chemo convulsive) as in humans by different analytical techniques. Additionally, some compounds are not yet identified, which are related to a metabolic consequence of seizures. This knowledge about the identity can define or clarify their role in seizures.

In general, our study emphasized the suitability of CE-MS to analyze volume-restricted plasma samples with an acceptable variation. Additionally, the method is sensitive enough to measure a suitable profile of polar components, differentiating the samples before and after an evoked seizure an define some amino acids involved in evoked seizures.

Acknowledgments

This work was supported by a Travel Grant of the Research Foundation Flanders (FWO) under Grant number V433318N for K. Segers. W. Zhang acknowledges the China Scholarship Council (CSC, No. 201507060011) for supporting his PhD project at Leiden University. R. Ramautar acknowledges the Netherlands Organization for Scientific Research (NWO) for support of the research with a Vidi grant. The authors would also thank N. Drouin for the support with the ROMANCE software as well as L. Walrave, A. Buckinx, Y. Van Den Herrewegen, A. Pierre and W. Allaoui for their excellent help with the animal experiments. Furthermore, we thank L. Dillen, T. Gevers, P. Anthonissen, H. Sieltjens, A. Vromans and C. Sas from Janssen Pharmaceutica - Johnson & Johnson to guide us with the use of capillary microsampling.

References

1. Chamberlain, C.A., V.Y. Rubio, and T.J. Garrett, *Impact of matrix effects and ionization efficiency in non-quantitative untargeted metabolomics.* Metabolomics, 2019. **15**(10),135.
2. Shyti, R., et al., *Plasma metabolic profiling after cortical spreading depression in a transgenic mouse model of hemiplegic migraine by capillary electrophoresis – mass spectrometry.* Molecular BioSystems, 2015. **11**(5),1462-1471.
3. Fisher, R.S., et al., *ILAE official report: a practical clinical definition of epilepsy.* Epilepsia, 2014. **55**(4),475-482.
4. Bazzigaluppi, P., et al., *Hungry Neurons: Metabolic Insights on Seizure Dynamics.* International Journal of Molecular Sciences, 2017. **18**(11).
5. Wang, D., et al., *GC-MS-Based metabolomics discovers a shared serum metabolic characteristic among three types of epileptic seizures.* Epilepsy Res, 2016. **126**,83-9.

6. Walker, D.I., et al., *Metabolome-wide association study of anti-epileptic drug treatment during pregnancy.* Toxicol Appl Pharmacol, 2019. **363**,122-130.
7. Li, S., et al., *In Situ Imaging of Cysteine in the Brains of Mice with Epilepsy by a Near-Infrared Emissive Fluorescent Probe.* Anal Chem, 2020.
8. Heischmann, S., et al., *Exploratory Metabolomics Profiling in the Kainic Acid Rat Model Reveals Depletion of 25-Hydroxyvitamin D3 during Epileptogenesis.* Sci Rep, 2016. **6**,31424.
9. Tan, X., et al., *Anticonvulsant and Neuroprotective Effects of Dexmedetomidine on Pilocarpine-Induced Status Epilepticus in Rats Using a Metabolomics Approach.* Med Sci Monit, 2019. **25**,2066-2078.
10. Kanawaku, Y., et al., *Pattern recognition analysis of proton nuclear magnetic resonance spectra of postmortem cerebrospinal fluid from rats with drug-induced seizure or coma.* Leg Med (Tokyo), 2017. **25**,52-58.
11. Li, P., et al., *(1)H NMR metabolomics to study the effects of diazepam on anisatin induced convulsive seizures.* J Pharm Biomed Anal, 2016. **117**,184-94.
12. Carmody, S. and L. Brennan, *Effects of pentylenetetrazole-induced seizures on metabolomic profiles of rat brain.* Neurochem Int, 2010. **56**(2),340-4.
13. Urban, M., et al., *Complexity and pitfalls of mass spectrometry-based targeted metabolomics in brain research.* Analytical Biochemistry, 2010. **406**(2),124-131.
14. Hogg, M.C., et al., *Elevation of plasma tRNA fragments precedes seizures in human epilepsy.* The Journal of clinical investigation, 2019. **129**(7).
15. McArdle, H., et al., *"TORNADO"–Theranostic One-Step RNA Detector; microfluidic disc for the direct detection of microRNA-134 in plasma and cerebrospinal fluid.* Scientific reports, 2017. **7**(1),1750.
16. Detour, J., et al., *Metabolomic characterization of human hippocampus from drug-resistant epilepsy with mesial temporal seizure.* Epilepsia, 2018. **59**(3),607-616.
17. Murgia, F., et al., *Metabolomics As a Tool for the Characterization of Drug-Resistant Epilepsy.* Front Neurol, 2017. **8**,459.
18. Al Zweiri, M., et al., *Response to drug treatment in newly diagnosed epilepsy: a pilot study of (1)H NMR- and MS-based metabonomic analysis.* Epilepsy Res, 2010. **88**(2-3),189-95.
19. Raynaud, F. and J. Roberts, *Capillary microsampling of mouse blood in pre-clinical studies: an alternative to dried blood spot sampling.* 2019.
20. Raje, A.A., et al., *Capillary microsampling in mice: effective way to move from sparse sampling to serial sampling in pharmacokinetics profiling.* Xenobiotica, 2019,1-7.
21. Patel, S.R., et al., *Microsampling for quantitative bioanalysis, an industry update: output from an AAPS/EBF survey.* Bioanalysis, 2019. **11**(07),619-628.
22. Xie, I., et al., *Extractability-mediated stability bias and hematocrit impact: high extraction recovery is critical to feasibility of volumetric adsorptive microsampling (VAMS) in regulated bioanalysis.* Journal of pharmaceutical and biomedical analysis, 2018. **156**,58-66.
23. Freeman, J.D., et al., *State of the science in dried blood spots.* Clinical chemistry, 2018. **64**(4),656-679.
24. Verhaeghe, T., et al., *The application of capillary microsampling in GLP toxicology studies.* Bioanalysis, 2017. **9**(7),531-540.
25. Verhaeghe, T., et al., *Comparison of toxicokinetic parameters of a drug and two metabolites following traditional and capillary microsampling in rat.* Bioanalysis, 2019(0).
26. Cobb, Z., et al., *Feedback from the European Bioanalysis Forum liquid microsampling consortium: capillary liquid microsampling and assessment of homogeneity of the resultant samples.* Bioanalysis, 2019. **11**(06),525-532.
27. Zhang, W., et al., *Utility of sheathless capillary electrophoresis-mass spectrometry for metabolic profiling of limited sample amounts.* J Chromatogr B Analyt Technol Biomed Life Sci, 2018. **1105**,10-14.

28. Ramautar, R., *Sheathless Capillary Electrophoresis-Mass Spectrometry for the Profiling of Charged Metabolites in Biological Samples.* Methods Mol Biol, 2018. **1738**,183-192.
29. Miggiels, P., et al., *Novel technologies for metabolomics: More for less.* TrAC Trends in Analytical Chemistry, 2018.
30. Sanchez-Lopez, E., et al., *Sheathless CE-MS based metabolic profiling of kidney tissue section samples from a mouse model of Polycystic Kidney Disease.* Sci Rep, 2019. **9**(1),806.
31. Hirayama, A., et al., *Development of a sheathless CE-ESI-MS interface.* Electrophoresis, 2018. **39**(11),1382-1389.
32. Fang, P., J.Z. Pan, and Q. Fang, *A robust and extendable sheath flow interface with minimal dead volume for coupling CE with ESI-MS.* Talanta, 2018. **180**,376-382.
33. Harada, S., et al., *Reliability of plasma polar metabolite concentrations in a large-scale cohort study using capillary electrophoresis-mass spectrometry.* PLoS One, 2018. **13**(1),e0191230.
34. Zhang, W., et al., *Assessing the suitability of capillary electrophoresis-mass spectrometry for biomarker discovery in plasma-based metabolomics.* ELECTROPHORESIS, 2019. **0**(0).
35. Drouin, N., et al., *Effective mobility as a robust criterion for compound annotation and identification in metabolomics: Toward a mobility-based library.* Analytica Chimica Acta, 2018. **1032**,178-187.
36. Brown, W.C., et al., *Comparative assay of an antiepileptic drugs by psychomotor seizure test and minimal electroshock threshold test.* J Pharmacol Exp Ther, 1953. **107**(3),273-83.
37. Barton, M.E., et al., *Pharmacological characterization of the 6 Hz psychomotor seizure model of partial epilepsy.* Epilepsy Res, 2001. **47**(3),217-27.
38. Walrave, L., et al., *Validation of the 6Hz refractory seizure mouse model for intracerebroventricularly administered compounds.* Epilepsy Research, 2015. **115**,67-72.
39. Albertini, G., et al., *6 Hz corneal kindling in mice triggers neurobehavioral comorbidities accompanied by relevant changes in c-Fos immunoreactivity throughout the brain.* Epilepsia, 2018. **59**(1),67-78.
40. Takach, E., T. O'Shea, and H. Liu, *High-throughput quantitation of amino acids in rat and mouse biological matrices using stable isotope labeling and UPLC–MS/MS analysis.* Journal of Chromatography B, 2014. **964**,180-190.
41. The Standard Metabolic Reporting Structures working, g., et al., *Summary recommendations for standardization and reporting of metabolic analyses.* Nature Biotechnology, 2005. **23**,833.
42. Madsen, R., T. Lundstedt, and J. Trygg, *Chemometrics in metabolomics--a review in human disease diagnosis.* Anal Chim Acta, 2010. **659**(1-2),23-33.
43. Ortiz-Villanueva, E., et al., *Knowledge integration strategies for untargeted metabolomics based on MCR-ALS analysis of CE-MS and LC-MS data.* Anal Chim Acta, 2017. **978**,10-23.
44. Gorrochategui, E., J. Jaumot, and R. Tauler, *A protocol for LC-MS metabolomic data processing using chemometric tools.* 2015.
45. Jaumot, J., A. de Juan, and R. Tauler, *MCR-ALS GUI 2.0: New features and applications.* Chemometrics and Intelligent Laboratory Systems, 2015. **140**,1-12.
46. Zhang, T. and D.G. Watson, *Evaluation of the technical variations and the suitability of a hydrophilic interaction liquid chromatography-high resolution mass spectrometry (ZIC-pHILIC-Exactive orbitrap) for clinical urinary metabolomics study.* Journal of Chromatography B, 2016. **1022**,199-205.
47. González-Ruiz, V., et al., *ROMANCE: A new software tool to improve data robustness and feature identification in CE-MS metabolomics.* ELECTROPHORESIS, 2018. **39**(9-10),1222-1232.
48. Gorrochategui, E., et al., *Data analysis strategies for targeted and untargeted LC-MS metabolomic studies: Overview and workflow.* TrAC Trends in Analytical Chemistry, 2016. **82**,425-442.
49. Zheng, F., et al., *Plasma metabolomics profiles in rats with acute traumatic brain injury.* PLoS One, 2017. **12**(8),e0182025.

50. Gosselin, R., D. Rodrigue, and C. Duchesne, *A Bootstrap-VIP approach for selecting wavelength intervals in spectral imaging applications.* Chemometrics and Intelligent Laboratory Systems, 2010. **100**(1),12-21.
51. During, M.J. and D.D. Spencer, *Extracellular hippocampal glutamate and spontaneous seizure in the conscious human brain.* Lancet, 1993. **341**(8861),1607-10.
52. Haglid, K.G., et al., *Excitotoxicity. Experimental correlates to human epilepsy.* Mol Neurobiol, 1994. **9**(1-3),259-63.
53. Wilson, C.L., et al., *Comparison of seizure related amino acid release in human epileptic hippocampus versus a chronic, kainate rat model of hippocampal epilepsy.* Epilepsy Res, 1996. **26**(1),245-54.
54. Boguszewicz, L., et al., *NMR-based metabolomics in pediatric drug resistant epilepsy - preliminary results.* Sci Rep, 2019. **9**(1),15035.
55. Szyndler, J., et al., *Changes in the concentration of amino acids in the hippocampus of pentylenetetrazole-kindled rats.* Neurosci Lett, 2008. **439**(3),245-9.
56. Eid, T., et al., *Loss of glutamine synthetase in the human epileptogenic hippocampus: possible mechanism for raised extracellular glutamate in mesial temporal lobe epilepsy.* The Lancet, 2004. **363**(9402),28-37.
57. Bejarano, E. and J.A. Rodriguez-Navarro, *Autophagy and amino acid metabolism in the brain: implications for epilepsy.* Amino Acids, 2015. **47**(10),2113-26.
58. Wu, G., *Amino acids: metabolism, functions, and nutrition.* Amino Acids, 2009. **37**(1),1-17.
59. Jobe, P.C. and J.W. Dailey, *Aspartame and seizures.* Amino Acids, 1993. **4**(3),197-235.
60. Wenger, G.R., R.E. Stitzel, and C.R. Craig, *The role of biogenic amines in the reserpine-induced alteration of minimal electroshock seizure thresholds in the mouse.* Neuropharmacology, 1973. **12**(7),693-703.
61. Svob Strac, D., et al., *Monoaminergic Mechanisms in Epilepsy May Offer Innovative Therapeutic Opportunity for Monoaminergic Multi-Target Drugs.* Frontiers in Neuroscience, 2016. **10**,492.
62. Kurian, M.A., et al., *The monoamine neurotransmitter disorders: an expanding range of neurological syndromes.* Lancet Neurol, 2011. **10**(8),721-33.
63. Lasley, S.M., *Roles of neurotransmitter amino acids in seizure severity and experience in the genetically epilepsy-prone rat.* Brain Res, 1991. **560**(1-2),63-70.
64. Yin, J., et al., *L-Cysteine metabolism and its nutritional implications.* Mol Nutr Food Res, 2016. **60**(1),134-46.
65. Pontes, Z.E., et al., *Proline administration decreases Na+,K+-ATPase activity in the synaptic plasma membrane from cerebral cortex of rats.* Metab Brain Dis, 1999. **14**(4),265-72.
66. Hirata, K., et al., *Effect of l-arginine on synaptosomal mitochondrial function.* Brain and Development, 2008. **30**(4),238-245.
67. Kakinoki, H., et al., *The effects of histamine H3-receptor antagonists on amygdaloid kindled seizures in rats*. Vol. 46. 1998. 461-5.

Chapter 8

A new dimension to nanosafety: the metabolite corona determined using a quantitative metabolomics approach

Based on

Andrew J. Chetwynd*, Wei Zhang*, James A. Thorn, Iseult Lynch, and Rawi Ramautar

A new dimension to nanosafety: the metabolite corona determined using a quantitative metabolomics approach

Submitted

* Authors contributed equally

Abstract

Nanomaterial corona research to date has predominantly focused on proteins and how they affect nanomaterial uptake, distribution and bioactivity. These studies demonstrate that proteins confer a biological identity to nanomaterials and enable them to interact with receptors to mediate cellular responses. Thus protein corona studies have been integral to nanosafety given its biological implications. However, a larger class of molecules, that is metabolites, has been overlooked. While orders of magnitude smaller than proteins, metabolites regulate key pathways in metabolism and interact with receptors. By ignoring metabolites, a significant resource in the corona has been overlooked, hampering our understanding of the bio-nano interface, development of computational predictions of corona formation and investigations into uptake or toxicity at the cellular level, including identification of molecular initiating events triggering adverse outcome pathways. Here a capillary electrophoresis – mass spectrometry based metabolomics approach reveals that polar ionogenic metabolites adsorb to nanomaterials, with nanomaterial properties impacting upon the qualitative and quantitative composition of the metabolite corona. The metabolite corona composition was quantitatively compared using protein-free and complete plasma samples, revealing that proteins in the sample significantly change the composition of the metabolite corona. This key finding provides the basis to include the metabolite corona in future nanosafety endeavors.

Introduction

The nanomaterial (NM) corona has been an area of intense research for a decade and is predominantly focused upon the adventitious adsorption of proteins to the NM surface from its local environment [1, 2]. This protein corona is instrumental in the biological recognition of NMs by cells and has a pivotal role in cellular uptake, distribution and toxicity [1, 3-5]. The qualitative and quantitative composition of the protein corona is reliant upon a wide range of NM properties including size [5-7], curvature [8-10], and surface modification [6, 7, 11], as well as being influenced by the biological matrix itself whose composition determines the biomolecules available for binding [8, 12]. A comprehensive understanding of the NM corona may help in the development of nanomedicines and nano-agrochemicals by manipulating its content to target specific tissues as a drug/pesticide delivery system [3]. Furthermore, a thorough knowledge of the corona may also help to predict environmental fate by understanding how proteins exchange in new environments as NMs are transported and how this affects the bioaccumulation of NMs in organisms.

However, studies to date have neglected a major set of biomolecules present in all biological matrices, i.e., endogenous metabolites. These are small molecules typically with a mass <1000 Da that act as substrates, intermediates and products of metabolism [13]. Metabolites are orders of magnitude smaller in size and significantly greater in number (>100,000 [14] vs 20,000 [15]) relative to their protein counterparts (excluding post-translationally modified proteins and chiral and positional isomers of metabolites). Metabolites contribute significantly to signaling cascades in biological systems and interact with receptors to initiate uptake and transport [16-21]. Overlooking this aspect of the corona is potentially deleterious to a comprehensive understanding of the role of the corona in determining the biological consequences of NMs both clinically and environmentally.

To date, the metabolite corona has been poorly investigated with only a few studies focusing on a subset of the metabolome, e.g. lipids, which constitute the initial barrier to cellular entry of NMs and are a major constitute of the lung lining (air-lung interface) and are thus the first point of contact for inhaled NMs [22-24]. Serum, a key transport media in the body, has also been assessed for its lipid corona forming ability [25]. These studies revealed that lipids adsorb to the surface of NMs and that they can impact upon the biological response to NMs. Furthermore, a limited number of studies have investigated a broader range of metabolites and demonstrated that a wide array of metabolites can interact with NMs to form a metabolite corona [26-28]. Yet, the concept of a small molecule corona, or indeed the realization that the presence of metabolites within the protein corona may mediate the NM behavior, has been overlooked in nanosafety to date. Here, for the first time, characterization of the selective adsorption of small molecules to NMs, forming a metabolite corona, and the impact of proteins on the composition of the small molecule corona are presented.

Metabolomics is a newer member of the omics family that aims to provide an answer to a well-defined biological question by the global profiling of metabolites in biological samples. As the metabolome is composed of compounds occupying a large physico-chemical space and spanning orders of magnitude in concentration, a combination of analytical separation techniques with complementary mechanisms are required in order to detect as many metabolites as possible. In this context, reversed-phase liquid chromatography-mass spectrometry (LC-MS) is well-suited for the analysis of relatively hydrophobic compounds such as lipids and steroids [29-31]. However, the current work implements capillary zone electrophoresis linked to mass spectrometry (CE-MS) which has recently been proposed as a novel method for NM corona analysis to characterize the highly polar charged metabolites [32]. CE-MS has found a niche in metabolomics for the analysis of highly polar and charged metabolites, such as amino acids, organic acids and nucleotides [33-36]. Due to the flat flow profile of the electro-osmotic flow and the fact that only longitudinal diffusion contributes to band broadening in CE, the use of CE-MS offers an analytical platform with an exceptionally high-resolution separation and highly selective detection. When employing a sheathless interfacing technique for coupling CE to MS, the intrinsically low flow-rate separation property of CE (about 20 nL/min under low-pH separation conditions) can be used effectively to significantly improve ionization efficiency in nano-ESI-MS [33, 37].

In the current proof-of-principle study, the metabolite coronas acquired by six different nanomaterials were analysed. Spherical SiO_2 is a common food additive and thus a significant source of human exposure, while anatase TiO_2, either naïve, PVP or poly acrylate (dispex) capped, is a common environmental contaminant from paints, sunscreen and food that also offers a human route of exposure [38]. The anatase structure offers a more complex structure which may impact upon the acquired corona compared to the other spherical particles in the study while the capping with ligands offers additional complexity and allows a comparison with the protein corona where surface modifications are known to significantly affect corona formation and composition. Moreover, spherical naïve and carboxylated polystyerene nanoparticles were investigated due to the rising interest in micro- and nano-plastics being both consumed by humans and other organisms but also released to the environment. The metabolite coronas were characterized in a quantitative manner by CE-MS, thereby complementing a recent protein corona study also performed with a CE-MS approach [39]. The role of proteins in the recruitment of endogenous metabolites to the corona was also examined and revealed that the presence of proteins in the sample is vital to characterize a biologically relevant and representative metabolite corona. This is an important and unique finding since neither proteins nor metabolites exist in isolation from one another in nature and are thus co-adsorbed into NM coronas as shown schematically in **Figure 1**. As part of rethinking nanosafety, characterisation of the interdependent metabolite and protein coronas may provide important new mechanistic insights allowing interpretation of systems toxicological effects and identification of molecular initiating events as part of adverse outcome pathways.

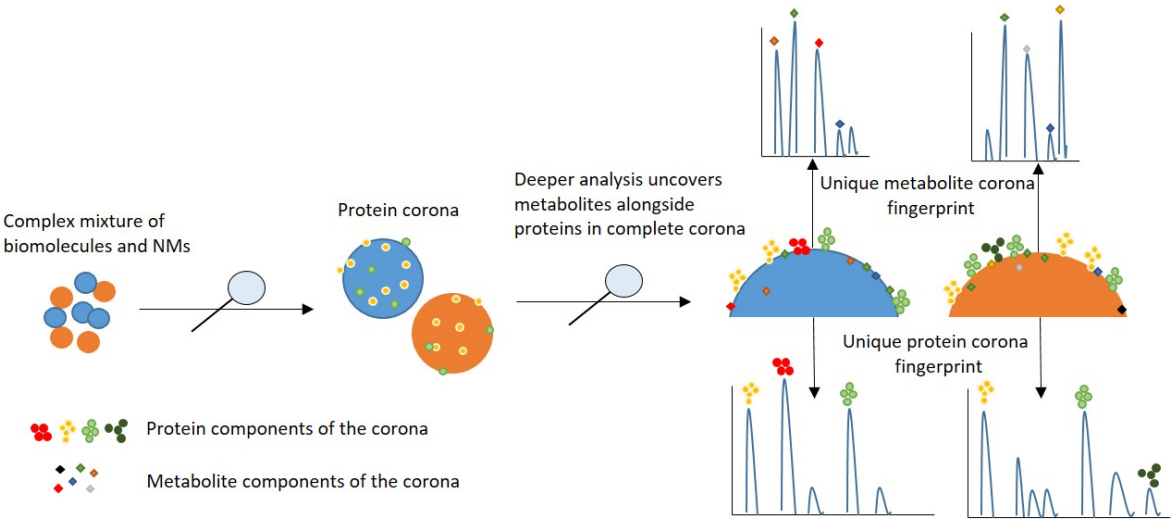

Figure 1. The analysis of unique protein and metabolite coronas as part of a complete corona analysis from various nanomaterials.

Results and Discussion

Initially this work assessed whether NMs exposed to equimolar mixtures of cationic (**Supplementary Table S1**) or anionic metabolites (**Supplementary Table S2**) selectively bound metabolites and determined which metabolites bound to the different NMs and the binding extent in order to determine whether each NM has a unique metabolite fingerprint. These standard metabolite solutions contained charged polar metabolites such as amino acids which can act as neurotransmitters, porphyrin and protein precursors; nucleotides and nucleosides which form the basis of DNA and RNA in addition to key organic acids from the TCA cycle and sugar phosphates which form part of the glycolysis and pentose phosphate pathways, all of which are key metabolic pathways in living organisms. Subsequently, NMs were exposed to human plasma, both with and without proteins in order to investigate the role of proteins in the recruitment of the metabolite corona, and to assess the utility of CE-MS to characterize the complete NM corona.

NM characterization

Table 1. NM characterisation in MilliQ water immediately following dispersion at 4 mg/mL

Nanomaterial	Hydrodynamic diameter (nm)	Polydispersity index	Zeta Potential (mV)	Electrophoretic mobility (µmcm/Vs)
SiO_2	34.8±0.6	0.16±0.01	-42.0±1.7	-3.3±0.1
TiO_2-un*	922.3±81.3	0.07±0.05	24.2±1.3	1.9±0.1
TiO_2-PVP	2076.5±666.7	0.58±0.32	8.4±1.1	0.65±0.1
TiO_2-Dispex	1757.7±793.4	0.27±0.16	24.85±1.5	2.0±0.1
PS	106.9±1.7	0.04±0.01	-61.2±2.7	-4.8±1.7
PS-COOH	111.2±2.6	0.03±0.02	-63.4±2.5	-5.0±0.2

* refers to uncapped titania NMs

These NMs have previously been characterized as part of a study of their acquired protein coronas and a summary of their physico-chemical characteristics in MilliQ water, which includes the size and zeta potential data, is provided in **Table 1** (details on the properties of the capping polymers is given in **Table S3**) [39]. The silica and polystyrene NMs maintain sizes close to their core particle size upon dispersion, however, the titania NMs show significant aggregation and agglomeration given their core size is 13 nm.

Suitability of the sheathless CE-MS platform and methodology

A brief assessment of the reproducibility of the sheathless CE-MS approach was performed by repeatedly injecting 5 μM of the cation metabolite mixture on three consecutive days. Both intra-day (n=16) and inter-day (n=36 across 3 days) reproducibility was assessed for peak area and migration (**Table S4**). The intra-day repeatability for peak area averaged 5.8% with all metabolites having an RSD ≤9.3%. The migration time values all fell below 2.7% and averaged 2.1%. Inter-day variability for peak area averaged 8.5% with all peaks having an RSD ≤ 16% with the corresponding values for migration time being 1.8% and ≤2.3%. Moreover, using the calibration curves generated for the standard mixtures the LODs were determined with the LOD for cations ranging from 1.3 nM to 22.3 nM and for anions ranging from 4.3 nM to 125.2 nM (**Supplementary Table S5**). These values demonstrate the excellent reproducibility and sensitivity of the sheathless CE-MS platform. Stability controls at the experimental concentrations were analyzed following the same experimental protocol minus the NMs confirming that there was no metabolite adsorption to any of the experimental vessels or degradation during incubation.

Adsorption of metabolites to NMs – metabolite corona formation

To characterize the metabolites that adsorb to NMs, two solutions were prepared, a 5 μM cation mixture and a 10 μM anion mixture (anions mixture was at a greater concentration due to negative mode ESI-MS being less sensitive). Following NM incubation in these solutions for 1 hr the NMs were removed and the amount of each metabolite remaining in the mixture was quantified, where the decrease in concentration was used as a surrogate for metabolite adsorption. To accurately determine the pre-exposure concentration, quality control (QC) and stability control samples were quantified as these were all from the same metabolite standard mixture stock.

1. **Silica nanoparticles**

The adsorption of both cations and anions to the SiNPs is very limited, with only 1.5 μM of the cationic, non-essential amino acid aspartic acid adsorbing to a significant extent ($p<0.0001$) (**Fig. 2**, **Table S6**) from the total pool of 30 cationic and 12 anionic metabolites. This is perhaps surprising given the negative zeta potential, suggesting electrostatic attraction plays a relatively

minor role in the adsorption of metabolites. Instead the adsorption mechanism may reflect the retention properties of hydrophilic interaction liquid chromatography (HILIC) columns, whereby polar metabolites are retained via interactions with a diffuse water layer surrounding the silica particles in the column, in this case the SiNPs behaving as a stationary phase during the incubation [40]. However, this exchange is highly pH-dependent and sensitive; in the current study a physiological pH is used which is incompatible with this retention mechanism and, therefore, adsorption of polar metabolites to the Ludox SiO_2 NMs is unlikely as seen here.

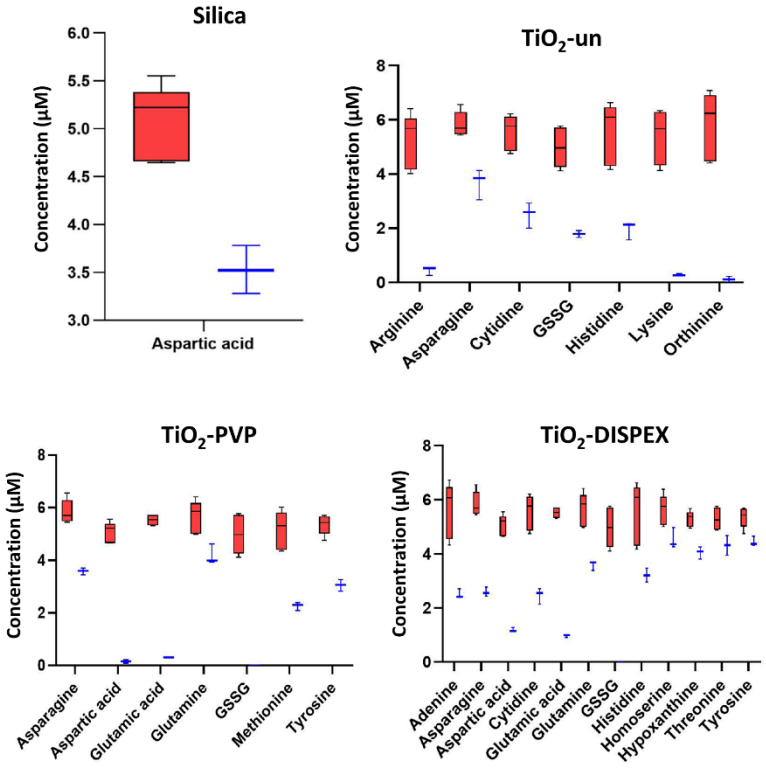

Figure 2. The adsorption of metabolites ($p<0.0001$) to SiO_2 and ($p<0.05$) to TiO_2 NMs after a 1 hr incubation with a metabolite mixture. Red refers to the initial concentration in the cation mixture whereas blue indicates the concentration of the cation remaining in solution following NM exposure, whereby the reduction is a result of binding to the NM surface.

2. Titania nanomaterials

The three titania NMs, uncoated, PVP capped and Dispex (polyacrylate) capped, displayed strong adsorption characteristics for both cations and anions. In the case of the cations, 7 adsorbed significantly to the TiO_2-un NMs (**Fig. 2**, **Table S6**) with arginine, lysine and ornithine almost completely depleted from the metabolite solution following NM incubation. This raises an interesting prospect whereby the depletion of key metabolites in a system may be a potential source of NM toxicity since their depletion may lead to disruption of key metabolic pathways including in the urea cycle, and protein synthesis and modification. Interestingly, only arginine and glutathione disulfide (GSSG) are adsorbed to significant extents across all three TiO_2 NMs. This implies that even in the presence of capping ligands the influence of the core material on the

formation of the corona is conserved, as has also been observed with protein corona formation [7, 41]. Interestingly, TiO_2-Dispex NMs, which possess a negative charge (**Table S3**), had 4 corona metabolites in common with TiO_2-un making them closer in terms of qualitative composition than either are to the TiO_2-PVP NMs. This is in contrast to previous protein corona studies with these NMs where the uncoated and PVP capped materials were well matched in terms of protein corona composition [39]. This is an interesting result as based on the protein corona data it may be tempting to assume metabolite behavior would also be conserved. These differences between metabolite and protein coronas highlight the need to characterize the complete corona to better inform future nanosafety, bio-nano interaction and modeling studies. The TiO_2-Dispex NMs adsorbed the greatest number of metabolites, i.e. 12 from the pool of 42 metabolites, potentially as a result of the carboxy groups available on the polyacrylate polymer and the net positive charge of the cations thus leading to electrostatic attraction, in addition to permanent covalent bonds formed via esterification of the carboxy groups on the polymer and hydroxyl groups on the amino acids. The TiO_2-PVP NMs carry a more neutral charge compared to TiO_2-un, thus the interactions between metabolites and the TiO_2-PVP NMs are likely a result of the core material itself, as well as hydrogen bonding or van der Waals interactions with the PVP chain. Interestingly, on both TiO_2-PVP and TiO_2-Dispex NMs the GSSG is completely depleted by the NMs potentially increasing the risk of antioxidant damage *in-vivo* as GSSG is a key component in the glutathione-ascorbate cycle which is a major metabolic pathway to detoxify hydrogen peroxide (H_2O_2).

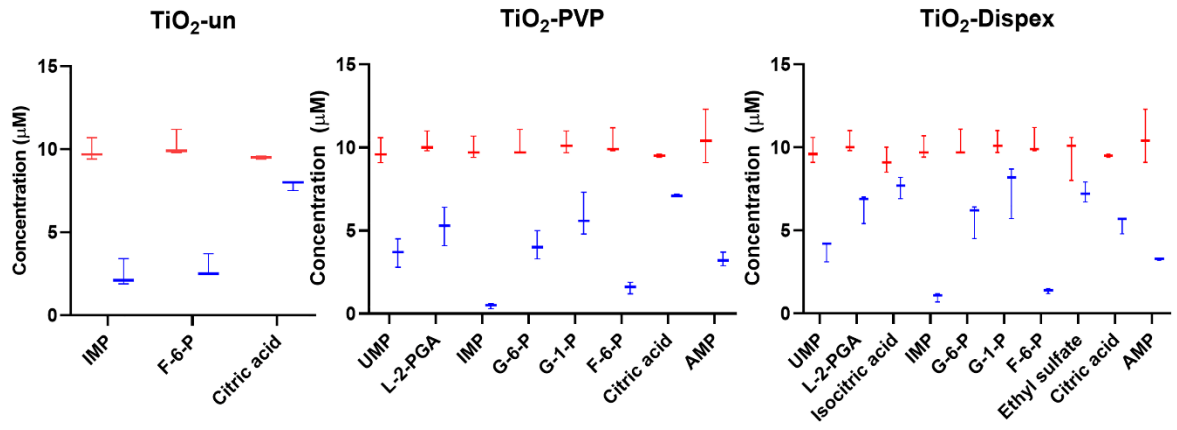

Figure 3. The adsorption of anions ($p<0.05$) to the 3 TiO_2 NMs after a 1 hr incubation in a standard metabolite mixture. Red refers to the concentrations in the initial anion mixture whereas blue indicates the concentration remaining in the anion solution following NM exposure.

The TiO_2 NMs were the only NMs to adsorb anions from the metabolite standard solutions (**Fig. 3**, **Table S7**), this is likely due to the over representation of phosphorylated metabolites in the mixture. These metabolites are vital in energy metabolism and DNA/RNA synthesis and their binding into the NM corona highlights an interesting property of corona formation, namely isomer selectivity. In the case of TiO_2-un NMs, 8.7 µM fructose 6-phosphate (F-6-P) formed part of the corona however the same was not the case for glucose 1-phopshate (G-1-P) or glucose 6-

phosphate (G-6-P), isomers of F-6-P. This isomer selectivity was also observed for citrate and isocitrate where citrate was the only form to adsorb to both TiO_2-un and TiO_2-PVP whereas both adsorbed to TiO_2-Dispex, though 4.6 µM of citrate adsorbed compared to 2.4 µM of isocitrate. The polymer capped TiO_2 NMs adsorbed 8 and 10 anions (from an available pool of 12, **Table S3**) for the TiO_2-PVP and TiO_2-Dispex, respectively, highlighting the key role of surface modification in the composition of the metabolite corona. Of the sugar phosphates, F-6-P was again well adsorbed to the polymer coated TiO_2 NMs (TiO_2-PVP and TiO_2-Dispex), however G-1-P and G-6-P were also adsorbed with a slight preference for the G-6-P isomer over the G-1-P evident from **Figure 3**. The adsorption of phosphate containing metabolites to TiO_2 NMs is unsurprising as titanium based solid phase extraction is used to enrich phosphopeptides and phosphoproteins due to the high affinity of phosphates for titania [42, 43], though the isomer selectivity provides an intriguing prospect for future work as this may be key to several biological interactions.

3. Polystyrene nanoparticles

From the cationic and anionic metabolite mixtures, COOH-PS NMs bound only 6 cations, adenine, arginine cytidine, histidine, lysine and tyramine with between 2.6 and 3.7 µM (52% and 74% respectively of the available amount) of each adsorbing (**Fig. 4**, **Table S6**), while the bare PS NMs bound none. Here, not only was electrostatic attraction a potential route for adsorption but also esterification via the carboxylic acid moieties on the PS-COOH particle surface. Given that there was no significant adsorption to the bare PS NM which shares a similar negative zeta potential, it is possible that the cationic metabolite adsorption to the carboxylated PS NMs is via the latter mechanism (esterification). However, the relatively large negative net charge of the two PS NMs is likely a reason behind the lack of anion adsorption via electrostatic repulsion. The difference in the adsorption of cations between the two PS NMs is not unexpected as the composition of the protein coronas for these two very similar NMs has recently been demonstrated to be (semi)quantitatively different [39].

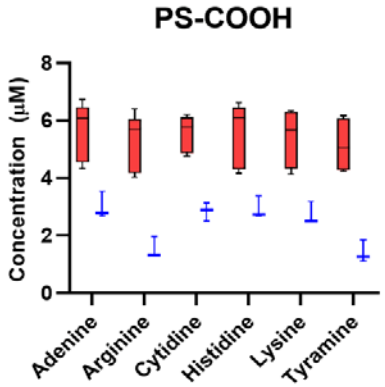

Figure 4. The adsorption of cations (p<0.05) to the PS-COOH NMs after a 1 hr incubation in a metabolite mixture. Red refers to the concentrations of cation in the initial mixture whereas blue indicates the concentration of the cations remaining in solution following NM exposure.

Time evolution of the metabolite corona

It is well known that the protein corona is dynamic and undergoes compositional changes over time whereby low affinity high abundance proteins are slowly exchanged for low abundance high

affinity proteins [2, 44]. To investigate whether this phenomenon also occurs with metabolites the 6 NMs were incubated with the 5 μM cationic mixture for 24 hrs at 37 ˚C and the amount and types of metabolites bound were compared to the above data from 1 hr incubations. Only the cations were examined as the phosphorylated anions are less stable over protracted periods of time at 37 ˚C [45].

The SiO_2 and bare PS NM metabolite coronas were unchanged following the extended incubation, however the three TiO_2 and the COOH-PS NMs displayed several significant changes in the metabolite corona over time, suggesting that equilibration of the metabolite corona is protracted (**Fig. S1**, **Table S8**). The TiO_2-un NM corona contained 6 metabolites that varied significantly with the 24 hr incubation, namely asparagine, cytidine and GSSG where the same trend in terms of ratios of absorbed amounts was observed as for the 1 hr incubation, suggesting that after an hour there are still adsorption sites on the NM available for further adsorption of these metabolites or that there are metabolite-metabolite interactions that are yet to be elucidated. Potentially further evidence of metabolite-metabolite interactions was seen with glutamine and methionine which were adsorbed significantly by 24 hrs but did not absorb at all in the 1 hr incubation. An alternative explanation could be that some of the slower binding metabolites displace early binders, as observed in the protein corona [1, 7]. For example, the quantity of lysine in the COOH-PS corona decreased by 2-fold between 1 and 24 hrs, suggesting it may have been displaced by one or several of the other 5 metabolites. It is worth noting that in the case of asparagine and glutamine the metabolites were completely depleted from the standard solution, thus it is possible more could have adsorbed if a greater concentration was used. Future work could help elucidate this mechanism by using a simpler metabolite mixture, adding one metabolite at a time or incorporating more time points over longer time periods.

The incubation of the TiO_2-PVP NMs returned 6 metabolites that varied significantly from the 1 hr incubations with asparagine, glutamine, methionine and tyrosine adsorbing to greater extents, 9, 7, 27 and 3 fold more at 24 hrs than at 1 hr, respectively. Creatine and tyramine were found to have adsorbed to the NM by 24 hrs whereas they had not done in the initial 1 hr study, further suggesting that one hour is insufficient time for the metabolite corona to reach equilibration in a standard mixture in water. As observed in the TiO_2-un NMs, a number of metabolites in the exposure medium were found to be depleted or close to depletion with 10- and 143-fold more asparagine and glutamine respectively adsorbing to the TiO_2-un NM in the additional 23 hrs compared to the 1 hr incubation. The TiO_2-Dispex corona also contained some of the same metabolites as the 1 hr incubation but with a 1.5-fold greater concentration, and with the addition of creatine and methionine to the corona. Interestingly aspartic acid levels in the corona decreased by nearly 2 fold suggesting that a limited amount of corona exchange has occurred. The small molecule corona of COOH-PS NMs remained quite stable with just the addition of creatine binding significantly by 24 hr, in addition to the 6 metabolites seen in the initial 1 hr corona.

These data suggest that the complex dynamics observed in the protein corona in terms of affinities and exchange kinetics are reflected also in the metabolite corona, which this pilot study only begins to uncover. The extended duration of formation of the metabolite corona, with continual adsorption of metabolites over at least 24 hrs, offers a key insight into a potential route for NM toxicity relating to NM sequestering of key signaling metabolites. It should be noted however that in this pilot study a high concentration of NMs and metabolites is used, however, it is reasonable to expect that the same trend and time course for metabolite corona evolution would occur in human or environmental conditions. Given that the metabolites used in this study represent those from key metabolic processes, it is likely that the effect on cellular metabolism will be dynamic and that upregulation of pathways to compensate for the loss of key metabolites may continue to feed the formation of the metabolite corona.

Recovery of adsorbed metabolites

The initial findings of this pilot study confirm that each NM has a unique metabolite fingerprint in terms of which metabolites bind to the NM surface and are incorporated into its metabolite corona. The approach used, whereby the corona is determined by looking at how metabolite levels change in a matrix as a result of binding to the NM, is however unsuitable for real world examples where it is not possible or feasible to characterize (and quantify all metabolites present in) the biological matrix before and after NM exposure. In these cases, a washing procedure will be required to isolate the metabolite corona from the NMs and directly identify the bound metabolites. As a result of the range of metabolite properties, several fractions may need to be recovered and characterized in parallel to ensure complete metabolite corona characterization.

Given the highly hydrophilic nature of the metabolite test mixtures, a three-step washing procedure was considered, comprising two washing steps with water and one washing step with methanol/water (1:1, v/v) [46]. All washing steps were assisted with sonication for 5 minutes in a water bath at room temperature.

The total recovery for each washing step of those metabolites found to adsorb significantly for all NMs are shown in **Figures S2** and **S3**. In the case of the cations, recovery from the SiO_2, TiO_2-un and the TiO_2-PVP is generally poor with no more than 20% of the cations, known to be there based on the amounts depleted from solution, being recovered. However, this washing process seems to be more appropriate for cations adsorbed to the TiO_2-Dispex and the COOH-PS NMs, with recoveries exceeding 60% for several of the metabolites (**Fig. S2**).

In the case of the anion recoveries the performance of the wash steps is poor with only glucose 6-phosphate and citric acid showing a recovery exceeding 50% from the TiO_2-un NMs. As with the adsorption of the anionic metabolites, the recovery of these metabolites also appears to follow an isomer specific recovery profile. These data clearly indicate that the amount of metabolite not detected in the supernatant samples at the end of the exposure periods was adsorbed to the NMs,

though, in many cases the adsorbed amount could not be fully recovered with the selected washing conditions. As such caution is warranted for work where it is claimed that metabolites are recovered from NMs where a recovery study has not been performed, as it is highly likely that each NM will require a unique recovery protocol.

Metabolite corona formation under competitive binding conditions: Effect of the absence or presence of proteins in plasma on the adsorption of metabolites

In all biological matrices proteins and metabolites co-exist; as such it is important to consider the effect of one on the other during the formation of the NM corona. This work has shown already that metabolites adsorb in an NM-dependent manner and it is well documented that proteins follow a similar trend, as recently demonstrated also for these 6 NMs [39]. To characterize the impact of proteins on the recruitment of the small molecule corona, a pooled human plasma sample was split into two aliquots, one of which was protein crashed to remove the proteins from the plasma (designated as protein free plasma, PFP) and the other of which was left as intact plasma (IP). The NMs were exposed to these samples for 1 hr at 37 ˚C and the concentration decrease in the same selected cations and anions was quantified.

1. **Silica nanoparticles**

As with the pure metabolite standards, the SiO_2 NM showed a poor affinity even in plasma for the metabolites being investigated. However, histidine, which did not adsorb significantly in the standard solutions, did adsorb 1.3 fold more in the protein free plasma (PFP) versus the intact plasma (IP), suggesting that the presence of proteins in plasma in this case inhibits the adsorption of histidine to the SiO_2 NMs (**Fig. 5**, **Tables S9** and **S10**). This inhibition could potentially occur through proteins occupying adsorption points or changing the surface chemistry to such an extent that it is no longer suitable for histidine interactions. Additionally, the fact that histidine adsorbed in the plasma samples but not the pure standards implies that there are other mechanisms playing a role in metabolite adsorption such as salt concentration/adsorption or metabolite-metabolite interactions on the NM surface. In terms of anion adsorption, inosine monophosphate (IMP), uridine monophosphate (UMP) and F-6-P were all adsorbed to greater extents (1.6-1.9 fold more) in the presence of proteins from the IP, providing strong evidence to suggest that proteins and metabolites are co-located in the NM corona, and that both are vital components. The role of proteins as mediators of metabolite incorporation into the corona is clear, as none of the metabolite cations being investigated were seen to adsorb to the SiO_2 NMs from the standard solution. Given the negative charge of the SiO_2 NMs the proteins in plasma will have a strong affinity for the surface which will reduce the net negative charge and lead to a more positive charge thus becoming a suitable environment for recruitment of the negatively charged anions. Conversely, the isomer of F-6-P, G-6-P was found at a higher concentration in the corona formed in the PFP conditions, again suggesting that there are other mechanisms involved in the

recruitment of metabolites to the corona which have isomer specificity. More detailed studies are needed to identify these mechanisms.

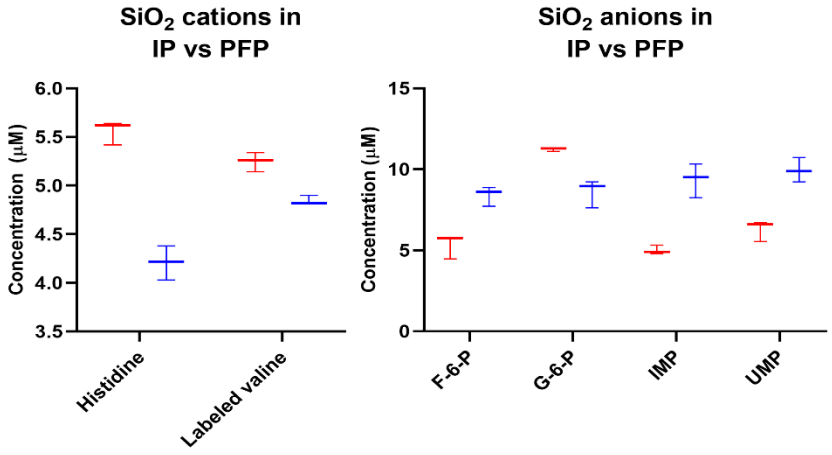

Figure 5. Differential adsorption of cations and anions to SiO_2 NMs from human plasma in the absence and presence of the plasma proteins. Red denotes the metabolite concentrations remaining in solution following SiO_2 NM exposure in intact plasma whereas blue denotes the metabolite concentrations remaining in solution following SiO_2 NM exposure in protein depleted plasma.

2. Titania nanomaterials

In the TiO_2-un NM corona, two cationic metabolites changed significantly between the PFP and the IP incubation solutions, cytidine and isoleucine (**Fig. 6**, **Tables S9** and **S10**). Cytidine was observed to adsorb in the pure water solutions and in the PFP solution approximately 25% of the cytidine adsorbed to the TiO_2 NMs this was further increased to 64% in the IP sample indicating that the presence of protein enhanced the recruitment of cytidine to the complete corona. In the case of isoleucine this metabolite was not previously observed to interact significantly with the bare TiO_2 NM in the pure solution, however, in the presence of proteins a significant quantity adsorbs to the NM. Furthermore, its isomer leucine was not significantly altered between the two solutions, indicating there is an apparent selectivity for isomers by the proteins in the corona. The isomer specificity was conserved for the anions in the TiO_2-un NMs of the anions being analyzed only citric acid was significantly altered between the incubation solutions. With 5-fold more citric acid being found in the corona of the TiO_2-un NMs incubated in IP than in PFP, its isomer isocitric acid was not observed to change and was not seen to adsorb in the initial tests using the standard solutions, further highlighting the potential for isomer specificity in the corona.

The TiO_2-PVP NMs showed the greatest differences of the titania NMs between the two plasma conditions, with the cations arginine, cytidine and histidine all demonstrating significant reductions in quantity in the IP corona (compared to the PFP corona) with histidine having a 40 fold greater concentration in the corona formed from the protein depleted sample (**Fig. 6**, **Tables S9** and **S10**). In contrast, methionine was 2.6 times greater in the IP corona, meaning that the

effects of proteins on the recruitment of metabolites to the corona is metabolite dependent. The presence of Sulphur in methionine is a potential mechanism for the disparity between samples as it may form disulphide bonds with the amino acids in the proteins of the corona. As with the bare titania, the specificity for citric acid rather than isocitric acid was conserved in TiO_2-PVP, with the citric acid being depleted from the IP whereas 50% remained in the PFP while isocitric acid was not observed to adsorb differently between the two preparations. Inosine monophosphate was present at greater levels in the IP corona.

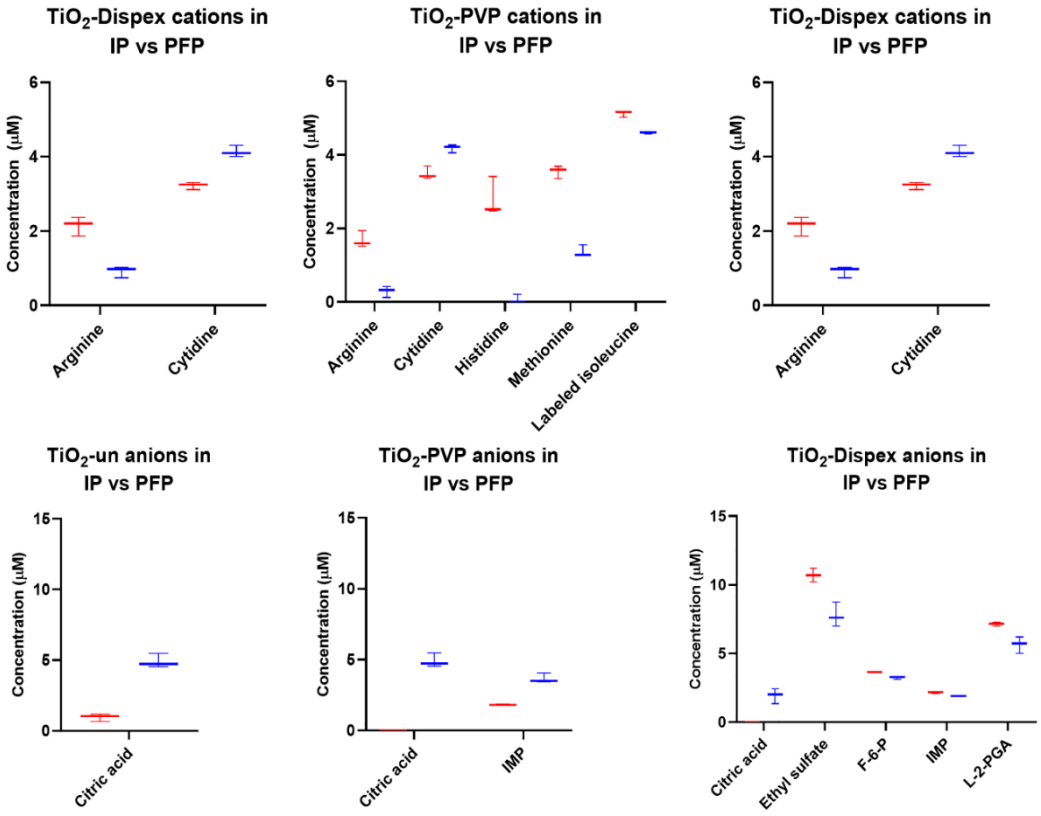

Figure 6. Differential adsorption of cations and anions to the TiO_2 NMs from human plasma in the absence and presence of the plasma proteins. Red denotes indicated concentration of metabolites bound in intact plasma whereas blue denotes the amount of the metabolite bound to the NM from the protein depleted plasma. Here, 5 µM of each metabolite was spiked into the human plasma on top of endogenous concentrations, explaining the higher values obtained for some metabolites.

Interestingly, with the TiO_2-Dispex the anions were predominantly found to be at a reduced concentration in the corona with the presence of proteins, which is counter-intuitive given the general trend for proteins to enhance metabolite recruitment to the corona (**Fig. 6**, **Tables S9** and **S10**). In the pure standards, the TiO_2-Dispex adsorbed the most anions of all the materials tested. Given the reversal in this trend here, it's likely that the carboxylated dispex coating is a key factor. Potentially these groups are saturated with proteins in the IP sample, and thus there are less adsorption points for metabolites. However, the trend for citric acid to bind to a greater extent in the presence of protein remains, suggesting that in the case of citric acid it is through the proteins

that the adsorption is driven whereas for the IMP, F-6-P, ethyl sulfate and L-2-phosphoslyceric acid it is direct interaction with the NM and its surface modification which is the most influential. This disparity between metabolites is also observed for the cations where cytidine is adsorbed to a greater extent in the IP whereas the presence of proteins inhibits the adsorption of arginine with a 2.4 fold decrease in arginine recruitment to the corona.

3. Polystyrene nanoparticles

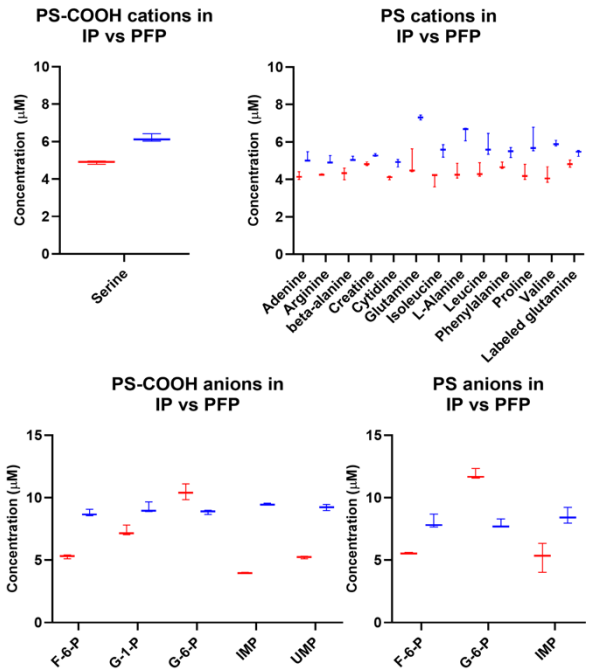

Figure 7. Differential adsorption of cations and anions to the PS NMs in human plasma with/without proteins. Red denotes intact plasma whereas blue denotes protein depleted plasma.

In both PSNPs, all cations bound significantly differently between the PFP and IP with greater concentrations observed in the presence of the intact plasma (**Fig. 7**, **Tables S9** and **S10**). This is likely a result of the overall net negative charge of the PSNPs showing a high affinity for the larger net positive charge proteins in the plasma, which then are instrumental in the recruitment of the metabolites portion of the corona. Interestingly, where 6 metabolites were seen to comprise the cation segment of the corona in pure standards for the COOH-PSNP, only serine was observed to be significantly bound when proteins were present. However, in the case of the bare PSNPs, 12 cationic metabolites were found to be present at higher concentrations in the protein-rich environment of the IP. This trend was also observed for anions for the PSNP corona with IMP, UMP, F-6-P and G-1-P binding to the COOH-PSNPs and IMP and F-6-P binding to the bare PSNPs to a greater extent in the presence of proteins, none of which adsorbed in the standard solution tests (metabolites only). As with the cations, this is likely a result of the negatively charged PSNPs adsorbing positively charged proteins which then directly recruit anions to the corona via protein-metabolite interactions. However, for both PSNPs and as seen for the SiNP corona, G-6-P

is recruited in an opposing fashion, as it is not identified in the corona of the pure standard anions but adsorbs in the PFP potentially as a result of salts or other metabolite interactions. G-6-P also opposes the behavior of its isomers of G-1-P and F-1-P in the presence of proteins, further indicating a strong isomer specificity of the corona.

Conclusion

This is the first quantitative analysis of the metabolome corona, which demonstrates that NMs recruit a unique metabolite fingerprint in much the same way as the protein corona and that variations in the protein corona do not necessarily reflect that of the metabolite corona. Moreover, this is the first work demonstrating that the protein portion of the corona is key to the formation of the metabolite corona to form a complete biomolecular corona. It is vital to follow this work up with an opposing study to investigate the role of metabolites in the formation of the protein corona as this may prove instrumental in the rising trend in modelling corona formation and its biological and environmental interactions. Furthermore, this work demonstrates that the formation of the metabolite corona is highly specific to the isomeric nature of the metabolites and that it enriches specific isomers over others. While this study uncovers many interesting properties of the metabolite and complete biomolecular corona and introduces CE-MS to the nanoscience field, the proposed work also generated a significant amount of unanswered and relevant questions for follow-up research. The key insight obtained by this study is that we need to consider (characterize and quantify) the full biomolecular corona at the bio-nano interface in order to get a comprehensive view of the interactions at this scale and to elucidate signaling impacts from NMs.

Experimental Section

All experiments and reporting were carried out in the spirit of the various guidelines and reporting standards for metabolomics and NM characterization [47-49].

Materials

Reagents were purchased from Sigma Aldrich, Actu-All Chemicals, Cambridge Isotope Laboratories and Buchem B.V. Pooled human plasma, anti-coagulated with heparin, was obtained from Sanquin Blood Bank (Leiden, the Netherlands). Two internal standards (ISTD) were used in this work 50 μM L-methionine sulfone (ISTD1) and 100 μM 2,2,4,4-D4-citric acid (ISTD2) for normalising peak areas of cations and anions, respectively.

Colloidal silica nanoparticles (SiO_2 NMs) Ludox TM-40, 40% w/v, were sourced from Sigma (Sigma, Merck, Darmstadt, Germany). 100 nm polystyrene nanoparticles (PS NMs) and 100 nm carboxylated PS NMs (PS-COOH) were purchased from Polysciences Inc. (Hirschberg an der Bergstrasse, Germany). Finally, 3 anatase titanium dioxide (TiO_2) NMs with the same primary

particle size (13 nm) but different capping states (uncapped denoted TiO_2-un, Polyvinylpyrrolidone capped (TiO_2-PVP) and dispex AA4040 capped (TiO_2-DISPEX)) were sourced from Promethean Particles Ltd (Nottingham, U.K). Details on the titania polymer coatings can be found in **Supplementary Table S3**.

NM Characterisation

The NMs used for this study are from the same batches of particles used in our recent protein corona characterization study, and thus were characterized for this initial study [39]. In brief, hydrodynamic diameter and zeta-potential were determined on a Malvern Zetasizer (nanoZS) (Malvern Panalytical, Malvern, UK). All particles were dispersed in deionized water (18.2 MΩ·cm at 25 °C) at 4 mg/mL at pH 6.98. All samples were allowed to equilibrate for 2 minutes prior to each measurement at 25 °C. Both DLS and zeta-potential measurements were taken in quadruplicate with each replicate incorporating 3 technical replicates.

Incubation experiments

Incubation experiments included two categories of metabolites (30 cations and 12 anions) and were carried out in water and in both intact and protein-free plasma using a fixed NM concentration. All metabolites are detailed in **Supplementary Table S1** and **S2**. In all cases the incubations were split into cationic and anionic metabolite incubations. Incubation was performed with an incubating microplate shaker (VWR, The Netherlands) at 37 °C for 60 min mixing at 350 RPM. Calibration curves for metabolite standards in the various sample matrices were constructed for quantitative studies over the range of 0.05 to 20 µM for cations and 0.5 to 20 µM for anions.

Incubation of NMs with metabolite standards in water

20 µL of an in-house metabolite standard mixture (cations at 50 µM or anions at 100 µM detailed in **Supplementary Table S1** and **S2**) were aliquoted into 1.5 mL Eppendorf tubes. Corresponding amounts of NM solutions and water were then added to achieve a final volume of 200 µL (**Table S11**). The final concentration of NMs in the mixtures was 5 mg/mL and of the metabolite standards was 5 µM (cations) or 10 µM (anions). The mixtures were vortexed for 15 seconds before incubation started. After incubation (37 °C, 1hr), samples were immediately centrifuged at 15,000 RPM at 4 °C for 30 min. 150 µL of the supernatant was transferred and filtered through centrifugal filters with 0.1 µm membrane, after which 95 µL of the filtrate was taken and mixed with 5 µL internal standards (100 µM ISTD1 in water for cations or 400 µM ISTD2 in water for anions). The final sample was vortexed and centrifuged prior to analysis by CE-MS.

Extraction and quantitation of the metabolites adsorbed to NMs

After the supernatant was transferred out of the incubation mix, residual liquid was removed. 200 µL water was then added to the tubes containing the NM pellets, followed by rigorous shaking and 5 minutes of sonication in a water bath. The mixtures were then centrifuged for 30 minutes at 15,000 RPM at 4 °C. Samples were then processed as described in the previous part and labelled as "Washing Fraction I (WF1)". The procedure for preparation of WF1 was repeated and subsequent collected samples were denoted as "Washing Fraction II (WF2)". The same washing step was then repeated again with water being substituted by 200 µL of methanol and water (1;1, v/v). After sonication and centrifugation, 150 µL of the supernatant was then taken and evaporated. Dried extracts were dissolved in 150 µL water, further processed as per fraction 1 and 2 and denoted as "Washing Fraction III (WF3)". All the samples were vortexed thoroughly and centrifuged prior to analysis by CE-MS.

Incubation of metabolite standards and NMs in plasma

Both intact and protein-free plasma was used in this study. All procedures were performed on ice. Intact plasma used for incubation was prepared by mixing 500 µL of pooled human plasma with 4500 µL water. The dilution factor was 10. To prepare protein-free plasma for incubation, 500 µL of the same plasma was divided evenly into 10 tubes. Into every tube, 200 µL chloroform, 250 µL methanol, and 350 µL water were added. The sample was vortexed for 2 minutes, followed by a 10 min centrifugation at 13,200 RPM at 4 °C. Then, 500 µL of supernatant was taken and filtered using 3 kDa cutoff membrane spin filters and centrifuged at 12,000 and 4 °C for 2 hours. 430 µL filtrate was subsequently transferred to Eppendorf tubes and evaporated. Dried extracts were resuspended in 345 µL water, followed by vigorous shaking and centrifugation. The processed samples were then combined and used as protein-free plasma, this is a commonly applied technique in metabolomics to eliminate proteins from biological matrices prior to metabolomics analysis where proteins are considered a contaminant. As for the intact plasma samples, the overall dilution factor was 10. Before incubation of metabolite standards in the plasma samples, 20 µL of a 50 µM mixture of L-Valine-D8, L-isoleucine-^{13}C,^{15}N, and L-glutamine-$^{13}C2$ was aliquoted into Eppendorf tubes and the solvent was evaporated. Then, 20 µL of a metabolite standard mixture (cations at 50 µM or anions at 100 µM, **Tables S1** and **S2**) and 100 µL of intact or protein-free plasma were added, followed by addition of NM solutions and water, resulting in a final volume of 200 µL. All NMs in the final mixture had the same concentration of 5 mg/mL. All the samples were vortexed for 15 seconds prior to incubation (37 °C, 1 hr). After incubation, samples were directly centrifuged for 30 minutes at 15,000 RPM at 4 °C, and 150 µL of the supernatant was transferred to a fresh Eppendorf tube for further operations. For samples incubated with intact plasma, 200 µL chloroform, 250 µL methanol, 220 µL water and 30 µL ISTD (50 µM ISTD1 for cations or 100 µM ISTD2 for anions) were added followed by vigorous shaking for 2 min and centrifugation for 10 min at 13,200 RPM and 4 °C. 500 µL supernatant was transferred to 3 kDa cutoff membrane filters and centrifuged at 12,000 g and 4 °C for 1.5 hours. 380 µL of filtrate was

transferred and evaporated and dried extracts were resuspended in water prior to CE-MS analysis. For samples incubated with protein-free plasma, 150 µL of supernatant taken after incubation was filtered through centrifugal filters with 0.1 µm membrane. Then, 95 µL of the filtrate was thoroughly mixed with 5 µL ISTDs in water (200 µM ISTD1 for cations or 400 µM ISTD2 for anions) and centrifuged at 13,200 RPM and 4 °C for 10 min prior to CE-MS analysis (**Fig. S4** for simplified workflow).

Analysis of metabolites by sheathless CE-MS

Sheathless CE-MS experiments were conducted with a CESI 8000 instrument from Sciex (Brea, CA, USA) with an OptiMS CESI cartridge (30 µm ID x 91 cm bare fused silica capillary), which was thermostatted at 25 °C with coolant. The CE equipment was coupled to a Sciex TripleTOF 6600 MS system using the NANOSpray® III source. Electrospray Ionisation (ESI) was performed in positive ion mode for cations and negative ion mode for anions, with the porous tip of the capillary positioned 2-4 mm from the entrance of the MS inlet. A description of the analytical methods employed is provided in our previous works [34, 35]. ESI-MS in positive ion mode was performed using an IonSpray Voltage Floating (ISVF) of 1350 V, while 1400 V was used in negative ion mode. New capillaries were conditioned and rinsing procedures were performed between runs as previously described [50]. All samples were hydrodynamically injected (at 2 psi for 30 seconds for cations and 40 seconds for anions, corresponding to 1.07% of the capillary volume or circa 6.89 nL and 1.43% and 9.19 nL respectively), and separated with 10% acetic acid (pH 2.2) as the background electrolyte (BGE). A voltage of 30 kV was used for electrophoretic separation. Full scan MS data acquisition covered the mass range from 65 to 1000 *m/z*.

Analysis of cationic metabolites incubated with human plasma matrices using sheath-liquid CE-MS

Analyses were conducted on an Agilent 7100 CE instrument hyphenated to an Agilent 6230 Time of Flight (TOF) mass spectrometer (Agilent Technologies, Santa Clara, California), equipped with an ESI source via a co-axial sheath-liquid interface. The employed method was adapted from the following works [51, 52]. In short, 10% acetic acid (pH 2.2) was used as the BGE and separation was conducted on a bare fused silica capillary (70 cm in length and 50 µm i.d.). Samples were injected hydrodynamically at 50 mbar for 20 s, corresponding to circa 1.2% (~17 nL) of the total capillary volume. A voltage of 30 kV was used for electrophoretic separation and MS detection was performed in positive mode. Full scan MS data acquisition covered the mass range from 50 to 1000 *m/z*.

Statistical analysis

Each NM, for adsorption vs control, protein free vs intact protein plasma and 1 vs 24 hrs was assessed by unpaired t-test ($p<0.05$) followed by a two-stage Benjamini, Krieger and Yekutieli false discovery rate test set to a 5% level using GraphPad Prism version 8.1.1.

Acknowledgements

A.J.C and W.Z contributed equally to this work.

A.J.C, I.L and J.A.T acknowledge funding from the European Commission via Horizon 2020 project ACEnano (Grant no. H2020-NMBP-2016-720952). W.Z. acknowledges PhD funding from the China Scholarship Council (CSC, No. 201507060011). R.R. acknowledges the financial support of the Vidi grant scheme of the Netherlands Organization of Scientific Research (NWO Vidi 723.016.003). I.L. thanks the University of Birmingham Institute of Global Innovation emerging theme Environmental Pollution Solutions who funded a collaborative visit and workshop.

References

1. Lynch, I. and K.A. Dawson, *Protein-nanoparticle interactions.* Nano Today, 2008. **3**(1-2),40-47.
2. Ke, P.C., et al., *A Decade of the Protein Corona.* Acs Nano, 2017. **11**(12),11773-11776.
3. Hellstrand, E., et al., *Complete high-density lipoproteins in nanoparticle corona.* Febs Journal, 2009. **276**(12),3372-3381.
4. Hadjidemetriou, M. and K. Kostarelos, *NANOMEDICINE Evolution of the nanoparticle corona.* Nature Nanotechnology, 2017. **12**(4),288-290.
5. Tenzer, S., et al., *Nanoparticle Size Is a Critical Physicochemical Determinant of the Human Blood Plasma Corona: A Comprehensive Quantitative Proteomic Analysis.* Acs Nano, 2011. **5**(9),7155-7167.
6. Zhang, H.Z., et al., *Quantitative proteomics analysis of adsorbed plasma proteins classifies nanoparticles with different surface properties and size.* Proteomics, 2011. **11**(23),4569-4577.
7. Lundqvist, M., et al., *Nanoparticle size and surface properties determine the protein corona with possible implications for biological impacts.* Proceedings of the National Academy of Sciences of the United States of America, 2008. **105**(38),14265-14270.
8. Lundqvist, M., et al., *The nanoparticle protein corona formed in human blood or human blood fractions.* Plos One, 2017. **12**(4).
9. Goy-Lopez, S., et al., *Physicochemical Characteristics of Protein-NP Bioconjugates: The Role of Particle Curvature and Solution Conditions on Human Serum Albumin Conformation and Fibrillogenesis Inhibition.* Langmuir, 2012. **28**(24),9113-9126.
10. Gu, Z.L., et al., *Surface Curvature Relation to Protein Adsorption for Carbon-based Nanomaterials.* Scientific Reports, 2015. **5**.
11. Mortensen, N.P., et al., *Dynamic development of the protein corona on silica nanoparticles: composition and role in toxicity.* Nanoscale, 2013. **5**(14),6372-6380.
12. Cox, A., et al., *Evolution of Nanoparticle Protein Corona across the Blood-Brain Barrier.* Acs Nano, 2018. **12**(7),7292-7300.
13. Dunn, W.B., et al., *Systems level studies of mammalian metabolomes: the roles of mass spectrometry and nuclear magnetic resonance spectroscopy.* Chemical Society Reviews, 2011. **40**(1),387-426.
14. Wishart, D.S., et al., *DrugBank 5.0: a major update to the DrugBank database for 2018.* Nucleic Acids Research, 2018. **46**(D1),D1074-D1082.
15. Kim, M.S., et al., *A draft map of the human proteome.* Nature, 2014. **509**(7502),575-+.
16. Serhan, C.N., J.Z. Haeggstrom, and C.C. Leslie, *Lipid mediator networks in cell signaling: Update and impact of cytokines.* Faseb Journal, 1996. **10**(10),1147-1158.

17. Thomas, C., et al., *Targeting bile-acid signalling for metabolic diseases.* Nature Reviews Drug Discovery, 2008. **7**(8),678-693.
18. Migliaccio, A., et al., *Sex steroid hormones act as growth factors.* Journal of Steroid Biochemistry and Molecular Biology, 2002. **83**(1-5),31-35.
19. Barnes, P.J., *Corticosteroid effects on cell signalling.* European Respiratory Journal, 2006. **27**(2),413-426.
20. Jenkins, C.M., A. Cedars, and R.W. Gross, *Eicosanoid signalling pathways in the heart.* Cardiovascular Research, 2009. **82**(2),240-249.
21. Wymann, M.P. and R. Schneiter, *Lipid signalling in disease.* Nature Reviews Molecular Cell Biology, 2008. **9**(2),162-176.
22. Ruge, C.A., et al., *The Interplay of Lung Surfactant Proteins and Lipids Assimilates the Macrophage Clearance of Nanoparticles.* Plos One, 2012. **7**(7).
23. Kapralov, A.A., et al., *Adsorption of Surfactant Lipids by Single-Walled Carbon Nanotubes in Mouse Lung upon Pharyngeal Aspiration.* Acs Nano, 2012. **6**(5),4147-4156.
24. Zhang, X., et al., *Quantification of Lipid Corona Formation on Colloidal Nanoparticles from Lipid Vesicles.* Analytical Chemistry, 2018. **90**(24),14387-14394.
25. Lee, J.Y., et al., *Analysis of lipid adsorption on nanoparticles by nanoflow liquid chromatography-tandem mass spectrometry.* Analytical and Bioanalytical Chemistry, 2018. **410**(24),6155-6164.
26. Pink, M., et al., *Identification and characterization of small organic compounds within the corona formed around engineered nanoparticles.* Environmental Science-Nano, 2018. **5**(6),1420-1427.
27. Go, M.R., et al., *Interactions between Food Additive Silica Nanoparticles and Food Matrices.* Frontiers in Microbiology, 2017. **8**.
28. Martel, J., et al., *Fatty acids and small organic compounds bind to mineralo-organic nanoparticles derived from human body fluids as revealed by metabolomic analysis.* Nanoscale, 2016. **8**(10),5537-5545.
29. Theodoridis, G.A., et al., *Liquid chromatography-mass spectrometry based global metabolite profiling: A review.* Analytica Chimica Acta, 2012. **711**,7-16.
30. Chetwynd, A.J., et al., *Evaluation of analytical performance and reliability of direct nanoLC-nanoESI-high resolution mass spectrometry for profiling the (xeno)metabolome.* Journal of Mass Spectrometry, 2014. **49**(10),1063-1069.
31. Gika, H.G., I.D. Wilson, and G.A. Theodoridis, *LC-MS-based holistic metabolic profiling. Problems, limitations, advantages, and future perspectives.* Journal of Chromatography B-Analytical Technologies in the Biomedical and Life Sciences, 2014. **966**,1-6.
32. Chetwynd, A.J., et al., *Current Application of Capillary Electrophoresis in Nanomaterial Characterisation and Its Potential to Characterise the Protein and Small Molecule Corona.* Nanomaterials, 2018. **8**(2).
33. Busnel, J.M., et al., *High Capacity Capillary Electrophoresis-Electrospray Ionization Mass Spectrometry: Coupling a Porous Sheathless Interface with Transient-Isotachophoresis.* Analytical Chemistry, 2010. **82**(22),9476-9483.
34. Gulersonmez, M.C., et al., *Sheathless capillary electrophoresis-mass spectrometry for anionic metabolic profiling.* Electrophoresis, 2016. **37**(7-8),1007-1014.
35. Ramautar, R., et al., *Enhancing the Coverage of the Urinary Metabolome by Sheathless Capillary Electrophoresis-Mass Spectrometry.* Analytical Chemistry, 2012. **84**(2),885-892.
36. Ramautar, R., G.W. Somsen, and G.J. de Jong, *CE-MS in metabolomics.* Electrophoresis, 2009. **30**(1),276-291.
37. Zhang, W., T. Hankemeier, and R. Ramautar, *Next-generation capillary electrophoresis-mass spectrometry approaches in metabolomics.* Current Opinion in Biotechnology, 2017. **43**,1-7.
38. Heringa, M.B., et al., *Detection of titanium particles in human liver and spleen and possible health implications.* Particle and Fibre Toxicology, 2018. **15**.

39. Faserl, K., et al., *Corona Isolation Method Matters: Capillary Electrophoresis Mass Spectrometry Based Comparison of Protein Corona Compositions Following On-Particle versus In-Solution or In-Gel Digestion.* Nanomaterials (Basel), 2019. **9**(6).
40. Buszewski, B. and S. Noga, *Hydrophilic interaction liquid chromatography (HILIC)-a powerful separation technique.* Analytical and Bioanalytical Chemistry, 2012. **402**(1),231-247.
41. Cui, M.H., et al., *Quantitative study of protein coronas on gold nanoparticles with different surface modifications.* Nano Research, 2014. **7**(3),345-352.
42. Yu, L.R. and T. Veenstra, *Phosphopeptide enrichment using offline titanium dioxide columns for phosphoproteomics.* Methods Mol Biol, 2013. **1002**,93-103.
43. Richardson, B.M., et al., *Automated, reproducible, titania-based phosphopeptide enrichment strategy for label-free quantitative phosphoproteomics.* J Biomol Tech, 2013. **24**(1),8-16.
44. Tenzer, S., et al., *Rapid formation of plasma protein corona critically affects nanoparticle pathophysiology.* Nat Nanotechnol, 2013. **8**(10),772-81.
45. Gil, A., et al., *Stability of energy metabolites-An often overlooked issue in metabolomics studies: A review.* Electrophoresis, 2015. **36**(18),2156-2169.
46. Grintzalis, K., et al., *Metabolomic method to detect a metabolite corona on amino-functionalized polystyrene nanoparticles.* Nanotoxicology, 2019. **13**(6),783-794.
47. Faria, M., et al., *Minimum information reporting in bio-nano experimental literature.* Nat Nanotechnol, 2018. **13**(9),777-785.
48. Sumner, L.W., et al., *Proposed minimum reporting standards for chemical analysis Chemical Analysis Working Group (CAWG) Metabolomics Standards Initiative (MSI).* Metabolomics, 2007. **3**(3),211-221.
49. Chetwynd, A.J., K.E. Wheeler, and I. Lynch, *Best practice in reporting corona studies: Minimum information about Nanomaterial Biocorona Experiments (MINBE).* Nano Today, 2019,100758.
50. Zhang, W., et al., *Sheathless Capillary Electrophoresis-Mass Spectrometry for Metabolic Profiling of Biological Samples.* J Vis Exp, 2016(116).
51. Drouin, N., et al., *Effective mobility as a robust criterion for compound annotation and identification in metabolomics: Toward a mobility-based library.* Analytica Chimica Acta, 2018. **1032**,178-187.
52. Zhang, W., et al., *Assessing the suitability of capillary electrophoresis-mass spectrometry for biomarker discovery in plasma-based metabolomics.* Electrophoresis, 2019. **40**(18-19),2309-2320.

Supplementary Materials

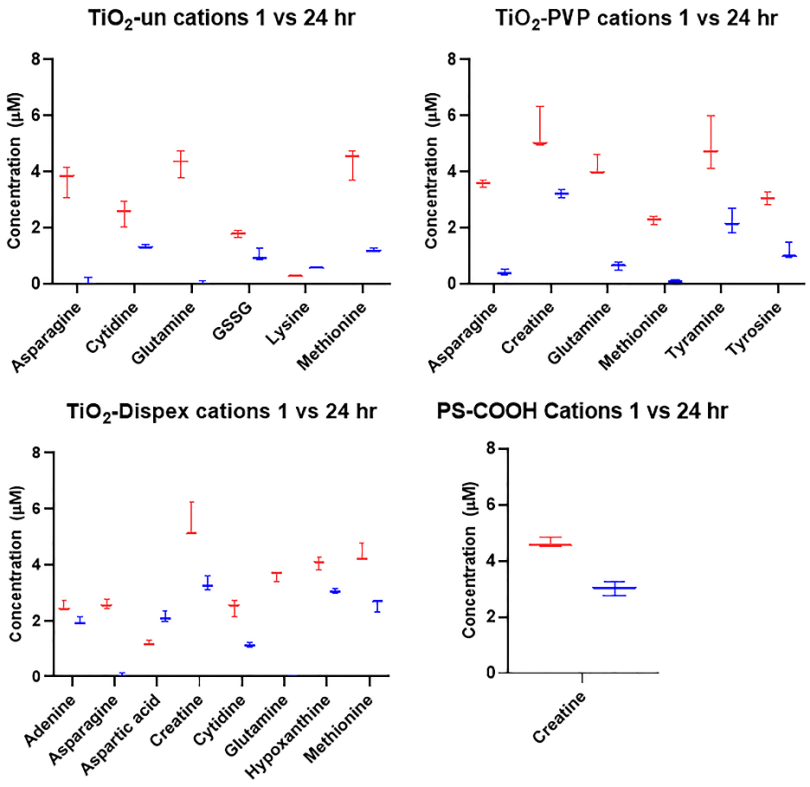

Figure S1: Time resolved analysis of the cationic metabolite corona. Red refers to 1 hr adsorption concentrations versus the blue concentrations at 24 hr adsorption. In all cases the initial amount of each metabolite was 5 µM and the amount remaining in solution at the end of the incubation period (1 or 24 hrs) was determined, from which the amount bound in the NM corona was inferred.

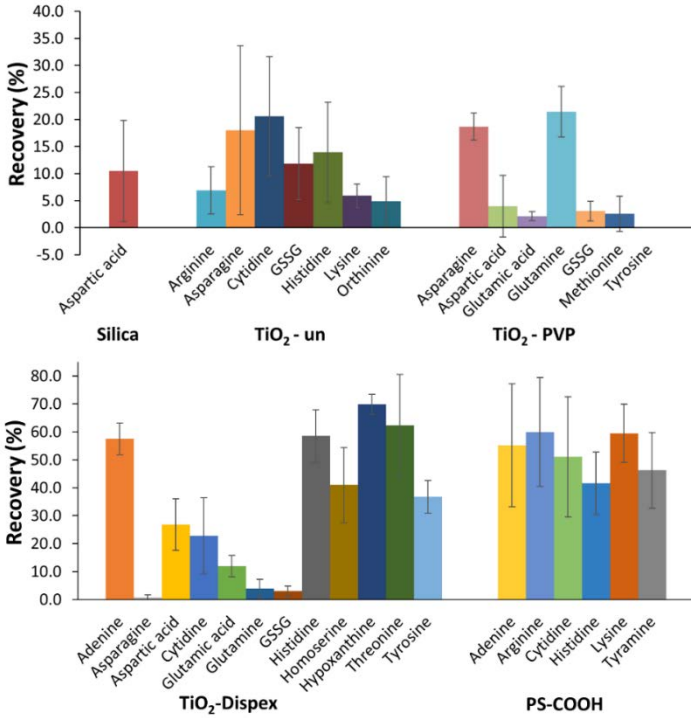

Figure S2. Recovery of cationic metabolites from the assessed NMs using the 3-step washing procedure.

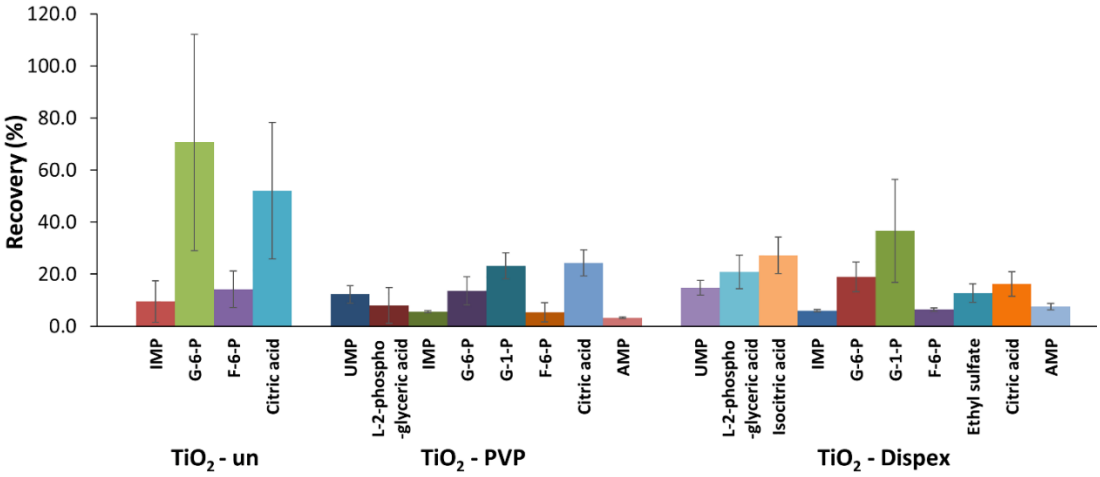

Figure S3. Recovery of anionic metabolites from the assessed NMs using the 3-step washing procedure.

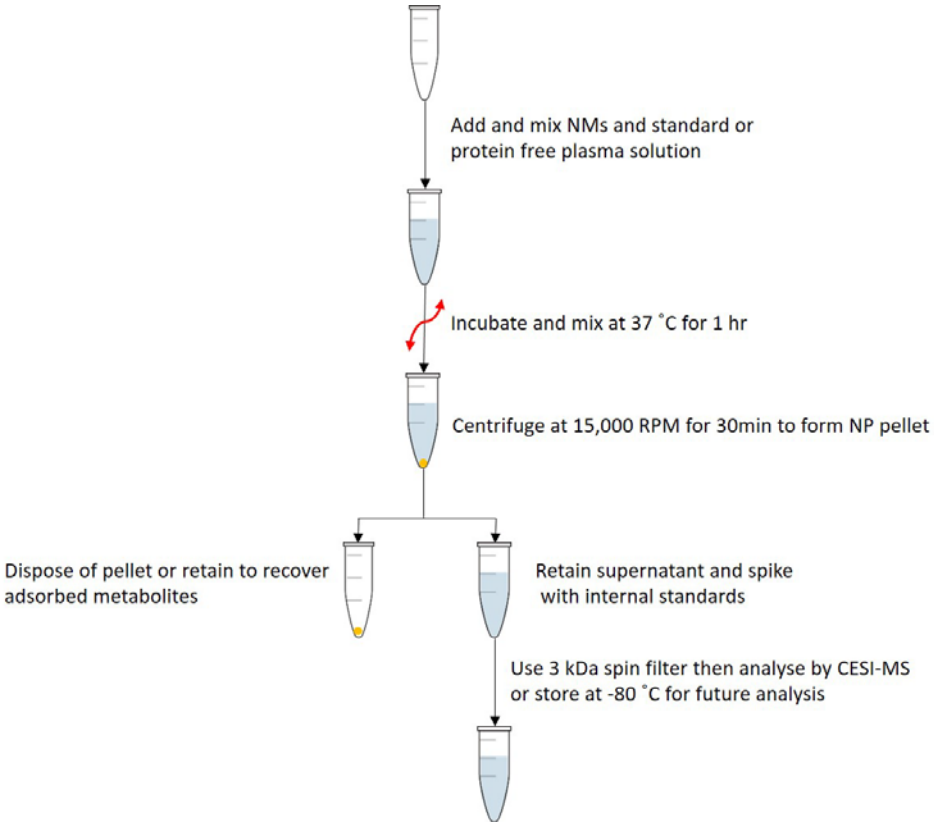

Figure S4. Simplified workflow for metabolite corona characterization

Table S1. Overview of the physico-chemical properties of the cationic metabolites used in this study for assessing metabolite adsorption to NMs.

Compound	Formula	m/z value	Migration time (min)	Log K_{ow} acidic	Log K_{ow} Basic	Hydrogen acceptor count	Hydrogen donor count	Polar surface area (Å^2)	Physiological charge state	Polarizability (Å^3)
4-hydroxyproline	$C_5H_9NO_3$	132.0661	19	1.64	10.62	4	3	69.56	0	12.29
Adenine	$C_5H_5N_5$	136.0618	9.9	10.29	5.32	4	2	80.48	0	12.29
Arginine	$C_6H_{14}N_4O_2$	175.119	10	2.41	12.41	6	5	125.22	1	17.8
Asparagine	$C_4H_8N_2O_3$	133.0608	14.3	2	8.43	4	3	106.41	0	11.66
Aspartic acid	$C_4H_7NO_4$	134.0448	15.5	1.7	9.61	5	3	100.62	-1	11.28
Beta-alanine	$C_3H_7NO_2$	90.055	9.5	4.08	10.31	3	2	63.32	0	8.62
Creatine	$C_4H_9N_3O_2$	132.0768	11.9	3.5	12.43	5	3	90.41	0	12.17
Cytidine	$C_9H_{13}N_3O_5$	244.0928	11.9	12.55	-0.062	7	4	128.61	0	54.54
Cytosine	$C_4H_5N_3O$	112.0505	9.4	9.83	3.8	3	2	67.48	0	9.88
Glutamic acid	$C_5H_9NO_4$	148.0604	15.1	1.88	9.54	5	3	100.62	-1	13.19
Glutamine	$C_5H_{10}N_2O_3$	147.0764	14.5	2.15	9.31	4	3	106.41	0	13.87
Glycine	$C_2H_5NO_2$	76.0393	11.9	2.31	9.24	3	2	63.32	0	6.65
GSSG	$C_{20}H_{32}N_6O_{12}S_2$	307.0833	17	1.44	9.61	14	10	317.64	-2	58.41
Histidine	$C_6H_9N_3O_2$	156.0768	10.1	1.85	9.44	4	3	92	0	38.06
Homoserine	$C_4H_9NO_3$	120.0655	13.8	2.22	9.16	4	3	83.55	0	11.44
Hypoxanthine	$C_5H_4N_4O$	137.0458	16.1	8.72	2.66	4	2	74.69	0	11.82
Iso/Leucine	$C_4H_9N_3O_2$	132.1019	13.7	2.79	9.52	3	2	63.32	0	14.16
L-Alanine	$C_3H_7NO_2$	90.055	12.6	2.47	9.48	3	2	63.32	0	8.49
Lysine	$C_6H_{14}N_2O_2$	147.1128	9.7	2.74	10.29	4	3	89.34	1	15.84
Methionine	$C_5H_{11}NO_2S$	150.0583	14.4	2.53	9.5	3	2	63.32	0	15.5
Ornithine	$C_5H_{12}N_2O_2$	133.0972	9.6	2.67	10.29	4	3	89.34	1	13.85
Phenylalanine	$C_9H_{11}NO_2$	166.0683	14.8	2.47	9.45	3	2	63.32	0	17.03
Proline	$C_5H_9NO_2$	116.0706	15	1.94	11.33	3	2	49.33	0	28.06
Serine	$C_3H_7NO_3$	106.0499	13.8	2.03	8.93	4	3	83.55	0	9.39
Threonine	$C_4H_9NO_3$	120.0655	14.3	2.21	9	4	3	83.55	0	11.08
Tyramine	$C_8H_{11}NO$	138.0913	10.5	10.41	9.66	2	2	46.25	1	15.33
Tyrosine	$C_9H_{11}NO_3$	182.0812	14.9	2	9.19	4	3	83.55	0	18.01
Valine	$C_5H_{11}NO_2$	118.0863	13.6	2.72	9.6	3	2	63.32	0	12.19

Table S2. Overview of the physico-chemical properties of the anionic metabolites used in this study for assessing metabolite adsorption to NMs.

Compound	Formula	m/z value	Migration time (min)	Log K_{ow} acidic	Log K_{ow} Basic	Hydrogen acceptor count	Hydrogen donor count	Polar surface area (Å^2)	Physiological charge state	Polarizability (Å^3)
Uridine monophosphate	$C_9H_{13}N_2O_9$	323.0286	13.9	1.23	-3.7	8	5	165.86	-2	26.3
Suberic acid	$C_8H_{14}O_4$	173.0819	23.4	4.15	N/A	4	2	76.6	-2	18.41
Phosphoglyceric acid	$C_3H_7O_7P$	184.9857	12.4	1.14	N/A	5	3	104.06	-3	10.67
Isocitric acid	$C_6H_8O_7$	191.0197	21.9	3.07	-4	7	4	132.13	-3	15.55
Inosine monophosphate	$C_{10}H_{13}N_4O_8$	347.0398	15.1	0.68	2.74	10	5	175.73	-3	28.69
Glucose 6 Phosphate	$C_6H_{13}O_9P$	259.0224	13.8	1.22	-3.6	8	6	156.91	-2	20.56
Glucose 1 Phosphate	$C_6H_{13}O_9P$	259.0224	13.5	1.16	-3	8	6	156.91	-2	20.66
Fructose 6 Phosphate	$C_6H_{13}O_9P$	259.0224	13.7	1.49	-3.3	8	6	164.75	-2	20.87
Ethyl Sulphate	$C_2H_6O_4S$	124.9914	9.1	-2.1	N/A	3	1	63.6	-1	10.54
Citric acid	$C_6H_8O_7$	191.0197	21.1	3.05	-4.2	7	4	132.13	-3	15.54
Adenosine monophosphate	$C_{10}H_{14}N_5O_7$	346.0558	23.5	1.23	4.97	10	5	186.07	-2	30
Adipic acid	$C_6H_{10}O_4$	145.0506	23.3	3.92	N/A	4	2	74.6	-2	14.24

Table S3. Physical and chemical properties of the PVP and Dispex polymers on Titania NMs.

	PVP	Dispex® AA 4040
Chemical structure	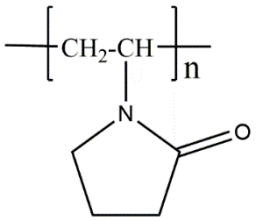	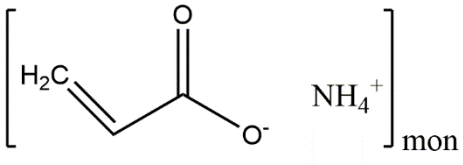
Description	Polyvinylpyrrolidone $(C6H9NO)_x$	Ammonium salt of an acrylic polymer (structure shown is simplest – may have additional functionalization on the 1st carbon
MW used	10	X
Charge	Neutral	Positive
pH		~7.5
pH stability range	5.0 – 8.0 at 10 g/L at 20 °C	5.0-10.5

Table S4. Intra-day and inter-day (3 day) repeatability (RSD, %) obtained for peak area of cationic metabolite standards in water (5 µM) used in this study to assess metabolite adsorption to NMs by sheathless CE-MS.

Compound	Intra-day peak area RSD (%) (n=16)	Intra-day migration time RSD (%) (n=16)	Inter-day peak area RSD* (%) (n=36)	Inter-day migration time RSD* (%) (n=36)
Adenine	4.6	1.8	6.0	1.5
Arginine	3.0	1.7	6.0	1.4
Asparagine	4.7	2.4	6.3	2.0
Aspartic acid	8.4	2.5	12.3	2.2
beta-alanine	5.9	1.7	7.0	1.4
Creatine	4.2	2.0	8.5	1.7
Cytidine	5.6	2.1	10.1	1.8
Cytosine	3.0	1.7	6.4	1.4
Glutamic acid	7.6	2.4	11.0	2.0
Glutamine	5.0	2.4	6.7	2.0
Glycine	6.5	2.0	11.6	1.7
GSSG	8.6	2.6	16.0	2.2
Histidine	3.9	1.8	6.9	1.5
Homoserine	6.3	2.3	7.7	2.0
Hypoxanthine	9.3	2.6	13.1	2.3
Iso/Leucine	5.8	2.3	6.2	2.0
L-Alanine	6.0	2.1	8.9	1.8
Lysine	2.8	1.7	5.9	1.4
Methionine	6.2	2.4	7.4	2.0
Orthinine	4.1	1.7	7.4	1.4
Phenylalanine	6.0	2.4	7.3	2.1
Proline	7.0	2.4	8.9	2.1
Serine	6.7	2.3	8.3	2.0
Threonine	5.7	2.3	7.0	2.0
Tyramine	6.4	1.8	8.6	1.6
Tyrosine	7.2	2.4	12.7	2.1
Valine	6.3	2.2	6.6	1.9

* n=10 on the second and third day

Table S5. LOD and LOQ values for all metabolites as a standard mixture in water.

Metabolite	LOD (nM)	LOQ (nM)	Metabolite	LOD (nM)	LOQ (nM)
4-Hydroxyproline	4.0	13.5	Orthinine	7.0	23.4
Adenine	1.3	4.5	Phenylalanine	3.7	12.3
Arginine	1.4	4.6	Proline	9.3	30.9
Asparagine	9.5	31.8	Serine	2.8	9.2
Aspartic acid	17.2	57.3	Threonine	13.2	43.9
beta-alanine	22.3	74.4	Tyramine	4.4	14.7
Creatine	2.0	6.7	Tyrosine	2.3	7.8
Cytidine	1.9	6.4	Valine	7.9	26.4
Cytosine	1.7	5.5	Citric acid	90.6	302.2
Glutamic acid	5.4	18.0	Ethyl sulfate	7.9	26.2
Glutamine	10.9	36.2	F-6-P	11.4	37.9
Glycine	13.8	45.9	G-1-P	7.0	23.2
GSSG	2.6	8.7	G-6-P	8.6	28.7
Histidine	1.8	5.9	IMP	5.6	18.6
Homoserine	15.8	52.6	Isocitric acid	35.3	117.6
Hypoxanthine	5.6	18.6	L-2-phosphoglyceric acid	125.2	417.3
Isoleucine/Leucine	3.8	12.7	UMP	4.3	14.4
L-Alanine	10.4	34.6	Adipic acid	47.4	157.9
Lysine	6.0	19.9	AMP	6.5	21.6
Methionine	8.0	26.7	Suberic acid	20.1	66.9

Table S6. Detailed analysis of cationic metabolites that significantly (p<0.05) bind to the surface of at least one of the 6 NMs following incubation cation metabolite mixture for 1 hour.

Metabolite	Control concentration (µM)	Post exposure concentration (µM)	Fold Change	p-value
SiO_2				
Aspartic acid	5.061	3.527	1.44	0.0009911
TiO_2-un				
Arginine	5.225	0.4333	12.05	0.000216
Asparagine	5.845	3.68	1.59	0.000985
Cytidine	5.541	2.51	2.21	0.000432
GSSG	4.983	1.79	2.78	0.000355
Histidine	5.522	1.953	2.83	0.00205
Lysine	5.38	0.29	18.55	0.000146
Orthinine	5.798	0.12	48.32	0.000274
TiO_2-PVP				
Asparagine	5.845	3.577	1.63	0.000183
Aspartic acid	5.061	0.15	33.74	<0.000001
Glutamic acid	5.52	0.29	19.03	<0.000001
GSSG	4.983	<LOD	N/A	0.000028
Methionine	5.143	2.257	2.28	0.000579
Tyrosine	5.355	3.047	1.76	0.000077
Glutamine	5.636	4.177	1.35	0.011372
TiO_2-Dispex				
Adenine	5.62	2.503	2.25	0.002255
Asparagine	5.845	2.583	2.26	0.000025
Aspartic acid	5.061	1.183	4.28	0.000003
Cytidine	5.541	2.463	2.25	0.000273
Glutamic acid	5.52	0.9667	5.71	<0.000001
Glutamine	5.636	3.593	1.57	0.001678
GSSG	4.983	<LOD	N/A	0.000028
Histidine	5.522	3.21	1.72	0.014738
Homoserine	5.62	4.53	1.24	0.026392
Hypoxanthine	5.289	4.053	1.31	0.000774
Threonine	5.284	4.313	1.23	0.025566
Tyrosine	5.355	4.45	1.20	0.008784
PS-COOH				
Adenine	5.62	3.00	1.87	0.006335
Arginine	5.225	1.533	3.41	0.001027
Cytidine	5.541	2.843	1.95	0.000585
Histidine	5.522	2.933	1.88	0.009662
Lysine	5.38	2.72	1.98	0.005241
Tyramine	5.134	1.413	3.63	0.001669
PS				
No significant adsorption				

Table S7. Detailed analysis of anionic metabolites that significantly ($p<0.05$) bind to the surface of at least one of the 6 NMs following incubation in anion metabolite mixture for 1 hour.

Metabolite	Control concentration (µM)	Post exposure concentration (µM)	Fold Change	p-value
SiO_2				
No significant adsorption				
TiO_2-un				
F-6-P	10.3	2.9	3.55	0.000253
IMP	9.933	2.467	4.03	0.00026
Citric acid	9.5	7.833	1.21	0.0007
TiO_2-PVP				
Citric acid	9.5	7.133	1.33	0.000004
IMP	9.933	0.4667	21.28	0.000019
F-6-P	10.3	1.567	6.57	0.00006
UMP	9.767	3.667	2.66	0.000762
G-6-P	10.17	4.1	2.45	0.000868
AMP	10.6	3.267	3.25	0.001565
L-2-phosphoglyceric acid	10.27	5.267	1.95	0.002775
G-1-P	10.27	5.9	1.74	0.006286
TiO_2-Dispex				
IMP	9.933	1.0	9.93	0.000029
F-6-P	10.3	1.367	7.53	0.000041
Citric acid	9.5	5.4	1.76	0.000178
UMP	9.767	3.833	2.55	0.000493
AMP	10.6	2.267	3.25	0.001397
L-2-phosphoglyceric acid	10.27	6.433	1.60	0.003837
G-6-P	10.17	5.7	1.78	0.004234
Isocitric acid	9.2	7.6	1.21	0.050265
G-1-P	10.27	7.533	1.36	0.052918
Ethyl Sulfate	9.567	7.267	1.32	0.057219
PS-COOH				
No significant adsorption				
PS				
No significant adsorption				

Table S8. Evolution of cation metabolite adsorption to NMs over 24 hr time period.

Metabolite	Post 1Hr Exposure concentration (µM)	Post 24 Hr exposure concentration (µM)	Fold Change	p-value
SiO_2				
No significant changes in adsorption				
TiO_2-un				
Asparagine	3.68	0.08333	44.16	0.000428
Cytidine	2.51	1.317	1.91	0.012172
Glutamine	4.29	0.03	143	0.000115
GSSG	1.79	1.017	1.76	0.006566
Lysine	0.29	0.5767	0.50	0.000252
Methionine	4.33	1.2	3.61	0.00059
TiO_2-PVP				
Asparagine	3.577	0.3967	9.02	0.000006
Creatine	5.43	3.217	1.69	0.008432
Glutamine	4.177	0.063	6.63	0.000114
Methionine	2.257	0.08333	27.09	0.00002
Tyramine	4.947	2.22	2.23	0.010784
Tyrosine	3.047	1.147	2.66	0.000921
TiO_2-Dispex				
Adenine	2.503	1.973	1.27	0.017
Asparagine	2.583	0.03667	70.44	0.000018
Aspartic acid	1.183	2.13	0.56	0.001836
Creatine	5.483	3.317	1.65	0.005587
Cytidine	2.463	1.12	2.20	0.001563
Glutamine	3.593	0.001667	215.54	0.000004
Hypoxanthine	4.053	3.04	1.33	0.001856
Methionine	4.377	2.573	1.70	0.001441
PS-COOH				
Creatine	4.643	3.027	1.53	0.000901
PS				
No significant changes in adsorption				

Table S9. Cationic metabolites with significant ($p<0.05$) variation in adsorption to NM surfaces depending upon the presence or absence of proteins.

Metabolite	Concentration remaining in Intact plasma (µM)	Concentration remaining in Protein free plasma (µM)	Fold Change	p-value
SiO_2				
Histidine	5.56	4.21	1.32	0.000393
Labelled valine	5.247	4.847	1.08	0.003331
TiO_2-un				
Cytidine	2.867	3.713	0.77	0.000176
Isoleucine	3.433	4.17	0.82	0.005349
TiO_2-PVP				
Arginine	1.68	0.2867	5.86	0.00093
Cytidine	3.493	4.18	0.84	0.00522
Histidine	2.80	0.07	40	0.000955
Labelled Isoleucine	5.12	4.603	1.11	0.000635
Methionine	3.547	1.363	2.60	0.000094
TiO_2-Dispex				
Cytidine	3.22	4.137	0.78	0.000991
Arginine	2.147	0.9133	2.35	0.001953
PS-COOH				
Serine	4.89	6.183	0.79	0.000601
PS				
Adenine	4.187	5.157	0.81	0.008274
Arginine	4.26	5.023	0.85	0.003562
Beta-alanine	4.31	5.1	0.85	0.014213
Creatine	4.83	5.293	0.91	0.003284
Cytidine	4.093	4.887	0.84	0.004091
Glutamine	4.84	7.307	0.66	0.003569
Isoleucine	4.03	5.54	0.73	0.006217
Labelled glutamine	4.83	5.42	0.89	0.015897
L-Alanine	4.387	6.49	0.68	0.002916
Leucine	4.453	5.797	0.77	0.029427
Phenylalanine	4.72	5.453	0.87	0.0183
Proline	4.333	5.993	0.72	0.023366
Valine	4.193	5.923	0.71	0.002851

Table S10. Anionic metabolites with significant (p<0.05) variation in adsorption to NM surfaces depending upon the presence or absence of proteins.

Metabolite	Concentration remaining in Intact plasma (µM)	Concentration remaining in Protein free plasma (µM)	Fold Change	p-value
SiO_2				
IMP	5.00	9.367	0.53	0.002187
UMP	6.28	9.947	0.63	0.002958
F-6-P	5.327	8.403	0.53	0.005393
G-6-P	11.23	8.607	1.31	0.00645
TiO_2-un				
Citric acid	0.95	4.917	0.19	0.000263
TiO_2-PVP				
Citric acid	<LOD	4.917	N/A	0.000068
IMP	1.817	3.667	0.4955	0.000803
TiO_2-Dispex				
IMP	2.16	1.907	1.32	0.00298
Citric acid	<LOD	1.933	N/A	0.003806
F-6-P	3.653	3.25	1.12	0.004082
Ethyl sulfate	10.7	7.78	1.36	0.007308
L-2-phosphoglyceric acid	7.15	5.643	1.27	0.013028
PS-COOH				
IMP	3.98	9.47	0.42	<0.000001
UMP	5.213	9.223	0.57	0.000014
F-6-P	5.273	8.757	0.60	0.00005
G-1-P	7.333	9.17	0.80	0.006361
G-6-P	10.45	8.857	1.18	0.013236
PS				
G-6-P	11.86	7.88	1.51	0.000225
F-6-P	5.553	8.047	0.69	0.001685
IMP	5.237	8.53	0.61	0.012565

Table S11. The detailed compositions of all incubation mixes used in this work.

Nanomaterials	Stock solution concentration (mg/mL)	Volume added to incubation mix (µL)	Volume of standards stock solution (µL)	Water (µL)
SiO_2	40	25	20	155
TiO_2-un	25	40	20	144
TiO_2-PVP	40	25	20	155
TiO_2-Dispex	13.7	73	20	107
PS	26	38.5	20	141.5
PS-COOH	26	38.5	20	141.5

Chapter 9

Conclusions and Perspectives

Conclusions and perspectives

The analytical toolbox used in present-day metabolomics encounters difficulties for the analysis of limited amounts of biological samples. As a result, a significant number of crucial biomedical/clinical questions cannot be addressed by the current metabolomics approach. Therefore, there is a strong need for analytical tools capable of addressing such challenges. CE is a microscale technique providing highly efficient separations for polar and charged compounds, while requiring only minute amounts of sample. The analytical technology used in this thesis was based on a combination of capillary electrophoresis (CE) and time-of-flight mass spectrometry (TOF-MS). For the design of the microscale analytical platform, both a sheath-liquid and a sheathless interface were used for coupling CE to MS.

CE-MS has shown its complimentary role in the field of metabolomics, but at the same time its application is still very limited compared to other MS-based platforms. The goal of this thesis is to develop reliable CE-MS methods for a wide range of polar metabolites and convince the scientific community about the usefulness of this technique in metabolomics research, especially for applications dealing with limited amounts of biological samples, such as small amounts of body fluids from mouse models for neurological diseases and microscale cell culture samples. In order to minimize the loss and acquire the correct information of potentially irreplaceable biological samples, it is imperative that the adopted analytical workflow is properly assessed and fit for the research purpose.

Prior to the application of an analytical method to metabolomics studies, the suitability of the designated approach should be investigated to assure its analytical performance. **Chapter 6** depicts an artificial metabolomics study where metabolic discrepancies were created manually by spiking isotope-labeled amino acids into human plasma. The labeled amino acids used for spiking were selected in a way that their *m/z* values and migration times were distributed across the investigated range so that the whole analysis window could be evaluated. Different spiking strategies were considered when creating simulated "markers" to mimic the absence/presence and increase/decrease situation of endogenous metabolites, and the samples were analyzed by CE-MS employing a (conventional) sheath-liquid interface. The recorded data were subjected to two different data analysis strategies conducted by two different individuals. Data analysis revealed that the main compounds contributing to the differences between the various groups of plasma were the spiked compounds, thereby emphasizing the reliability of CE-MS for plasma-based biomarker discovery studies.

The choice of sample preparation strategy is of crucial importance in metabolomics studies for that it not only affects the observed metabolome but also the biological interpretation of the data later on. The two main types of biological samples used in this thesis are plasma and mammalian cells. Throughout this thesis, a combination of water/methanol/chloroform proved to be an

effective way of extracting polar metabolites from cells (and plasma). The sample preparation of mammalian cells prior to instrumental analysis also includes quenching before the metabolite extraction process. The quenching of intracellular enzymatic reactions is essential to capture the representative metabolic profile that reflects the physiological status of cells at the time of sampling [1]. **Chapter 3** (**Part 2**), **Chapter 4**, and **Chapter 5** are all cell-based studies despite different metabolites of interest. The first two chapters regarding cellular metabolites are general proof-of-principle research, while the study described in **Chapter 5** aimed to accurately quantitate intracellular nucleotides. Nucleotides are among the fastest changing endogenous metabolites and, therefore, an effective and swift quenching approach is key to uncovering the accurate concentrations of compounds like ATP. A mixture of methanol/water(8:2,v/v) at -20 °C was quickly added for quenching all enzymatic reactions in this work. An essential component in sample preparation is the application of ultrafilters with cutoff membrane of 3 or 5 kDa. Ultrafiltration has been successfully applied as a clean-up step in various studies [2-4]. This technique is beneficial in delivering excellent coverage of polar metabolites [5] and is in perfect alignment with the applications of CE-MS. The inclusion of ultrafiltration in sample preparation has proven in practice that it can help deliver stable performance on the instruments. The proposed workflow in **Chapter 5** can be employed to capture the state of energy metabolism in various organisms and has the potential to expand its usefulness even further. Moreover, the proposed sample preparation greatly increased the lifespan of sheathless capillary cartridges, and an average of around 200 runs could be achieved for bare fused-silica capillaries. To further increase the number of electrophoretic runs of each capillary, special attention should be given to developing even better sample handling processes in the future.

Our sheathless CE-MS work conducted on nucleotides in **Chapter 5** utilized a high pH separation condition in combination with positive ESI mode, which totally circumvented commonly observed corona discharge that takes place when coupling high pH nano separation to negative ESI mode. The sample preparation incorporated liquid-liquid extraction and ultrafiltration. Good linearity was observed for all the nucleotides investigated, including mono-, di- and tri-phosphate compounds. This chapter also demonstrated the repeatability obtained for nucleotides concentrations from three different petri dishes prepared at the same time. 1000 and 2500 HepG2 cells were used in comparison for inter-dish precision. Excellent RSD values of 3.0% and 3.9% were obtained for ATP concentrations observed in cell extracts of 1000 and 2500 HepG2 cells derived from three different petri dishes. One indicator that can be used to reflect good sample preparation is the adenylate energy charge (AEC) value that falls between 0.7 and 0.95 when growing under optimal conditions. The calculated AEC values in this chapter using different numbers of HepG2 cells as the starting material were between 0.72 to 0.85, indicating that the analytical method proposed here can be used to assess AEC values in studies dealing with minute amount of mammalian cells. This method showed great potential of sheathless CE-MS in the accurate quantitation of nucleotides in biomass-limited samples.

One aspect that still needs to be properly addressed regarding sample preparation in this thesis is miniaturization. The dried-up samples after liquid-liquid extraction and solvent evaporation were always reconstituted in a volume between 20 to 30 µL prior to CE-MS analyses to ensure thorough and consistent recovery, while only as little as 5 µL is needed in sample vials for successful sample injections on the sheathless CE instrument. Sanchez-Lopez et al. [6, 7] applied multiple solvent evaporation/resuspension processes and analyzed the samples after each resuspension. Although these multiple evaporation/resuspension processes were performed to fit different analytical platforms, this could be a potential way of miniaturizing samples efficiently. However, this procedure needs to be rigorously assessed and validated for it might accelerate the degradation process of compounds like nucleotide triphosphates.

The advantage of CE being a microscale separation technique can be a drawback when very high detection sensitivity is needed in profiling limited amount of samples. In this thesis, we mainly adopted transient ITP (tITP) as an online preconcentration technique in both **Chapter 4** and **Chapter 5** for analyzing samples derived from the content of low numbers of HepG2 cells on sheathless CE-MS. The tITP method employed in **Chapter 4** utilized 250 mM ammonium acetate (pH=7.0) as the leading electrolyte (LE) when 10% acetic acid was used as the BGE. The employment of tITP enabled a 6 times larger injection volume than regular hydrodynamic injections. With the increase of injection volumes, the content of 500 HepG2 cells (the injected volume is less than a single HepG2 cell) already led to the identification of over 24 metabolites. However, the preliminary attempt in **Chapter 5** using 2 M acetic acid as LE in combination with 16 mM NH_4Ac (pH=9.7) still needs further optimization before overall sensitivity boost can be achieved. Overall, the two works aforementioned emphasized the utility of sheathless CE-MS in analyzing ultra-small biological samples.

Reproducibility is a necessity when it comes to untargeted metabolomics. Despite the developments over the years, CE-MS is still considered by the analytical community as a technique that lacks reproducibility. One of the reasons that contribute to the poor reproducibility with CE-MS analyses is the absence of standard operating protocols. In **Chapter 3**, two protocols regarding the coupling of CE to MS and the extraction of intracellular metabolites are provided. The first part of this chapter offers an operation protocol using 10% acetic acid as an example BGE for both cationic and anionic metabolites on sheathless CE-MS. The second part summarizes key points in dealing with HepG2 cells to help ensure continuous analyses on such narrow-bore capillaries. The introduction of such technical notes should in theory help the CE-MS community obtain reproducible results and make inter-lab comparative studies more feasible. **Chapter 5** evaluated the repeatability of a proposed sheathless CE-MS method using triplicates of low numbers of HepG2 cells as the starting material, and obtained data clearly indicated that CE-MS can be used in a reproducible way for metabolomics studies.

The analytical methods described in **Chapter 3** were later used for the application that's summarized in **Chapter 8**. **Chapter 8** described the application of sheathless CE-MS in analyzing small molecule corona on the surface of nanomaterials (NMs) . Two different solutions of standard mixes were used to investigate the interactions between NMs and cations or anions separately. This study included six types of clinically and environmentally relevant NMs and illustrated that NMs can form a unique metabolite fingerprint when incubated in water solutions with standard mix solutions. In order to better simulate biological scenarios, plasma was added into the incubation mixes and this is the first work that demonstrates that the protein portion of the corona is essential for the formation of metabolite corona. This work revealed many interesting characteristics of the metabolite and complete biomolecular corona, but at the time also raised a plethora of questions that call for follow-up research.

The major issue caused by irregular migration patterns is the lack of confidence in metabolite annotation and identification when comparing data obtained from different institutes. A common counteractive measure is to use one or more internal standards, as illustrated throughout this thesis. In **chapter 5**, two labeled nucleotides were used as internal standards for correcting peak areas and migration times of the evaluated compounds. The relative migration times (RMT) after correction showed excellent RSD values of no larger than 1.1%, and this greatly improved the repeatability of the method and potentially made metabolite annotation more reliable. Another possibility to increase the level of confidence in metabolite annotation is with the use of ROMANCE [8]. By selecting a known reference marker in analyses, one can easily calculate the electrophoretic mobility of other features and compare those with known metabolites analyzed under the same condition. **Chapter 7** was designed to identify potential biomarkers related to induced epilepsy onsets in mouse plasma using sheath liquid CE-MS. As little as 10 μL mouse plasma was collected at each time point. The same analytical approach from Chapter 6 was adopted. During data analysis, ROMANCE was employed to help confirm detected "markers" in this study. This is the first attempt to investigate metabolic profiles for seizures in mouse plasma. Although specific pathways are still unclear without sophisticated investigation, the initial metabolic profiling could be a starting point for future research.

MS measurements typically contain multiple data points, derived from diverse sources such as biological differences in samples, instrumental condition variation and instrumental error [9]. It is of utmost importance to apply strict quality control and preprocessing of acquired data. The implementation of QC process has been extensively reviewed in literature [10, 11]. Common practice for implementing QC process is by generating a QC pool with equivalent aliquots taken from each sample, however, this procedure can be potentially expanded by serial-diluting pooled QCs [12]. A set of pooled QC samples are diluted within a certain range and analyzed to check if a positive correlation can be observed between obtained signal and nominal concentration. In this way, the data cleaning process during preprocessing can be done more efficiently.

In order to accurately extract relevant and meaningful information from hundreds of MS measurements, proper data analysis workflows are urgently needed. A generic data handling workflow includes feature list generation, uni-/multi-variate analysis, and data interpretation. Lamichhane et al. [9] provided an overview of the currently available tools for metabolomics data analysis and discussed their strengths and weaknesses in detail. A plethora of strategies have been developed to help unravel metabolic mysteries, however, the choice of the method is largely dependent on the study design and purpose. Data analysis also plays a key role in integrating multiple layers of omics research, which helps obtain deeper insights and lower false discovery rates [13].

The CE-MS methods described in this thesis have been applied in the analyses of various types of samples. Despite the different sample sizes involved, the goal for all the aforementioned CE-MS methods is the application for large-scale metabolic studies.

With the accumulated knowledge in the scientific community about single cells, it still remains unclear whether any components, if at all, of cell heterogeneity serves a function and carry meaningful information [14]. Heterogeneity is observed at different scales of biology, from cultured cell populations [15] to tumor tissues [16]. By profiling the intracellular metabolome from a small group of homogenous cells or even a single cell, researchers may find answers to a lot of medical issues, such as antibacterial resistance and tumor relapses [17]. There are a few bottlenecks to consider in single-cell analyses, including intracellular metabolite extraction, instrumental analysis and bridging metabolic snapshot with biological relevance. CE-MS has become a powerful tool in single-cell metabolomics study [18]. Sweedler's group used a modified patch-clamp tool to extract cytoplasm from neurons and astrocytes of rat brain and detected about 60 metabolites on a custom-built CE-ESI-MS platform [19]. Striking differences in the abundance and presence of metabolites were observed in this work for different cell types and cells of the same type. However, this technique lacks the sensitivity to detect some metabolites of low concentration from smaller cancer cells. Kawai et al. [20] recently illustrated their single-cell work utilizing CE-MS with a homemade thin-walled tapered emitter. The proposed method can inject as much as 1200 nL sample into the capillary with the proposed dual preconcentration technique. The utility of this method was exemplified with the profiling of single HeLa cells, from which the authors could annotate 51 metabolites, including amino acids and amines, among others.

Although the great potential of CE-MS has been demonstrated for single-cell metabolomics studies, the improved performance of the aforementioned examples to some extent relied on the in-house fabrication of hardware and cannot be easily replicated. Recent work carried out by Wells et al. achieved a 5000-fold sensitivity improvement by applying electrokinetic supercharging on a conventional sheath liquid CE-MS system [21]. The reported method was successfully applied in the analysis of neurotransmitters in biological samples. This work can serve as an example of how to maximize the loadability of sample into the capillary, combining electrokinetic injection with

isotachophoresis. The effective introduction of sample fraction into the capillary is of crucial importance for limited sample amounts (or even single cells). The other aspect that might facilitate CE-MS for better sensitivity is the use of MS/MS. The MS/MS-based methods could potentially provide a series of advantages such as higher sensitivity, lower background interferences, and better identification confidence for targeted metabolomics studies.

Another intriguing subject that requires further investigation lies within the field of nanoscience and will attempt to better explain the interactions between nanomaterials and biomolecules. The formation of corona changes the way NMs get identified by cells and alters cellular functions and toxicological profiles of NMs [22, 23]. Better understanding of the NM corona formation is significant for understanding NMs-cell interaction in vivo. In this thesis, we were unable to fully recover the metabolites in the formed coronas, and most metabolites showed recovery rates under 60%. In an attempt to study toxicological interactions of polar pharmaceuticals from wastewater with different types nanomaterials [24], the authors applied two times of methanol washing and the recovery for most compounds fell in the 70-90% range. Future work will look for better washing procedures and more accurately describe relevant characteristics of NM coronas. So far our investigation regarding NMs has only included in-vitro situations, and already shown some fascinating results reflecting complex interactions between NMs and biomolecules. To properly assess the influence of coronas on biological systems, it is important to incubate NMs of interest with cell lines and see if there are changes in the intra- and extracellular metabolome, where our proposed CE-MS methods can be of good use.

References

1. Leon, Z., et al., *Mammalian cell metabolomics: experimental design and sample preparation.* Electrophoresis, 2013. **34**(19),2762-75.
2. Courant, F., et al., *Development of a metabolomic approach based on liquid chromatography-high resolution mass spectrometry to screen for clenbuterol abuse in calves.* Analyst, 2009. **134**(8),1637-46.
3. Soga, T., *Capillary electrophoresis-mass spectrometry for metabolomics.* Methods Mol Biol, 2007. **358**,129-37.
4. Tiziani, S., et al., *Optimized metabolite extraction from blood serum for 1H nuclear magnetic resonance spectroscopy.* Anal Biochem, 2008. **377**(1),16-23.
5. Vuckovic, D., *Current trends and challenges in sample preparation for global metabolomics using liquid chromatography–mass spectrometry.* Analytical and Bioanalytical Chemistry, 2012. **403**(6),1523-1548.
6. Sanchez-Lopez, E., et al., *A cross-platform metabolomics workflow for volume-restricted tissue samples: application to an animal model for polycystic kidney disease.* Molecular Biosystems, 2017. **13**(10),1940-1945.
7. Sanchez-Lopez, E., et al., *Sheathless CE-MS based metabolic profiling of kidney tissue section samples from a mouse model of Polycystic Kidney Disease.* Sci Rep, 2019. **9**(1),806.

8. Gonzalez-Ruiz, V., et al., *ROMANCE: A new software tool to improve data robustness and feature identification in CE-MS metabolomics.* Electrophoresis, 2018. **39**(9-10),1222-1232.
9. Lamichhane, S., et al., *Chapter Fourteen - An Overview of Metabolomics Data Analysis: Current Tools and Future Perspectives*, in *Comprehensive Analytical Chemistry*, J. Jaumot, C. Bedia, and R. Tauler, Editors. 2018, Elsevier. p. 387-413.
10. Broadhurst, D., et al., *Guidelines and considerations for the use of system suitability and quality control samples in mass spectrometry assays applied in untargeted clinical metabolomic studies.* Metabolomics, 2018. **14**(6).
11. Dunn, W.B., et al., *The importance of experimental design and QC samples in large-scale and MS-driven untargeted metabolomic studies of humans.* Bioanalysis, 2012. **4**(18),2249-64.
12. Lewis, M.R., et al., *Development and Application of Ultra-Performance Liquid Chromatography-TOF MS for Precision Large Scale Urinary Metabolic Phenotyping.* Anal Chem, 2016. **88**(18),9004-13.
13. Zhang, W., F. Li, and L. Nie, *Integrating multiple 'omics' analysis for microbial biology: application and methodologies.* Microbiology, 2010. **156**(Pt 2),287-301.
14. Altschuler, S.J. and L.F. Wu, *Cellular Heterogeneity: Do Differences Make a Difference?* Cell, 2010. **141**(4),559-563.
15. Tang, L., *Investigating heterogeneity in HeLa cells.* Nat Methods, 2019. **16**(4),281.
16. Alizadeh, A.A., et al., *Toward understanding and exploiting tumor heterogeneity.* Nat Med, 2015. **21**(8),846-53.
17. Fessenden, M., *Metabolomics: Small molecules, single cells.* Nature, 2016. **540**(7631),153-155.
18. DeLaney, K., et al., *Recent Advances and New Perspectives in Capillary Electrophoresis-Mass Spectrometry for Single Cell "Omics".* Molecules, 2018. **24**(1).
19. Aerts, J.T., et al., *Patch clamp electrophysiology and capillary electrophoresis-mass spectrometry metabolomics for single cell characterization.* Anal Chem, 2014. **86**(6),3203-8.
20. Kawai, T., et al., *Ultrasensitive Single Cell Metabolomics by Capillary Electrophoresis-Mass Spectrometry with a Thin-Walled Tapered Emitter and Large-Volume Dual Sample Preconcentration.* Anal Chem, 2019. **91**(16),10564-10572.
21. Wells, S.S., M. Dawod, and R.T. Kennedy, *CE-MS with electrokinetic supercharging and application to determination of neurotransmitters.* Electrophoresis, 2019.
22. Ritz, S., et al., *Protein corona of nanoparticles: distinct proteins regulate the cellular uptake.* Biomacromolecules, 2015. **16**(4),1311-21.
23. Mirshafiee, V., et al., *Impact of protein pre-coating on the protein corona composition and nanoparticle cellular uptake.* Biomaterials, 2016. **75**,295-304.
24. Martin-de-Lucia, I., et al., *Reverse Trojan-horse effect decreased wastewater toxicity in the presence of inorganic nanoparticles.* Environmental Science-Nano, 2017. **4**(6),1273-1282.

Appendix

Nederlandse Samenvatting

Acknowledgements

Curriculum Vitae

List of publications

Samenvatting

In het huidige biomedisch/klinisch onderzoek wordt er naast de proefdieren steeds meer gebruik gemaakt van 3D in vitro celcultuurmodelsystemen om inzicht te krijgen in het pathofysiologisch mechanisme van complexe ziektebeelden. Dergelijke systemen vinden ook steeds meer hun toepassing voor het achterhalen van het werkingsmechanisme van potentiële geneesmiddelen. Inzicht in complexe ziektebeelden op moleculair niveau kan o.a. verkregen worden met metabolomics. Deze discipline houdt zich bezig met de bestudering van het metaboloom, d.w.z. de verzameling van alle (lichaamseigen) metabolieten in een cel, orgaan, lichaamsvloeistof of organisme. Deze metabolieten zijn onderdeel van het metabolisme of de stofwisseling. Metabolomics is dus zeer geschikt om onderscheid te maken tussen ziek en gezond op basis van de onderliggende metabole/biochemische processen. Een goed voorbeeld hiervan is de hielprikscreening waarin in het bloed van pasgeborenen een serie lichaamseigen metabolieten (in dit geval overwegend aminozuren) kwantitatief wordt gemeten voor het opsporen van erfelijke stofwisselingsziekten.

Inzicht verkrijgen in complexe ziektebeelden of in het werkingsmechanisme van mogelijke nieuwe geneesmiddelen aan de hand van 3D in vitro celcultuurmodellen met een metabolomics benadering kan een enorme analytische uitdaging zijn. In tegenstelling tot de klassieke biochemische experimenten waarbij doorgaans met minimaal 1000000 cellen wordt gewerkt, ligt dit aantal doorgaans in de orde van grootte van 1000 tot 10000 cellen in 3D microfluidische celcuursystemen. Voor het gevoelig en selectief meten van metabolieten in dergelijke materiaal-gelimiteerde biologische systemen, en dus om biochemisch inzicht te verkrijgen, zijn nieuwe analytische technieken nodig.

In dit proefschrift zijn de mogelijkheden van capillaire elektroforese (CE) gekoppeld aan electrospray ionisatie time-of-flight massaspectrometrie (ESI-TOF-MS) bestudeerd voor het meten van metabole profielen in materiaal- en volume-gelimiteerde biologische monsters. CE is een zeer efficiënte micro-scheidingstechniek die met name geschikt is voor het analyseren van polaire en geladen metabolieten, aangezien de scheiding van componenten in CE gebaseerd is op verschillen in lading en grootte. CE wordt doorgaans uitgevoerd in een fused-silica capillair dat gevuld is met een waterige buffer en waarover een hoge elektrische spanning wordt aangelegd. In CE zijn zeer kleine monstervolumina nodig voor de analyse en daarmee is deze techniek zeer geschikt voor het bestuderen van materiaal/volume-gelimiteerde biologische problemen.

Bij aanvang van dit proefschrift was de bruikbaarheid van CE-TOF-MS voor het metabolomics onderzoek al beschreven. Enkele onderzoeksgroepen hebben de potentie van CE-MS reeds onderzocht voor de analyse van metabolieten in een enkele cel, echter, slechts een beperkt aantal componenten kon gedetecteerd worden met deze systemen.

Het hoofddoel van de studies beschreven in dit proefschrift was de ontwikkeling van CE-TOF-MS methoden voor het analyseren van zoveel mogelijk metabolieten in zeer schaars monstermateriaal. Deze analytische methodes zouden dan de bestudering van materiaal/volume-gelimiteerde biologische vraagstukken met een metabolomics benadering mogelijk moeten maken.

In **Hoofdstuk 1** worden de uitgangspunten en het doel van het uitgevoerde onderzoek beschreven. Een overzicht van het gebruik van CE-MS voor metabolomics wordt gegegeven in **Hoofdstuk 2**, waarbij nadruk wordt gelegd op technologische ontwikkelingen om CE-MS een bruikbare tool voor de analyse van materiaal-gelimiteerde monsters te maken. In **Hoofstuk 3** wordt uitvoerig ingegaan op het koppelen van CE aan MS via een sheathless interface (vergezeld van een video) en hoe deze methode verder geoptimaliseerd kan worden voor het gevoelig en efficiënt profileren van metabolieten in biologische monsters.

De potentie van sheathless CE-MS voor het profileren van (endogene) metabolieten in extracten van kleine hoeveelheden cellen (≤10000) is onderzocht in **Hoofdstuk 4**. Hiertoe werd het HepG2 cellijn als modelsysteem gebruikt. De focus lag op het ontwikkelen van een assay voor de analyse van metabolieten met een basische groep, zoals aminozuren, nucleosiden en amines, in extracten van 500 tot 10000 HepG2 cellen. Een in-capillaire preconcentratie-stap werd geïmplementeerd in de CE scheiding om de gevoeligheid van het sheathless CE-MS systeem verder te bevorderen, resulterend in sub-nanomolair detectielimitieten voor de basische metabolieten.

De analyse van metabolieten met een zure groep, zoals nucleotiden en organische zuren, gebeurt doorgaans in negative ion mode ESI-MS. Echter, wanneer de scheiding plaatsvindt onder basische condities met nano-ESI-MS in negative ion mode dan kan corona discharge een nadelige effect hebben op de analyse. In **Hoofdstuk 5** wordt corona discharge volledig omzeild door de nucleotiden te analyseren met sheathless CE-MS in positive ion mode. De toepasbaarheid wordt aangetoond voor de gevoelige en efficiënte analyse van deze verbindingen in extracten van 500 tot 10000 HepG2 cellen. Er wordt voorgesteld om het ontwikkelde assay in te zetten voor de bepaling van de adenylate energy charge als een aanvullende evaluatieparameter voor metabolomics onderzoek aan kleine hoeveelheden cellen.

In **Hoofdstuk 6** wordt de bruikbaarheid van een standaard CE-MS systeem getest voor het vinden van de juiste metabole markers (=biochemische informatie) in een vergelijkende metabolomics studie. Hiertoe werd een artificiële metabolomics studie opgezet, waarbij zgn. ziek versus gezond humane plasma groepen werden geïntroduceerd op basis van aangebrachte verschillen in isotoop-gelabelde metabolieten. De uitkomst van de studie was dat de isotoop-gelabelde metabolieten als de belangrijkste metabole markers (d.w.z. mogelijke biomarkers) naar voren kwam. Kortom, CE-MS is in staat om de juiste (biochemische) informatie te extraheren uit een vergelijke metabolomics studie. Op basis van deze bevindingen is de CE-MS methode in

Hoofdstuk 7 gebruikt voor het vinden van metabole markers voor epileptische aanvallen gebruikmakend van een muizenmodel voor epilepsie.

Nanodeeltjes hebben om zich een biomoleculaire laag, ook wel de corona genoemd. Een goed begrip van de corona is essentieel aangezien deze een cruciale rol speelt bij de interactie van een nanodeeltje met een biologisch systeem. Tot nu toe lag de focus met name op de karakterisering van de eiwitten in de corona. **Hoofdstuk 8** beschrijft de toepassing van sheathless CE-MS voor de kwantitatieve analyse van de metabolieten in de corona van verscheidene nanodeeltjes. Er wordt aangetoond dat metabolieten zich op een specifieke manier hechten aan de verschillende nanodeeltjes.

Hoofdstuk 9 geeft algemene conclusies en opmerkingen over de bruikbaarheid van de ontwikkelde CE-MS methodes voor het gevoelig en efficiënt profileren van metabolieten in materiaal-gelimiteerde monsters. Daarnaast worden suggesties gedaan voor vervolgonderzoek.

Acknowledgements

First of all, I would like to express my sincere gratitude to everyone who contributed to the completion of this thesis. This thesis would not have been possible without you.

I am grateful to Prof. dr. Thomas Hankemeier for giving me the opportunity to come to Leiden for the PhD program. His patience, enthusiasm and immense knowledge has always been a great inspiration. I would also like to thank Dr. Rawi Ramautar, my supervisor, who has been my biggest supporter since day one. Thank you for all your guidance with my experiments, and for your tremendous help with the writing of this thesis.

Many thanks to my external collaborators, from whom I have learned a lot. I am grateful to my collaborators from Vrije Universiteit Brussel, Karen, Debby, Ann, and Yvan for conducting interesting research programs together and imparting their knowledge on data analysis. To Iseult and Andy from the University of Birmingham, thanks for the good work we carried out together and making those wonderful arrangements for us during our stay in the UK. I'm looking forward to working with all of you in the future.

I would like to thank all the past and present colleagues at ABS and BMFL. Thank you, Loes, for taking good care of us and helping us with all sorts of issues; Faisa, for your expertise and assistance with the instruments; Nicolas, for selflessly sharing your knowledge with me. My genuine appreciation goes to everybody and thank you for making the last four years such an amazing experience. I want to especially thank my Chinese colleagues, Zhengzheng, Wei, Tian, Yupeng, Xinyu, Luojiao, Pingping, and Bingshu, for the good food and laughs we shared.

I want to express my appreciation to Jelte Liemburg for designing the nice cover of this thesis.

Last but not least, I would also like to thank my family for their faith in me and encouragement along the way.

Curriculum vitae

Wei Zhang was born on Nov 18th, 1989 in Yangzhou, China. After graduating from Gaoyou High School of Jiangsu Province in 2008, he got admitted to the major of Traditional Chinese Pharmacy at China Pharmaceutical University in Nanjing. One year later, he got transferred to the National Academic Base for Pharmaceutical Science due to his excellent academic performance. In 2012, he obtained his bachelor's degree and got recommended to the graduate school at the same university to pursue a master's degree in pharmacokinetics. During his master's study, he focused on the investigation of pharmacokinetic properties of acteoside in animals, which led to his first scientific publication as the first author in 2015, titled "Pharmacokinetics of acteoside following single dose intragastric and intravenous administrations in dogs". In October 2015, he started his PhD project under the supervision of Prof. Dr. Thomas Hankemeier and Dr. Rawi Ramautar at Leiden Academic Centre for Drug Research (LACDR). Between 2015 and 2019, he dedicated his research to the development of nanoscale separation strategies for metabolic profiling of ultra-small samples using capillary electrophoresis-mass spectrometry(CE-MS).

List of publications

1. **Zhang, W.**, Gulersonmez, M. C., Hankemeier, T., & Ramautar, R. (2016). Sheathless Capillary Electrophoresis–Mass Spectrometry for Metabolic Profiling of Biological Samples. *JoVE (Journal of Visualized Experiments)*, (116), e54535.
2. **Zhang, W.**, Hankemeier, T., & Ramautar, R. (2017). Next-generation capillary electrophoresis–mass spectrometry approaches in metabolomics. *Current opinion in biotechnology*, *43*, 1-7.
3. **Zhang, W.**, Guled, F., Hankemeier, T., & Ramautar, R. (2019). Utility of sheathless capillary electrophoresis-mass spectrometry for metabolic profiling of limited sample amounts. *Journal of Chromatography B*, *1105*, 10-14.
4. **Zhang, W.**, Hankemeier, T., & Ramautar, R. (2019). Capillary Electrophoresis-Mass Spectrometry for Metabolic Profiling of Biomass-Limited Samples. In *Clinical Applications of Capillary Electrophoresis* (pp. 165-172). Humana Press, New York, NY.
5. **Zhang, W.***, Segers, K., Mangelings, D., Van Eeckhaut, A., Hankemeier, T., Vander Heyden, Y., & Ramautar, R. (2019). Assessing the suitability of capillary electrophoresis-mass spectrometry for biomarker discovery in plasma-based metabolomics. *Electrophoresis*, *40*(18-19), 2309-2320.
6. **Zhang, W.**, Guled, F., Hankemeier, T., & Ramautar, R. (2020). Profiling nucleotides in low numbers of mammalian cells by sheathless CE-MS in positive ion mode: circumventing corona discharge. *Electrophoresis*.

Not part of this thesis

1. **Zhang, W.**, Huo, S. X., Wen, Y. L., Xing, H., Zhang, Q., Li, N., ... & Chen, X. J. (2015). Pharmacokinetics of acteoside following single dose intragastric and intravenous administrations in dogs. *Chin J Nat Med*, 13, 634-640.
2. Zhao, J., Wen, Y., **Zhang, W.**, Zhao, D., Fan, A., Zhang, Y., ... & Wang, Z. (2014). Investigation on pharmacokinetics, tissue distribution and excretion of a novel platinum anticancer agent in rats by inductively coupled plasma mass spectrometry (ICP-MS). *Xenobiotica*, 44(8), 757-762.
3. Deng, S., Wang, C., **Zhang, W.**, Gao, W., Fan, A., Zhang, Q., ... & Zhao, J. (2014). Effect of triacontanol on the pharmacokinetics of docetaxel in rats associated with induction of cytochrome P450 3A1/2. *Xenobiotica*, 44(7), 583-590.
4. Wen, Y., Huo, S., **Zhang, W.**, Xing, H., Qi, L., Zhao, D., ... & Chen, X. (2016). Pharmacokinetics, biodistribution, excretion and plasma protein binding studies of acteoside in rats. *Drug research*, 66(03), 148-153.
5. Burgos, R. C. R., **Zhang, W.**, van Wijk, E. P., Hankemeier, T., Ramautar, R., & van der Greef, J. (2017). Cellular glutathione levels in HL-60 cells during respiratory burst are not correlated with ultra-weak photon emission. *Journal of Photochemistry and Photobiology B: Biology*, 175, 291-296.

* *Authors contributed equally*